PHD DISSERTATION / TESIS DOCTORAL

AUTHOR:

CLÉMENT LOPEZ-CANFIN

UNIVERSIDAD
DE GRANADA

DRYLAND SOIL-ATMOSPHERE CO_2 EXCHANGE ASSOCIATED TO MICROCLIMATE AND GEOCHEMISTRY OVER A BIOCRUSTS SUCCESSION

DIRECTORS:

ROBERTO A. LÁZARO SUAU

ENRIQUE PÉREZ SÁNCHEZ-CAÑETE

FEBRUARY 2022

UNIVERSITY OF GRANADA

PHD PROGRAM IN EARTH SCIENCE

PHD DISSERTATION / TESIS DOCTORAL

AUTHOR

CLÉMENT LOPEZ-CANFIN

DRYLAND SOIL-ATMOSPHERE CO_2 EXCHANGE ASSOCIATED TO MICROCLIMATE AND GEOCHEMISTRY OVER A BIOCRUSTS SUCCESSION

PROGRAMA DE DOCTORADO EN CIENCIAS DE LA TIERRA

UNIVERSIDAD
DE
GRANADA

CONSEJO SUPERIOR DE
INVESTIGACIONES
CIENTIFICAS

Grupo Física
de la Atmósfera

Editor: Universidad de Granada. Tesis Doctorales
Autor: Clément López Canfin
ISBN: 978-84-1117-269-1
URI: http://hdl.handle.net/10481/73974

TESIS DOCTORAL

DRYLAND SOIL-ATMOSPHERE CO_2 EXCHANGE ASSOCIATED TO MICROCLIMATE AND GEOCHEMISTRY OVER A BIOCRUSTS SUCCESSION

Trabajo de investigación presentado por **Clément Lopez-Canfin**
para aspirar al grado de Doctor por la Universidad de Granada

Esta Tesis Doctoral ha sido dirigida y supervisada por:

Dr. Roberto A. Lázaro Suau y Dr. Enrique Pérez Sánchez-Cañete

Febrero 2022

La Tesis doctoral que se expone en la siguiente memoria, titulada: "Dryland soil-atmosphere CO_2 exchange associated to microclimate and geochemistry over a biocrusts succession" ha sido realizada por Clément Lopez-Canfin para aspirar al grado de Doctor por la Universidad de Granada. Se ha realizado conjuntamente en el Departamento de Desertificación y Geoecología de la Estación Experimental de Zonas Áridas (CSIC, Almería) y el Departamento de Física Aplicada de la Universidad de Granada. La realización de esta Tesis ha sido financiada por el proyecto "Dinámica de Biocostras" (DINCOS) del Plan Estatal de Investigación Científica, Técnica y de Innovación 2016-2020 (CGL2016-78075-P), y por el proyecto "Intercambios de Carbono y Agua en Ecosistemas Singulares y Representativos de Andalucía" (ICAERSA) de la Junta de Andalucía (P18-RT-3629), incluyendo fondos europeos de desarrollo regional (FEDER).

ABSTRACT

This thesis arose in response to several gaps in the current understanding and modelling of the carbon cycle: (1) in spite of its importance on ecosystem and global CO_2 emissions, the soil-atmosphere CO_2 flux (F_c) was still not well constrained, and its feedback with climate change and F_c was still uncertain; (2) biological soil crusts (biocrusts) were believed to play a considerable role in the global carbon budget due to their photosynthetic activity but little was known about the spatio-temporal variability of F_c under those communities of microorganisms that cover drylands soils worldwide; (3) a nocturnal soil CO_2 uptake has been increasingly reported in those areas but the involved biogeochemical mechanisms remained unclear; (4) recent evidence suggested that liquid water input *via* water vapor adsorption (WVA) by soil had been overlooked in water-limited ecosystems, though it might represent an important process to take into account in climate-carbon cycle feedback models. This thesis aimed to contribute to improve the available knowledge required to address those issues.

To this end, a semi-permanent experiment was designed in the Tabernas Desert (Southeastern Spain). A network of environmental sensors was installed to monitor continuously the microclimate over an ecological succession of biocrusts, including CO_2 and water vapor measurements in the topsoil and atmosphere. Those measurements were coupled to a geochemical characterization of the soil and soil water.

To assess the role of geochemistry and in particular soil carbonates in F_c dynamics, it was necessary to obtain accurate measurements of parameters used as inputs in geochemical models. Therefore, Chapter 1 presents a methodological advance to determine accurately the carbonate chemistry in the soil solid and aqueous phase: a new low-cost device was developed to quantify the calcium carbonate content and reactive surface area in solid samples as well as the dissolved inorganic carbon content in water samples.

Chapter 2 presents two years of continuous measurements of the topsoil CO_2 molar fraction (χ_c) and pedoclimatic variables, including soil water content (θ_w) and soil temperature (T_s). Those data were used to develop statistical spatio-temporal models of the χ_c dynamics over the biocrusts succession. We found that soil CO_2 emissions were more sensitive to θ_w and T_s

in late successional stages, and that a future enhancement of soil CO_2 emissions is a likely outcome of global warming at this site. Nevertheless, we also found that calcite played a role in mitigating CO_2 emissions through the uptake of CO_2 by soil at night. Our measurements suggested that CO_2 consumption processes were progressively masked by the increase in biological CO_2 production during succession. That is probably why those processes could mainly be detected in early successional stages and more generally in drylands, as they sustain a low biological activity.

In Chapter 3, water vapor measurements were added to the dataset of Chapter 2 and analyzed in association with CO_2 measurements. Our main findings were (1) the occurrence of WVA fluxes during hot and dry periods, and new insights on their underlying mechanisms; (2) a coupling between water vapor and CO_2 fluxes, well predicted by our models; and (3) cumulative soil CO_2 uptake increasing with specific surface area in early succession stages, thus mitigating CO_2 emissions. During summer drought, as WVA was the main water source, it probably maintained ecosystem processes such as microbial activity and mineral reactions. Therefore, at this stage of the thesis, we suggested that WVA could drive the detected nocturnal CO_2 uptake.

In Chapter 4, we further explored the underlying mechanisms involved in this uptake. To this end, measurements of CO_2 and water vapor were combined to analyses of the composition of the soil solution after simulated rain events and subsequent geochemical and statistical modelling. We found strong evidence for the occurrence of a geochemical mechanism of coupled gypsum dissolution-carbonate precipitation due to a common-ion effect, and proposed a pathway for its implication in the nocturnal soil CO_2 uptake. The main factor limiting the process in this dryland was water availability, but our observations supported that nocturnal water vapor adsorption by soil might lift this limitation under drought conditions. We also discussed the role of soil dissolved organic carbon on calcite precipitation, and a possible connection with the nitrogen cycle and biomineralizing microorganisms among biocrusts. We suggest that this natural geochemical process has the potential to constitute an active long-term carbon sink because the Ca involved in $CaCO_3$ precipitation came from an exogenic source.

In summary, this thesis contributed to improve the understanding and modelling of the soil-atmosphere CO_2 exchange in semiarid biocrusted soils,

by identifying the environmental variables and potential biogeochemical processes controlling those fluxes. It especially emphasizes the role of overlooked natural processes able to mitigate CO_2 emissions. A general discussion is provided at the end of this thesis, which connects the contents of the different chapters together with the current state of knowledge.

RESUMEN

Esta tesis tomó forma como respuesta a ciertas lagunas que el ciclo del Carbono presenta actualmente en cuanto a la comprensión y la modelización de los procesos: (1) a pesar de su importancia en el ecosistema y en las emisiones globales de CO_2, el flujo de CO_2 suelo-atmósfera (F_c) aún no estaba bien acotado, y la retroalimentación entre el cambio climático y F_c era aún incierta; (2) se creía que las costras biológicas del suelo (biocostras) desempeñaban un papel considerable en el balance global de carbono debido a su actividad fotosintética, pero se sabía poco sobre la variabilidad espacio-temporal de F_c en esas comunidades de microorganismos que cubren el suelo en una amplia parte de las tierras secas en todo el mundo; (3) aunque han ido apareciendo evidencias de absorción nocturna de CO_2 en el suelo en esas áreas, los mecanismos biogeoquímicos involucrados seguían sin estar claros; (4) la entrada de agua líquida en el sistema por la adsorción de vapor de agua (WVA) por el suelo no se había tenido suficientemente en cuenta en estos ecosistemas limitados por el agua, aunque podría ser un proceso importante a considerar en los modelos de retroalimentación del ciclo del carbono y el clima. Esta tesis tuvo como objetivo contribuir a mejorar el conocimiento actual sobre estos problemas.

Para ello se diseñó un experimento semipermanente en el Desierto de Tabernas (sureste de España). Se instaló una red de sensores ambientales para registro en continuo del microclima y medición de CO_2 y vapor de agua en la capa superior del suelo y la atmósfera, en una serie de puntos representativos de la sucesión ecológica en las biocostras. Esas mediciones se acoplaron a una caracterización geoquímica del suelo y del agua del suelo.

Para evaluar el papel de la geoquímica y, en particular, de los carbonatos del suelo en la dinámica de F_c, fue necesario obtener mediciones precisas de los parámetros utilizados como entradas en los modelos geoquímicos. Es por ello que el Capítulo 1 presenta un avance metodológico para determinar con precisión la química del carbonato en las fases sólida y acuosa del suelo: Se desarrolló un nuevo dispositivo, de bajo coste, para cuantificar el contenido de carbonato de calcio y el área superficial reactiva en muestras sólidas, así como el carbono inorgánico disuelto contenido en muestras de agua.

El Capítulo 2 presenta dos años de mediciones continuas de la fracción molar de CO_2 de la capa superior del suelo (χ_c), junto con variables pedoclimáticas, incluido el contenido de agua del suelo (θ_w) y la temperatura del suelo (T_s). Esos datos se usaron para desarrollar modelos estadísticos espacio-temporales de la dinámica de χ_c a lo largo de la sucesión en las

biocostras. Descubrimos que las emisiones de CO_2 del suelo eran más sensibles a θ_w y T_s en las últimas etapas de la sucesión, y que un aumento futuro de las emisiones de CO_2 del suelo es un resultado probable del calentamiento global en este sitio. Sin embargo, también encontramos que la calcita desempeñó un papel en la mitigación de las emisiones de CO_2, a través de la absorción de CO_2 por parte del suelo durante la noche. Nuestras mediciones sugirieron que los procesos de consumo de CO_2 fueron progresivamente más enmascarados por el aumento en la producción biológica de CO_2 a lo largo de la sucesión. Probablemente por eso estos procesos se detectarían principalmente en etapas sucesionales tempranas, y particularmente en tierras secas, ya que mantienen una baja actividad biológica.

En el Capítulo 3, mediciones de flujos de vapor de agua se agregaron al conjunto de datos del Capítulo 2 y se analizaron en asociación con las mediciones de CO_2. Nuestros principales hallazgos fueron (1) la aparición de flujos WVA durante períodos cálidos y secos, y nuevos conocimientos sobre sus mecanismos subyacentes; (2) la existencia de un acoplamiento entre los flujos de vapor de agua y CO_2, acertadamente predicho por nuestros modelos; y (3) que la absorción acumulativa de CO_2 del suelo aumenta con el área de superficie específica en las primeras etapas de sucesión, mitigando así las emisiones de CO_2. Durante la sequía del verano, dado que WVA era la principal fuente de agua, probablemente mantuvo procesos del ecosistema, como la actividad microbiana y las reacciones minerales. Es por esto que, en esta etapa de la tesis, sugerimos que WVA podría impulsar la captación nocturna de CO_2 detectada.

En el Capítulo 4, exploramos más a fondo los mecanismos subyacentes implicados en esta captación. Con este fin, las mediciones de CO_2 y vapor de agua se combinaron con análisis de la composición de la solución del suelo después de eventos de lluvia simulados y la posterior modelización geoquímica y estadística. Encontramos fuerte evidencia de la existencia de un mecanismo geoquímico de precipitación de carbonatos acoplada con disolución de yeso debido a un efecto de ion común, y hemos propuesto una vía para su implicación en la absorción nocturna de CO_2 por el suelo. El factor principal que limitó el proceso en esta tierra seca fue la disponibilidad de agua, pero nuestras observaciones respaldaron la hipótesis de que la adsorción nocturna de vapor de agua por parte del suelo podría eliminar esta limitación en condiciones de sequía. También discutimos el papel del carbono orgánico disuelto en el suelo en la precipitación de calcita y una posible conexión con el ciclo del nitrógeno y los microorganismos bio-mineralizadores de las biocostras. Sugerimos que este proceso geoquímico natural tiene el potencial

de constituir un sumidero de carbono activo a largo plazo porque el Ca involucrado en la precipitación de $CaCO_3$ proviene de una fuente exógena.

En resumen, esta tesis ha contribuido a mejorar la comprensión y el modelado del intercambio de CO_2 suelo-atmósfera en suelos semiáridos con biocostra, al identificar las variables ambientales y los posibles procesos biogeoquímicos que controlan esos flujos. Enfatiza especialmente el papel de los procesos naturales pasados por alto capaces de mitigar las emisiones de CO_2. Se incluye una discusión general al final de esta tesis, que conecta los contenidos de los diferentes capítulos junto con el estado actual del conocimiento.

ACKNOWLEDGEMENTS

Deseo especialmente agradecer a mis directores de tesis, Roberto Lázaro y Enrique P. Sánchez-Cañete. Sin ellos, la realización de este trabajo no hubiera sido posible. Agradezco a los dos sin distinción por haber confiado en mí y darme carta blanca del inicio hasta el final. A Roberto, al cual le estoy profundamente agradecido por haber estado disponible en todo momento para responder a mis interrogaciones, por su capacidad de escucha, su gran humanidad y su mentalidad abierta. Nunca olvidaré nuestras conversaciones apasionantes, siempre constructivas y llenas de sabiduría de su parte. Sintiendo una gran admiración frente a su filosofía de vida, moral de acero y resistencia al trabajo de campo. A Enrique, al cual le tengo profundo respeto e inmenso agradecimiento por apostar por mí, primero para mi tesina de Máster, luego como técnico y finalmente como estudiante de doctorado. Mostró una eficiencia incomparable para aclarar mis dudas y guiarme durante estos años. Admiro especialmente su gran pragmatismo frente a las situaciones más complejas. De Enrique aprendí que, si hay un problema, hay una solución, sino no hay problema. Le estoy fuertemente agradecido por su gran paciencia conmigo, su capacidad de análisis y sus consejos siempre sensatos. Sinceramente, no hubiera podido soñar mejores directores de tesis. A la vez su pasión por la ciencia y sus cualidades humanas me procuraron una inagotable fuente de motivación para avanzar sobre un camino esparcido de obstáculos. Mucho más que directores de tesis, ahora forman parte de las personas que han marcado profundamente mi vida.

También quiero agradecer a Andrew S. Kowalski por su atento seguimiento como tutor durante todo el desarrollo de mi tesis, por sus recomendaciones tan relevantes, y su contribución al mejoramiento de la redacción de los artículos.

Agradezco a la UGR y su programa de doctorado en Ciencias de la Tierra por su calidad académica y numerosas oportunidades para los estudiantes (conferencias, cursos, becas, etc.).

Me gustaría también agradecer a Francisco Domingo por haberme recibido en la EEZA con los brazos abiertos, y por su mirada benévola sobre mis avances durante estos años.

Agradezco también a Encarnación Ruiz Agudo por haberme abierto las puertas de su laboratorio para realizar análisis de superficie especifica de la calcita, y por su colaboración en el último capítulo de la tesis. También agradezco a Aurelia Ibañez Velasco por haber supervisado estos análisis.

Gracias a Albert Solé-Benet por haber compartido con entusiasmo su brillante conocimiento y por haberme prodigado consejos y datos valiosos en relación con la pedología del sitio experimental. Le deseo una excelente jubilación, bien merecida.

Gracias a Cecilio Oyonarte por haberme permitido realizar los análisis de carbono orgánico en su laboratorio, por haberme guiado a lo largo del proceso y por haberme prestado su IRGA de campo.

Gracias también a Penélope Serrano-Ortiz por haberme prestado su IRGA de campo, permitiendo calibrar un modelo de difusión del CO_2.

Gracias a Mónica Ladrón de Guevara por haberme acogido y capacitado sobre el uso de otro IRGA de campo y a Fernando Maestre por haberme recibido en su laboratorio durante esta capacitación.

Gracias también a los técnicos de la EEZA Angel Belmonte, Domingo Álvarez, Pilar Fuentetaja, Olga Corona Forero y Montserrat Guerrero por echarme una mano con distintas actividades de laboratorio.

Gracias también a Consuelo Rubio y Marietta Daskalaki por su participación en el trabajo de campo y la caracterización de algunas propiedades del suelo.

Gracias a Enrique Cortés-Sánchez por su ayuda en resolver problemas relacionados con la electrónica de las instalaciones y la instrumentación.

Gracias al personal administrativo de la EEZA, estas personas que actúan en la sombra pero que hacen posible la investigación, en particular Almudena Delgado, Andrés Castro y Mercedes Salvador por su dedicación día a día.

Gracias también a mis compañeros de trabajo de la EEZA y de la UGR por su amabilidad a diario, especialmente Christian, Cristina, Gustavo, Iñaki, Jordi, Jorge, Juan, Lourdes y Miguel (EEZA), así como Emilio, Enrique, Félix, Juan Jo, Marcela, Patricio y Sergio (UGR).

Finalmente, quiero agradecer fraternalmente a un amigo especial, Daniel, y a dos miembros de mi familia particularmente importantes, mi primo Cyrille y mi hermano Théo, por su presencia a pesar de la distancia, y por su apoyo infalible, incluso cuando más lo necesitaba.

Je dédie cette thèse à mon père et à celui qui a repris son flambeau, mon grand-père, qui me répétait souvent cette phrase, tirée d´une chanson de Jean Gabin et inspirée de Socrate :

« *Maintenant je sais, je sais qu´on ne sait jamais* »

À mon père, je dédie le poème suivant, en espérant qu´il eut été fier de moi, même s´il me reste encore beaucoup à apprendre :

Si tu peux voir détruit l'ouvrage de ta vie
Et sans dire un seul mot te mettre à rebâtir,
Ou perdre en un seul coup le gain de cent parties
Sans un geste et sans un soupir ;

Si tu peux être amant sans être fou d'amour,
Si tu peux être fort sans cesser d'être tendre,
Et, te sentant haï, sans haïr à ton tour,
Pourtant lutter et te défendre ;

Si tu peux supporter d'entendre tes paroles
Travesties par des gueux pour exciter des sots,
Et d'entendre mentir sur toi leurs bouches folles
Sans mentir toi-même d'un mot ;

Si tu peux rester digne en étant populaire,
Si tu peux rester peuple en conseillant les rois,
Et si tu peux aimer tous tes amis en frère,
Sans qu'aucun d'eux soit tout pour toi ;

Si tu sais méditer, observer et connaître,
Sans jamais devenir sceptique ou destructeur,
Rêver, mais sans laisser ton rêve être ton maître,
Penser sans n'être qu'un penseur ;

Si tu peux être dur sans jamais être en rage,
Si tu peux être brave et jamais imprudent,
Si tu sais être bon, si tu sais être sage,
Sans être moral ni pédant ;

Si tu peux rencontrer Triomphe après Défaite
Et recevoir ces deux menteurs d'un même front,
Si tu peux conserver ton courage et ta tête
Quand tous les autres les perdront,

Alors les Rois, les Dieux, la Chance et la Victoire
Seront à tout jamais tes esclaves soumis,
Et, ce qui vaut mieux que les Rois et la Gloire
Tu seras un homme, mon fils.

" *Tu seras un Homme mon fils »,* Rudyard Kipling (translated by André Maurois)

TABLE OF CONTENTS

1. INTRODUCTION

1.1. Climate-carbon cycle feedbacks

The CO_2 concentration of atmosphere has increased from ca. 278 ppm during pre-industrial times to ca. 410 ppm at the present time and has been growing recently at a rate of ca. 2.5 ppm $year^{-1}$, mainly because of anthropogenic emissions due to fossil fuel combustion and land use change [*Lan et al.*, 2021]. It is now unequivocal that those anthropogenic emissions of CO_2 have substantially magnified the Earth's greenhouse effect triggering a change in climate through global warming, and the resulting forcing continues to rise. As a result, widespread, abrupt and irreversible changes in the atmosphere, ocean, cryosphere and biosphere have already occurred and many of the observed changes are unprecedented over decades to millennia. As temperature rises, more water evaporates and therefore continued global warming intensifies the global water cycle, including its variability, global monsoon precipitation and the severity of wet and dry events [*IPCC*, 2013, 2021]. This ongoing climate change is also responsible for biodiversity loss and alteration of ecosystem functioning and services [*Reid et al.*, 2005].

Soils and biocenosis continuously exchange carbon with the atmosphere. In terrestrial ecosystems, the soil CO_2 flux (F_c) is globally the second largest contributor to CO_2 exchange with atmosphere [*Raich & Schlesinger*, 1992] and the first contributor to CO_2 emissions in many ecosystems [*Davidson & Janssens*, 2006]. This flux is mostly the resultant of CO_2 production in soil and its transport towards atmosphere, mainly by biological respiration and diffusion, respectively [*Šimůnek & Suarez*, 1993]. In spite of its magnitude, F_c is the least constrained component of the terrestrial carbon cycle [*Bond-Lamberty & Thomson*, 2010] and its estimates are largely uncertain [*Bahn et al.*, 2010]. In particular, even if a future global trend of positive feedback between F_c and climate change is likely [*Hashimoto et al.*, 2015], no consensus has been achieved yet to confirm this future feedback. These uncertainties are partly attributable to the considerable variation in F_c related to the many controlling factors that interact over different temporal and spatial scales [*Lopez-Canfin et al.*, 2018; *Vargas et al.*, 2011]. It is thus a major challenge to

better characterize ecosystems carbon cycling in order to improve modeling and forecasts of climate and ecosystems responses.

1.2. The role of dryland biocrusts in the carbon cycle

In natural soils, carbon tends to be sequestered in organic matter over time due to the autotrophic CO_2 assimilation by photosynthesis and its subsequent carbon transfer to soil that exceeds the release of CO_2 by heterotrophic respiration during decomposition. In dryland ecosystems where vegetation is sparse and short, carbon inputs to the soil through photosynthesis are mainly ensured by microscopic (cyanobacteria, algae, fungi and bacteria) and macroscopic (lichens and mosses) poikilohydric organisms that occur on or within the top few centimeters of the soil, namely biological soil crusts (hereafter biocrusts) [*Weber et al.*, 2016]. Under optimal conditions, biocrusts photosynthetic rates are similar to those of vascular leaves; therefore, when biocrusts are wet, their carbon fixation is equivalent to that of a layer of vascular leaves lying on soil surface [*Pointing & Belnap*, 2012]. As drylands cover ca. 45% of the Earth´s land surface area [*Lal*, 2019] and those communities can represent up to 70% of the living cover in those areas [*Belnap*, 1990], biocrusts are believed to play a considerable role in the global carbon budget [*Belnap*, 2012]: the global net carbon uptake of biocrusts has been estimated to range between 0.34 and 3.9 Gt C yr-1 worldwide [*Elbert et al.*, 2012; *Porada et al.*, 2013], with the upper estimate corresponding to around 7% of net primary production by terrestrial vegetation. As a result, over several years biocrusts can increase the total amount of carbon in soil by up to 300% [*Rogers & Burns*, 1994], stimulating the respiration of the underlying community of heterotrophs, which is often carbon- limited [*Belnap & Lange*, 2003; *Beymer & Klopatek*, 1991].

Nevertheless, little is known about the spatio-temporal variability of F_c under biocrusts as most research has measured the CO_2 exchange of biocrusts in controlled conditions after separating them from the underlying soil [*Wilske et al.*, 2008]. This component is crucial to assess the potential of ecosystems dominated by biocrusts as carbon sinks because the carbon balance of water-limited ecosystems is often close to neutrality and therefore can easily switch between sink and source in response to even small variations in F_c. It is

generally assumed that biocrusts develop worldwide following an ecological succession [*Lan et al.*, 2015; *Lázaro et al.*, 2008], gradually from bare soil (or physical crust) to *Cyanobacteria* to lichens to mosses. However, few studies have measured F_c *in-situ* in soils covered by biocrusts [e.g. *Bowling et al.*, 2011; *Wilske et al.*, 2008] and so far, those measurements have not been performed over the whole ecological succession, nor continuously over several years, and with spatial representativeness. Continuous measurements are essential to capture the temporal variability of F_c which is known to exhibit ephemeral soil CO_2 pulses after precipitation in drylands [*Lopez-Canfin et al.*, 2018; *Vargas et al.*, 2018]. That is especially important in soils covered by biocrusts as those organisms can stay dormant during long periods of time and respond very quickly (in few minutes) to rewetting [*Karnieli et al.*, 2001]. Spatial representativeness of measurements is also critical as dryland ecosystems present "hot-spots" of CO_2 emissions [*Leon et al.*, 2014] and the distribution of biocrust types is particularly heterogeneous in space. Furthermore, as ecological succession can last up to millennia, measuring and sampling succession stages allows space-for-time substitution, i.e. to infer long-term temporal dynamics from spatial data [*Pickett*, 1989]. Besides, the ecological succession of biocrusts could represent a convenient *in-situ* model to study the interaction between biotic and abiotic factors on F_c as the biotic influence on soil is expected to increase gradually from physical crusts to lichens-dominated late succession stages.

1.3. Potential abiotic processes of CO_2 consumption in drylands

In ecosystems where biological activity is limited, the prevalence of CO_2 consumption rates over CO_2 production rates can sometimes result in negative values of F_c (influx or CO_2 uptake by the soil). Such "anomalies" in F_c have generally been reported in drylands during nighttime [*Ball et al.*, 2009; *Fa et al.*, 2016; *Hamerlynck et al.*, 2013; *Li et al.*, 2015], revealing the non-negligible role of soil CO_2 consumption processes on the carbon balance of these ecosystems. It has been recently reported that a considerable fraction of soil CO_2 is not emitted directly towards atmosphere, but rather reacts into the soil where it is consumed by various biogeochemical processes [*Sánchez-Cañete et al.*, 2018]. The biotic processes able to consume CO_2 in the soil gaseous

phase are: (1) photosynthesis by biological soil crusts [*Máguas et al.*, 2013]; (2) root uptake by plants [*Stemmet et al.*, 1962] and (3) chemoautotrophy. For example, chemolithoautotrophic bacteria fix CO_2 into organic matter via the oxidation of reduced inorganic compounds such as nitrogen, sulfur and iron [*Gobat et al.*, 2004]. The abiotic mechanisms that can consume gaseous CO_2 in soil are (1) CO_2 dissolution in the aqueous phase [*Ma et al.*, 2013, 2014] and (2) reaction with some minerals, such as carbonates [*Hamerlynck et al.*, 2013; *Roland et al.*, 2013]; (3) adsorption of CO_2 on soil particles [*Davidson et al.*, 2013]. Other processes such as bioweathering and/or biomineralization of carbonates [*Cuezva et al.*, 2012; *Liu et al.*, 2018] are at the frontier between the biotic and the abiotic. There is no consensus so far about which biogeochemical processes are involved in the negative anomalies of F_c, and they are not necessarily unique nor identical from one site to another.

Reactions with soil minerals involving CO_2, such as carbonates, deserve special attention since it is estimated that soils contain between 940 Gt and 1558 GtC inorganic carbon (mainly as carbonates), of which 80 to 97% (916-1237 GtC) is located in drylands [*Bernoux & Chevallier*, 2014; *Lal*, 2019]. The upper estimate of the inorganic carbon pool in drylands represents an amount of carbon 20% greater than in permafrost soils, 138% greater than in vegetation, and 49% greater than that in the atmosphere [*Plaza et al.*, 2018]. In some site-specific conditions, the inorganic carbon pool can be up to 10-17 times the organic pool [*Lal*, 2019]. In addition, the residence time of mineral carbon is much greater than organic matter: 10^2-10^6 years and 0.1-10^3 years, respectively [*Bernoux & Chevallier*, 2014; *Cailleau et al.*, 2004] and carbonates have the capacity to stabilize organic matter [*Rowley et al.*, 2018]. Therefore, mineral carbon represents a much more interesting pool for carbon storage, but due to its magnitude it should be monitored more closely in the context of climate change as its alteration could potentially release more carbon to the atmosphere.

Among carbonates, calcite ($CaCO_3$) is dominant in soils and particularly reactive, with a dissolution rate approximately 100 times greater than dolomite and a dissolution time generally on the order of 0.5 to 3 days [*Loeppert & Suarez*, 1996]. Diel patterns of precipitation/dissolution of $CaCO_3$ affecting the net ecosystem carbon exchange have already been described [*Roland et al.*, 2013], and hence are compatible with the nocturnal CO_2 uptake

increasingly reported in drylands. The reactions of precipitation and dissolution of $CaCO_3$ produce and consume CO_2 respectively but their effect on the carbon balance depends on the considered time- and spatial scale [*Serrano-Ortiz et al.*, 2010], as well as the calcium source [*Monger et al.*, 2015]. That is due to dissolution and subsequent reprecipitation of $CaCO_3$ that can have overriding effects on the carbon balance over time in soils developed from preexisting carbonate bedrock, and transient storage of CO_2 as dissolved inorganic carbon (DIC). Soils can store an order of magnitude greater CO_2 as DIC in the aqueous phase than in the gas phase [*Angert et al.*, 2015]. Global stocks of DIC in groundwater have been estimated to 1404 GtC, thus surpassing the soil organic carbon pool (1530 GtC) when added to carbonate [*Monger et al.*, 2015]. However, estimates of DIC pools in drylands could not be found in the scientific literature, probably due to the scarcity of soil water in those ecosystems and its large spatio-temporal variability. The lack of water in drylands has also challenged the assumption according to which calcite dissolution consuming CO_2 could explain the nocturnal CO_2 uptake by soil [*Schlesinger et al.*, 2009].

1.4. Water vapor adsorption: an overlooked water input in drylands

In drylands, due to the infrequency and variability of precipitation, non-rainfall water inputs (NRWIs) (i.e. fog deposition, dew formation and water vapor adsorption by soil) can be the sole water supply for plants and biocrusts during large periods of time. There is also increasing evidence that multiple ecosystem functions including biogeochemical dynamics and organism survival (e.g. microorganisms and animals) critically depend on NRWIs; however, to better predict the ecosystem responses to environmental changes, especially in drylands, a better understanding and quantification of the NRWI contributions are essential [*Wang et al.*, 2017]. The later authors have identified several critical gaps in the knowledge of NRWIs, including: (1) the mechanisms of NRWIs (especially dew and water vapor adsorption) effects on various ecosystem functions, (2) the quantitative contributions of NRWIs components to ecosystem functions, and (3) the separation of different NRWIs contributions.

Among NRWIs, most research efforts on quantifying those inputs and assessing their role on ecosystem functions have focused on fog deposition and dew formation, whereas water vapor adsorption (WVA) by soil has received very little attention. WVA is the movement of water vapor from atmosphere to soil, forming liquid water on the surface of soil particles. It occurs when the water vapor pressure of the soil is lower than the water vapor pressure of the atmosphere. Due to absence of standardized methods to measure NRWIs and the difficulty to differentiate between dew formation and WVA, the role of dew has probably been overestimated to the detriment of WVA [*Agam & Berliner*, 2006]. Moreover, as warmer air has the capacity to hold more water vapor, and soil drying is predicted with high confidence in some regions of the globe [*Collins et al.*, 2013], WVA by soil might be enhanced by climate change.

In addition, WVA could represent an overlooked but important process to take into account in climate-carbon cycle feedbacks model. The process has been shown to enhance CO_2 release from microbial litter decomposition [*Dirks et al.*, 2010; *Newell et al.*, 1985]. More recently, WVA was found to increase soil CO_2 production thus revealing that dryland microorganisms were able to use this water input to sustain their metabolic activity [*McHugh et al.*, 2015]. WVA could also affect the CO_2 exchange by enhancing CO_2 dissolution in the adsorbed water and mineral reactions. Dew, which is a surficial process, can stimulate weathering processes like the hydration of salts and other mineral components [*Verheye*, 2009]. Therefore, a similar effect can be expected regarding WVA into soil. Furthermore, WVA has been commonly reported to occur at night when the soil-atmosphere water vapor pressure gradient inverts because of increasing atmosphere relative humidity and previous soil drying [*Agam & Berliner*, 2006; *Kool et al.*, 2021; *Kosmas et al.*, 1998]. Hence, WVA could potentially drive the nocturnal CO_2 uptake increasingly reported in drylands by providing water to sustain either biotic or abiotic CO_2 consumption processes.

1.5. Objectives of the thesis and general assumption

The main objective of this thesis is to improve the understanding and modelling of the soil-atmosphere CO_2 exchange in semiarid biocrusted soils, by identifying the environmental variables and biogeochemical processes controlling it.

In the different chapters of this thesis, we will try to achieve the main objective by meeting the specific objectives identified for each chapter:

- To develop a low-cost device to determine accurately the carbonate chemistry in the soil solid and aqueous phase (Chapter 1).

- To identify the main factors controlling the *in-situ* spatio-temporal dynamics in soil-atmosphere CO_2 exchange, with a particular focus on assessing the effect of biocrust succession and developing a predictive model (Chapter 2).

- To measure soil water vapor adsorption continuously, at low-cost and with little time investment, and to evaluate its role on the soil-atmosphere CO_2 exchange, in particular as a potential explanatory process of nocturnal soil CO_2 uptake (Chapter 3).

- To evaluate the role of the precipitation-dissolution dynamics of $CaCO_3$ in the soil-atmosphere CO_2 exchange (Chapter 4).

In all the chapters of this thesis, we assume that the following biocrust types are representative of the stages of the ecological succession in this ecosystem [*Lázaro et al.*, 2008]: (1) physical depositional crust (PD); (2) incipient cyanobacterial (IC); (3) mature cyanobacterial (MC); (4) lichen community dominated by *Squamarina lentigera* (Web.) Poelt and *Diploschistes diacapsis* (Ach.) Lumbsch (SD); and (5) lichen community characterized by *Lepraria isidiata* (Llimona) Llimona & Crespo (LI).

References

Agam, N., & Berliner, P. R. (2006). Dew formation and water vapor adsorption in semi-arid environments—a review. *Journal of Arid Environments*, *65*(4), 572–590.

Angert, A., Yakir, D., Rodeghiero, M., Preisler, Y., Davidson, E., & Weiner, T. (2015). Using O2 to study the relationships between soil CO2 efflux and soil respiration. *Biogeosciences*, *12*, 2089–2099. https://doi.org/10.5194/bg-12-2089-2015

Bahn, M., Reichstein, M., Davidson, E. A., Grünzweig, J., Jung, M., Carbone, M. S., Epron, D., Misson, L., Nouvellon, Y., & Roupsard, O. (2010). Soil respiration at mean annual temperature predicts annual total across vegetation types and biomes. *Biogeosciences*, *7*(7), 2147.

Ball, B. A., Virginia, R. A., Barrett, J. E., Parsons, A. N., & Wall, D. H. (2009). Interactions between physical and biotic factors influence CO2 flux in Antarctic dry valley soils. *Soil Biology and Biochemistry*, *41*(7), 1510–1517. https://doi.org/10.1016/j.soilbio.2009.04.011

Belnap, J. (1990). Microbiotic crusts: their role in past and present ecosystems. *Park Science*, *10*(3), 3–4.

Belnap, J. (2012). Unexpected uptake. *Nature Geoscience 2012 5:7*, *5*(7), 443–444. https://doi.org/10.1038/ngeo1514

Belnap, J., & Lange, O. L. (2003). *Biological Soil Crusts: Structure, Function, and Management*. Springer-Verlag Berlin Heidelberg New York.

Bernoux, M., & Chevallier, T. (2014). Carbon in dryland soils. Multiple essential functions. *Les Dossiers Thématiques Du CSFD*, *10*.

Beymer, R. J., & Klopatek, J. M. (1991). Potential contribution of carbon by microphytic crusts in pinyon-juniper woodlands. *Arid Land Research and Management*, *5*(3), 187–198. http://doi.org/10.1080/15324989109381279

Bond-Lamberty, B., & Thomson, A. (2010). A global database of soil respiration data. *Biogeosciences*, *7*(6), 1915–1926.

Bowling, D. R., Grote, E. E., & Belnap, J. (2011). Rain pulse response of soil CO2 exchange by biological soil crusts and grasslands of the semiarid Colorado Plateau, United States. *Journal of Geophysical Research: Biogeosciences*, *116*(G3). https://doi.org/10.1029/2011JG001643

Cailleau, G., Braissant, O., & Verrecchia, E. P. (2004). Biomineralization in plants as a long-term carbon sink. *Naturwissenschaften 2004 91:4*, *91*(4), 191–194. https://doi.org/10.1007/S00114-004-0512-1

Collins, M., Knutti, R., Arblaster, J., Dufresne, J.-L., Fichefet, T., Friedlingstein, P., Gao, X., Gutowski, W. J., Johns, T., & Krinner, G. (2013). Long-term climate change: projections, commitments and irreversibility. In *Climate Change 2013-The Physical Science Basis: Contribution of Working Group I to the Fifth Assessment Report of the Intergovernmental Panel on Climate Change* (pp. 1029–1136). Cambridge University Press.

Cuezva, S., Fernandez-Cortes, A., Porca, E., Pašić, L., Jurado, V., Hernandez-Marine, M., Serrano-Ortiz, P., Hermosin, B., Cañaveras, J. C., & Sanchez-Moral, S. (2012). The biogeochemical role of Actinobacteria in Altamira cave, Spain. *FEMS Microbiology Ecology*, *81*(1), 281–290.

Davidson, E. A., & Janssens, I. A. (2006). Temperature sensitivity of soil carbon decomposition and feedbacks to climate change. *Nature*, *440*(7081), 165–173.

Davidson, G. R., Phillips-Housley, A., & Stevens, M. T. (2013). Soil-zone adsorption of atmospheric CO2 as a terrestrial carbon sink. *Geochimica et Cosmochimica Acta*, *106*, 44–50.

Dirks, I., NAVON, Y., KANAS, D., DUMBUR, R., & GRÜNZWEIG, J. M. (2010). Atmospheric water vapor as driver of litter decomposition in Mediterranean shrubland and grassland during rainless seasons. *Global Change Biology*, *16*(10), 2799–2812. https://doi.org/10.1111/J.1365-2486.2010.02172.X

Elbert, W., Weber, B., Burrows, S., Steinkamp, J., Büdel, B., Andreae, M. O., & Pöschl, U. (2012). Contribution of cryptogamic covers to the global cycles of carbon and nitrogen. *Nature Geoscience*, *5*(7), 459–462. https://doi.org/10.1038/ngeo1486

Fa, K.-Y., Zhang, Y.-Q., Wu, B., Qin, S.-G., Liu, Z., & She, W.-W. (2016). Patterns and possible mechanisms of soil CO2 uptake in sandy soil. *Science of the Total Environment*, *544*, 587–594. https://doi.org/10.1016/j.scitotenv.2015.11.163

Gobat, J. M., Aragno, M., & Matthey, W. (2004). *The Living Soil – Fundamentals of Soil Science and Soil Biology.* Enfield: Science Publishers.

Hamerlynck, E. P., Scott, R. L., Sánchez-Cañete, E. P., & Barron-Gafford, G. A. (2013). Nocturnal soil CO2 uptake and its relationship to subsurface soil and ecosystem carbon fluxes in a Chihuahuan Desert shrubland. *Journal of Geophysical Research: Biogeosciences*, *118*(4), 1593–1603. https://doi.org/10.1002/2013JG002495

Hashimoto, S., Carvalhais, N., Ito, A., Migliavacca, M., Nishina, K., & Reichstein, M. (2015). Global spatiotemporal distribution of soil respiration modeled using a global database. *Biogeosciences*, *12*, 4121–4132. https://doi.org/10.5194/bg-12-4121-2015

IPCC. (2013). Climate change 2013: The physical science basis. In T. F. Stocker, D. Qin, G.-K. Plattner, M. Tignor, S. K. Allen, J. Boschung, A. Nauels, Y. Xia, V. Bex, & P. M. Midgley (Eds.), *Contribution of Working Group I to the Fifth Assessment Report of the Intergovernmental Panel on Climate Change*. Cambridge University Press.

IPCC. (2021). *Climate Change 2021: The Physical Science Basis. Contribution of Working Group I to the Sixth Assessment Report of the Intergovernmental Panel on Climate Change* (V. Masson-Delmotte, P. Zhai, P. A., S. L. Connors, C. Péan, S. Berger, N. Caud, Y. Chen, L. Goldfarb, M. I. Gomis, M. Huang, K. Leitzell, E. Lonnoy, J. B. R. Matthews, T. K. Maycock, T. Waterfield, O. Yelekçi, R. Yu, & B. Zhou (eds.)). Cambridge University Press. In Press.

Karnieli, A., Kokaly, R. F., West, N. E., & Clark, R. N. (2001). *Remote Sensing of Biological Soil Crusts*. 431–455. https://doi.org/10.1007/978-3-642-56475-8_31

Kool, D., Agra, E., Drabkin, A., Duncan, A., Fendinat, P. P., Leduc, S., Lupovitch, G., Nambwandja, A. N., Ndilenga, N. S., & Thị, T. N. (2021). The overlooked non-rainfall water input sibling of fog and dew: Daily water vapor adsorption on a! Nara hummock in the Namib Sand Sea. *Journal of Hydrology*, *598*, 126420.

Kosmas, C., Danalatos, N. G., Poesen, J., & Van Wesemael, B. (1998). The effect of water vapour adsorption on soil moisture content under Mediterranean climatic conditions. *Agricultural Water Management*, *36*(2), 157–168.

Lal, R. (2019). Carbon Cycling in Global Drylands. *Current Climate Change Reports 2019 5:3*, *5*(3), 221–232. https://doi.org/10.1007/S40641-019-

00132-Z

Lan, S., Wu, L., Zhang, D., & Hu, C. (2015). Analysis of environmental factors determining development and succession in biological soil crusts. *Science of The Total Environment*, *538*, 492–499. https://doi.org/10.1016/J.SCITOTENV.2015.08.066

Lan, X., Tans, P., Hall, B. D., Dutton, G., Mühle, J., Elkins, J. W., & Vimont, I. (2021). Long-lived greenhouse gases. In J. Blunden & T. Boyer (Eds.), *State of the Climate in 2020* (Vol. 102, Issue 8, pp. S1–S475). American Meteorological Society. https://doi.org/10.1175/2021BAMSStateoftheClimate.1

Lázaro, R., Cantón, Y., Solé-Benet, A., Bevan, J., Alexander, R., Sancho, L. G., & Puigdefábregas, J. (2008). The influence of competition between lichen colonization and erosion on the evolution of soil surfaces in the Tabernas badlands (SE Spain) and its landscape effects. *Geomorphology*, *102*(2), 252–266. https://doi.org/10.1016/j.geomorph.2008.05.005

Leon, E., Vargas, R., Bullock, S., Lopez, E., Panosso, A. R., & La Scala, N. (2014). Hot spots, hot moments, and spatio-temporal controls on soil CO2 efflux in a water-limited ecosystem. *Soil Biology and Biochemistry*, *77*, 12–21. https://doi.org/10.1016/j.soilbio.2014.05.029

Li, Y., Wang, Y., Houghton, R. A., & Tang, L. (2015). Hidden carbon sink beneath desert. *Geophysical Research Letters*, *42*(14), 5880–5887.

Liu, Z., Zhang, Y., Fa, K., Zhao, H., Qin, S., Yan, R., & Wu, B. (2018). Desert soil bacteria deposit atmospheric carbon dioxide in carbonate precipitates. *Catena*, *170*, 64–72.

Loeppert, R. H., & Suarez, D. L. (1996). Carbonate and gypsum. *Methods of Soil Analysis: Part 3 Chemical Methods*, *5*, 437–474. https://doi.org/10.2136/sssabookser5.3.c15

Lopez-Canfin, C., Sánchez-Cañete, E. P., Serrano-Ortiz, P., López-Ballesteros, A., Domingo, F., Kowalski, A. S., & Oyonarte, C. (2018). From microhabitat to ecosystem: identifying the biophysical factors controlling soil CO2 dynamics in a karst shrubland. *European Journal of Soil Science*, *69*(6), 1018–1029. https://doi.org/10.1111/ejss.12710

Ma, J., Liu, R., Tang, L.-S., Lan, Z.-D., & Li, Y. (2014). A downward CO2 flux seems to have nowhere to go. *Biogeosciences Discussions*, *11*(7), 10419–

10450.

Ma, J., Wang, Z.-Y., Stevenson, B. A., Zheng, X.-J., & Li, Y. (2013). An inorganic CO2 diffusion and dissolution process explains negative CO2 fluxes in saline/alkaline soils. *Scientific Reports*, *3*, 2025. https://doi.org/10.1038/srep02025

Máguas, C., Pinho, P., Branquinho, C., Hartard, B., & Lakatos, M. (2013). Carbon-Water-Nitrogen relationships between lichens and the atmosphere: Tools to understand metabolism and ecosystem change. *MycoKeys*, *6*, 95.

McHugh, T. A., Morrissey, E. M., Reed, S. C., Hungate, B. A., & Schwartz, E. (2015). Water from air: an overlooked source of moisture in arid and semiarid regions. *Scientific Reports*, *5*(1), 1–6.

Monger, H. C., Kraimer, R. A., Khresat, S., Cole, D. R., Wang, X., & Wang, J. (2015). Sequestration of inorganic carbon in soil and groundwater. *Geology*, *43*(5), 375–378. https://doi.org/10.1130/G36449.1

Newell, S. Y., Fallon, R. D., Cal Rodriguez, R. M., & Groene, L. C. (1985). Influence of rain, tidal wetting and relative humidity on release of carbon dioxide by standing-dead salt-marsh plants. *Oecologia 1985 68:1*, *68*(1), 73–79. https://doi.org/10.1007/BF00379477

Pickett, S. T. A. (1989). Space-for-Time Substitution as an Alternative to Long-Term Studies. *Long-Term Studies in Ecology*, 110–135. https://doi.org/10.1007/978-1-4615-7358-6_5

Plaza, C., Zaccone, C., Sawicka, K., Méndez, A. M., Tarquis, A., Gascó, G., Heuvelink, G. B. M., Schuur, E. A. G., & Maestre, F. T. (2018). Soil resources and element stocks in drylands to face global issues. *Scientific Reports 2018 8:1*, *8*(1), 1–8. https://doi.org/10.1038/s41598-018-32229-0

Pointing, S. B., & Belnap, J. (2012). Microbial colonization and controls in dryland systems. *Nature Reviews Microbiology 2012 10:8*, *10*(8), 551–562. https://doi.org/10.1038/nrmicro2831

Porada, P., Weber, B., Elbert, W., Pöschl, U., & Kleidon, A. (2013). Estimating global carbon uptake by lichens and bryophytes with a process-based model. *Biogeosciences*, *10*(11), 6989–7033. https://doi.org/10.5194/bg-10-6989-2013

Raich, J. W., & Schlesinger, W. H. (1992). The global carbon dioxide flux in soil

respiration and its relationship to vegetation and climate. *Tellus B*, *44*(2), 81–99.

Reid, W. V, Mooney, H. A., Cropper, A., Capistrano, D., Carpenter, S. R., Chopra, K., Dasgupta, P., Dietz, T., Duraiappah, A. K., & Hassan, R. (2005). Millennium Ecosystem Assessment. Ecosystems and human well-being: synthesis. *World Resources Institute, Washington, DC*.

Rogers, S. L., & Burns, R. G. (1994). Changes in aggregate stability, nutrient status, indigenous microbial populations, and seedling emergence, following inoculation of soil with Nostoc muscorum. *Biology and Fertility of Soils*, *18*(3), 209–215. https://doi.org/10.1007/BF00647668

Roland, M., Serrano-Ortiz, P., Kowalski, A. S., Goddéris, Y., Sánchez-Cañete, E. P., Ciais, P., Domingo, F., Cuezva, S., Sanchez-Moral, S., & Longdoz, B. (2013). Atmospheric turbulence triggers pronounced diel pattern in karst carbonate geochemistry. *Biogeosciences*, *10*(7), 5009–5017. https://doi.org/10.5194/bg-10-5009-2013

Rowley, M. C., Grand, S., & Verrecchia, É. P. (2018). Calcium-mediated stabilisation of soil organic carbon. *Biogeochemistry*, *137*(1), 27–49.

Sánchez-Cañete, E. P., Barron-Gafford, G. A., & Chorover, J. (2018). A considerable fraction of soil-respired CO2 is not emitted directly to the atmosphere. *Scientific Reports*, *8*(1), 13518. https://doi.org/10.1038/s41598-018-29803-x

Schlesinger, W. H., Belnap, J., & Marion, G. (2009). On carbon sequestration in desert ecosystems. *Global Change Biology*, *15*(6), 1488–1490.

Serrano-Ortiz, P., Roland, M., Sanchez-Moral, S., Janssens, I. A., Domingo, F., Goddéris, Y., & Kowalski, A. S. (2010). Hidden, abiotic CO 2 flows and gaseous reservoirs in the terrestrial carbon cycle: review and perspectives. *Agricultural and Forest Meteorology*, *150*(3), 321–329.

Šimůnek, J., & Suarez, D. L. (1993). Modeling of carbon dioxide transport and production in soil: 1. Model development. *Water Resources Research*, *29*(2), 487–497.

Stemmet, M. C., De Bruyn, J. A., & Zeeman, P. B. (1962). The uptake of carbon dioxide by plant roots. *Plant and Soil*, *17*(3), 357–364.

Vargas, R., Carbone, M. S., Reichstein, M., & Baldocchi, D. D. (2011). Frontiers and challenges in soil respiration research: from measurements to

model-data integration. *Biogeochemistry*, *102*(1–3), 1–13. https://doi.org/10.1007/s10533-010-9462-1

Vargas, R., Sánchez-Cañete P, E., Serrano-Ortiz, P., Curiel Yuste, J., Domingo, F., López-Ballesteros, A., & Oyonarte, C. (2018). Hot-moments of soil CO2 efflux in a water-limited grassland. *Soil Systems*, *2*(3), 47. https://doi.org/10.3390/soilsystems2030047

Verheye, W. (2009). *Land Use, Land Cover and Soil Sciences - Volume V: Dry Lands and Desertification*. 394.

Wang, L., Kaseke, K. F., & Seely, M. K. (2017). Effects of non-rainfall water inputs on ecosystem functions. *Wiley Interdisciplinary Reviews: Water*, *4*(1), e1179. https://doi.org/10.1002/WAT2.1179

Weber, B., Büdel, B., & Belnap, J. (2016). Biological soil crusts as an organizing principle in drylands. In *Biological soil crusts: an organizing principle in drylands*. Springer International Publishing AG. https://doi.org/http://dx.doi.org/10.1007/978-3-319-30214-0_1

Wilske, B., Burgheimer, J., Karnieli, A., Zaady, E., Andreae, M. O., Yakir, D., & Kesselmeier, J. (2008). The CO2 exchange of biological soil crusts in a semiarid grass-shrubland at the northern transition zone of the Negev desert, Israel. *Biogeosciences Discussions*, *5*(3), 1969–2001. https://doi.org/10.5194/bg-5-1411-2008

2. MATERIAL AND METHODS

2.1. Experimental Site

2.1.1. Location and climate

This research was conducted in the experimental site of El Cautivo, located in the Tabernas Desert in south-east Spain, some 25 km north of the city of Almería (Figure 1). The area belongs to the driest part of Europe. The climate is classified as semi-arid thermo-Mediterranean with a mean annual temperature of 17.9 °C and an average annual precipitation of ca. 230 mm with great inter- and intra-annual variation (coefficient of variation (CV) of 36%) and intra-annual variation (CV of up to 207%) based on a 30-year rainfall record from 1967 to 1997 [*Lázaro et al.*, 2001, 2004]. Summers are hot and dry while winters are mild, with most precipitation falling as intense storm rainfall, particularly in September and October. The average diurnal air temperature variation is 14 °C, varying between 12.8 °C in winter and 15.6 °C in summer. Further information about the study site can be found in Calvo-Cases et al. [2014].

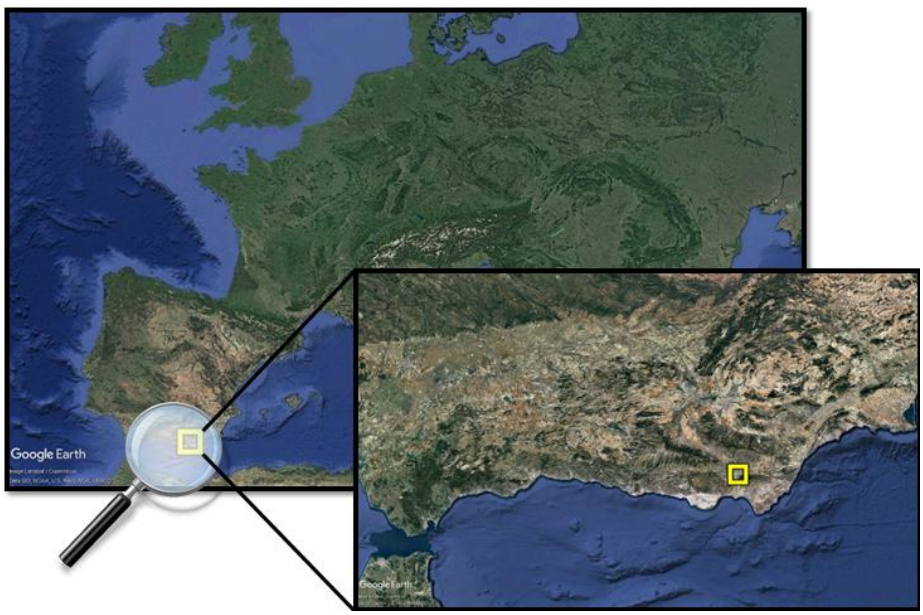

Figure 1 Location of the experimental site of El Cautivo (Almería, Spain).

2.1.2. Geology and Soil

The area is a part of the most extensive badlands in southeastern Spain. The Tabernas Basin is mainly filled with marine sediments deposited during the Miocene. The bedrock horizon starts at a depth ranging from ca. 0.5 to 1.5 m and consists of gypsum-calcareous mudstones and calcaric sandstones . It is composed dominantly by silt-size (> 60%) siliceous and calcareous particles; the coarse sand fraction is almost absent, the fine sand fraction ranges from 20 to 35%, and clay ranges from 5% to 10%. Bulk mineralogical composition is quartz, muscovite, paragonite, calcite (up to ca. 30%), gypsum (up to ca. 30% in some strata), and minor amounts of smectite (< 5% of the clay fraction) [*Cantón et al.*, 2001]; the weathering of mudrock is presumably caused by the combined effects of wetting-drying and gypsum solubilisation-recrystallisation [*Solé-Benet et al.*, 1997]. Soils in the area are mainly Epileptic and Endoleptic Leptosols, Calcaric Regosols and Eutric Gypsisols [*FAO*, 1998], and the soil texture is classified as silty-loam. The piezometric level in the area oscillates between 22 and 26 m depth (data from 1985 to 2020 of the Spanish Geological Survey, IGME).

2.1.3. Biocrusts succession and vegetation

Bare soil, eroded or originated from sediment deposition, occupies a third of the territory. Another third is covered by short vascular vegetation with biocrusts in the interspaces and the rest is covered mainly by biocrusts [*Lázaro et al.*, 2000]. Different biocrust types can be distinguished and associated with stages of ecological succession [*Lázaro et al.*, 2008]: (1) physical depositional crust (PD); (2) incipient cyanobacterial (IC); (3) mature cyanobacterial (MC); (4) lichen community dominated by *Squamarina lentigera* (Web.) Poelt and *Diploschistes diacapsis* (Ach.) Lumbsch (SD); and (5) lichen community characterized by *Lararia isidiata* (Llimona) Llimona & Crespo (LI). In the SD stage, patches of mature *Cyanobacteria* (MC2) are also present. In the LI stage, lichens coexist mainly with vascular plants *Macrochloa tenacissima* (L.) Kunth, but other species such as *Salsola genistoides* Juss. ex Poir. and *Lygeum spartum* L. are also commonly found. The ecological succession is summarized in figure 2. A microsite representative of each stage

of the succession was chosen to conduct this research. The maximum distance between microsites was ca. 500 m.

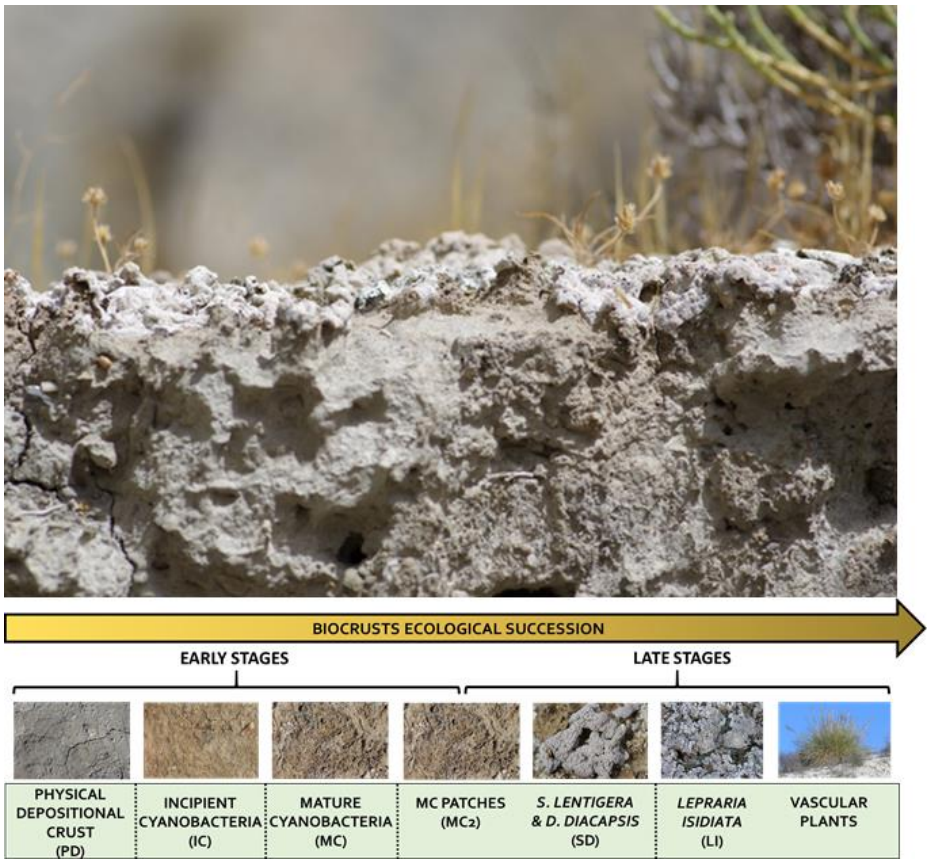

Figure 2 Schematic representation of the ecological succession in the Tabernas Desert. The upper photo is from the SD microsite.

2.2. Fundamentals

2.2.1. Operating principle of CO_2 sensors

The main results of this thesis were obtained from CO_2 measurements. As it is part of the greenhouse gases family, CO_2 absorbs infrared radiation in a characteristic wavelength and reemits it in all directions. This specific property of greenhouse gases is used by CO_2 sensors. The principle of operation of the CO_2 sensors here used is presented in figure 3. The gas penetrates the measurement chamber by diffusion through a porous

membrane. Inside this chamber, infrared radiation is emitted by a lamp and reflected by a mirror towards an infrared detector that measures the light intensity at a wavelength determined by a Fabry–Pérot interferometer (FPI) and a band pass filter. The FPI is tuned electrically so that its measurement wavelength is changed between the CO_2 absorption band and a reference band (i.e. where no absorption occurs, in order to get a reference signal). When the passband of the FPI coincides with the absorption wavelength of CO_2, the detector detects a decrease in the light transmission. The ratio of these two signals, one at the absorption wavelength and the other at the reference wavelength, gives the fraction of light absorption. This absorption is calculated internally by the sensor using the Beer-Lambert law. Then, the sensor uses the absorption value to calculate the CO_2 number density and finally outputs the CO_2 molar fraction from the ideal gas law.

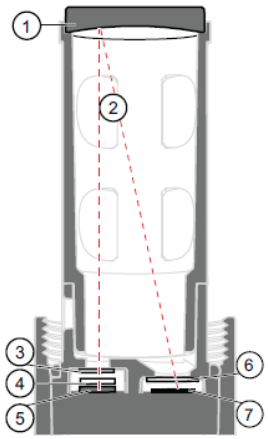

Figure 3. Operating principle of a GMP252 CO_2 sensor (Vaisala, Vantaa, Finland). (1) Mirror, (2) light absorbed by CO_2, (3) Hermetic window, (4) Fabry–Pérot interferometer, (5) Light source, (6) Hermetic window, (7) Infrared detector. The figure is taken from the sensor user guide.

In order to improve accuracy, CO_2 measurements can be compensated for temperature, pressure, relative humidity (RH) and O_2 concentration. In the chapter one of this thesis, the CO_2 sensor that was used (MH-Z16, Zhengzhou Winseng Electronics Technology Co., Zhengzhou, China) internally applied compensation for real-time temperature. The CO_2 measurement was additionally corrected for real-time pressure and dilution due to water vapor [*Hupp*, 2011] in post-processing as:

$$\chi_{\mathrm{c\ (corrected)}} = \chi_{\mathrm{c\ (measured)}} \frac{P_0}{P} (1 - \chi_{\mathrm{h}})^{-1} \qquad (1)$$

where χ_c is the CO_2 molar fraction (ppm), P is the ambient pressure (kPa), P_0 is the reference pressure (101.325 kPa) and χ_h is the water vapor molar fraction (mol) calculated as:

$$\chi_{\mathrm{h}} = \frac{P_{\mathrm{h}}}{P} \qquad (2)$$

where P_h is the partial pressure of water vapor (kPa), obtained as:

$$P_{\mathrm{h}} = P_{\mathrm{s}}\, RH \qquad (3)$$

where RH is the relative humidity (%) and P_s is the saturation vapor pressure calculated according to Buck [1981]:

$$P_{\mathrm{s}} = 0.61365\ \mathrm{e}^{\frac{17.502\,T}{240.97+T}} \qquad (4)$$

where T is the air temperature (°C).

In the chapter two of this thesis, the CO_2 sensor that was used (GMP252, Vaisala, Vantaa, Finland) internally applied compensation for real-time temperature, a fixed value of relative humidity and a fixed value of O_2 concentration. According to the manufacturer, in practice, when CO_2 is measured at the ppm level, RH and O_2 compensations have a very small effect on the accuracy of the measurements.

2.2.2. Soil water extractors

A large variety of soil water extractors exist to sample the vadose zone, with different operating principles and materials; their choice depends on criteria such as the required spatial representativeness, temporal resolution, installation effort, maintenance, and cost expense [*Weihermüller et al.*, 2007]. Porous ceramic extractors are the most universally used tools to extract soil water; they offer the advantages of being relatively easy to install compared to other sampling devices, causing only limited disturbance of the soil profile, being cost-effective and benefiting from a wide knowledge due to their extensive use [*Curley et al.*, 2011]. Therefore, in this study, porous ceramic extractors (1910PL06; Soilmoisture Equipment Corp., CA, USA) were

used. The selected extractors have the additional advantage to comply with the ASTM D4696-92 (2000) standard and have a “zero dead volume”, meaning that there is limited space for collecting water samples inside the sampler itself. That is an important feature as a reduced air volume in the sampling chamber limits pH errors that could otherwise compromise the determination of specific mineralogical controls on soil solution composition [*Suarez*, 1986, 1987]. Another important parameter to consider was the air entry value (AEV) of the porous material. The AEV is the pressure at which air will break through a wetted pore channel. In order to avoid air to bubble inside the extractor, the AEV should be greater than the vacuum pressure applied to extractor. The AEV is related to the pore size of the material [*Fredlund et al.*, 2012] as:

$$\mathrm{AEV} = \frac{2T_s}{R_s} \qquad (5)$$

where T_s is the surface tension of the contractile skin or the air-water interface (e.g. T_s = 73.75 mN/m at 20 ◦C), R_s is the radius of the maximum pore size (m). The soil water samplers were chosen to have an AEV of 100 kPa as this value was greater than the vacuum pressure that would be applied to the soil, i.e. 50 kPa. The use of higher vacuum pressure in order to speed up the water flow is not recommendable as it could favor clogging of the sampler pores.

2.2.3. Carbonate reactivity

In soils, carbonates are most commonly present as calcium carbonate in the form of calcite ($CaCO_3$). To a lesser extent, dolomite ($CaMg(CO_3)_2$) can also be found but is less reactive, with a dissolution rate approximately 100-fold lower. In soils, calcite undergo dissolution and precipitation processes that can be summarized according to the following reversible reaction:

$$CaCO_{3\,(s)} + H_2O_{\,(l)} + CO_{2\,(g)} \leftrightarrow Ca^{2+}{}_{(aq)} + 2HCO_3{}^-{}_{(aq)} \qquad (6)$$

The dissolution of calcite (from left to right) or the direct dissolution of CO_2 in water produces dissolved inorganic carbon (DIC) species (H_2CO_3, HCO_3^- or CO_3^{2-}) in proportions that depend on pH. The effect of pH on the proportion of dissolved carbonate species is illustrated in Figure 4. The reaction (6) reaches a dynamic equilibrium (or steady state) when precipitation and dissolution rates are equal and therefore, compensate.

According to the Le Châtelier principle, in response to a change in conditions (concentration, temperature, volume, or pressure), the position of the equilibrium will move in such a way as to counteract the change. For example, if CO_2 is added to the system, the reaction will move to the right (i.e. towards $CaCO_3$ dissolution) so that CO_2 concentration decreases again.

In practice, in soils, equilibrium is rarely met. Disequilibrium between the solid carbonates and liquid phase can almost always be expected for soil-water systems, especially when equilibrium is approached from supersaturation [1], due to the presence of dissolved organics which inhibit precipitation [*Loeppert & Suarez*, 1996]. In addition, biological effects (e.g. respiration) or chemical reactions (e.g. proton producing or consuming reactions) also may cause disequilibrium between the liquid and gas phases [*Suarez*, 1995].

The rates of precipitation and dissolution of calcite and more generally of minerals increase with the mineral surface area. Therefore, this parameter is critical to model mineral dynamics [e.g. *Kräutle et al.*, 2021; *Noiriel et al.*, 2012; *Suarez and Šimůnek*, 1997). In soils, a portion of carbonate surface is coated with organic matter or oxides and thus is not reactive [*Lebron & Suarez*, 1996; *Lebron & Suarez*, 1998; *Suarez & Wood*, 1984]. Therefore, the reactive surface area is a more realistic parameter affecting the precipitation-dissolution dynamics of calcite in soils.

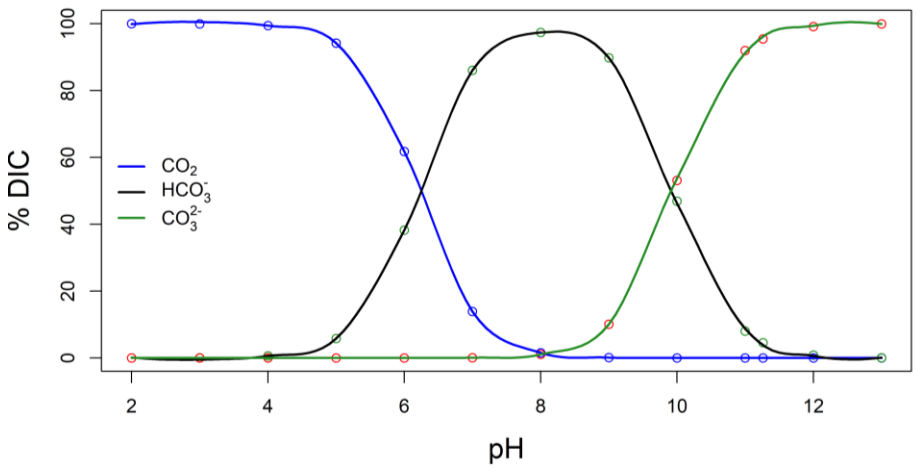

Figure 4 Proportion of dissolved inorganic carbon species as a function of pH. The simulation was performed with the PHREEQC software

[1] Soil solution is saturated with respect to calcite if calcite has dissolved until it is unable to dissolve anymore. Soil solution is supersaturated with respect to calcite when it contains more (undissolved) calcite than the saturated solution (i.e. precipitation is favored over dissolution). Soil solution is undersaturated when calcite dissolves completely (i.e. dissolution is favored over precipitation).

2.3. Applied methodology

2.3.1. Measuring CO_2 fluxes with portable soil chambers

Soil chambers are the most widely used technique to measure soil CO_2 fluxes (F_c). Several different types of chambers exist [*Pumpanen et al.*, 2004]. In this research, a non-steady-state through-flow chamber (EGM-4, PP-system, Amesbury, MA, USA), also known as closed dynamic chamber, was used to measure F_c. To this end, a PVC collar of 0.0069 m^2 surface area was inserted into the soil. We took the precaution of inserting gently the collar in order to limit soil and crust disturbance and measurements were started one month later to allow for the recovery of soil surface. During measurements, the portable chamber was placed over the soil collar and the flux was calculated by measuring the rate of linear change in CO_2 molar fraction with an infrared CO_2 sensor. The water vapor molar fraction, ambient pressure and air temperature inside the chamber were measured at the same time by the instrument. All variables were measured every 3 s over 120 s. The F_c was measured regularly (during 14 days over two years) and measurements were irregularly spaced in time, trying to cover the natural range of θ_w variability. During post-processing, the measured CO_2 fractions were corrected for temperature, pressure and dilution due to water vapor as:

$$\chi_{\mathrm{c\ (corrected)}} = \chi_{\mathrm{c\ (measured)}} \frac{T}{T_0} \frac{P_0}{P} (1 - \chi_{\mathrm{h}})^{-1} \quad (7)$$

where T is the air temperature inside the chamber (K) and T_0 is the reference temperature (273.15 K), P is the measured pressure and P_0 is the reference pressure (101.325 kPa).

Then, the soil CO_2 flux was calculated based on the ideal gas law, according to Pérez-Priego et al. [2015]:

$$F_{\mathrm{c}} = \frac{\partial \chi_{\mathrm{c}}}{\partial t} \frac{(P-e)V}{RT} \quad (8)$$

where F_c is the soil CO_2 flux (µmol m^{-2} s^{-1}), $\frac{\partial \chi_{CO2}}{\partial t}$ is the slope of the change in the corrected CO_2 molar fraction over time (µmol mol s^{-1}), the term *(P – e)* refers to the partial pressure of dry air, P is the ambient pressure (Pa), e is the partial pressure of water vapor (Pa), V is the total volume of the chamber and

collar, R is the ideal gas constant (8.314 m^3 J mol^{-1} K^{-1}), and T is the air temperature.

The F_c measured with portable soil chambers were used in the Chapter 2, Chapter 3, and Chapter 4 of this thesis.

2.3.2. The gradient method

The soil CO_2 flux can be calculated as a diffusive flux from the gradient in CO_2 molar fraction between soil and atmosphere, namely by the gradient method. This method has gained popularity in the last few years due to the recent development of solid-state sensors allowing to measure greenhouse gases fluxes in the soil-atmosphere continuum [*Maier & Schack-Kirchner*, 2014; *Sánchez-Cañete & Kowalski*, 2014]. It presents several advantages over manual soil chamber measurements or manual gas sampling: (1) it allows continuous measurements at high frequency; (2) it limits or avoids disturbance of the CO_2 molar fraction gradient between soil and atmosphere, changes in the chamber headspace and microclimate; (3) it provides further understanding on belowground CO_2 production or consumption; (4) it requires low effort of maintenance after installation as measurements are automated; (5) CO_2 sensors have a low-cost compared to chamber systems, allowing to combine temporal resolution with spatial representativeness. The gradient method has usually been employed to estimate CO_2, CH_4 and N_2O diffusive fluxes [*Maier & Schack-Kirchner*, 2014; *Sánchez-Cañete & Kowalski*, 2014]. However, soil-atmosphere diffusive fluxes of water vapor (F_h) have seldom been estimated and most studies were limited to laboratory experiments [e.g. Jabro and Jabro, 2008; Rao and Rekapalli, 2020; Reyzabal and Bazán, 1992]. Only one study estimating F_h *in-situ* was found in the literature [*Bittelli et al.*, 2008].

The gradient method is based on the main assumption that molecular diffusion is the dominant gas transport process between soil and atmosphere, a condition that is generally considered to be fulfilled both for CO_2 [*Šimůnek & Suarez*, 1993] and water vapor [*Liu et al.*, 2020]. Therefore, the soil-atmosphere CO_2 and water vapor fluxes can be estimated from the first Fick´s law of molecular diffusion:

$$F = -\rho_a k_s \frac{d\chi}{dz} \qquad (9)$$

where F is the soil-atmosphere flux (mmol m^{-2} s^{-1} and µmol m^{-2} s^{-1} for F_h and F_c, respectively), ρ_a is the average molar density of air (mol m^{-3}), dχ is the gradient in water vapor or CO_2 molar fraction (mmol mol^{-1} and µmol mol^{-1}) between atmosphere and soil, dz is the vertical gradient between atmosphere and soil (m), and k_s is the diffusion coefficient or empirical soil transfer coefficient (m^2 s^{-1}).

As k_s is a major source of uncertainty in the diffusive flux calculation, it is recommended to apply a site-specific calibration to improve the accuracy of the gradient method [*Sánchez-Cañete et al.*, 2017]. Therefore, the k_s of CO_2 fluxes was calibrated from 225 chamber measurements by rearranging eq. 9:

$$k_s = -\frac{F_{soil}\,dz}{\rho_a\,d\chi} \qquad (10)$$

where F_{soil} values were obtained from the soil chamber measurements.

Since k_s is generally considered to depend on the diffusion coefficient of CO_2 in free air and the air-filled pore space (i.e. the difference between total porosity and soil water content), then k_s was modeled as a function of these variables. The following model provided the best fit to the data and therefore was retained for the CO_2 flux estimation:

$$k_s = D_a a e^{b\theta_a} \qquad (11)$$

where θ_a is the air-filled pore space, a and b are empirical coefficients obtained by non-linear least squares regression, and D_a is the diffusion coefficient of CO_2 in free air calculated according to Jones [1992]:

$$D_a = D_{a,0}\left(\frac{T}{T_0}\right)^{1.75}\left(\frac{P_0}{P}\right) \qquad (12)$$

where $D_{a,0}$ $1.47 \cdot 10^{-5}$ m^{-2} s^{-1}, T is the measured soil temperature, P the measured atmospheric pressure (Pa), T_0 is 293.15 K and P_0 is 101 325 Pa.

For the estimation of water vapor fluxes (F_h), since no standardized procedures exist yet to calibrate k_s, the coefficient was calculated according to the only *in-situ* study found in the litterature [*Bittelli et al.*, 2008]:

$$k_s = D_a \beta \theta_a^m \qquad (13)$$

where D_a is the diffusion coefficient of water vapor in free air calculated according to Jones [1992] using $D_{a,0}$ of water vapor ($2.4 \cdot 10^{-5}$ m^{-2} s^{-1} according

to Campbell and Norman [1998]), and β and m are constants that account for the shape of soil particles. Values of 0.9 and 2.3 were used for the later parameters, respectively, as according to Bittelli et al. [2015], those values are good approximations for undisturbed samples.

For comparative purpose of the resulting F_h, k_s was also calculated according to Xu et al. [1992] as:

$$k_s = D_a \frac{\theta_a^{2.58}}{\varphi^2} \qquad (14)$$

where φ is the soil porosity.

2.3.3. Continuous environmental measurements

Continuous measurements of soil and above-surface variables were conducted during two years (from December 2017 to December 2019). At 5 cm depth, the CO_2 molar fraction (χ_c) of soil was measured mainly by GMP252 probes (accuracy of ±2% of reading in the range 0-10000 ppm) and some measurements were completed with GMM222 transmitter modules (accuracy of ± (1.5% of the range + 2% of reading in the range 0-10000 ppm)) (Vaisala, Vantaa, Finland).

The soil water content (θ_w) was measured by EC-5 and 5TM sensors (Meter Group, Pullman, WA, USA). The θ_w sensors were calibrated according to the general equation for mineral soils provided by the manufacturer. This equation should apply for all mineral soils up to an electrical conductivity (EC) of 8 dS m^{-1} in saturation extract according to the instructions of the manufacturer. Preliminary tests showed that most soils at our study site had an EC < 1 dS m^{-1} in 1:5 soil to water ratios. Based on those values, it was reasonable to expect that EC in saturation extracts would not exceed the recommended threshold [*Kargas et al.*, 2020]. The 5TM sensors also measured the soil temperature (T_s); T_s measurements were also replicated with thermistors (108, Campbell Scientific, Logan, UT, USA; hereafter CSI).

All such measurements were performed within each stage of biocrusts succession, in triplicates. Since mature cyanobacterial patches (MC2) were also present within the SD site and lichens in the LI site covered the interstices between vascular plants, for comparison purpose, measurements were also performed in MC2 (in duplicate) and under plants (*Macrochloa tenacissima*

(L.) Kunth, *Salsola genistoides* Juss. ex Poir. and *Lygeum spartum* L.). Since the biotic and abiotic contributions to soil CO_2 dynamics are respectively expected to decrease and increase with depth, a χ_c sensor was also installed at 45 cm in depth (close to bedrock) in the MC site, in order to provide information about those contributions.

Within each site, air temperature (T_a) and atmosphere relative humidity at 30 cm aboveground were measured by a S-THB-M00x Smart Sensor (Onset Computer Corporation, Bourne, MA, USA; hereafter Onset); the surface temperature (T_{surf}) was measured by a S-TMB-M0xx Smart Sensor (Onset) and the photosynthetically active radiation (PAR) by a S-LIA-M003 Smart Sensor (Onset); precipitation was measured by a Rain-O-Matic-Pro tipping-bucket rain gauge of 0.25 mm resolution (Pronamic, Ringkoebing, Denmark) at 1.5 meters above the ground surface.

At 2 cm aboveground, the χ_c, of atmosphere (same sensors as soil χ_c) was monitored in the PD and SD microsites, and atmospheric pressure was monitored in the LI microsite. The relative humidity in soil at 5 cm depth and in atmosphere in contact with soil (RH_s and RH_a, respectively) were measured by iButton® DS1923 logger (accuracy of ±5% of reading in the range 0-100%) (Maxim Integrated, San Jose, CA, USA); those measurements were started a bit later (in February, 2018). The rain gauge was connected to an on–off Hobo Event data logger (Onset) and all other variables were measured every 30 seconds and stored as 20-minute averages by data-loggers CR1000 (CSI) and H21 (Onset).

A summary of the continuous environmental measurements and associated instruments is provided in Table 1, and the experimental design containing the most important measurements over biocrusts succession is summarized in Fig. 5. The database generated from those measurements was used in Chapter 2, Chapter 3 and Chapter 4 of this thesis.

Table 1 Continuous environmental measurements and associated instruments

Measurement	Height (m)	Variable	Instrument(s)	Manufacturer
Atmospheric CO_2 molar fraction	0.02	χ_c	GMP252	Vaisala
Soil CO_2 molar fraction	-0.05	χ_c	GMP252 GMM222	Vaisala
Soil water content	-0.05	θ_w	EC-5 5TM	Meter Group
Soil temperature	-0.05	T_s	5TM Thermistors 108	Meter Group Campbell Scientific
Soil relative humidity	-0.05	RH_s	iButton® DS1923 logger	Maxim Integrated
Atmospheric relative humidity	0	RH_a	iButton® DS1923 logger	Maxim Integrated
	0.3	RH_a	S-THB-M00x Smart Sensor	Onset Computer Corporation
Atmospheric temperature	0.3	T_a	S-THB-M00x Smart Sensor	Onset Computer Corporation
Surface temperature	0	T_{surf}	S-TMB-M0xx Smart Sensor	Onset Computer Corporation
Photosynthetically active radiation	0	PAR	S-LIA-M003 Smart Sensor	Onset Computer Corporation
Precipitation	1.5	-	Rain-O-Matic-Pro tipping-bucket rain gauge	Pronamic

All variables were measured every 30 seconds and stored as 20-minute averages by data-loggers CR1000 (Campbell Scientific) and H21 (Onset), except the rain gauge which was connected to an on–off Hobo Event data logger (Onset).

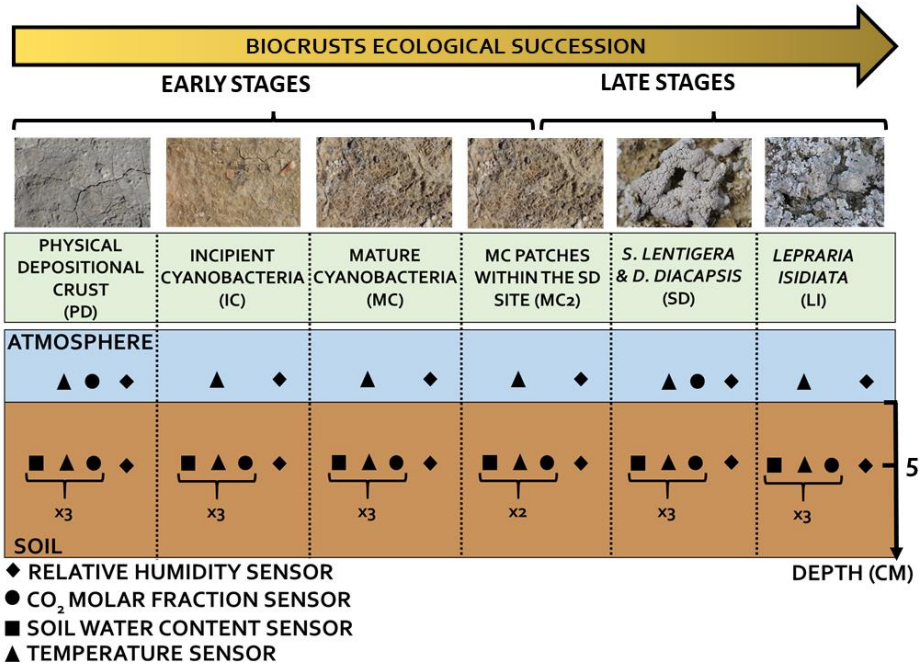

Figure 5 Summary of the experimental design. In the LI site, since lichens covered the interstices between vascular plants, for comparison purpose, measurements of the soil CO_2 molar fraction, soil water content and soil temperature were also performed under plants.

2.3.4. Preparation, installation, and operation of soil water samplers

Since the production process of ceramic samplers leaves over contaminants that can be released in the soil solution, they have to be cleaned prior to installation by flushing them with dilute acid and repeatedly rinsed with deionized water [*Curley et al.*, 2011]. In this study, 0.01M HCl (pH ~ 2) was used for flushing and then distilled water for rinsing until the pH of water flowing through the sampler stabilized.

The samplers were inserted vertically in the soil at 5 cm depth after previous wetting of soil surface and using a soil auger provided by the manufacturer, to ensure a good contact between the soil and the extractor. In order to study specifically the abiotic component of soil CO_2, extractors were installed in two microsites both covered by cyanobacterial biocrust but

differing in their $CaCO_3$ content (MC and MC2). Among each microsite, samplers were installed in triplicates.

The design of the water sampling system is presented in figure 6. The extraction procedure of Suarez [1987, 1986] was used to minimize pH errors; to this end, in addition to the small volume of the extractor, thin PVC tubing (0.8 mm inner diameter) was used to further minimize the volume of the system. Besides, applying a vacuum of 50 kPa to the samplers, the sampling vials were flushed with at least three times their volume of soil water before collection of the water samples.

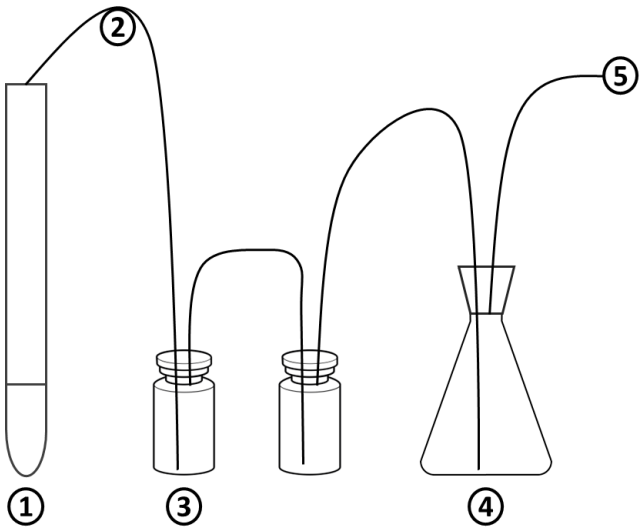

Figure 6 Water extraction system. (1) "Zero dead volume" soil water extractor with porous ceramic tip; (2) tubing (0.8 mm inner diameter); (3) sampling vial (10 mL); (4) reservoir (100 mL); (5) output to vacuum (-50 kPa).

2.3.5. Improvement of the determination of carbonate chemistry in the soil solid and aqueous phase

In natural soil systems, the dissolution time of calcite is generally on the order of 0.5 to 3 days [*Loeppert & Suarez*, 1996]. According to eq. 6, it is enhanced by CO_2 due its acidifying effect on soil solution. In the laboratory, the dissolution time can be greatly reduced to force the complete dissolution of $CaCO_3$ within minutes by the addition of an acid. This reaction can be summarized as [*Loeppert & Suarez*, 1996]:

$$\mathrm{CaCO_{3\,(s)}} + \mathrm{H^{+}}_{(aq)} \leftrightarrow \mathrm{Ca^{2+}}_{(aq)} + \mathrm{CO_{2(g)}} + \mathrm{H_2O_{(l)}} \qquad (15)$$

Compared to the natural calcite dissolution (eq. 6), during this enhanced reaction, calcite dissolution produces gaseous CO_2 instead of DIC species. That is due to the equations of CO_2 equilibrium in water:

$$CO_{2(g)} \leftrightarrow CO_{2(aq)} \quad (16)$$

$$CO_{2(aq)} + H_2O_{(l)} \leftrightarrow H_2CO_{3\ (aq)} \quad (17)$$

$$H_2CO_{3\ (aq)} \leftrightarrow H^+_{(aq)} + HCO_3^-{}_{(aq)} \quad (18)$$

$$HCO_3^-{}_{(aq)} \leftrightarrow H^+_{(aq)} + CO_3^{2-}{}_{(aq)} \quad (19)$$

In an acidic medium, the presence of protons shifts the equilibria towards CO_2 degassing. Therefore, the gaseous CO_2 released from carbonate dissolution can be used to quantify the amount of calcite. Other methods exist to quantify the calcite content in soils but methods involving determination of CO_2 have usually been preferred, since in the absence of decomposition of organic matter, the measurement of CO_2 production provides an absolute measure of carbonate [*Loeppert & Suarez*, 1996]. However, current available methods measure only indirectly CO_2 production (e.g. with manometric, volumetric or gravimetric systems). At the beginning of this thesis, there was so far no procedure that measured directly the increase in CO_2 molar fraction during the reaction of either solid carbonates or aqueous carbonate species with acid. That was therefore the purpose of Chapter 1 of this thesis.

2.4. Data analysis

2.4.1. Gap Filling

Gaps in *in-situ* environmental time series are unavoidable due to several factors including power or instrument failure, maintenance or quality check. However, continuous data are often necessary to calculate cumulative fluxes over defined periods or in order to use particular statistical techniques. The gap-filling of the dataset is therefore required prior to the application of these procedures. The choice of an appropriate gap-filling technique is important to limit uncertainty in fluxes estimation or bias in statistical inference.

Several techniques exist to fill gaps in datasets. Traditional statistical techniques, such as mean/mode and regression, have been applied for this purpose during several decades while machine learning techniques have been emerging and became increasingly popular in the last 10 years [*Lin & Tsai*, 2020]. Machine learning is a data-driven approach in which algorithms use statistics to find patterns in large amounts of data and can improve automatically through experience. Among machine learning methods, imputation of missing values based on random forests was tested prior to this thesis. To this end, the package "missForest" of the R software was used to impute missing values in a similar dataset from a nearby ecosystem that also contained continuous measurements of CO_2 fluxes replicated in space. This algorithm was chosen because it was able to deal with mixed-type data and as a non-parametric method, it was particularly effective to deal with complex interactions and non-linear data structures [*Stekhoven & Bühlmann*, 2012]. The good performance of the algorithm was verified by generating artificial gaps in the dataset; as it was observed than "missForest" performed better than other imputation methods, the algorithm was used for gap-filling [*Lopez-Canfin et al.*, 2018]. Further information about random forests can be found in Breiman [2001].

More recently, other studies have confirmed that imputation of missing values based on random forests could equal or outperform other machine learning procedures [*Emmanuel et al.*, 2021; *Platias & Petasis*, 2020], including for the imputation of time series of greenhouse gases fluxes [*Huang & Hsieh*, 2020; *Irvin et al.*, 2021; *Kang et al.*, 2019; *Kim et al.*, 2020; *Mahabbati et al.*, 2021; *Yao et al.*, 2021]. Moreover, it has been reported that the performance of "missForest" was enhanced when data presented highly correlated variables [*Platias & Petasis*, 2020], a typical feature in micrometeorological datasets due to spatial correlation. Therefore, this algorithm was used again for gap-filling in Chapter 2 to 4..

2.4.2. Statistical modelling

All analyses were performed with R software *[R Core Team*, 2019]. The statistical protocol of Zuur and Ieno [2016] was followed as closely as possible to model the data. This protocol include the following steps: (1) Formulate

appropriate questions; (2) Visualize the experimental design; (3) Conduct data exploration, following as closely as possible the procedure of Zuur et al. (2010); (4) Identify the dependency structure in the data, e.g. spatial and/or temporal correlation; (5) Present the statistical model; (6) Fit the model; (7) Validate the model, i.e. check the validity of underlying assumptions and the absence of non-linear patterns in residuals; (8) Interpret the numerical output of the model; (9) Create a visualization of the model; (10) Simulate or perform cross-validation from the model.

There is an ongoing debate on whether research should rather use statistics based on a traditional frequentist approach or based on a Bayesian approach, both approaches having advantages and limitations [*Hackenberger*, 2019]. In brief, the frequentist method makes statistical inferences using only data from the current experiment. By contrast, the Bayesian approach uses previous knowledge of similar experiments encoded into a "prior", and this prior is combined with current experiment data to make a conclusion on the test. One of the main objections against frequentist hypothesis testing is the use of *p* values, because the *p* value is partly determined by data that have never been observed. Bayesian methods use no null and alternative hypotheses, but in their case the main objection is that a prior is subjective and that there is no single, prescribed and well-defined method for choosing a prior [*Hackenberger*, 2019].

In this thesis, most models were developed in a frequentist framework, using either generalized least squares (GLS) models, linear mixed effects (LME) models, non-linear least squares (NLS) models or non-linear mixed effects (NLME) models during model construction. Those models are thoroughly described by Pinheiro and Bates [2000]. For linear model construction using the frequentist approach, the protocol of Zuur et al. [2009] was followed as closely as possible whereas non-linear models were developed following the instructions of Pinheiro and Bates [2000]. In Chapter 2 of this thesis, linear models were also developed in a Bayesian framework with the R "INLA" package [*Rue et al.*, 2009; *A. F. Zuur et al.*, 2017] as it has the great advantage of allowing to model spatio-temporal dependencies that were inherent to the experimental design.

2.4.3. Geochemical modelling

Various software programs are available to model the carbonate chemistry in soils [*Suarez*, 1995]. Their choice depends on the system to model ("open" or "closed"), the objectives and the available variables. In this thesis, it was chosen to use the PHREEQC software as it is free and allows both systems to be modelled for specific purposes [*Parkhurst & Appelo*, 2011]. The "open system" corresponds to an infinite CO_2 reservoir that equilibrates with the dissolving solution (or sustained supply of CO_2). The "closed system" corresponds to the case where a given initial amount of CO_2 equilibrates with the solution and no further supply is provided [*Romero-Mujalli et al.*, 2019]. The closed system can be used for some laboratory experiments or for descriptions of the chemistry of groundwater systems [*Suarez*, 1995]. For example, it can be useful to simulate the enhancing effect of a solution pH on CO_2 dissolution. To illustrate that, solutions of varying pH were simulated to get in contact with a gas phase containing 400 ppm of CO_2 in a closed system (Figure 7).

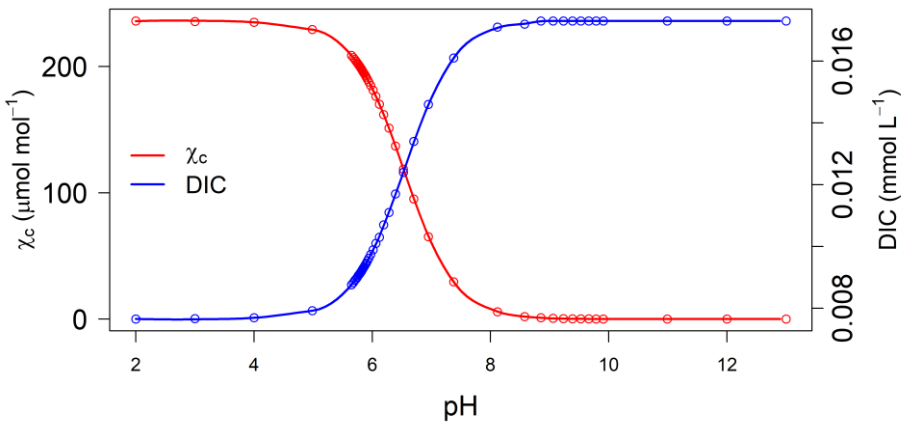

Figure 7 Effect of solution pH on CO_2 uptake in a closed system with a gas phase containing 400 ppm of CO_2, at 25°C. χ_c, gas phase CO_2 molar fraction. DIC, dissolved inorganic carbon. Simulations were performed with the PHREEQC software.

The results of the simulation indicate that CO_2 uptake increases with the pH of the solution, following a sigmoid relationship that confirms the statement according to which soils with pH > 6.5 can retain substantial amounts of CO_2 in the solution phase [*Sparling & West*, 1990]. That is because

at those values of pH, most of the dissolved CO_2 converts to HCO_3^- or CO_3^{2-} (equilibria of eq. 18 and 19 are pushed to the right). Therefore, the depletion of CO_2 allows more CO_2 to dissolve (eq. 16 and 17). However, in spite of some advantages, the "closed system" is generally unrealistic for soil systems. Since soils undergo a continuous flux of CO_2, the open system model, is a more realistic model for Earth surface conditions and thus is more commonly used.

In order to model the saturation status of soil solution with respect to a mineral, the saturation index (SI) is an informative tool. A positive SI indicates that the solution is supersaturated with respect to the considered mineral, and therefore that it may precipitate. A negative indicates that the solution is undersaturated with respect to the considered mineral, and therefore that it may dissolve. A SI equal to zero indicates that the solution is saturated and therefore in equilibrium with the mineral of interest. The SI is calculated by comparing the chemical activities of the dissolved ions of the mineral (ion activity product, IAP) with their solubility product (K_{sp}), as:

$$\mathrm{SI} = \log_{10}\left(\frac{\mathrm{IAP}}{\mathrm{K_{sp}}}\right) \qquad (20)$$

For example, the SI of calcite is equal to:

$$\mathrm{SI} = \log_{10}\left(\frac{a_{\mathrm{Ca^{2+}}} a_{\mathrm{HCO_3^-}}}{\mathrm{K_{sp}}}\right) \qquad (21)$$

where a_i denotes the ion activity of the aqueous species *i,* calculated as:

$$a_i = C_i\,\gamma_i \qquad (22)$$

where C_i is the molar concentration and γ_i is the activity coefficient of the aqueous species, calculated as:

$$\ln\gamma_i = -A{z_i}^2\left(\frac{\sqrt{I}}{1+\sqrt{I}} - 0.3I\right) \qquad (23)$$

where z_i is the ionic charge of aqueous species *i*, *A* is a constant dependent only on temperature, and *I* is the ionic strength calculated as:

$$I = \frac{1}{2}\sum_{i=1}^{n} C_i\,{z_i}^2 \qquad (24)$$

where *n* is the number of species in the solution, and C_i is the molar concentration of i^{th} present in the solution.

2.5. Summary of applied methodology and data analysis by chapter

The applied methodology and data analysis in each chapter to fulfill the objectives of the thesis can be summarized as:

- Chapter 1: (i) development of a new low-cost device to determine accurately the carbonate chemistry in the soil solid and aqueous phase, based on direct measurements of the CO_2 evolved from an acidic reaction, and (ii) fit of linear regression models on the generated data, in a frequentist framework.

- Chapter 2: (i) implementation of the gradient method with a network of environmental sensors including CO_2 sensors in soil and atmosphere to estimate the soil-atmosphere CO_2 flux over the biocrusts ecological succession, (ii) gap-filling, and (iii) fit of linear regression models on the generated data, both in a frequentist and Bayesian framework (in order to take into account spatio-temporal dependency in the data).

- Chapter 3: (i) implementation of the gradient method with a network of environmental sensors including relative humidity sensors in soil and atmosphere to estimate the soil-atmosphere water vapor flux over the biocrusts ecological succession; (ii) gap-filling, and (iii) fit of linear and non-linear regression models on the generated data, in a frequentist framework.

- Chapter 4: (i) operation of soil water extractors to analyze and model the chemistry of the soil $CaCO_3$-CO_2-H_2O system in microsites dominated by *Cyanobacteria*; (ii) gap-filling, and (iii) fit of linear regression models on the generated data, in a frequentist framework.

References

ASTM D4696-92, 2000. Standard Guide for Pore-Liquid Sampling from the Vadose Zone. West Conshohocken, PA.

Bittelli, M., Campbell, G. S., & Tomei, F. (2015). *Soil physics with Python: transport in the soil-plant-atmosphere system*. OUP Oxford.

Bittelli, M., Ventura, F., Campbell, G. S., Snyder, R. L., Gallegati, F., & Pisa, P. R. (2008). Coupling of heat, water vapor, and liquid water fluxes to compute evaporation in bare soils. *Journal of Hydrology*, *362*(3–4), 191–205. https://doi.org/10.1016/J.JHYDROL.2008.08.014

Breiman, L. (2001). Random Forests. *Machine Learning 2001 45:1*, *45*(1), 5–32. https://doi.org/10.1023/A:1010933404324

Buck, A. L. (1981). New equations for computing vapor pressure and enhancement factor. *Journal of Applied Meteorology*, *20*(12), 1527–1532.

Calvo-Cases, A., Harvey, A. M., Alexander, R. W., Cantón, Y., Lázaro, R., Solé-Benet, A., & Puigdefábregas, J. (2014). Badlands in the Tabernas basin, Betic chain. In *Landscapes and Landforms of Spain* (pp. 197–211). Springer. https://doi.org/10.1007/978-94-017-8628-7_17

Campbell, G. S., & Norman, J. M. (1998). An Introduction to Environmental Biophysics. *An Introduction to Environmental Biophysics*. https://doi.org/10.1007/978-1-4612-1626-1

Cantón, Y., Solé-Benet, A., Queralt, I., Pini, R. (2001). Weathering of a gypsum-calcareous mudstone under semi-arid environment at Tabernas, SE Spain: laboratory and field-based experimental approaches. *Catena, 44*, 111–132. https://doi.org/10.1016/S0341-8162(00)00153-3

Curley, E. M., O'Flynn, M. G., & McDonnell, K. P. (2011). The use of porous ceramic cups for sampling soil pore water from the unsaturated zone. *International Journal of Soil Science*, *6*(1), 1–11. https://doi.org/10.3923/IJSS.2011.1.11

Emmanuel, T., Maupong, T., Mpoeleng, D., Semong, T., Mphago, B., & Tabona, O. (2021). A survey on missing data in machine learning. *Journal of Big Data 2021 8:1*, *8*(1), 1–37. https://doi.org/10.1186/S40537-021-00516-9

FAO. (1998). *World reference base for soil resources* (Vol. 3). Food & Agriculture Org.

Fredlund, D. G., Rahardjo, H., & Fredlund, M. D. (2012). Unsaturated Soil Mechanics in Engineering Practice. *Unsaturated Soil Mechanics in Engineering Practice*. https://doi.org/10.1002/9781118280492

Hackenberger, B. K. (2019). Bayes or not Bayes, is this the question? *Croatian Medical Journal*, *60*(1), 50. https://doi.org/10.3325/CMJ.2019.60.50

Huang, I. H., & Hsieh, C. I. (2020). Gap-Filling of Surface Fluxes Using Machine Learning Algorithms in Various Ecosystems. *Water 2020, Vol. 12, Page 3415*, *12*(12), 3415. https://doi.org/10.3390/W12123415

Hupp, J. (2011). The importance of water vapor measurements and corrections. *LI-COR Biosciences Inc. Application Note*, *129*, 8.

Irvin, J., Zhou, S., McNicol, G., Lu, F., Liu, V., Fluet-Chouinard, E., Ouyang, Z., Knox, S. H., Lucas-Moffat, A., Trotta, C., Papale, D., Vitale, D., Mammarella, I., Alekseychik, P., Aurela, M., Avati, A., Baldocchi, D., Bansal, S., Bohrer, G., … Jackson, R. B. (2021). Gap-filling eddy covariance methane fluxes: Comparison of machine learning model predictions and uncertainties at FLUXNET-CH4 wetlands. *Agricultural and Forest Meteorology*, *308–309*, 108528. https://doi.org/10.1016/J.AGRFORMET.2021.108528

Jabro, J. D., & Jabro, J. D. (2008). Water Vapor Diffusion Through Soil as Affected by Temperature and Aggregate Size. *Transport in Porous Media 2008 77:3*, *77*(3), 417–428. https://doi.org/10.1007/S11242-008-9267-Z

Jones, H. G. (1992). *Plants and microclimate: a quantitative approach to environmental plant physiology*. Cambridge university press.

Kang, M., Ichii, K., Kim, J., Indrawati, Y. M., Park, J., Moon, M., Lim, J. H., & Chun, J. H. (2019). New Gap-Filling Strategies for Long-Period Flux Data Gaps Using a Data-Driven Approach. *Atmosphere 2019, Vol. 10, Page 568*, *10*(10), 568. https://doi.org/10.3390/ATMOS10100568

Kargas, G., Londra, P., & Sgoubopoulou, A. (2020). Comparison of Soil EC Values from Methods Based on 1:1 and 1:5 Soil to Water Ratios and ECe from Saturated Paste Extract Based Method. *Water 2020, Vol. 12, Page 1010*, *12*(4), 1010. https://doi.org/10.3390/W12041010

Kim, Y., Johnson, M. S., Knox, S. H., Black, T. A., Dalmagro, H. J., Kang, M., Kim, J., & Baldocchi, D. (2020). Gap-filling approaches for eddy covariance methane fluxes: A comparison of three machine learning algorithms and

a traditional method with principal component analysis. *Global Change Biology*, *26*(3), 1499–1518. https://doi.org/10.1111/GCB.14845

Kräutle, S., Hodai, J., & Knabner, P. (2021). Robust simulation of mineral precipitation–dissolution problems with variable mineral surface area. *Journal of Engineering Mathematics*, *129*(1), 1–26. https://doi.org/10.1007/S10665-021-10132-4

Lázaro, R., Alexander, R. W., & Puigdefabregas, J. (2000). *Cover distribution patterns of lichens, annuals and shrubs in the Tabernas Desert, Almería, Spain* (pp. 19–39). Wiley, Chichester.

Lázaro, R., Cantón, Y., Solé-Benet, A., Bevan, J., Alexander, R., Sancho, L. G., & Puigdefábregas, J. (2008). The influence of competition between lichen colonization and erosion on the evolution of soil surfaces in the Tabernas badlands (SE Spain) and its landscape effects. *Geomorphology*, *102*(2), 252–266. https://doi.org/10.1016/j.geomorph.2008.05.005

Lázaro, R., Rodrigo, F. S., Gutiérrez, L., Domingo, F., & Puigdefábregas, J. (2001). Analysis of a 30-year rainfall record (1967–1997) in semi–arid SE Spain for implications on vegetation. *Journal of Arid Environments*, *48*(3), 373–395. https://doi.org/10.1006/jare.2000.0755

Lázaro, R., Rodríguez-Tamayo, M. L., Ordiales, R., & Puigdefábregas, J. R. (2004). El clima. *Subdesiertos de Almería: Naturaleza de Cine*, 62–79.

Lebron, I., & Suarez, D. L. (1996). Calcite nucleation and precipitation kinetics as affected by dissolved organic matter at 25°C and pH > 7.5. *Geochimica et Cosmochimica Acta*, *60*(15), 2765–2776. https://doi.org/10.1016/0016-7037(96)00137-8

Lebron, I., & Suarez, D. L. (1998). Kinetics and mechanisms of precipitation of calcite as affected by PCO2 and organic ligands at 25 C. *Geochimica et Cosmochimica Acta*, *62*(3), 405–416.

Lin, W. C., & Tsai, C. F. (2020). Missing value imputation: a review and analysis of the literature (2006–2017). *Artificial Intelligence Review*, *53*(2), 1487–1509. https://doi.org/10.1007/S10462-019-09709-4

Liu, F. fei, Mao, X. song, Zhang, J. xun, Wu, Q., Li, Y. ying, & Xu, C. (2020). Isothermal diffusion of water vapor in unsaturated soils based on Fick's second law. *Journal of Central South University 2020 27:7*, *27*(7), 2017–2031. https://doi.org/10.1007/S11771-020-4427-6

Loeppert, R. H., & Suarez, D. L. (1996). Carbonate and gypsum. *Methods of Soil*

Analysis: Part 3 Chemical Methods, *5*, 437–474. https://doi.org/10.2136/sssabookser5.3.c15

Lopez-Canfin, C., Sánchez-Cañete, E. P., Serrano-Ortiz, P., López-Ballesteros, A., Domingo, F., Kowalski, A. S., & Oyonarte, C. (2018). From microhabitat to ecosystem: identifying the biophysical factors controlling soil CO2 dynamics in a karst shrubland. *European Journal of Soil Science*, *69*(6), 1018–1029. https://doi.org/10.1111/ejss.12710

Mahabbati, A., Beringer, J., Leopold, M., McHugh, I., Cleverly, J., Isaac, P., & Izady, A. (2021). A comparison of gap-filling algorithms for eddy covariance fluxes and their drivers. *Geoscientific Instrumentation, Methods and Data Systems*, *10*(1), 123–140. https://doi.org/10.5194/GI-10-123-2021

Maier, M., & Schack-Kirchner, H. (2014). Using the gradient method to determine soil gas flux: A review. *Agricultural and Forest Meteorology*, *192*, 78–95.

Noiriel, C., Steefel, C. I., Yang, L., & Ajo-Franklin, J. (2012). Upscaling calcium carbonate precipitation rates from pore to continuum scale. *Chemical Geology*, *318*, 60–74.

Parkhurst, D., & Appelo, C. A. J. (2011). PHREEQC (Version 3)—A computer program for speciation, batch-reaction, one-dimensional transport, and inverse geochemical calculations. *Water Resources Div., Denver, CO*.

Pérez-Priego, O., López-Ballesteros, A., Sánchez-Cañete, E. P., Serrano-Ortiz, P., Kutzbach, L., Domingo, F., Eugster, W., & Kowalski, A. S. (2015). Analysing uncertainties in the calculation of fluxes using whole-plant chambers: random and systematic errors. *Plant and Soil*, *393*(1–2), 229–244. https://doi.org/10.1007/S11104-015-2481-X

Pinheiro, J. C., & Bates, D. M. (2000). *Mixed-Effects Models in S and S-Plus*. Springer-Verlag New York.

Platias, C., & Petasis, G. (2020). A Comparison of Machine Learning Methods for Data Imputation. *11th Hellenic Conference on Artificial Intelligence*, *10*(2020). https://doi.org/10.1145/3411408

Pumpanen, J., Kolari, P., Ilvesniemi, H., Minkkinen, K., Vesala, T., Niinistö, S., Lohila, A., Larmola, T., Morero, M., Pihlatie, M., Janssens, I., Yuste, J. C., Grünzweig, J. M., Reth, S., Subke, J. A., Savage, K., Kutsch, W., Østreng,

G., Ziegler, W., … Hari, P. (2004). Comparison of different chamber techniques for measuring soil CO2 efflux. *Agricultural and Forest Meteorology*, *123*(3–4), 159–176. https://doi.org/10.1016/J.AGRFORMET.2003.12.001

R Core Team (2019). *R: A Language and Environment for Statistical Computing*. R Foundation for Statistical Computing. https://www.r-project.org/

Rao, S. M., & Rekapalli, M. (2020). Identifying the dominant mode of moisture transport during drying of unsaturated soils. *Scientific Reports 2020 10:1*, *10*(1), 1–9. https://doi.org/10.1038/s41598-020-61302-w

Reyzabal, M. L., & Bazán, J. C. (1992). A method for measurement of water vapor diffusion in dry soils. *Geoderma*, *53*(1–2), 105–110. https://doi.org/10.1016/0016-7061(92)90024-2

Romero-Mujalli, G., Hartmann, J., Börker, J., Gaillardet, J., & Calmels, D. (2019). Ecosystem controlled soil-rock pCO2 and carbonate weathering--Constraints by temperature and soil water content. Chemical Geology, 527, 118634.

Rue, H., Martino, S., & Chopin, N. (2009). Approximate Bayesian inference for latent Gaussian models by using integrated nested Laplace approximations. *Journal of the Royal Statistical Society: Series b (Statistical Methodology)*, *71*(2), 319–392. https://doi.org/10.1111/j.1467-9868.2008.00700.x

Sánchez-Cañete, E. P., & Kowalski, A. S. (2014). Comment on “Using the gradient method to determine soil gas flux: A review” by M. Maier and H. Schack-Kirchner. *Agricultural and Forest Meteorology*, *197*, 254–255.

Sánchez-Cañete, E. P., Scott, R. L., van Haren, J., & Barron-Gafford, G. A. (2017). Improving the accuracy of the gradient method for determining soil carbon dioxide efflux. *Journal of Geophysical Research: Biogeosciences*, *122*(1), 50–64.

Šimůnek, J., & Suarez, D. L. (1993). Modeling of carbon dioxide transport and production in soil: 1. Model development. *Water Resources Research*, *29*(2), 487–497.

Solé-Benet, A., Calvo, A., Cerda, A., Laīzaro, R., Pini, R., & Barbero, J. (1997). Influences of micro-relief patterns and plant cover on runoff related processes in badlands from Tabernas (SE Spain). *Catena*, *31*(1–2), 23–38.

Sparling, G. P., & West, A. W. (1990). A comparison of gas chromatography

and differential respirometer methods to measure soil respiration and to estimate the soil microbial biomass. *Pedobiologia*, *34*(2), 103–112.

Stekhoven, D. J., & Bühlmann, P. (2012). MissForest—non-parametric missing value imputation for mixed-type data. *Bioinformatics*, *28*(1), 112–118. https://doi.org/10.1093/bioinformatics/btr597

Suarez, D. L. (1986). A soil water extractor that minimizes CO2 degassing and pH errors. *Water Resources Research*, *22*(6), 876–880.

Suarez, D. L. (1987). Prediction of pH Errors in Soil-water Extractors Due to Degassing 1. *Soil Science Society of America Journal*, *51*(1), 64–67.

Suarez, D. L. (1995). Carbonate chemistry in computer programs and application to soil chemistry. *SSSA SPECIAL PUBLICATION*, *42*, 53.

Suarez, D. L., & Šimůnek, J. (1997). UNSATCHEM: Unsaturated water and solute transport model with equilibrium and kinetic chemistry. *Soil Science Society of America Journal*, *61*(6), 1633–1646.

Suarez, D. L., & Wood, J. D. (1984). Simultaneous Determination of Calcite Surface Area and Content in Soils 1. *Soil Science Society of America Journal*, *48*(6), 1232–1235.

Weihermüller, L., Siemens, J., Deurer, M., Knoblauch, S., Rupp, H., Göttlein, A., & Pütz, T. (2007). In Situ Soil Water Extraction: A Review. *Journal of Environmental Quality*, *36*(6), 1735–1748. https://doi.org/10.2134/JEQ2007.0218

Yao, J., Gao, Z., Huang, J., Liu, H., & Wang, G. (2021). Technical note: Uncertainties in eddy covariance CO₂ fluxes in a semiarid sagebrush ecosystem caused by gap-filling approaches. *Atmospheric Chemistry and Physics*, *21*(20), 15589–15603. https://doi.org/10.5194/ACP-21-15589-2021

Zuur, A. F., & Ieno, E. N. (2016). A protocol for conducting and presenting results of regression-type analyses. *Methods in Ecology and Evolution*, *7*(6), 636–645. https://doi.org/10.1111/2041-210X.12577

Zuur, A. F., Ieno, E. N., & Elphick, C. S. (2010). A protocol for data exploration to avoid common statistical problems. *Methods in Ecology and Evolution*, *1*(1), 3–14. https://doi.org/10.1111/J.2041-210X.2009.00001.X

Zuur, A. F., Ieno, E. N., & Saveliev, A. A. (2017). Spatial, temporal and spatial–temporal ecological data analysis with R-INLA. *Highland Statistics Ltd*, *1*.

Zuur, A., Ieno, E. N., Walker, N., Saveliev, A. A., & Smith, G. M. (2009). *Mixed effects models and extensions in ecology with R*. Springer Science & Business Media.

3. RESULTS

3.1. CHAPTER 1

Development of a new low-cost device to measure calcium carbonate content, reactive surface area in solid samples and dissolved inorganic carbon content in water samples

Clément Lopez-Canfin, Roberto Lázaro**,** Enrique P. Sánchez-Cañete

Published in *Methods in Ecology and Evolution*

Lopez-Canfin, C., Sánchez-Cañete, E. P., & Lázaro, R. (2021). Development of a new low-cost device to measure calcium carbonate content, reactive surface area in solid samples and dissolved inorganic carbon content in water samples. *Methods in Ecology and Evolution*. https://doi.org/10.1111/2041-210X.13579

Device registered the 27/05/2021 in the Spanish Office of Patents and Trademarks as Utility Model (n° ES1262569).

Abstract

1. Estimates of soil carbonate dynamics are still very scarce, despite their importance in the global carbon budget. Geochemical models used to estimate carbonate precipitation-dissolution rates require important inputs including carbonate content and calcite reactive surface area in soil as well as dissolved inorganic carbon (DIC) content in soil solution. However, most methods currently available to accurately measure these parameters can be time consuming and/or often require expensive laboratory equipment.

2. To tackle this problem, we aimed to develop a sensitive device to measure these variables at low cost and with little time investment. By taking advantage of the recent development of low-cost CO_2 sensors and microcontrollers, a low-cost and easy-to-mount analyzer was developed based on direct measurements of CO_2 evolved during an acidic reaction.

3. The new instrument proved to be sensitive, accurate, precise and able to quickly perform the analyses. It was therefore used in a pilot experiment on the inorganic component of CO_2 flows from crusted semi-arid soils, and to evaluate the variation in DIC content through a spring-cave-downstream river water continuum.

4. The device could facilitate these analyses for scientists from different fields since it can potentially analyze any solid or aqueous sample.

3.1.1. Introduction

The current rise in atmospheric CO_2 and temperature as well as the modification of precipitation patterns could affect the precipitation-dissolution dynamics of soil carbonates, potentially altering both the inorganic and recalcitrant organic carbon (bounded to carbonates) storage capacity of soils and modifying the global carbon balance. It is thus urgent to assess the sensitivity of soil carbonates to climate change by monitoring their precipitation-dissolution dynamics.

Geochemical models used to estimate carbonate precipitation-dissolution rates require important inputs including the carbonate content and reactive surface area (RSA) in soil as well as the dissolved inorganic carbon content (DIC) in soil solution [*Suarez*, 1995; *Suarez & Šimůnek*, 1997]. However, most methods currently available to accurately measure these parameters can be time consuming and/or often require expensive laboratory equipment [*Del Campillo et al.*, 1992; *Kindler et al.*, 2011; *Kristl et al.*, 2016; *Rounds & Wilde*, 2012].

By contrast, the pressure calcimeter has proven to be an accurate, simple and rather inexpensive instrument for measuring carbonate content and calcite RSA in soils [*Suarez & Wood*, 1984]. It measures with a manometer/pressure transducer the CO_2 evolved from the reaction of soil carbonates with an acid. Nevertheless, the cost of digital manometers/pressure transducers and dataloggers can still be substantial. In addition, although methods involving direct determination of CO_2 have been recommended for their accuracy [*Loeppert & Suarez*, 1996], there is so far no procedure that measures directly the increase in CO_2 molar fraction (χ_{CO2}) during the reaction of either solid carbonates or aqueous carbonate species with acid.

The objective of this study was to develop a sensitive device based on the direct measurement of χ_{CO2}, to measure $CaCO_3$ equivalent (CCE) content, calcite RSA in soil and DIC content in water at low cost and low time investment. We examined the behavior of the new instrument in a pilot experiment on the inorganic component of CO_2 flows from crusted semi-arid

soils, and to evaluate the variation in DIC content through a spring-cave-downstream river water continuum.

We assumed that the manometric procedure could be improved by the recent development of low-cost CO_2 sensors and microcontrollers [e.g. *Greenspan et al.*, 2016; *Harmon et al.*, 2015; *Heger et al.*, 2020], and adapted in order to also measure DIC. The new device was used to test the following research hypotheses: (1) the calcite specific surface area (SSA, calcite RSA per weight of calcite) should increase over the ecological succession of biocrusts due to a gradual increase in small-size secondary carbonates during soil development; (2) the colonization of the soil by lichens and plants should decrease the CCE due to their ability to enhance mineral weathering; (3) in a spring-cave-downstream river continuum, the DIC content should increase progressively due to the enhanced dissolution of CO_2 in CO_2-rich caves, combined with the accumulation of aqueous carbonate species during $CaCO_3$ weathering.

3.1.1.1. Device design and set-up

The device design and working principle is presented in Fig. 1. Three wide-mouth jars with flat bottoms are used as reaction, desiccation and measurement vessels; jars have volumes of 0.72 L, 0.25L and 1L, respectively. For measuring DIC, a smaller reaction vessel (0.125 L) is used instead. In the cap of every jar, two holes are drilled to attach hose connectors. Another hole is drilled in the cap of the reaction vessel to attach a two-way acid-resistant stopcock. In the cap of the measurement vessel, two additional holes are drilled, to attach a nondispersive infrared CO_2 sensor (MH-Z16, Zhengzhou Winseng Electronics Technology Co., Zhengzhou, China) that outputs χ_{CO2} in the range 0-50,000 ppm (version Gravity UART, DFRobot, Shanghai, China), and a sensor that measures temperature, relative humidity and pressure (BME280, Bosch, Gerlingen-Schillerhöhe, Germany). In the desiccation vessel, a thin layer of desiccant, in our case Drierite (W. A. Hammond DRIERITE, OH, USA) is added in order to limit relative humidity increase during the reaction. The vessels are connected with tubing. A diaphragm pump (SP 200 EC-LC, Schwarzer Precision, Essen, Germany) ensures airflow in a closed loop. A

liquid-crystal display (LCD) shows sensor information in real time. System control and datalogging on an SD card are ensured by a microcontroller (Arduino Uno Rev3, Arduino, Ivrea, Italy) coupled to a datalogger shield (Adafruit Industries, NY, USA). Measurements are recorded every 5 seconds. The connection diagram is presented in Fig. 2. A good sealing of the system is essential. The total cost of the device is ca. US$ 200.

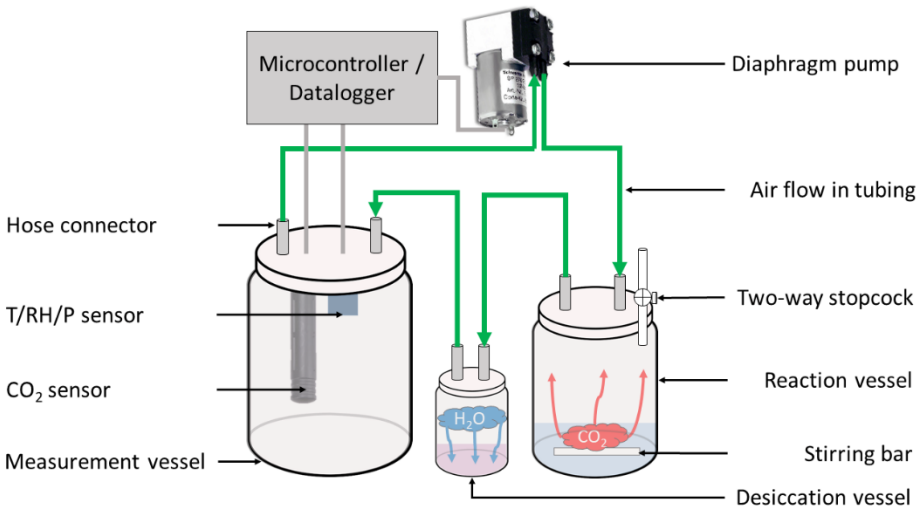

Figure 1 Device design

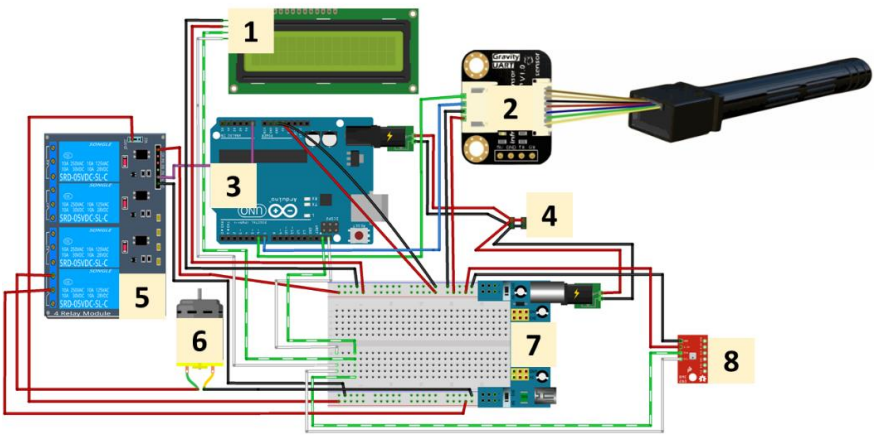

Figure 2 Connection diagram. 1, liquid-crystal display screen; 2, nondispersive infrared CO2 sensor; 3, microcontroller (coupled to a datalogger shield on it, not represented

here); 4, power supply (9-volt direct current); 5, relay module; 6, diaphragm pump; 7, breadboard power supply module (5-volt direct current); 8, sensor of temperature, relative humidity, and pressure. Black and red wires are for negative and positive current, respectively.

Calibrations and analyses should be performed at the same temperature in a temperature-controlled room and preferably by placing the reaction vessel in a water bath. While χ_{CO2} measurements are internally corrected for temperature by the sensor, they are manually corrected in post-processing for pressure and water vapor.

3.1.1.2. Calibrations

To calibrate the analysis of CCE, amounts from 0.01 to 0.40g of pure calcite are added to the reaction vessel. An amount of 0.001g is also added to test the sensitivity of the device. A large stirring bar is also introduced. After closing the vessels, the device is turned on. Once χ_{CO2} is steady, 40 mL of 3M hydrochloric acid (HCl) with 3% (by weight) ferrous chloride ($FeCl_2$) is injected inside the reaction vessel with a syringe through the stopcock and the valve is rapidly closed. The solution is stirred at 300 rpm. The reaction is complete when χ_{CO2} increase stops (after ca. 10-20 minutes). The difference between the final and initial χ_{CO2} (ΔCO_2) is plotted against $CaCO_3$ amount.

To calibrate the analysis of calcite RSA, it is first necessary to obtain pure calcite standards of known SSA. In this study, Iceland spar calcite was broken and wet-sieved through screens of 63 µm and 100 µm. The SSA of the collected fraction was measured by the N_2-BET method (0.1 m^2 g^{-1} $CaCO_3$). Different calcite amounts (from 0.001 to 0.1g) from this standard were successively added to the reaction vessel to construct a calibration curve covering the RSA range 0 – 0.01 m^2. A large stirring bar is inserted into the reaction vessel (good mixing between the sample and the reagents is crucial). Distilled water (100 mL) is added to the sample. After closing the vessels, the device is turned on and 5 mL of 1M $C_2H_3NaO_2$ is injected through the stopcock with a micropipette and the valve is closed. The solution is stirred at 300 rpm. Once χ_{CO2} is steady, 5 mL of 2M $C_2H_4O_2$ is injected into the reaction vessel. The RSA is proportional to the maximum dissolution rate of the reaction, which is achieved in few minutes. A general rule of thumb is to wait ca. 5-10 minutes or to check the CO_2 increase on the LCD screen before stopping the reaction.

After that, the χ_{CO2} curve is smoothed using a moving average with a one-minute window, the maximum slope of χ_{CO2} (δCO_2) is calculated and plotted against RSA. More details about solutions preparation for CCE and SA determinations are available in the original manometric method described in [*Loeppert & Suarez*, 1996].

To calibrate the DIC analysis, samples of commercial still water are selected according to their bicarbonate content, ensuring to cover a range of values as wide as possible. Sample dilution and evaporation can be performed to complete the range. In this study, mineral water samples containing 108, 243, 284, and 409 mg L^{-1} of DIC as HCO_3^- were used. A 5 mL water sample is introduced gently into the reaction vessel with a stirring bar and the vessel is closed. The device is turned on. Once χ_{CO2} stabilizes, 15 mL of 0.15M HCl are injected through the stopcock with a micropipette. The valve is rapidly closed and the solution stirred at 300 rpm. The reaction ends when χ_{CO2} stops increasing. The $\Delta\chi_{CO2}$ is calculated and plotted against the DIC content.

3.1.1.3. Sampling and analysis of soil and water samples

The device was tested with soil samples from the experimental site of *El Cautivo*, an area of badlands located in the Tabernas Desert (Almería, Spain) (more information about the study site is available in Section 2.1).

Soil samples were collected in triplicates from the 0-5 cm layer, randomly spaced within each successional stage as well as in mature cyanobacteria patches within the SD site (referred as MC2, hereafter) and under plants. Soils were dried at 105 ^oC and sieved to collect the < 1 mm fraction without crushing the aggregates.

Water samples of different origins (tap water, soil water, sea water, spring water, cave water, river water and water from a “rambla”, i.e. the dry bed of a temporary or transitory stream) were collected. The soil water was extracted from an intact soil core with a porous ceramic extractor (1910PL06, Soilmoisture Equipment Corp., CA, USA). Water samples were passed through a 0.22 µm filter, placed in a cooler and analyzed within few hours. The same analytical procedures as for calibrations were used to analyze soil and water samples.

Measured DIC contents were compared to values estimated by the PHREEQC software [*Parkhurst & Appelo*, 2011], using pH and alkalinity as

inputs. The pH was measured by a laboratory pH-meter (pH 50+ DHS, XS Instruments, Carpi MO, Italy) and alkalinity was determined by titration with 0.1M HCl, using the inflection point method and calculator of the United States Geological Survey (https://or.water.usgs.gov/alk/). As an additional validation procedure, the measured DIC contents in 11 soil water samples were compared to those measured according to the standard *ASTM D7573-09* [2009] using a carbon analyzer TOC-Vcsh coupled to an automatic sampler ASI-V (Shimadzu, Kyoto, Japan).

3.1.1.4. Statistical analyses

Statistical analyses were performed with R software v. 3.6.3 [*R Core Team*, 2019] and the significance level was set to 5%. The repeatability of the analyses was assessed by calculating the coefficient of variation (CV) of the replicated sample. Linear models were used to fit calibration data as well as to explore relationships between CCE, calcite RSA and calcite SSA and to test if these variables differed significantly over the ecological succession. Pairwise comparisons of means were performed after ANOVA models and models assumptions of independence, homoscedasticity, and normality were checked.

3.1.2. Results

The calibration models of CCE, calcite RSA and DIC analyses are presented in Figs 3A, 3B and 3C, respectively ($R^2 \geq 0.99$). Over 5 repetitions of the same sample, the measured CCE was on average 0.18 g g^{-1} soil, with a CV of 0.6 %. The measured calcite RSA was on average 0.0162 m^2 g^{-1} soil, with a CV of 3.2 %. The measured DIC was on average 342 mg L^{-1}, with a CV of 0.9 %. The CCE as well as RSA and SSA are presented and plotted along the ecological succession (Table 1, Fig. 4). The CCE is significantly higher in the IC, MC2, SD and LI sites, compared to the PD site ($P < 0.05$) (Fig. 4A). It tends to decrease in the late successional stages, after lichen colonization, but not significantly. Since there is a significant positive relationship between RSA and CCE ($P < 0.001$) (Fig. 5), they show similar trends over the ecological succession (Fig. 4B). A gradual trend of increase is observed over ecological succession for SSA, before dropping in plants, but differences are not significant. The measured

DIC in water samples is compared to estimated DIC from pH and alkalinity using the PHREEQC software (Table 2) and results are plotted in Fig. 6 (R^2 > 0.99). The DIC contents (as HCO_3^-) measured with the device in 11 soil water samples (ranging from 14.8 to 119.4 mg L^{-1}) differ on average by |9.5| mg L^{-1} from those measured with the commercial carbon analyzer (R^2 = 0.91).

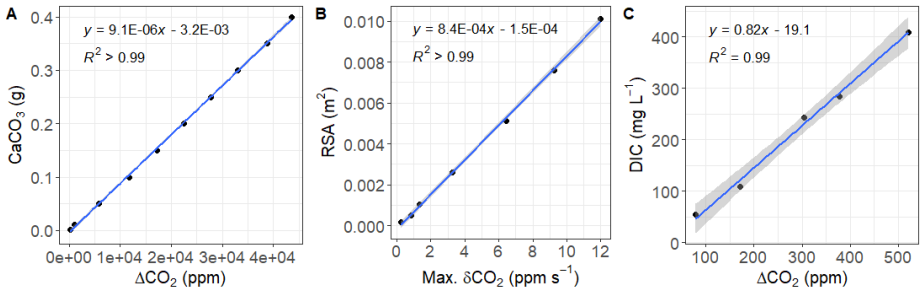

Figure 3 Calibration models (blue lines) for the determination of (A) $CaCO_3$ equivalent content; (B) reactive surface area (RSA) and (C) dissolved inorganic carbon (DIC) content. The grey area delimits the 95% confidence interval.

Table 1 Mean values ± standard deviation of the soil parameters measured with the developed device.

Succession stage	CCE	RSA	SSA
-	(g g^{-1})	(m^2 g^{-1} soil)	(m^2 g^{-1} $CaCO_3$)
PD	0.193 ± 0.012	0.017 ± 0.001	0.088 ± 0.005
IC	0.297 ± 0.020	0.025 ± 0.004	0.085 ± 0.008
MC	0.247 ± 0.012	0.021 ± 0.003	0.087 ± 0.010
MC2	0.306 ± 0.028	0.028 ± 0.003	0.092 ± 0.003
SD	0.282 ± 0.044	0.025 ± 0.003	0.090 ± 0.005
LI	0.267 ± 0.023	0.026 ± 0.004	0.098 ± 0.005
Plants	0.219 ± 0.026	0.019 ± 0.002	0.085 ± 0.005

CCE, $CaCO_3$ equivalent content; RSA, reactive surface area; SSA, specific surface area.

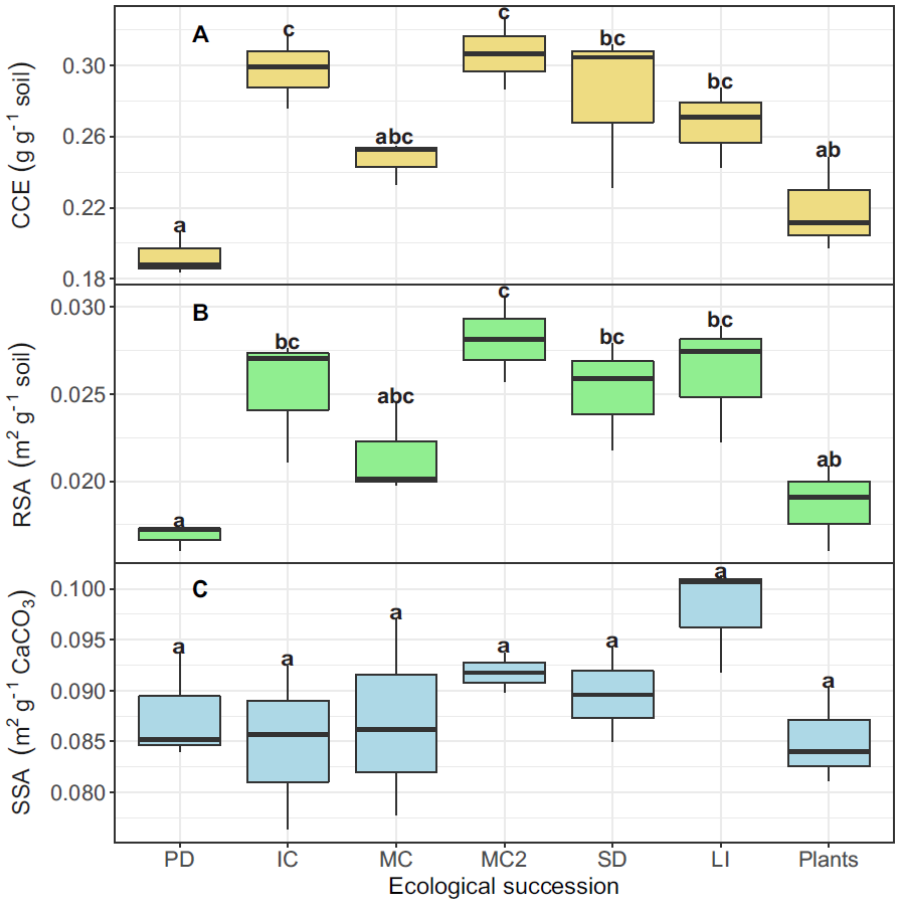

Figure 4 Evolution of the $CaCO_3$ (A) equivalent (CCE) content, (B) reactive surface area (RSA) and (C) specific surface area (SSA) over ecological succession. PD, physical depositional crust; IC, incipient cyanobacterial crust; MC, mature cyanobacterial crust; SD, lichen community characterized by *S. lentigera* and *D. diacapsis*; LI, lichen community characterized by *L. isidiata*; MC2, mature cyanobacterial patches within SD site. Boxes that do not share the same letters indicate significant differences of the means.

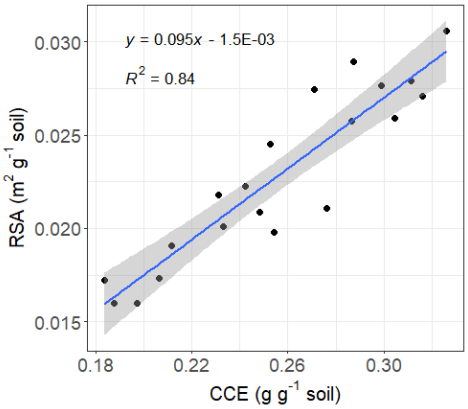

Figure 5 Linear model (blue line) of reactive surface area (RSA) as a function of $CaCO_3$ equivalent (CCE) content. The grey area delimits the 95% confidence interval.

Table 2 Comparison of DIC measured with the developed device and DIC estimated from alkalinity and pH.

Sample	Alkalinity (meq L^{-1})	pH -	Measured DIC (mg L^{-1})	Estimated DIC (mg L^{-1})
Tap water	0.67	8.09	36	41
Spring water	1.13	7.67	65	71
Soil water	2.27	8.07	140	140
Cave water	2.28	7.42	145	147
Sea water	2.43	8.06	151	149
River water	3.17	7.67	210	200
Rambla water	5.04	8.02	342	310

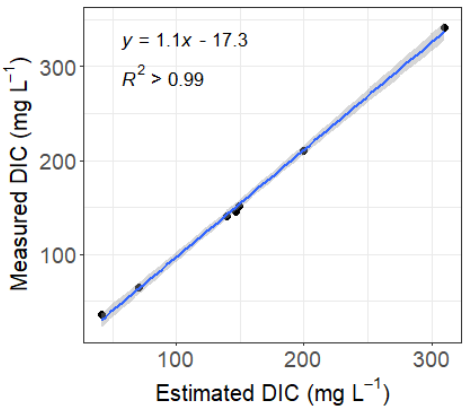

Figure 6 Linear model (blue line) of measured dissolved inorganic carbon (DIC) content as a function of estimated DIC content. The grey area delimits the 95% confidence interval.

3.1.3. Discussion

3.1.3.1. Device features

The novel system has six interesting features: (1) it determines CCE, calcite RSA and DIC with excellent accuracy, as reflected by the R^2 of the calibration models (≥0.99) (Fig. 3), the small difference between measured and calculated DIC values (Table 2) and the small difference between DIC contents measured with the device and those measured with the commercial carbon analyzer (|9.5| mg L^{-1} on average, R^2 = 0.91). (2) The system is very sensitive, and detected amounts as low as 0.001g of $CaCO_3$, 1.10^{-4} m^2 of RSA and 36 mg L^{-1} of DIC. For other demanding applications, the device sensitivity can be improved by reducing the system volume. (3) The system is precise, as reflected by the CVs of repeatability tests (0.7%, 3.2% and 0.9 % for CCE, RSA and DIC, respectively). (4) Analyses are fast, ranging from few minutes for RSA to less than half an hour for CCE and DIC (5). The device is very affordable, with a total cost of ca. US$ 200. (6) It is simple to mount and to program because it is built on Arduino, an open-source hardware and software.

3.1.3.2. Protocol considerations

The protocol used in this study for CCE and RSA determination was adapted from [*Suarez & Wood*, 1984]. Like those authors, we recommend the use of a 1-mm or 0.5-mm sieve and not to crush aggregates since this procedure would increase sample RSA. If aggregates need to be included in the analysis, they should be dispersed previously. For all analyses, a new calibration should be performed for any change in the system volume. Since the RSA analysis measures a reaction rate, the calibration of this analysis is also sensitive to changes in pump rate, stirring bar size and stirring rate, and so the user should recalibrate the device for any change in those settings.

3.1.3.3. Pilot experiment

The SSA tended to increase over the ecological succession, before dropping in plants (Table 1, Fig. 4C). This is compatible with our assumption of progressive formation of small-size pedogenic carbonates during pedogenesis. This type

of carbonate is formed by dissolution of preexisting carbonates and re-precipitation, and is common near the soil surface in dry and hot climates due the supersaturation of the soil solution with respect to calcite [*Zamanian et al.*, 2016]. However, the formation of small-size $CaCO_3$ could also be due to biomineralization by cyanobacteria from atmospheric CO_2 [*Benzerara et al.*, 2014] and/or by oxalotrophs through the oxalate-carbonate pathway [*Verrecchia et al.*, 2006]. Oxalate is abundantly produced by lichens and has been identified as the most frequent biomolecule in lichens species at this experimental site [*Miralles et al.*, 2017]. In this study, we also assumed an enhancement of carbonate dissolution by the rhizosphere. The biocrust community characterized by the lichen species *Lepraria isidiata* covers the interstices between the sampled plants. In spite of this proximity, the CCE and SSA were substantially lower in plants than in this lichen species. Although this observation is congruent with our assumption, a potential biomineralization of $CaCO_3$ from oxalate produced by *Lepraria isidiata* also could explain this difference. We also assumed that the colonization of soil by lichens should decrease the CCE since these organisms are able to enhance bedrock weathering up to 100 times [*Schwartzman & Volk*, 1989] but no conclusive patterns were detected here, probably because other important factors control mineral weathering. In general, the trends for CCE and SSA observed in this study should be completed with further microscopic observations and biogeochemical analyses after separating the crust and subcrust soil layers in order to disentangle the underlying mechanisms involved in $CaCO_3$ precipitation and dissolution. We also found a significant positive relationship between RSA and CCE content (Fig. 5).

Regarding water samples, as expected the DIC content increased following the spring-cave-downstream river continuum. This increase in DIC concentration is attributable to (1) the enhanced CO_2 dissolution in cave water, favored by high CO_2 concentrations (frequently caves exhibit values exceeding ten times the atmospheric concentration [*Sánchez-Cañete et al.*, 2013]) and lower temperatures, according to Henry´s law; (2) the enhanced weathering of $CaCO_3$ by more acidic CO_2-rich subterranean water, releasing additional carbonate species into water; and (3) the progressive removal of

pure water by evaporation, especially because samples were collected during summer.

3.1.4. Conclusion

A new device was developed to determine the CCE content and calcite RSA in soil as well as DIC in water. The device, based on the direct measurement of the evolution of χ_{CO2} during an acidic reaction, proved to be accurate, sensitive, precise and not time-consuming. Its low cost (ca. US$ 200) makes it particularly attractive where research suffers most from resource limitations. Moreover, as it is built on open-source hardware and software, it is simple to mount and program, thus holding the potential to make such measurements widespread and allowing future system improvements to be easily shared within the scientific community. The device has the potential to analyze any solid or aqueous sample by adjusting calibration ranges.

Analyses performed in our pilot experiment seem to support the assumption of a gradual increase in small-size secondary carbonates over biocrust succession but the exact nature and origin of these minerals still have to be characterized. The gradual DIC increase in the spring-cave-downstream river continuum highlights the enhanced CO_2 dissolution in water from cool CO_2-rich caves and the progressive weathering of $CaCO_3$ by this more acidic, CO_2-rich subterranean water. The measured parameters can be used as inputs in geochemical models to estimate the precipitation-dissolution rates of carbonates.

Acknowledgements

This research was part of the DINCOS project (Biocrust Dynamics, key CGL2016-78075-P) funded by the Spanish State Plan for Scientific and Technical Research and Innovation 2013–2016, which funds the first author. CLC thanks the PhD program in Earth Sciences (University of Granada) in which he is enrolled, Encarnación Ruiz Agudo and Aurelia Ibañez Velasco (University of Granada) for supervising and providing facilities for the N_2-BET analysis, as well as Francisco Contreras for the field expedition in Sorbas caves. The data from the El Cautivo experimental field site were obtained thanks to the courtesy of the Viciana brothers, the landowners.

Authors´ contributions

CLC conceived the idea and developed the device; RLS and EPSC supervised and funded its development; CLC, RLS and EPSC collected the samples; CLC analyzed the samples and the data; CLC led the writing of the manuscript. All authors contributed critically to the drafts and gave final approval for publication.

Peer review

The peer review history for this article is available at https://publons.com/publo n/10.1111/2041- 210X.13579.

Data availability statement

The data used in this research are publicly available from the fig-share repository https://doi.org/10.6084/m9.figsh are.13713 448.v1. The Arduino source code used in this study is publicly available from the GitHub and Zenodo repositories http://doi.org/10.5281/zenodo.4520391 [*Lopez-Canfin et al.*, 2021].

References

ASTM D7573-09, A. (2009). *Standard Test Method for Total Carbon and Organic Carbon in Water by High Temperature Catalytic Combustion and Infrared Detection*. ASTM International. https://doi.org/10.1520/D7573-09

Benzerara, K., Skouri-Panet, F., Li, J., Férard, C., Gugger, M., Laurent, T., Couradeau, E., Ragon, M., Cosmidis, J., & Menguy, N. (2014). Intracellular Ca-carbonate biomineralization is widespread in cyanobacteria. *Proceedings of the National Academy of Sciences*, *111*(30), 10933–10938.

Del Campillo, M. C., Torrent, J., & Loeppert, R. H. (1992). The reactivity of carbonates in selected soils of southern Spain. *Geoderma*, *52*(1–2), 149–160.

Greenspan, S. E., Morris, W., Warburton, R., Edwards, L., Duffy, R., Pike, D. A., Schwarzkopf, L., & Alford, R. A. (2016). Low-cost fluctuating-temperature chamber for experimental ecology. *Methods in Ecology and Evolution*, *7*(12), 1567–1574.

Harmon, T. C., Dierick, D., Trahan, N., Allen, M. F., Rundel, P. W., Oberbauer, S. F., Schwendenmann, L., & Zelikova, T. J. (2015). Low-cost soil CO2 efflux and point concentration sensing systems for terrestrial ecology applications. *Methods in Ecology and Evolution*, *6*(11), 1358–1362.

Heger, A., Kleinschmidt, V., Gröngröft, A., Kutzbach, L., & Eschenbach, A. (2020). Application of a low-cost NDIR sensor module for continuous measurements of in situ soil CO2 concentration. *Journal of Plant Nutrition and Soil Science*.

Kindler, R., Siemens, J. A. N., Kaiser, K., Walmsley, D. C., Bernhofer, C., Buchmann, N., Cellier, P., Eugster, W., Gleixner, G., & Grünwald, T. (2011). Dissolved carbon leaching from soil is a crucial component of the net ecosystem carbon balance. *Global Change Biology*, *17*(2), 1167–1185.

Kristl, M., Muršec, M., Šuštar, V., & Kristl, J. (2016). Application of thermogravimetric analysis for the evaluation of organic and inorganic carbon contents in agricultural soils. *Journal of Thermal Analysis and Calorimetry*, *123*(3), 2139–2147.

Loeppert, R. H., & Suarez, D. L. (1996). Carbonate and gypsum. *Methods of Soil Analysis: Part 3 Chemical Methods*, *5*, 437–474. https://doi.org/10.2136/sssabookser5.3.c15

Lopez-Canfin, C., Sánchez-Cañete, E. P., & Lázaro, R. (2021). *Low-cost CaCO3-RSA-DIC device: source code (Version v1.0.0)*. Zenodo. https://doi.org/http://doi.org/10.5281/zenodo.4520391

Miralles, I., Jorge-Villar, S. E., van Wesemael, B., & Lázaro, R. (2017). Raman spectroscopy detection of biomolecules in biocrusts from differing environmental conditions. *Spectrochimica Acta Part A: Molecular and Biomolecular Spectroscopy*, *171*, 40–51.

Parkhurst, D., & Appelo, C. A. J. (2011). PHREEQC (Version 3)—A computer program for speciation, batch-reaction, one-dimensional transport, and inverse geochemical calculations. *Water Resources Div., Denver, CO*.

R Core Team. (2019). *R: A Language and Environment for Statistical Computing*. R Foundation for Statistical Computing. https://www.r-project.org/

Rounds, S. A., & Wilde, F. D. (2012). *Chapter A6. Section 6.6. Alkalinity and acid neutralizing capacity*.

Sánchez-Cañete, E. P., Serrano-Ortiz, P., Domingo, F., & Kowalski, A. S. (2013). Cave ventilation is influenced by variations in the CO2-dependent virtual temperature. *International Journal of Speleology*, *42*(1), 1.

Schwartzman, D. W., & Volk, T. (1989). Biotic enhancement of weathering and the habitability of Earth. *Nature*, *340*(6233), 457.

Suarez, D. L. (1995). Carbonate chemistry in computer programs and application to soil chemistry. *SSSA SPECIAL PUBLICATION*, *42*, 53.

Suarez, D. L., & Šimůnek, J. (1997). UNSATCHEM: Unsaturated water and solute transport model with equilibrium and kinetic chemistry. *Soil Science Society of America Journal*, *61*(6), 1633–1646.

Suarez, D. L., & Wood, J. D. (1984). Simultaneous Determination of Calcite Surface Area and Content in Soils 1. *Soil Science Society of America Journal*, *48*(6), 1232–1235.

Verrecchia, E. P., Braissant, O., & Cailleau, G. (2006). The oxalate-carbonate pathway in soil carbon storage: the role of fungi and oxalotrophic bacteria. *Fungi in Biogeochemical Cycles*, 289–310.

Zamanian, K., Pustovoytov, K., & Kuzyakov, Y. (2016). Pedogenic carbonates: Forms and formation processes. *Earth-Science Reviews*, *157*, 1–17.

3.2. CHAPTER 2

Disparate responses of soil-atmosphere CO_2 exchange to biophysical and geochemical factors over a biocrust ecological succession in the Tabernas Desert

Clément Lopez-Canfin, Roberto Lázaro, Enrique P. Sánchez-Cañete

Submitted for publication to *Geoderma*. January 2022.

Lopez-Canfin, C.; Lázaro R.; Sánchez-Cañete, E.P (under review). Disparate responses of soil-atmosphere CO_2 exchange to biophysical and geochemical factors over a biocrust ecological succession in the Tabernas Desert.

Graphical abstract

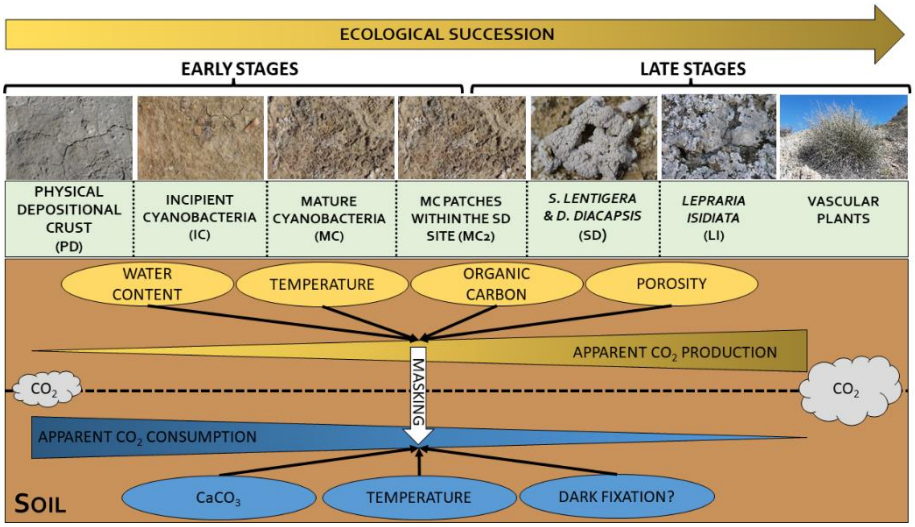

Abstract

In drylands, potential abiotic processes of CO_2 uptake are still debated while estimates of the biotic contribution of photosynthetizing biocrusts to the net carbon uptake remain uncertain. This uncertainty is partly attributable to a common neglect of the underlying soil and spatio-temporal variability of soil CO_2 fluxes. Moreover, it is still unknown how those fluxes evolve during the ecological succession of biocrusts, and which factors control them.

Therefore, we aimed to (1) identify those factors and use them for predictions, and (2) explain the variation of annual CO_2 fluxes over the succession. We conducted 2 years of continuous measurements of the topsoil CO_2 molar fraction (χ_s) and microclimatic variables. Statistical spatio-temporal models were developed of χ_s dynamics and annual fluxes.

The succession stage, soil water content (θ_w), and temperature (T_s) and the interactions of these variables explained and efficiently predicted the χ_s dynamics. Soil CO_2 emissions were more sensitive to θ_w and T_s in late successional stages, apparently because of organic carbon accumulation and higher porosity. The calcite content also played a role in explaining the uptake of CO_2 at night. The annual CO_2 influx represented up to 115% of the CO_2 efflux, generating a net annual carbon uptake in some locations.

Our measurements suggest that CO_2 consumption processes were progressively masked by the increase in biological CO_2 production during succession. That is probably why those processes could mainly be detected in early successional stages and more generally in drylands, as they sustain a low biological activity. However, such processes could be ubiquitous in ecosystems if difficult to detect.

Here, we propose that a geochemical process of calcite dissolution might be involved. Nevertheless, the possibility of a (geo)biological origin through dark CO_2 fixation should not be discarded. It is crucial to elucidate whether a biotic and/or abiotic process is acting and to better characterize its sensitivity to interacting environmental drivers, because they have disparate feedback to climate change. Abiotic CO_2 uptake must also be isolated to avoid overestimating biocrust photosynthesis (or underestimating respiration) when interpreting net surface CO_2 fluxes and determining the roles of biocrusts in the global carbon budget.

Our observations and modelling results suggest that a future enhancement of soil CO_2 emissions is a likely outcome of global warming at this site. However, it is urgent to invest more research efforts in understanding, quantifying and assessing the climatic sensitivity of natural ecosystem processes able to mitigate CO_2 emissions, such as those involved in the CO_2 uptake by the extensive drylands soils.

3.2.1. Introduction

It is now unequivocal that anthropogenic emissions of CO_2 have substantially magnified the Earth's greenhouse effect and the resulting forcing continues to rise [*IPCC*, 2013]. This process is triggering a change in climate through global warming that is expected to exacerbate the current disruption of water and carbon cycles as well as biodiversity loss and alteration of ecosystem services [*Reid et al.*, 2005]. It is thus a major challenge to better characterize the carbon cycle in order to improve modeling and forecasts of climate and ecosystems responses. It is also critical to find innovative solutions to mitigate climate change [*Esteban et al.*, 2008; *Grubb*, 2004]. Terrestrial ecosystems are good candidates to achieve this purpose because of their well-known effect as carbon sinks, offsetting at least one-fourth of fossil fuel emissions [*Le Quéré et al.*, 2018]. However, models of ecosystem-climate carbon feedbacks still suffer from a lack of predictability under such unprecedented environmental conditions [*Huntzinger et al.*, 2017; *Luo et al.*, 2015]**.**

Previously suggested critical gaps (especially regarding the understanding of soil and microbial processes) include nutrient and other controls that couple photosynthetic carbon input to respiratory carbon outputs, and climate feedbacks including the carbon balance [*Chapin III et al.*, 2009]. For example, although it is clear that climatic variations are the major factors controlling the net land carbon flux, it is still debated whether the main regulator is temperature or moisture variability, and it is becoming increasingly evident that their interaction is fundamental but still largely neglected in most studies [*Piao et al.*, 2020; *Quan et al.*, 2019]. In particular, even if a positive feedback between the soil CO_2 efflux (F_s) and temperature is likely [*Hashimoto et al.*, 2015], global models are often simplified for drylands

with respect to their hydric status and underrepresent those areas. Therefore, future predictions require confirmation of their modelled processes in water-limited ecosystems where the effect of soil temperature (T_s) is essentially constrained by soil water content (θ_w), and antecedent moisture conditions play a key role in triggering ephemeral CO_2 pulses that can be difficult to capture by observations and models [*Lopez-Canfin et al.*, 2018; *Vargas et al.*, 2018]. In addition, the issue of the unknown "residual terrestrial carbon sink" (previously termed the "missing carbon sink") raised in order to explain the unbalanced global carbon budget, has remained unsolved for decades [*Houghton et al.*, 2018].

There is growing evidence that dryland soils could act as substantial but so far disregarded carbon sinks at the global scale. Such soils represent ca. 40 % of the Earth´s land surface, and thus even small CO_2 uptake at a local scale could have large-scale repercussions. Dryland soils can take up atmospheric CO_2 through either biotic or abiotic processes. On the one hand, abiotic processes that have been suggested to explain the recent observational convergence of atypical CO_2 uptake by different soils, are still a matter of debate [e.g. *Ball et al.*, 2009; *Hamerlynck et al.*, 2013; *Ma et al.*, 2013]. One possible explanation could arise from the dissolution of soil calcite ($CaCO_3$), a geochemical reaction consuming CO_2. This hypothesis deserves special attention since it is estimated that soils contain ca. 940 Gt inorganic carbon (mainly as carbonates), of which 97% is located in drylands, exceeding the amount of carbon in the atmosphere (ca. 780 GtC) [*Bernoux & Chevallier*, 2014]. On the other hand, the main known and largely studied biotic process able to take up atmospheric CO_2 is photosynthesis. In drylands, where plants are typically scarce, microbial communities of biological soil crusts also ensure this crucial ecosystem process**.**

Biological soil crusts (biocrusts) consist of microscopic (cyanobacteria, algae, fungi and bacteria) and macroscopic (lichens, mosses and microarthropods) poikilohydric organisms that occur on or within the top few centimeters of the soil [*Weber et al.*, 2016]. They are key ecosystem engineers as they sustain many important ecological functions including an ability to fix CO_2. Other functions consist of improvement of water infiltration and thus runoff reduction, limitation of soil water evaporation, soil stabilization against erosion, plant recruitment and atmospheric N_2 fixation**.** These communities

are very abundant in drylands where they colonize bare soil interspaces between plants, covering up to 70% of the soil surface. Due to the widespread of drylands, these organisms are believed to play a considerable role in the global carbon budget: the global net carbon uptake of biocrusts has been estimated to range between 0.34 and 3.9 Gt C yr^{-1} worldwide [*Elbert et al.*, 2012; *Porada et al.*, 2013], with the upper estimate corresponding to around 7% of net primary production by terrestrial vegetation.

Those estimates remain largely uncertain presumably because (1) many studies have measured the CO_2 exchange of biocrusts in controlled conditions after separating them from the underlying soil [*Wilske et al.*, 2008], thus neglecting the soil CO_2 efflux which is a crucial component of the net ecosystem CO_2 exchange; (2) both biocrust photosynthesis and the soil CO_2 efflux have an ephermeral pulse response to rain [*Bowling et al.*, 2011] that makes it difficult to obtain representative measurements of soil-atmosphere CO_2 fluxes; (3) the spatial distribution of biocrust types is highly heterogeneous and hence, has the potential to modulate locally these fluxes. *In situ* long-term continuous measurements of soil-atmosphere CO_2 exchange conducted with representative spatial coverage have the potential to overcome these issues; however, such measurements are still lacking in biocrusted ecosystems to confidently assess their carbon sequestration potential [*Weber et al.*, 2016]. In addition, we currently lack sufficient spatiotemporal data on biocrust function, cover, and community structure to confidently assess their ecological roles across the extensive dryland biome [*Ferrenberg et al.*, 2017].

Evaluating how biocrusts colonization of bare soil affects the spatio-temporal variability of F_s is of particular importance because dryland ecosystems where they develop are characterised by “hot-spots” (i.e. patches) and “hot-moments” (i.e. bursts) of CO_2 emission that can substantially affect their net carbon balance [*Leon et al.*, 2014; *Vargas et al.*, 2018] . Many biophysical and geochemical factors control F_s and interact over different temporal and spatial scales [*Vargas et al.*, 2011]. In the absence of plants, important drivers of F_s (through the regulation of soil CO_2 production, consumption and transport processes) include soil porosity [*Sánchez-Cañete et al.*, 2017], microbial community composition [*Liu et al.*, 2018], substrate

availability [*Gershenson et al.*, 2009], soil mineralogy, especially calcite [*Gallagher & Breecker*, 2020; *Roland et al.*, 2013], soil pH [*Ma et al.*, 2013], and pedoclimate [*Lopez-Canfin et al.*, 2018]. As a matter of fact, biocrust colonization can affect all these factors, thus having potential repercussions for local F_s dynamics.

It remains unknown, both how soil-atmosphere CO_2 exchanges evolve during the ecological succession of biocrusts, and which are the factors that control it. Observations suggest that biocrusts gradually develop according an ecological succession [*Lázaro et al.*, 2008]**.** It has been suggested that a successional community framework has strong potential to provide predictive and scaling power regarding biocrust relationships with function, but this type of assessment has not been consistently performed across variable biocrust or ecosystem types [*Ferrenberg et al.*, 2017]. However, since successional stages are associated with typical microclimates and soil develops in parallel with succession over time, it can be challenging to disentangle the respective roles of biology, microclimate and pedogenesis on the soil-atmosphere CO_2 exchange. Nevertheless, the use of appropriate statistical modelling techniques, besides helping to validate mechanistic models [*Reichstein et al.*, 2003], has the potential to provide insight regarding those effects and offer useful predictions.

In this research, our objective was to identify the factors controlling the soil-atmosphere CO_2 exchanges (daily dynamics and inter-annual balance), with a particular focus on assessing the effect of biocrust succession and taking into account spatio-temporal variability to obtain robust predictions. We hypothesized that (1) biocrust succession should gradually increase substrate availability for microorganisms in the underlying soil (through carbon and nitrogen fixation), thus enhancing CO_2 production by microbial respiration in this soil layer; (2) this gradual mitigation of a substrate limitation for microbial activity during succession should increase the sensitivity of respiration to pedoclimatic variables, mainly θ_w and T_s; (3) soil porosity should increase with biocrust succession thus enhancing CO_2 transport by diffusion towards the atmosphere; (4) both enhanced CO_2 production and diffusion should result in increasing soil CO_2 effluxes with succession; and (5) due to the abundance of soil carbonates in the studied ecosystem, they could affect the

soil-atmosphere CO_2 exchange as $CaCO_3$ precipitation-dissolution reactions respectively produce-consume CO_2.

3.2.2. Material and methods

3.2.2.1. Experimental Site

This study was conducted in the experimental site of El Cautivo, an area of badlands located in the Tabernas Desert (Almería, Spain) (more information about the study site is provided in Section 2.1).

3.2.2.2. Environmental measurements and soil analyses

Continuous measurements of soil and above-surface variables were conducted during two years (see Section 2.3.3). The soil CO_2 efflux (F_s) was also measured regularly with portable chambers (see Section 2.3.1).

In the topsoil (0-5cm), physical and chemical properties (porosity, (ϕ), soil organic carbon content (SOC), total nitrogen (N) content, pH, electrical conductivity (EC), calcium carbonate equivalent content (CCE) and calcite specific surface area (SSA)) were measured within each site described above. The SOC content was measured by a modified wet oxidation method [*Mingorance et al.*, 2007] and determination with a spectrophotometer (Spectronic Helios Alpha 9423 UVA 1002E, Thermo Fisher Scientific, Waltham, MA, USA). The total N content was determined by the Kjeldahl method, using an automatic distillation unit (UDK 129, Velp Scientifica, Usmate Velate, MB, Italy). The pH and EC were measured using a soil:water ratio of 1:2.5 and 1:5 respectively, with an electrode 50 12 T (Hach Company, Loveland, CO, USA) connected to a pH-meter Sension+ pH3 (Hach Company) and an electrode 5292 (Hach Company) connected to a conductimeter Basic 30 (Crison Instruments, Barcelona, Spain) respectively. The CCE and SSA were quantified by measuring the CO_2 released during an acidic reaction [*Lopez-Canfin et al.*, 2021].

3.2.2.3. Data processing

To reduce the computing time of the subsequent gap-filling process, hourly averages were calculated on data. For the variable of main interest in

this study, i.e. χ_s, the average of gaps within each successional stage was 1.72%, ranging from 0.42% (in IC, MC, LI and plants) to 6.4% (in SD). A gap-filling procedure was used to impute missing values (see Section 2.4.1).

The χ_s and χ_a were corrected for real-time changes in atmospheric pressure and temperature (see Section 2.2.1) and F_s were calculated based on the gradient method (see. Section 2.3.2).

3.2.2.4. Statistical modelling

All analyses were performed with R software v.3.6.3 [*R Core Team*, 2019]. The 10-step statistical protocol of Zuur and Ieno [2016] was used to analyze the data:

(1) step 1: formulate appropriate questions. Our model construction aimed to explore specifically assumptions (1), (2) and (5) of this research, that can be summarized with the statistical questions: Does pedoclimate (θ_w and T_s), SOC and CCE affect cumulative annual F_s? Does pedoclimate affect differently the daily dynamics of χ_s in each stage of biocrusts succession?

(2) step 2: visualize the experimental design (see Section 2.3.3 Fig. 5);

(3) step 3: conduct data exploration. Based on this exploration, we identified non-normality, homoscedasticity, spatio-temporal dependency, and collinearity in the data structure. To solve non-normality and homoscedasticity issues, the daily χ_s was log-transformed, and the residual variance was modeled in models of cumulative F_s. We also ensured that the variance inflation factor (VIF) was below 1.5 to avoid collinearity issues.

(4) step 4: identify the dependency structure in the data. Violation of independence was expected due to spatial and/or temporal dependence inherent to the experimental design.

(5, 6) step 5 and 6: present and fit the model. Initial models were built in a Bayesian framework using integrated nested Laplace approximations (INLA) with the *inla* R package which allows modelling of spatio-temporal dependencies [*Rue et al.*, 2009; *Zuur et al.*, 2017]. Those models included variables and interactions to test our research hypotheses. They were compared with more complex models: (i) a mixed model treating the measurement location as a random intercept; and (ii) a spatial intercept model in which the spatial dependence relies on GPS coordinates of measurements

locations. The latter model was based on a dense covariance matrix Matérn model, a Gaussian field with a Matérn correlation function, which assumes that observations that are closer in space are more similar. The best model was always retained as the one that minimized the deviance information criterion (DIC, a Bayesian measure analogous to the Akaike Information Criterion (*AIC*)). If the random intercept model was better, it was fitted in a frequentist framework with the *nlme* package [*Pinheiro & Bates*, 2000] using AIC to compare models when possible.

To build a model of χ_s dynamics over time and over the succession, daily averages were computed from the data. The dataset was split into a training set (first year) for calibration and a testing set (second year) for prediction. The initial model contained the variables θ_w, T_s, succession stage, and up to three-way interactions in order to allow the effect of θ_w, T_s and their interaction to vary for each successional stage. The serial correlation was modeled with a first-order autoregressive (AR1) process. We also tried to add a random slope of either θ_w or T_s. Then, we tried to remove fixed terms one by one, starting from the higher order interaction.

The following spatio-temporal model was retained to explain the log-transformed χ_s at location *i* and time *t* (Y_{it}):

$$Y_{it} = X_{it}\beta + Z_{it}v + w_{it} + \varepsilon_{it} \quad (1)$$

$$w_{it} = \phi w_{it-1} + u_{it} \quad (2)$$

Briefly, the equations define a hierarchical model characterized by a Gaussian field Y_{it} built from a design matrix of the fixed explanatory variables X_{it} (with all the original terms having been conserved), a vector β of regression coefficients associated with the fixed effects, a design matrix Z_{it} of the random explanatory variable (random slope of θ_w), a vector *v* of regression parameters associated with the random effect, the residual ε and a first order autoregressive dynamic model for the latent process *w*, with an autoregressive parameter φ ($|\varphi|<1$) and spatially correlated innovations u_{it}. More details about this kind of spatio-temporal model can be found in [*Cameletti et al.*, 2013].

Explanatory models of the following annual cumulative F_s were also fitted: the efflux, the influx and the total flux. They refer to, respectively: the positive flux

(CO_2 emissions from soil to atmosphere), the negative flux (CO_2 uptake from atmosphere to soil) and the sum of both fluxes (positive and negative), calculated from hourly data for both years. Since this subset had 42 observations and a general rule of thumb in statistics is to have a minimum of 10 observations per model term, four terms were included in the model. After centering and scaling variables to zero mean and unit variance, we tested for the effect of annual average θ_w and T_s including their interaction, as well as the effect of calcium carbonate equivalent content (CCE). We also tried to substitute T_s by SOC since those variables were collinear. Residual variance was modelled as proportional to θ_w in the influx model and proportional to fitted values in the efflux model. Non- significant/important fixed terms were removed based on the *t*-statistic.

Mixed models retained to model cumulative annual fluxes have the general form:

$$Y = X\beta + zu + \varepsilon \qquad (3)$$

Where *Y* is the response variable (either the annual efflux, influx or total F_s), $X\beta$ is the model's fixed part with *X* being the design matrix of the fixed explanatory variables and β a vector of regression coefficients associated with the fixed effects, *Zu* is the model's random part with *Z* being the design matrix of the random explanatory variables and *u* a vector of regression parameters associated with the random effects, and ε is the residual.

(7) step 7: validate the model. In every model, the validity of underlying assumptions and the absence of non-linear patterns in residuals was inspected visually;

(8, 9) step 8 and 9: interpret and present the numerical output and create a visualization of the model (see Results Section);

(10) step 10: simulate or perform cross-validatation from the model. The predictive accuracy of the model of χ_s dynamics was tested by cross-validation over the second year. We also performed predictions from simulated θ_w and T_s data. Simulated values for θ_w ranged from the minimum to the maximum observed θ_w over the two years and predictions were performed at three levels of T_s corresponding to (1) low (mean – standard deviation); (2) medium (mean); (3) high (mean + standard deviation), and vice-versa for predictions from simulated T_s at low, medium and high θ_w.

3.2.3. Results

3.2.3.1. Spatio-temporal trends

Daily time series of soil CO_2 molar fractions (χ_s) and fluxes (F_s) were highly variable in time and space (Fig. 1A-B, Table 1). Their variations mainly followed those in soil water content (θ_w) (Fig. 1C). Differences in χ_s and F_s between stages of succession were mainly marked in non-limiting soil moisture conditions (i.e. after rainfalls), especially when antecedent θ_w was low (Fig. 1C) and soil temperature (T_s) was high (Fig. 1D), typically after extended summer drought. In those moments, the rewetting of hot dry soil produced CO_2 pulses (short periods with high CO_2 emissions from soil to atmosphere). Two of these pulses were recorded in this study and occurred in concomitance with two extreme precipitation events (36 mm at an average intensity of 30 mm hr^{-1} and 86 mm at an average intensity of 12 mm hr^{-1}, respectively). In both cases, during those precipitation events, the magnitude of the CO_2 pulses tended to increase over the succession: χ_s rose from 13% in the PD site to up to 487% in plants, compared to its initial value before rain (Table 1). In addition, the CO_2 bursts were always greater after the largest rain event, regardless of the stage of succession.

3.2.3.2. Short-term spatio-temporal dynamics

During most of the year, the diel variation of χ_s, reflected by its diel standard deviation, was greater in the early stages of succession than in late stages (i.e. before and after lichen dominance of biocrusts) (Fig. 2A). That seems mainly due to a greater diel variation of T_s in early stages than in late stages of succession (Fig. 2B). The main exceptions to this pattern occurred during the first CO_2 pulse after the summer drought.

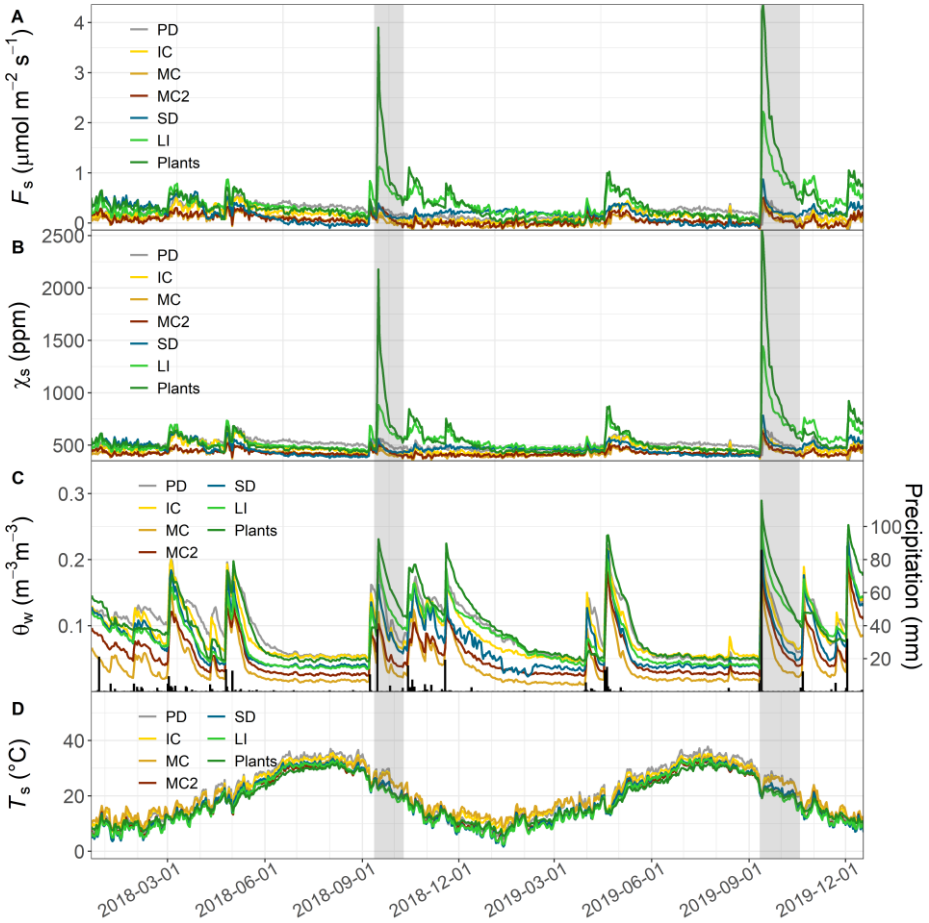

Fig. 1 Daily time series of (A) estimated soil CO_2 flux (F_s), (B) soil CO_2 molar fraction (χ_s), (C) soil water content (θ_w) and precipitation (black); (D) soil temperature (T_s). Shaded areas delimit moments of CO_2 pulses analyzed in Table 1. PD, physical depositional crust; IC, incipient cyanobacterial crust; MC, mature cyanobacterial crust; SD (line), lichen community characterized by *S. lentigera* and *D. diacapsis*; LI, lichen community characterized by *L. isidiata*; MC2, mature cyanobacterial patches within SD site.

Inverted patterns of χ_s dynamics were sometimes observed, with the soil having a lower CO_2 molar fraction than the atmosphere, usually at night. This potentially induced negative F_s, i.e. atmospheric CO_2 uptake by soil, and was particularly detectable in early-successional stages, especially in *Cyanobacteria* sites (Fig. 3). Overnight, χ_s progressively decreased following

closely the T_s pattern until reaching a minimum that coincided with the T_s minimum at early morning (data not shown). Those negative F_s were confirmed by nocturnal chamber measurements that were performed on 2019-03-15, during T_s minima. Among 15 locations distributed over the biocrust succession, we measured with the chambers negative F_s at 11 locations. All stages of biocrust succession exhibited influxes except the last one (*L. isidiata* mixed with plants) and the influx of greater magnitude occurred in the first stage of succession (physical depositional crust). Measured influxes were on average -0.12 ± 0.06 µmol m^{-2} s^{-1}, ranging from -0.07 to -0.23 µmol m^{-2} s^{-1}. Even at 45 cm depth, the χ_s dropped below atmospheric CO_2 values, but only during periods of T_s minima in winter (data not shown).

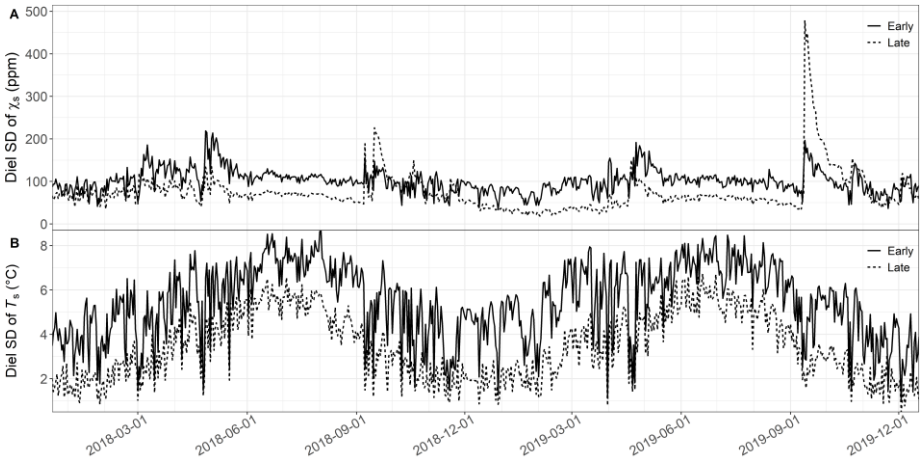

Fig. 2 Diel standard deviations across time of (A) soil CO_2 molar fraction (χ_s); (B) soil temperature (T_s), for early and late successional stages (solid and dashed lines, respectively). Plants were not included in late successional stages for this representation to focus on crusts, but similar patterns were observed.

Table 1 Spatio-temporal variation of soil CO_2 molar fraction

Successional stage	Spatial variation			Temporal variation pulse 1			Temporal variation pulse 2		
	Mean ($\mu mol\ mol^{-1}$)	SD ($\mu mol\ mol^{-1}$)	CV (%)	Mean initial value ($\mu mol\ mol^{-1}$)	Increase ($\mu mol\ mol^{-1}$)	Increase (%)	Mean initial value ($\mu mol\ mol^{-1}$)	Increase ($\mu mol\ mol^{-1}$)	Increase (%)
PD	504	59	12	499	66	13	484	184	38
IC	467	39	8	436	72	16	441	213	48
MC	424	19	4	412	79	19	409	175	43
MC2 (Ads)	427	45	11	406	106	26	409	230	56
SD	468	30	6	393	176	45	403	381	95
LI	542	73	13	455	429	94	443	1000	226
Plants	551	197	36	444	1735	391	435	2120	487
Inter-crust	483	103	21	-	-	-	-	-	-

PD, physical depositional crust; IC, incipient cyanobacterial crust; MC, mature cyanobacterial crust; SD (line), lichen community characterized by *S. lentigera* and *D. diacapsis*; LI, lichen community characterized by *L. isidiata*; MC2, mature cyanobacterial patches within SD site. SD (column), standard deviation; CV, coefficient of variation. The two CO_2 pulses started on 2018-09-15 and 2019-09-12.

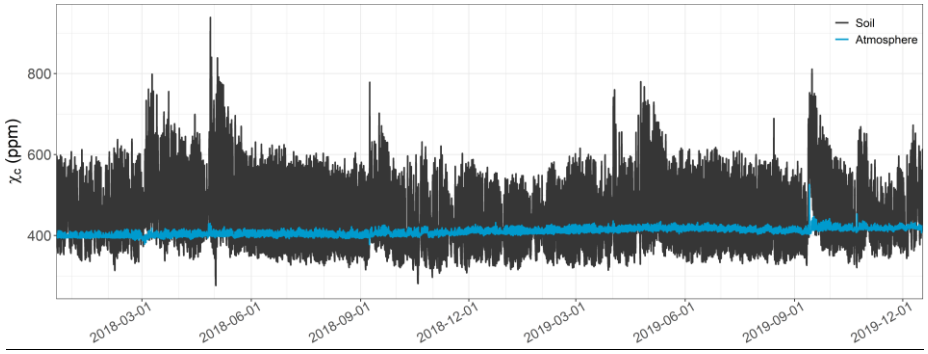

Fig. 3 Hourly time series of CO_2 molar fraction (χ_c) in soil and atmosphere (black and blue lines, respectively). Soil CO_2 molar fraction is the mean of replicated time series within all *Cyanobacteria* sites.

3.2.3.3. Carbon balances over ecological succession

The evolution over two years of the total cumulative, negative and positive F_s is represented for each successional stage in Fig. 4. The effect of precipitation events greater than 15 mm on CO_2 emissions was barely notable in early successional stages but tended to accentuate in late stages, as reflected by the broken-stick aspect of the curves with increasingly sharp slopes after most such events.

On average, the magnitude of the cumulative negative F_s tended to increase in the early stages of succession (-20, -50 and -65 gC m^{-2} in PD, IC and MC, respectively) and decrease in later stages (-55, -15, -4 and -7 gC m^{-2} in MC2, SD, LI and plants, respectively). Negative F_s in lichens and plants sites occurred essentially during summer drought whereas in early succession stages, they occurred all over the year. The cumulative positive F_s tended to decrease in the early stages of the succession (190, 164 and 101 gC m^{-2} in PD, IC and MC sites, respectively) before increasing in later successional stages (101, 154, 291 and 307 gC m^{-2} in MC2, SD, LI and plants sites, respectively). The resultant cumulative total F_s followed the same trend as the positive F_s of initial decrease (170, 114 and 36 gC m^{-2} in PD, IC and MC sites, respectively) and later increase (46, 139, 288 and 300 gC m^{-2} in MC2, SD, LI and plants sites, respectively).

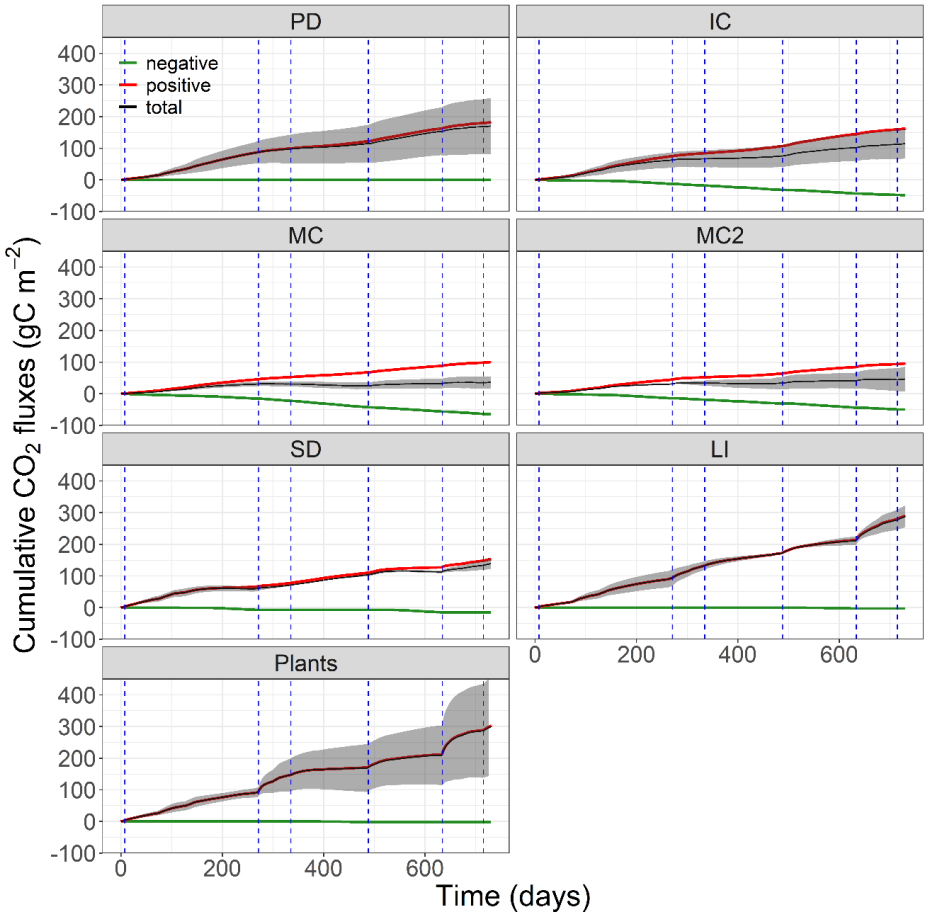

Fig. 4 Cumulative CO_2 fluxes over two years for each succession stage. The shaded area delimits ± the spatial standard deviation of the total CO_2 flux (i.e. the resultant of positive and negative fluxes). Dashed lines mark precipitation events greater than 15 mm. PD, physical depositional crust; IC, incipient cyanobacterial crust; MC, mature cyanobacterial crust; SD (line), lichen community characterized by *S. lentigera* and *D. diacapsis*; LI, lichen community characterized by *L. isidiata*; MC2, mature cyanobacterial patches within SD site.

The mean annual θ_w also decreased in early successional stages (0.096, 0.087, 0.040 $m^3\ m^{-3}$ in PD, IC and MC sites, respectively) and increased in later stages (0.053, 0.071, 0.082, 0.097 $m^3\ m^{-3}$ in MC2, SD, LI and Plants sites, respectively). The mean annual T_s was overall higher in early stages (21.3, 21.3 and 21.2 °C in PD, IC and MC sites) than in later stages (18.6, 18.7, 18.2 and 18.6 °C in MC2, SD, LI and plants sites).

The ratio of cumulative negative F_s to positive F_s increased in the early stages of succession (0.11, 0.30, 0.64 in PD, IC and MC sites, respectively) and decreased in later stages (0.54, 0.10, 0.01 and 0.02 in MC2, SD, LI and Plants sites, respectively). During the second year, the cumulative negative F_s reached locally greater values than the positive F_s (by 108% and 115% in two locations situated in the MC and MC2 sites, respectively), generating a net annual carbon uptake by the soil (-3 and -7 gC m^{-2}, respectively).

3.2.3.4. Soil properties over ecological succession

Some soil properties exhibited clear trends of increase over ecological succession (Table 2): (1) the soil porosity (0.47, 0.48, 0.51, 0.55, 0.53, 0.54, 0.58 m^3 m^{-3} in the PD, IC, MC, MC2, SD, LI and plants sites, respectively); (2) the soil organic carbon (SOC) content (5.4, 4.9, 7.5, 8.1, 9.0, 12.4 and 16.2 mg g^{-1} in the PD, IC, MC, MC2, SD, LI and plants sites, respectively), and (3) the total soil nitrogen (N) content (0.7, 0.7, 0.8, 1.2, 1.3, 1.5 and 1.4 mg g^{-1} in the PD, IC, MC, MC2, SD, LI and plants sites, respectively). The correlation between pairs of these variables was high (Pearson´s coefficient of correlation $r > 0.84$).

Table 2 Soil properties

Succession	Local SOC		Local CCE		Local SSA		SOC		N		pH		EC		ϕ	
	Mean	SD	Mean	SD	Mean	SD	Mean	SD	Mean	SD	Mean	SD	Mean	SD	Mean	SD
	(mg g^{-1})	(mg g^{-1})	(g g^{-1})	(g g^{-1})	(m^2 g^{-1})	(m^2 g^{-1})	(mg g^{-1})	(mg g^{-1})	(mg g^{-1})	(mg g^{-1})	-	-	(dS m^{-1})	(dS m^{-1})	-	-
PD	5.6	0.3	0.19	0.01	0.088	0.005	5.4	1.8	0.7	0.1	7.91	0.06	2.2	0.1	0.47	0.05
IC	7.6	0.6	0.30	0.02	0.085	0.008	4.9	2.3	0.7	0.1	8.05	0.41	1.3	1.0	0.48	0.04
MC	6.4	0.1	0.25	0.01	0.087	0.010	7.5	3.5	0.8	0.2	8.37	0.44	0.4	0.2	0.51	0.02
MC2	11.2	0.2	0.31	0.03	0.092	0.003	8.1	1.4	1.2	0.3	8.53	0.26	0.3	0.1	0.55	0.04
SD	8.2	2.7	0.28	0.04	0.090	0.005	9.0	1.9	1.3	0.4	8.05	0.45	0.7	0.6	0.53	0.05
LI	9.7	1.8	0.27	0.02	0.098	0.005	12.4	4.7	1.5	0.3	8.09	0.33	0.6	0.2	0.54	0.05
Plants	12.6	3.7	0.22	0.03	0.085	0.005	16.2	4.9	1.4	0.4	8.22	0.23	0.6	0.62	0.58	0.05

PD, physical depositional crust; IC, incipient cyanobacterial crust; MC, mature cyanobacterial crust; SD, lichen community characterized by *S. lentigera* and *D. diacapsis*; LI, lichen community characterized by *L. isidiata*; MC2, mature cyanobacterial patches within SD site. SOC, soil organic carbon content; CCE, calcium carbonate equivalent content; SSA, specific surface area of calcite; N, nitrogen content; EC, electrical conductivity; ϕ, porosity. Local variables were measured in the proximity of soil sensors. Otherwise, variables were measured at random locations within succession stages.

3.2.3.5. Modeling the dynamics of soil CO_2 molar fractions

The cross-validation of the model of χ_s dynamics using predictions over the second year of data is presented in Fig. 5. The root mean square errors (RMSEs) of the predictions were in average (± standard deviation) 64 ± 39, 79 ± 1, 27 ± 6, 44 ± 22, 53 ± 11, 92 ± 16 and 111 ± 73 ppm for PD, IC, MC, MC2, SD, LI and plants, respectively. A model summary with the β coefficients of regression is provided in Table S1). The three-way interaction between θ_w, T_s and crust type was of particular importance, indicating that the interaction between θ_w and T_s differed between crust types. This relationship could be well visualized by plotting the predicted response of the model from the simulated values of θ_w and T_s (Fig. 6). Globally, the effect of θ_w was positive and tended to be magnified by T_s, as reflected by the increase in the steepness of the slopes from low T_s to high T_s. However, the effect of θ_w was greater and more sensitive to T_s in late successional stages (particularly for LI and plants, and more markedly for *M. tenacissima*).

3.2.3.6. Modeling annual carbon balances

The summary of annual models fixed effects is presented in Table 3 and models fits in Fig. 7. The variables θ_w (annual average), SOC and their interaction explained 64% of the variation in the annual efflux, the rest being explained by the random part. The interaction between θ_w and SOC can be visualized in Fig. 8: the positive effect of SOC was magnified by θ_w and vice versa. The variables T_s (annual average), θ_w and CCE explained 60% of the variation in the annual influx, and the variables SOC and θ_w explained 53% of the variation in the annual total flux.

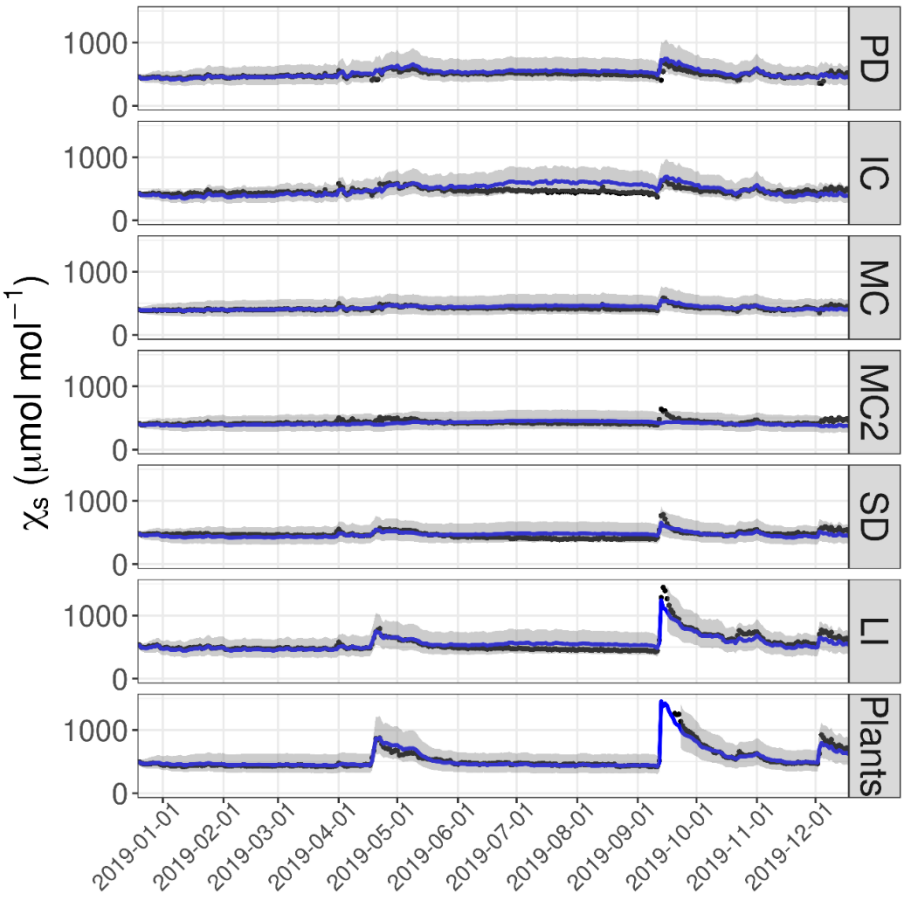

Fig. 5 Prediction of soil CO_2 molar fraction (χ_s) across time for each succession stage. To simplify representation, data and predictions from spatial replicates were averaged within each succession stage. The blue line is the mean prediction. The grey band is the 95% credible interval. Black points represent the observed data. PD, physical depositional crust; IC, incipient cyanobacterial crust; MC, mature cyanobacterial crust; SD, lichen community characterized by *S. lentigera* and *D. diacapsis*; LI, lichen community characterized by *L. isidiata*; MC2, mature cyanobacterial patches within SD site.

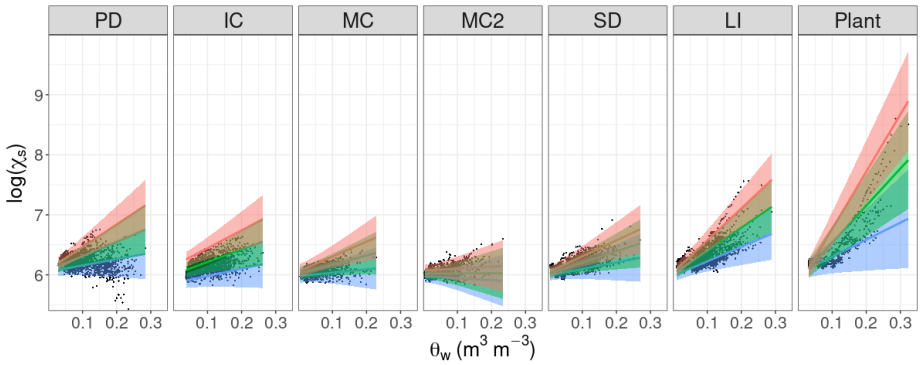

Fig. 6 Predictions of the model of soil CO_2 molar fraction (χ_s, log-transformed) from simulated values of θ_w at low soil temperature (blue), medium soil temperature (green) and high soil temperature (red). Lines are the mean predicted values and bands are the 95% credible intervals. Black points are the observed data. Simulated values of θ_w ranged from the minimum to the maximum values observed during the study period and temperature levels correspond to the observed mean – standard deviation, mean and mean + standard deviation, respectively for the low, medium and high levels. Among plants, only *M. tenacissima* is represented to optimize space. PD, physical depositional crust; IC, incipient cyanobacterial crust; MC, mature cyanobacterial crust; SD, lichen community characterized by *S. lentigera* and *D. diacapsis*; LI, lichen community characterized by *L. isidiata*; MC2, mature cyanobacterial patches within SD site.

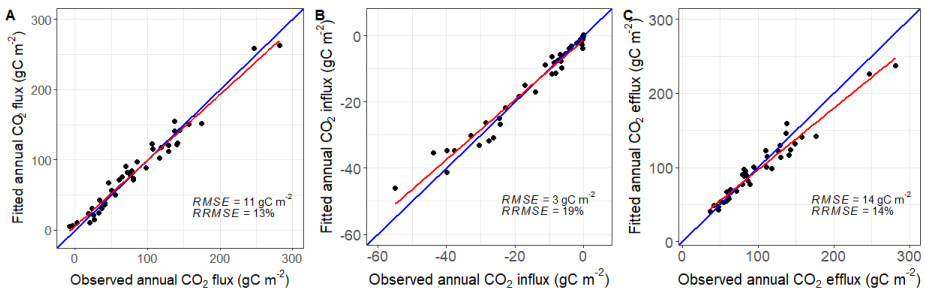

Fig. 7 Fits of models of cumulative annual (A) CO_2 flux, (B) CO_2 influx, (C) CO_2 efflux. The fit is the red line and the 1:1 line is the blue line

Table 3 Summary of annual models

Response variable	Explanatory variable	β	SE	*t*-statistic	*p*-value
Positive F_s	(Intercept)	94.9	6.6	14.4	<0.001
	θ_w	26.8	5.1	5.2	<0.001
	SOC	23.6	7.4	3.2	<0.01
	θ_w:SOC	14.8	5.6	2.6	<0.05
Negative F_s	(Intercept)	-14.2	1.9	-7.5	<0.001
	T_s	-8.5	1.8	-4.8	<0.001
	θ_w	5.3	1.5	3.6	<0.01
	CCE	-5.0	2.0	-2.5	<0.05
Total F_s	(Intercept)	84.1	9.7	8.7	<0.001
	SOC	35.2	9.8	3.6	<0.01
	θ_w	31.5	6.4	4.9	<0.001

β, vector of regression coefficients; SE, standard error. F_s, soil CO_2 flux; θ_w, mean annual soil water content; SOC, soil organic carbon content; T_s, mean annual soil temperature; CCE, calcium carbonate equivalent content.

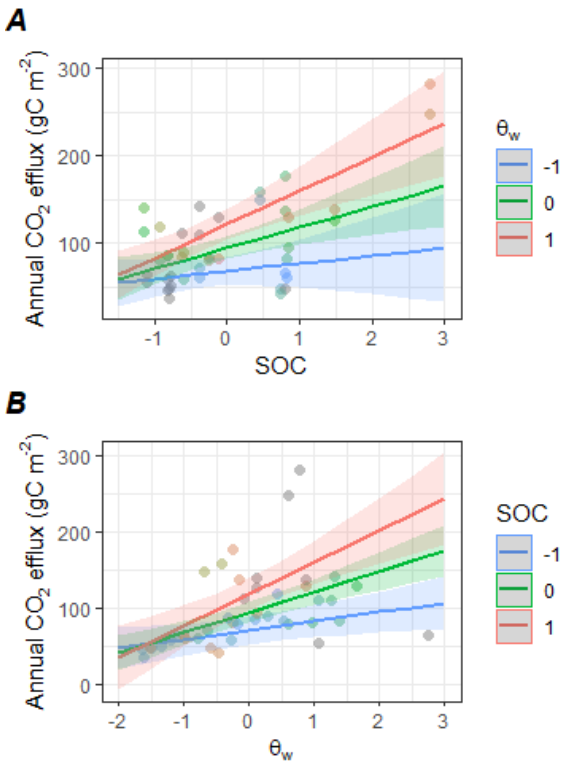

Fig. 8 Conditional plots for the interaction between soil organic carbon (SOC) and soil water content (θ_w) in the model of cumulative annual CO_2 efflux. (A) Effect of SOC at three θ_w levels; (B) Effect of θ_w at three SOC levels. Predictors are standardized to zero-mean and unit-variance. Lines are estimated marginal means and bands are the 95% confidence intervals.

3.2.4. Discussion

In this study we modelled and characterized the spatio-temporal variation of the soil-atmosphere CO_2 exchange in the Tabernas Desert, for different soil crust types related with biocrust succession. Our models of the daily dynamics of the soil CO_2 molar fraction (χ_s) and of the cumulative annual soil CO_2 flux (F_s) predicted and fitted well the data (Figs. 5-8). They revealed that those variables depended on biophysical and geochemical factors that acted in opposition (Table S1, Table 3). The factors affecting χ_s and F_s identified in this study were: the soil biota (biocrust succession), the soil organic matter (SOM; mainly the soil organic carbon content, SOC), the pedoclimate (soil water content, θ_w and soil temperature, T_s) and the pedostructure (soil porosity, φ). A geochemical factor, the calcium carbonate equivalent (CCE) content was also identified here as a potential factor explaining the occurrence of nocturnal net soil CO_2 influxes (i.e. soil CO_2 uptake) in this ecosystem. In order to highlight possible relationships between abiotic and biotic factors, we discuss hereafter the effect of the identified quantitative variables and interactions, emphasizing the role of biocrust succession. We also discuss the relevance of those results in the context of climate change.

3.2.4.1. The enhancing effect of soil organic matter

The SOC content had a positive effect on the cumulative annual soil CO_2 efflux and total soil CO_2 flux (Table 3). The release of CO_2 through microbial respiration is the result of SOM decomposition by microorganisms. During this process, SOM is broken down by heterotrophs and a fraction enters the SOC pool, stored either as microbial biomass or as recalcitrant carbon compounds. Therefore, a positive correlation between the SOC content and the soil CO_2 efflux was anticipated. Since the measured positive F_s was generally the main component of the total resultant F_s (Fig. 4), this positive correlation also partly explained the variation in the annual total F_s.

In drylands, where SOC content is generally low due to the scarcity of plants, biocrusts contribute substantially to the SOC pool within plant interspaces [Belnap, 2003a]. Here we found that the SOC content tended to increase over the succession (Table 2). That seems to partly explain why the

cumulative annual soil CO_2 efflux tended to increase in late successional stages (Fig. 4), as significant amounts of SOC come from better-developed biocrusts [*Weber et al.*, 2016]. Biocrusts may have contributed in different ways to SOC accumulation: (1) through carbon fixation by photosynthesis; (2) through biocrusts turnover via mortality and decomposition; (3) through wind- and water-borne trapping of allochthonous organic matter due to increased surface roughness and sticky polysaccharide sheaths [*Belnap*, 2003b; *Belnap et al.*, 2003]; (4) through secretion of photosynthates to the underlying soil, stimulating microbial activity *via* a "priming effect", a process well described in plants [*Guenet et al.*, 2018] that explains together with roots respiration, the disproportionnally high CO_2 emissions under plants at our site. In *Cyanobacteria*, these secretions can represent up to 50 % of total fixed carbon [*Belnap & Lange*, 2003]. A small fraction of those carbohydrates is leached downwards whereas a substantial part can be assimilated by the underlying microbial community [*Beymer & Klopatek*, 1991], benefiting heterotrophic microbes which are often carbon-limited [*Belnap et al.*, 2003]. For example, Burow et al. [2013] reconstructed a metabolic pathway occurring in cyanobacterial mats, in which photosynthates from *Cyanobacteria* are fermented to organic acids and subsequently used under anoxic conditions at night by *Chloroflexi*, a facultative autotroph. In drylands, microbes are strongly carbon-limited and thus particularly responsive to fresh carbon inputs [*Bastida et al.*, 2019]. Such processes are able to translocate organic carbon from biocrusts to the underlying soil microbial biomass, stimulating its development. For example, Maier et al. [2018] reported an increase in abundance and diversity of the heterotrophic community associated with biocrust succession.

The total N content also increased over the biocrust succession. Other studies also reported a simultaneous increase in SOC and N contents associated with biocrust development, either at this experimental site [*Chamizo et al.*, 2012] or in other drylands [*Maier et al.*, 2018; *Moreira-Grez et al.*, 2019]. Since some degree of collinearity was observed in our study between SOC and N contents, the N content could also be involved in explaining the occurrence of greater positive F_s in late successional stages, through (1) organic N accumulation in SOM over the succession and potentially more N mineralization during SOM decomposition; or (2) biological

fixation of atmospheric N_2. Diazotrophy is a ubiquitous process in biocrusts that likely constitutes a dominant source of N in drylands [*Evans & Ehleringer*, 1993]. Diazotrophy is performed by nitrogenase enzymes, whose activity has been shown to be enhanced in late successional stages [*Housman et al.*, 2006], and as a matter of fact, adequate N supply increases the SOM decomposition rate [*Luo & Zhou*, 2006].

3.2.4.2. The enhancing effect of pedoclimate

All selected models highlighted θ_w as an important predictor of the daily dynamics of χ_s (and by extension F_s) and of the cumulative annual F_s. The daily dynamics of χ_s and F_s was mainly affected by the variations in θ_w following precipitation events (Fig. 1A-C) and annual positive and total F_s followed the same trend as mean annual θ_w over the succession. That is because θ_w is the main factor limiting soil respiration in drylands. However, we found extensive evidence that the magnitude of the response of χ_s to θ_w was dependent on:

(1) The precipitation timing, which was related to T_s and antecedent soil moisture conditions. For example, for a similar precipitation amount (ca. 35 mm on day 2018-09-15 and 30 mm on day 2019-12-03), the increase in χ_s was moderate on the later day whereas it was disproportionately high on the former day, producing in the latter case a large CO_2 pulse also known as a "hot-moment" [*Leon et al.*, 2014]. The precipitation event on day 2019-12-03 occurred in winter during a period of T_s minima and in a previously wetted soil while the precipitation event on day 2018-09-15 occurred at the end of summer during a period of T_s maxima and a previously dried soil. Such CO_2 pulses after drought are characteristic of water-limited ecosystems; in Mediterranean climates, they occur after summer drought, at the onset of the rainy season [*Vargas et al.*, 2018]. During those moments, the lifting of water limitation allows biological reactions to be catalyzed by T_s and the rewetting of dry soil enhances microbial CO_2 release via the Birch effect [*Lopez-Canfin et al.*, 2018]. The effect of the interaction between θ_w and T_s on χ_s was well described by our model. According to our model representation (Fig. 6), the response of χ_s was always magnified when increasing simultaneously θ_w and T_s, regardless of the successional stage.

(2) Biocrusts succession, which was potentially related to the SOC and N content. Continuous measurements over 2 years captured two sporadic "hot-moments" of CO_2 emissions occurring at the end of summer, during which differences in χ_s between successional stages were revealed. In both cases, the magnitude of the CO_2 pulses tended to increase over the succession, revealing increased CO_2 emissions in late succession stages, namely "hot-spots" [*Leon et al.*, 2014]. For example, during the first CO_2 pulse, χ_s increased on average by 66, 72, 79, 106, 176, 429 and 1735 ppm for PD, IC, MC, MC2, SD, LI and plants, respectively, compared to initial values before rain (Table 1). This gradual increase is likely related to the observed increase in SOC and N content over the succession because some of the previously mentioned processes potentially involved in their accumulation can be enhanced in optimal θ_w and T_s conditions: (i) the autotrophic metabolism and subsequent "priming effect" beneath the crust or in plants rhizosphere [*Blagodatskaya & Kuzyakov*, 2011]; and (ii) decomposition/mineralization of organic matter by heterotrophs [*Quemada & Cabrera*, 1997]. In particular, biocrust photosynthesis and release of carbohydrates occurs within minutes to a few days after rewetting [*Belnap et al.*, 2003]. This short-time response to rain is compelling to explain the ephemeral differences in χ_s increments measured in this study. In addition, the presence of a significant interaction between θ_w and SOC in the annual model of positive F_s confirms the existence of a tight relationship between those variables. The effect of the biocrust succession on the sensitivity of χ_s to θ_w (and indirectly to T_s) was also detectable in our model representation (Fig. 6) but to a lesser extent, as the increase in sensitivity was only clearly marked in late successional stages. This enhanced sensitivity of χ_s to θ_w in late successional stages was confirmed by Fig. 4, as the effect of substantial precipitation events (> 15 mm) on CO_2 emissions was barely notable in early successional stages but tended to accentuate in later stages. During the modelling process, it was observed that removing the biocrust term from the model considerably degraded the fit and predictions, thus confirming that a successional community framework has strong potential to provide predictive and scaling power regarding biocrust relationships with function [*Ferrenberg et al.*, 2017].

(3) The precipitation amount. Even though the two detected "hot-moments" occurred at the same time of the year (in September) at similar T_s

values, they differed in terms of precipitation amount (ca. 35 mm versus 85 mm). The heavier precipitation event induced a greater χ_s increment in all successional stages, probably because θ_w rose to a higher level (Fig. 1C). However, the response of soil respiration to the lighter event could also have been mitigated by the occurrence of a small precipitation event few days before. During this initial event, χ_s reached higher values under *L. isidiata* than under surrounding plants, but this trend was reversed after the following rainfall (Fig. 1B-C), in agreement with other studies stating that plant metabolism is delayed and requires heavier or repeated rainfalls for the water to reach deeper roots [*Sponseller*, 2007].

3.2.4.3. The enhancing effect of pedostructure

We found that soil porosity (ϕ) gradually increased over biocrusts succession and that this variable was highly correlated to the SOC content. In agreement with this result, organic matter is known to contribute to the formation of soil aggregates. For example, Rogers and Burns, [1994] reported a positive correlation between soil aggregate stability and soil carbohydrates induced by the inoculation of soil with biocrusts. A well aggregated, granular structure increases the proportion of larger pores, thus increasing the infiltration rate of water [*Warren*, 2001]. Other studies also have reported an increase in ϕ during biocrust development and succession [*Lan et al.*, 2012; *Miralles-Mellado et al.*, 2011]. In particular, Lan et al. [2012] observed a simultaneous increase in crust photosynthetic biomass, exopolysaccharides and fine soil particle content, and thus attributed the changes in ϕ over the succession to those parameters.

Apart from providing organic carbon inputs to the soil (in the form of porous organic bodies, presumably extracellular polymeric substances), biocrusts are also able to delineate additional pores on surface with their penetrating filaments [*Malam Issa et al.*, 1999]. The increase in ϕ that we measured over succession provided better soil aeration, which can favor oxidative decomposition of SOM [*Luo & Zhou*, 2006]. Therefore, more porosity has the potential to enhance biological CO_2 production. It also has the potential to enhance the transport of CO_2 towards atmosphere by diffusion as

ϕ is a key parameter of CO_2 diffusion models in soils [*Sánchez-Cañete et al.*, 2017].

Consequently, as initially assumed, both enhanced CO_2 production and diffusion can partly explain together the greater CO_2 emissions as well as greater annual positive and total F_s in late successional stages. Further research should investigate through continuous measurements if those greater emissions could be offset by a parallel increase in photosynthesis in late successional stages, as already suggested by *ex-situ* experiments [e.g. *Grote et al.*, 2010]. That would explain why SOC accumulates in late succession stages in spite of greater CO_2 losses.

3.2.4.4. The mitigating effect of geo(bio)chemistry

Atypical patterns of χ_s reaching values below atmospheric CO_2 were measured at night, particularly in early stages of biocrust succession and most importantly in *Cyanobacteria* sites (Fig. 3). In theory, based on the First Fick´s law of molecular diffusion, the inversion of the soil-atmosphere CO_2 gradient due to low nocturnal χ_s values should generate negative F_s (uptake of atmospheric CO_2 by the soil). Negative F_s have been increasingly reported recently from drylands soils, which are now regarded as potential carbon sinks [e.g. *Ball et al.*, 2009; *Hamerlynck et al.*, 2013; *Ma et al.*, 2013]. The occurrence of such negative F_s was confirmed by chamber measurements at our site, where they exhibited values (on average -0.12 ± 0.06 µmol m^{-2} s^{-1}, ranging from -0.07 to -0.23 µmol m^{-2} s^{-1}) similar to those reported by Fa et al. [2016] (-0.11 and -0.20 µmol m^{-2} s^{-1}), Ball et al. [2009] (ca. 0.1-0.15 µmol m^{-2} s^{-1}) and Parsons et al. [2004] (-0.1 µmol m^{-2} s^{-1}). The nocturnal influxes that we measured were relatively small in magnitude but as they occurred almost continuously throughout the study, they were able to offset annual CO_2 emissions at some locations, generating an annual net carbon uptake, independently of photosynthesis. Sporadic influxes of greater magnitude were estimated from continuous χ_s measurements (up to -0.75 µmol m^{-2} s^{-1}) but still have to be confirmed by direct F_s measurements with chambers.

Soil CO_2 influxes have generally been attributed to different abiotic processes which are still debated and probably not unique. In this ecosystem, in light of our observations, we assume that a geochemical process of CO_2

dissolution in soil water followed by $CaCO_3$ dissolution might be involved. Soils can store an order of magnitude greater CO_2 as dissolved inorganic carbon (DIC) in the aqueous-filled relative to gas-filled pore space [*Angert et al.*, 2015]. In particular, soils with pH > 6.5 (like at this site, Table 2) can retain substantial amounts of CO_2 in the solution phase [*Sparling & West*, 1990] and a soil solution charged with CO_2 can enhance carbonates dissolution, thus consuming CO_2. Dissolution reaction time for soil calcite in solution is fast, generally on the order of 0.5 to 3 days [*Loeppert & Suarez*, 1996] and diel patterns have already been described e.g. [*Roland et al.*, 2013].

Here we present some evidence indicating that such a geochemical origin is likely:

(1) Our model of the annual cumulative negative F_s identified the CCE as a significant explanatory variable. The negative effect of CCE is in accordance with the following reaction of $CaCO_3$ dissolution removing CO_2 from the soil:

$$CaCO_{3\,(s)} + H_2O_{\,(l)} + CO_{2\,(g)} \rightarrow Ca^{2+}{}_{(aq)} + 2HCO_3^-{}_{(aq)} \qquad (4)$$

(2) At night, χ_s covaried with T_s closely following its pattern of decrease, and both minima coincided. This observation is in agreement with the well-known enhancement of gas dissolution in water (Henry´s law) and carbonate solubility at lower temperature.

(3) Our model of the annual cumulative negative F_s showed that fluxes were more negative where the mean annual T_s was higher (i.e. negative correlation, Table 3). This is congruent with our observations of greater negative F_s in early successional stages that receive more solar radiation and therefore have a greater mean annual T_s. Early successional stages underwent a larger diel amplitude of T_s (Fig. 2B). Larger diel thermal variations are likely to trigger diel cycles of $CaCO_3$ dissolution and precipitation of greater magnitude that respectively consume and produce CO_2 (according to the reverse reaction as eq. 4);

(4) Even at 45 cm in depth, χ_s became lower than atmospheric CO_2 values, but only during periods of T_s minima in winter, i.e. exactly when $CaCO_3$ solubility was expected to be maximal due to its enhancement by cold and moisture. Altogether, those observations suggest that negative F_s might be driven by an abiotic process of $CaCO_3$ dissolution in this ecosystem. Further

research should focus on the geochemical characterization and modeling of carbonate reactions from soil water samples in order to validate this assumption.

In addition, recent studies pointed out the existence of dark CO_2 fixation mechanisms by chemotrophs [*Akinyede et al.*, 2020; *Spohn et al.*, 2020; *Yang et al.*, 2017], even in deep soil horizons [*Šantrůčková et al.*, 2018] and thus a potential biotic origin should not be discounted. Biological and geochemical processes could also be tightly linked, as we measured maximal negative F_s below *Cyanobacteria*. Those organisms have been reported to be able to decrease the local extracellular ion activity product of $CaCO_3$ by taking up Ca^{2+}, promoting the dissolution of the mineral, the weathering capacity of *Cyanobacteria* being optimal in the presence of a short daily dark phase [*Garcia-Pichel et al.*, 2010].

The negative F_s of lower magnitude in late successional stages and their observation only in summer (when soil respiration was dramatically reduced) suggest that CO_2 consumption processes were masked by biological CO_2 production there. That is probably why those processes could mainly be detected in early successional stages and more generally in drylands, as they sustain only low biological activity. However, such processes could be ubiquitous in ecosystems but difficult to detect from F_s measurements alone [*Sánchez-Cañete et al.*, 2018].

3.2.4.5. Implications for climate-carbon cycle feedbacks

According to our predictive model, θ_w was the main driver of the χ_s dynamics and overall, its effect tended to be enhanced by T_s (Fig. 6). This result provides relevant information to the ongoing debate on whether the main regulator of the net land carbon flux is temperature or moisture variability, supporting recent studies stating that it is becoming increasingly evident that their interaction is fundamental but still largely neglected in most [*Piao et al.*, 2020; *Quan et al.*, 2019]. This is particularly true in drylands where the effect of T_s is strongly constrained by θ_w and antecedent moisture conditions play a key role in triggering ephemeral soil CO_2 pulses. This result also confirms that even if a positive feedback between the F_s and temperature is likely [*Hashimoto et al.*, 2015], global models still underrepresent drylands and are

often simplified in those areas with respect to their hydric status; therefore, future predictions require confirmation of their modelled processes in water-limited ecosystems.

One of the main difficulties in establishing predictions of the future feedback between F_s and climate change in drylands comes from the fact that climate change can have disparate effects: (1) from the one hand, soil drying is expected to reduce θ_w by 25% in a substantial portion of drylands worldwide [*Maestre et al.*, 2012]. This soil drying has the potential to reduce basal respiration over long periods of drought; (2) from the other hand, the rewetting of soils that have previously experienced long droughts can trigger short-lived but very large CO_2 emissions, which according to the results at our site, should be enhanced by the future rise in temperature (Fig. 6). Therefore, one question arises: which of these disparate effects will dominate the carbon balance of water-limited ecosystems?

In the ecosystem studied here, it was observed that basal F_s was close to zero most of the year, except after rain pulses (Fig. 1A-C). As a result, a reduction of basal F_s in response to increasing drought should be limited in comparison with the enhanced pulse response to precipitation in response to the combined effect of rising temperature and increasing drought that stimulates the Birch effect. Consequently, a future enhancement of soil CO_2 emissions is a more likely outcome of global warming at this site. However, the future response of F_s might differ in other drylands such as in those from subhumid climates as they are expected to sustain a greater basal respiration. In addition, since climate change is predicted to have a harmful effect on biocrusts cover and their carbon assimilation capacity [*Ferrenberg et al.*, 2015; *Maestre et al.*, 2013, 2015], biocrusted drylands like the one studied here which often have a carbon balance close to neutrality, could dangerously switch from carbon sinks to carbon sources. That could potentially generate a vicious cycle of positive feedback with climate change.

In order to predict with higher confidence the future trajectory of ecosystem carbon-climate feedbacks in drylands, it is urgent to invest more research efforts in understanding, quantifying and assessing the climatic sensitivity of natural ecosystem processes that mitigate CO_2 emissions, such as those involved in the CO_2 uptake by drylands soils. As those ecosystems

represent ca. 40% of the terrestrial surface, even small but continuous CO_2 uptake could significantly impact the global carbon budget and contribute to explain the “residual terrestrial carbon sink”.

3.2.5. Conclusions

The biocrust succession stage, soil water content (θ_w) and temperature (T_s) explained and predicted efficiently the soil CO_2 molar fraction (χ_s) daily dynamics. Among those factors, the effect of θ_w was preponderant and dependent on T_s and biocrust succession stage, as revealed by the important triple interaction in the developed model. Soil CO_2 emissions tended to be more sensitive to θ_w (and indirectly T_s) in late successional stages, most likely as a result of progressive soil organic carbon (SOC) accumulation mediated by biocrusts, resulting in greater substrate availability for microbial respiration, and higher porosity enhancing CO_2 diffusion. The calcium carbonate equivalent (CCE) content also played a role in explaining the occurrence of negative CO_2 fluxes (i.e. atmospheric CO_2 uptake by the soil) at nighttime. The cumulative annual CO_2 influx represented up to 115% of the cumulative annual CO_2 efflux, generating a net annual carbon uptake by soil in some locations. Here, we suggest that a geochemical process of CO_2 dissolution in soil water followed by $CaCO_3$ dissolution might be involved. However, a potential biological or geobiological origin should not be disregarded.

It is crucial to elucidate whether a biotic and/or an abiotic process is involved as (i) the global atmospheric CO_2 increase, warming and disruption of precipitation patterns can potentially affect in complex interacting, opposing and scale-dependent ways the carbonate dissolution rates; (ii) abiotic processes consuming CO_2 in soil would need to be separated from biocrust photosynthesis and respiration when measuring net surface CO_2 fluxes (especially at sunrise or sunset), to not overestimate and underestimate respectively the biotic contribution of those communities of microorganisms to the global carbon budget, and (iii) the sensitivity of carbon assimilation and respiration by soil chemotrophs to environmental factors such as pCO_2, θ_w and T_s is largely unknown.

Our modelling results suggest that a future enhancement of soil CO_2 emissions is a more likely outcome of global warming at this site. However, it is urgent to invest more research efforts in understanding, quantifying and assessing the climatic sensitivity of natural ecosystem processes able to mitigate CO_2 emissions, such as those involved in the CO_2 uptake by the extensive drylands soils.

Acknowledgements

This work was funded by the research project CGL2016-78075-P, Biocrust Dinamics (DINCOS), of the Spanish National Program of Scientific and Technical Research, and by the ICAERSA research project (P18-RT-3629) of the Andalusian Regional Government including European Union ERDF funds. We are grateful to Andrew S. Kowalski for the proofreading and insightful suggestions that considerably improved the manuscript, to Consuelo Rubio, for her help with the fieldwork, to Angel Belmonte, Montserrat Guerrero, Domingo Alvarez and Cecilio Oyonarte for helping us with the laboratory work; and we are grateful to the Viciana brothers, landowners of the El Cautivo experimental site, without whose kind consent to set up semi-permanent installations on their land, this research would not have been possible.

Supporting information

Table S1 Summary of fixed effects of the model of soil CO_2 molar fraction dynamics

Model fixed effect	Factor level	Mean β	SD	Lower	Upper
(Intercept)	(PD)	6.032	0.056	5.921	6.142
Succession stage	IC	-0.398	0.088	-0.570	-0.225
	MC	-0.126	0.085	-0.294	0.042
	MC2	-0.121	0.079	-0.276	0.034
	SD	-0.072	0.075	-0.219	0.075
	LI	-0.078	0.083	-0.242	0.085
	Salsola sp.	0.038	0.112	-0.181	0.257
	Lygeum sp.	0.090	0.109	-0.124	0.303
	Macrochloa sp.	0.140	0.105	-0.067	0.346
θ_w	(PD)	-0.688	0.779	-2.217	0.839
θ_w × Succession stage	IC	0.494	1.108	-1.682	2.668
	MC	-0.542	1.138	-2.776	1.691
	MC2	0.010	1.241	-2.427	2.445
	SD	0.923	1.086	-1.209	3.053
	LI	1.534	1.125	-0.675	3.741
	Salsola sp.	0.424	1.566	-2.651	3.496
	Lygeum sp.	1.946	1.344	-0.692	4.581
	Macrochloa sp.	-1.461	1.573	-4.549	1.624
T_s	(PD)	0.002	0.001	-0.001	0.005
T_s × Succession stage	IC	0.015	0.002	0.011	0.020
	MC	0.003	0.002	-0.001	0.007
	MC2	0.004	0.002	0.000	0.008
	SD	0.001	0.002	-0.002	0.005
	LI	0.001	0.002	-0.003	0.006
	Salsola sp.	-0.017	0.004	-0.025	-0.010
	Lygeum sp.	-0.015	0.004	-0.023	-0.006
	Macrochloa sp.	-0.016	0.003	-0.022	-0.009
$\theta_w \times T_s$	(PD)	0.145	0.011	0.124	0.167
$\theta_w \times T_s$ × Succession stage	IC	-0.038	0.017	-0.072	-0.004
	MC	-0.015	0.023	-0.061	0.030
	MC2	-0.108	0.022	-0.151	-0.065
	SD	-0.057	0.015	-0.087	-0.028

LI	0.021	0.021	-0.020	0.062
Salsola sp.	0.083	0.029	0.027	0.139
Lygeum sp.	0.032	0.036	-0.040	0.103
Macrochloa sp.	0.303	0.028	0.248	0.357

θ_w, soil water content; T_s, soil temperature; β, vector of regression coefficients; SD (column), standard deviation of β. PD, physical depositional crust; IC, incipient cyanobacterial crust; MC, mature cyanobacterial crust; SD (line), lichen community characterized by *S. lentigera* and *D. diacapsis*; LI, lichen community characterized *by L. isidiata*; MC2, mature cyanobacterial patches within SD site. Prior to modelling, the response variable was transformed with a natural logarithm. The model takes PD as baseline to generate β. Therefore, the intercept is the absolute estimated mean for this factor level. For strictly quantitative terms, β is also an absolute estimate corresponding to this baseline. By contrast, for terms involving factors, β describes relative variations from the baseline β of the considered factor. "Lower" and "upper" columns correspond to the 2.5% and 97.5% quantiles, respectively.

References

Akinyede, R., Taubert, M., Schrumpf, M., Trumbore, S., & Küsel, K. (2020). Rates of dark CO2 fixation are driven by microbial biomass in a temperate forest soil. *Soil Biology and Biochemistry*, *150*, 107950. https://doi.org/10.1016/j.soilbio.2020.107950

Angert, A., Yakir, D., Rodeghiero, M., Preisler, Y., Davidson, E., & Weiner, T. (2015). Using O2 to study the relationships between soil CO2 efflux and soil respiration. *Biogeosciences*, *12*, 2089–2099. https://doi.org/10.5194/bg-12-2089-2015

Ball, B. A., Virginia, R. A., Barrett, J. E., Parsons, A. N., & Wall, D. H. (2009). Interactions between physical and biotic factors influence CO2 flux in Antarctic dry valley soils. *Soil Biology and Biochemistry*, *41*(7), 1510–1517. https://doi.org/10.1016/j.soilbio.2009.04.011

Bastida, F., García, C., Fierer, N., Eldridge, D. J., Bowker, M. A., Abades, S., Alfaro, F. D., Berhe, A. A., Cutler, N. A., & Gallardo, A. (2019). Global ecological predictors of the soil priming effect. *Nature Communications*, *10*(1), 1–9. https://doi.org/10.1038/s41467-019-11472-7

Belnap, J. (2003a). Microbes and microfauna associated with biological soil crusts. In *Biological soil crusts: structure, function, and management* (pp. 167–174). Springer. https://doi.org/10.1007/978-3-642-56475-8_14

Belnap, J. (2003b). The world at your feet: desert biological soil crusts. *Frontiers in Ecology and the Environment*, *1*(4), 181–189. https://doi.org/10.1890/1540-9295(2003)001[0181:TWAYFD]2.0.CO;2

Belnap, J., & Lange, O. L. (2003). *Biological Soil Crusts: Structure, Function, and Management*. Springer-Verlag Berlin Heidelberg New York.

Belnap, J., Prasse, R., & Harper, K. T. (2003). Influence of biological soil crusts on soil environments and vascular plants. In *Biological soil crusts: structure, function, and management* (pp. 281–300). Springer. https://doi.org/10.1007/978-3-642-56475-8_21

Bernoux, M., & Chevallier, T. (2014). Carbon in dryland soils. Multiple essential functions. *Les Dossiers Thématiques Du CSFD*, *10*.

Beymer, R. J., & Klopatek, J. M. (1991). Potential contribution of carbon by microphytic crusts in pinyon-juniper woodlands. *Arid Land Research and Management*, *5*(3), 187–198.

https://doi.org/http://doi.org/10.1080/15324989109381279

Blagodatskaya, E., & Kuzyakov, Y. (2011). Priming effects in relation to soil conditions–mechanisms. *Encyclopedia of Agrophysics. Springer, Dordrecht*, 657–667. https://doi.org/10.1007/978-90-481-3585-1_128

Bowling, D. R., Grote, E. E., & Belnap, J. (2011). Rain pulse response of soil CO2 exchange by biological soil crusts and grasslands of the semiarid Colorado Plateau, United States. *Journal of Geophysical Research: Biogeosciences*, *116*(G3). https://doi.org/10.1029/2011JG001643

Burow, L. C., Woebken, D., Marshall, I. P. G., Lindquist, E. A., Bebout, B. M., Prufert-Bebout, L., Hoehler, T. M., Tringe, S. G., Pett-Ridge, J., & Weber, P. K. (2013). Anoxic carbon flux in photosynthetic microbial mats as revealed by metatranscriptomics. *The ISME Journal*, *7*(4), 817–829. https://doi.org/10.1038/ismej.2012.150

Cameletti, M., Lindgren, F., Simpson, D., & Rue, H. (2013). Spatio-temporal modeling of particulate matter concentration through the SPDE approach. *AStA Advances in Statistical Analysis*, *97*(2), 109–131. https://doi.org/10.1007/s10182-012-0196-3

Chamizo, S., Cantón, Y., Miralles, I., & Domingo, F. (2012). Biological soil crust development affects physicochemical characteristics of soil surface in semiarid ecosystems. *Soil Biology and Biochemistry*, *49*, 96–105. https://doi.org/10.1016/J.SOILBIO.2012.02.017

Chapin III, S. F., McFarland, J., David McGuire, A., Euskirchen, E. S., Ruess, R. W., & Kielland, K. (2009). The changing global carbon cycle: linking plant–soil carbon dynamics to global consequences. *Journal of Ecology*, *97*(5), 840–850. https://doi.org/10.1111/j.1365-2745.2009.01529.x

Elbert, W., Weber, B., Burrows, S., Steinkamp, J., Büdel, B., Andreae, M. O., & Pöschl, U. (2012). Contribution of cryptogamic covers to the global cycles of carbon and nitrogen. *Nature Geoscience*, *5*(7), 459–462. https://doi.org/10.1038/ngeo1486

Esteban, M., Webersik, C., Leary, D., & Thompson-Pomeroy, D. (2008). *Innovation in Responding to Climate Change: Nanotechnology, Ocean Energy and Forestry, United Nations University Institute of Advanced Studies*.

Evans, R. D., & Ehleringer, J. R. (1993). A Break in the Nitrogen Cycle in

Aridlands? Evidence from δ ^{15}N of Soils. *Oecologia*, *94*(3), 314–317. http://www.jstor.org/stable/4220356

Fa, K.-Y., Zhang, Y.-Q., Wu, B., Qin, S.-G., Liu, Z., & She, W.-W. (2016). Patterns and possible mechanisms of soil CO2 uptake in sandy soil. *Science of the Total Environment*, *544*, 587–594. https://doi.org/10.1016/j.scitotenv.2015.11.163

Ferrenberg, S., Reed, S. C., Belnap, J., & Schlesinger, W. H. (2015). Climate change and physical disturbance cause similar community shifts in biological soil crusts. *Proceedings of the National Academy of Sciences of the United States of America*, *112*(39), 12116–12121. https://doi.org/10.1073/PNAS.1509150112/-/DCSUPPLEMENTAL

Ferrenberg, S., Tucker, C. L., & Reed, S. C. (2017). Biological soil crusts: diminutive communities of potential global importance. *Frontiers in Ecology and the Environment*, *15*(3), 160–167. https://doi.org/10.1002/fee.1469

Gallagher, T. M., & Breecker, D. O. (2020). The Obscuring Effects of Calcite Dissolution and Formation on Quantifying Soil Respiration. *Global Biogeochemical Cycles*, *34*(12), e2020GB006584. https://doi.org/10.1029/2020GB006584

Garcia-Pichel, F., Ramírez-Reinat, E., & Gao, Q. (2010). Microbial excavation of solid carbonates powered by P-type ATPase-mediated transcellular Ca2+ transport. *Proceedings of the National Academy of Sciences*, *107*(50), 21749–21754. https://doi.org/10.1073/pnas.1011884108

Gershenson, A., Bader, N. E., & Cheng, W. (2009). Effects of substrate availability on the temperature sensitivity of soil organic matter decomposition. *Global Change Biology*, *15*(1), 176–183. https://doi.org/10.1111/j.1365-2486.2008.01827.x

Grote, E. E., Belnap, J., Housman, D. C., & Sparks, J. P. (2010). Carbon exchange in biological soil crust communities under differential temperatures and soil water contents: implications for global change. *Global Change Biology*, *16*(10), 2763–2774. https://doi.org/10.1111/j.1365-2486.2010.02201.x

Grubb, M. (2004). Technology innovation and climate change policy: an overview of issues and options. *Keio Economic Studies*, *41*(2), 103–132.

Guenet, B., Camino-Serrano, M., Ciais, P., Tifafi, M., Maignan, F., Soong, J. L.,

& Janssens, I. A. (2018). Impact of priming on global soil carbon stocks. *Global Change Biology*, *24*(5), 1873–1883. https://doi.org/10.1111/gcb.14069

Hamerlynck, E. P., Scott, R. L., Sánchez-Cañete, E. P., & Barron-Gafford, G. A. (2013). Nocturnal soil CO2 uptake and its relationship to subsurface soil and ecosystem carbon fluxes in a Chihuahuan Desert shrubland. *Journal of Geophysical Research: Biogeosciences*, *118*(4), 1593–1603. https://doi.org/10.1002/2013JG002495

Hashimoto, S., Carvalhais, N., Ito, A., Migliavacca, M., Nishina, K., & Reichstein, M. (2015). Global spatiotemporal distribution of soil respiration modeled using a global database. *Biogeosciences*, *12*, 4121–4132. https://doi.org/10.5194/bg-12-4121-2015

Houghton, R. A., Baccini, A., & Walker, W. S. (2018). Where is the residual terrestrial carbon sink? *Global Change Biology*, *24*(8), 3277–3279. https://doi.org/10.1111/gcb.14313

Housman, D. C., Powers, H. H., Collins, A. D., & Belnap, J. (2006). Carbon and nitrogen fixation differ between successional stages of biological soil crusts in the Colorado Plateau and Chihuahuan Desert. *Journal of Arid Environments*, *66*(4), 620–634. https://doi.org/10.1016/j.jaridenv.2005.11.014

Huntzinger, D. N., Michalak, A. M., Schwalm, C., Ciais, P., King, A. W., Fang, Y., Schaefer, K., Wei, Y., Cook, R. B., & Fisher, J. B. (2017). Uncertainty in the response of terrestrial carbon sink to environmental drivers undermines carbon-climate feedback predictions. *Scientific Reports*, *7*(1), 1–8. https://doi.org/10.1038/s41598-017-03818-2

IPCC. (2013). Climate change 2013: The physical science basis. In T. F. Stocker, D. Qin, G.-K. Plattner, M. Tignor, S. K. Allen, J. Boschung, A. Nauels, Y. Xia, V. Bex, & P. M. Midgley (Eds.), *Contribution of Working Group I to the Fifth Assessment Report of the Intergovernmental Panel on Climate Change*. Cambridge University Press.

Lan, S., Wu, L., Zhang, D., & Hu, C. (2012). Successional stages of biological soil crusts and their microstructure variability in Shapotou region (China). *Environmental Earth Sciences*, *65*(1), 77–88. https://doi.org/http://dx.doi.org/10.1007/s12665-011-1066-0

Lázaro, R., Cantón, Y., Solé-Benet, A., Bevan, J., Alexander, R., Sancho, L. G., & Puigdefábregas, J. (2008). The influence of competition between lichen colonization and erosion on the evolution of soil surfaces in the Tabernas badlands (SE Spain) and its landscape effects. *Geomorphology*, *102*(2), 252–266. https://doi.org/10.1016/j.geomorph.2008.05.005

Le Quéré, C., Andrew, R. M., Friedlingstein, P., Sitch, S., Hauck, J., Pongratz, J., Pickers, P. A., Korsbakken, J. I., Peters, G. P., & Canadell, J. G. (2018). Global carbon budget 2018. *Earth System Science Data*, *10*(4), 2141–2194. https://doi.org/10.5194/essd-10-2141-2018

Leon, E., Vargas, R., Bullock, S., Lopez, E., Panosso, A. R., & La Scala, N. (2014). Hot spots, hot moments, and spatio-temporal controls on soil CO2 efflux in a water-limited ecosystem. *Soil Biology and Biochemistry*, *77*, 12–21. https://doi.org/10.1016/j.soilbio.2014.05.029

Liu, Y.-R., Delgado-Baquerizo, M., Wang, J.-T., Hu, H.-W., Yang, Z., & He, J.-Z. (2018). New insights into the role of microbial community composition in driving soil respiration rates. *Soil Biology and Biochemistry*, *118*, 35–41. https://doi.org/10.1016/j.soilbio.2017.12.003

Loeppert, R. H., & Suarez, D. L. (1996). Carbonate and gypsum. *Methods of Soil Analysis: Part 3 Chemical Methods*, *5*, 437–474. https://doi.org/10.2136/sssabookser5.3.c15

Lopez-Canfin, C., Sánchez-Cañete, E. P., & Lazaro, R. (2021). Development of a new low-cost device to measure calcium carbonate content, reactive surface area in solid samples and dissolved inorganic carbon content in water samples. *Methods in Ecology and Evolution*. https://doi.org/10.1111/2041-210X.13579

Lopez-Canfin, C., Sánchez-Cañete, E. P., Serrano-Ortiz, P., López-Ballesteros, A., Domingo, F., Kowalski, A. S., & Oyonarte, C. (2018). From microhabitat to ecosystem: identifying the biophysical factors controlling soil CO2 dynamics in a karst shrubland. *European Journal of Soil Science*, *69*(6), 1018–1029. https://doi.org/10.1111/ejss.12710

Luo, Y., Keenan, T. F., & Smith, M. (2015). Predictability of the terrestrial carbon cycle. *Global Change Biology*, *21*(5), 1737–1751. https://doi.org/10.1111/gcb.12766

Luo, Y., & Zhou, X. (2006). *Soil respiration and the environment*. Academic Press.

Ma, J., Wang, Z.-Y., Stevenson, B. A., Zheng, X.-J., & Li, Y. (2013). An inorganic CO2 diffusion and dissolution process explains negative CO2 fluxes in saline/alkaline soils. *Scientific Reports*, *3*, 2025. https://doi.org/10.1038/srep02025

Maestre, F. T., Escolar, C., Bardgett, R. D., Dungait, J. A. J., Gozalo, B., & Ochoa, V. (2015). Warming reduces the cover and diversity of biocrust-forming mosses and lichens, and increases the physiological stress of soil microbial communities in a semi-arid Pinus halepensis plantation. *Frontiers in Microbiology*, *6*(AUG). https://doi.org/10.3389/FMICB.2015.00865/ABSTRACT

Maestre, F. T., Escolar, C., de Guevara, M. L., Quero, J. L., Lázaro, R., Delgado-Baquerizo, M., Ochoa, V., Berdugo, M., Gozalo, B., & Gallardo, A. (2013). Changes in biocrust cover drive carbon cycle responses to climate change in drylands. *Global Change Biology*, *19*(12), 3835–3847. https://doi.org/10.1111/GCB.12306

Maestre, F. T., Salguero-Gó Mez, R., Quero, J. L., Rey, U., Carlos, J., & Tulipán, C. /. (2012). It is getting hotter in here: determining and projecting the impacts of global environmental change on drylands. *Philosophical Transactions of the Royal Society B: Biological Sciences*, *367*(1606), 3062–3075. https://doi.org/10.1098/RSTB.2011.0323

Maier, S., Tamm, A., Wu, D., Caesar, J., Grube, M., & Weber, B. (2018). Photoautotrophic organisms control microbial abundance, diversity, and physiology in different types of biological soil crusts. *The ISME Journal*, *12*(4), 1032–1046. https://doi.org/10.1038/s41396-018-0062-8

Malam-Issa, O., Trichet, J., Défarge, C., Couté, A., & Valentin, C. (1999). Morphology and microstructure of microbiotic soil crusts on a tiger bush sequence (Niger, Sahel). *Catena*, *37*(1–2), 175–196.

Mingorance, M. D., Barahona, E., & Fernández-Gálvez, J. (2007). Guidelines for improving organic carbon recovery by the wet oxidation method. *Chemosphere*, *68*(3), 409–413. https://doi.org/10.1016/j.chemosphere.2007.01.021

Miralles-Mellado, I., Cantón, Y., & Solé-Benet, A. (2011). Two-dimensional porosity of crusted silty soils: Indicators of soil quality in semiarid rangelands? *Soil Science Society of America Journal*, *75*(4), 1330–1342.

https://doi.org/10.2136/sssaj2010.0283

Moreira-Grez, B., Tam, K., Cross, A. T., Yong, J. W. H., Kumaresan, D., Nevill, P., Farrell, M., & Whiteley, A. S. (2019). The bacterial microbiome associated with arid biocrusts and the biogeochemical influence of biocrusts upon the underlying soil. *Frontiers in Microbiology*, *10*, 2143. https://doi.org/10.3389/fmicb.2019.02143

Parsons, A. N., Barrett, J. E., Wall, D. H., & Virginia, R. A. (2004). Soil carbon dioxide flux in Antarctic dry valley ecosystems. *Ecosystems*, *7*(3), 286–295. https://doi.org/10.1007/s10021-003-0132-1

Piao, S., Wang, X., Wang, K., Li, X., Bastos, A., Canadell, J. G., Ciais, P., Friedlingstein, P., & Sitch, S. (2020). Interannual variation of terrestrial carbon cycle: Issues and perspectives. *Global Change Biology*, *26*(1), 300–318. https://doi.org/10.1111/gcb.14884

Pinheiro, J. C., & Bates, D. M. (2000). *Mixed-Effects Models in S and S-Plus*. Springer-Verlag New York.

Porada, P., Weber, B., Elbert, W., Pöschl, U., & Kleidon, A. (2013). Estimating global carbon uptake by lichens and bryophytes with a process-based model. *Biogeosciences*, *10*(11), 6989–7033. https://doi.org/10.5194/bg-10-6989-2013

Quan, Q., Tian, D., Luo, Y., Zhang, F., Crowther, T. W., Zhu, K., Chen, H. Y. H., Zhou, Q., & Niu, S. (2019). Water scaling of ecosystem carbon cycle feedback to climate warming. *Science Advances*, *5*(8), eaav1131. https://doi.org/http://dx.doi.org/10.1126/sciadv.aav1131

Quemada, M., & Cabrera, M. L. (1997). Temperature and moisture effects on C and N mineralization from surface applied clover residue. *Plant and Soil*, *189*(1), 127–137. https://doi.org/10.1023/A:1004281804058

R Core Team (2019). *R: A Language and Environment for Statistical Computing*. R Foundation for Statistical Computing. https://www.r-project.org/

Reichstein, M., Rey, A., Freibauer, A., Tenhunen, J., Valentini, R., Banza, J., Casals, P., Cheng, Y., Grünzweig, J. M., & Irvine, J. (2003). Modeling temporal and large-scale spatial variability of soil respiration from soil water availability, temperature and vegetation productivity indices. *Global Biogeochemical Cycles*, *17*(4). https://doi.org/10.1029/2003GB002035

Reid, W. V, Mooney, H. A., Cropper, A., Capistrano, D., Carpenter, S. R.,

Chopra, K., Dasgupta, P., Dietz, T., Duraiappah, A. K., & Hassan, R. (2005). Millennium Ecosystem Assessment. Ecosystems and human well-being: synthesis. *World Resources Institute, Washington, DC*.

Rogers, S. L., & Burns, R. G. (1994). Changes in aggregate stability, nutrient status, indigenous microbial populations, and seedling emergence, following inoculation of soil with Nostoc muscorum. *Biology and Fertility of Soils*, *18*(3), 209–215. https://doi.org/10.1007/BF00647668

Roland, M., Serrano-Ortiz, P., Kowalski, A. S., Goddéris, Y., Sánchez-Cañete, E. P., Ciais, P., Domingo, F., Cuezva, S., Sanchez-Moral, S., & Longdoz, B. (2013). Atmospheric turbulence triggers pronounced diel pattern in karst carbonate geochemistry. *Biogeosciences*, *10*(7), 5009–5017. https://doi.org/10.5194/bg-10-5009-2013

Rue, H., Martino, S., & Chopin, N. (2009). Approximate Bayesian inference for latent Gaussian models by using integrated nested Laplace approximations. *Journal of the Royal Statistical Society: Series b (Statistical Methodology)*, *71*(2), 319–392. https://doi.org/10.1111/j.1467-9868.2008.00700.x

Sánchez-Cañete, E. P., Barron-Gafford, G. A., & Chorover, J. (2018). A considerable fraction of soil-respired CO2 is not emitted directly to the atmosphere. *Scientific Reports*, *8*(1), 13518. https://doi.org/10.1038/s41598-018-29803-x

Sánchez-Cañete, E. P., Scott, R. L., van Haren, J., & Barron-Gafford, G. A. (2017). Improving the accuracy of the gradient method for determining soil carbon dioxide efflux. *Journal of Geophysical Research: Biogeosciences*, *122*(1), 50–64.

Šantrůčková, H., Kotas, P., Bárta, J., Urich, T., Čapek, P., Palmtag, J., Alves, R. J. E., Biasi, C., Diáková, K., & Gentsch, N. (2018). Significance of dark CO2 fixation in arctic soils. *Soil Biology and Biochemistry*, *119*, 11–21. https://doi.org/http://dx.doi.org/10.1016/j.soilbio.2017.12.021

Sparling, G. P., & West, A. W. (1990). A comparison of gas chromatography and differential respirometer methods to measure soil respiration and to estimate the soil microbial biomass. *Pedobiologia*, *34*(2), 103–112.

Spohn, M., Müller, K., Höschen, C., Mueller, C. W., & Marhan, S. (2020). Dark microbial CO2 fixation in temperate forest soils increases with CO2

concentration. *Global Change Biology*, *26*(3), 1926–1935. https://doi.org/10.1111/gcb.14937

Sponseller, R. A. (2007). Precipitation pulses and soil CO2 flux in a Sonoran Desert ecosystem. *Global Change Biology*, *13*(2), 426–436. https://doi.org/10.1111/j.1365-2486.2006.01307.x

Vargas, R., Carbone, M. S., Reichstein, M., & Baldocchi, D. D. (2011). Frontiers and challenges in soil respiration research: from measurements to model-data integration. *Biogeochemistry*, *102*(1–3), 1–13. https://doi.org/10.1007/s10533-010-9462-1

Vargas, R., Sánchez-Cañete P, E., Serrano-Ortiz, P., Curiel Yuste, J., Domingo, F., López-Ballesteros, A., & Oyonarte, C. (2018). Hot-moments of soil CO2 efflux in a water-limited grassland. *Soil Systems*, *2*(3), 47. https://doi.org/10.3390/soilsystems2030047

Warren, S. D. (2001). Synopsis: influence of biological soil crusts on arid land hydrology and soil stability. In *Biological soil crusts: Structure, function, and management* (pp. 349–360). Springer. https://doi.org/http://dx.doi.org/10.1007/978-3-642-56475-8_26

Weber, B., Büdel, B., & Belnap, J. (2016). Biological soil crusts as an organizing principle in drylands. In *Biological soil crusts: an organizing principle in drylands*. Springer International Publishing AG. https://doi.org/http://dx.doi.org/10.1007/978-3-319-30214-0_1

Wilske, B., Burgheimer, J., Karnieli, A., Zaady, E., Andreae, M. O., Yakir, D., & Kesselmeier, J. (2008). The CO2 exchange of biological soil crusts in a semiarid grass-shrubland at the northern transition zone of the Negev desert, Israel. *Biogeosciences Discussions*, *5*(3), 1969–2001. https://doi.org/10.5194/bg-5-1411-2008

Yang, J., Kang, Y., Sakurai, K., & Ohnishi, K. (2017). Fixation of carbon dioxide by chemoautotrophic bacteria in grassland soil under dark conditions. *Acta Agriculturae Scandinavica, Section B—Soil & Plant Science*, *67*(4), 362–371. https://doi.org/10.1080/09064710.2017.1281433

Zuur, A. F., & Ieno, E. N. (2016). A protocol for conducting and presenting results of regression-type analyses. *Methods in Ecology and Evolution*, *7*(6), 636–645. https://doi.org/10.1111/2041-210X.12577

Zuur, A. F., Ieno, E. N., & Saveliev, A. A. (2017). Spatial, temporal and spatial–temporal ecological data analysis with R-INLA. *Highland Statistics Ltd*, *1*.

3.3. CHAPTER 3

Water vapor adsorption by dry soils: a potential link between the water and carbon cycles

Accepted for publication in *Science of the Total Environment.* February 2022.

Lopez Canfin, C., Lázaro, R., & Sánchez-Cañete P, E. (2022). Water vapor adsorption by dry soils: a potential link between the water and carbon cycles. Science of the Total Environment.

Graphical abstract

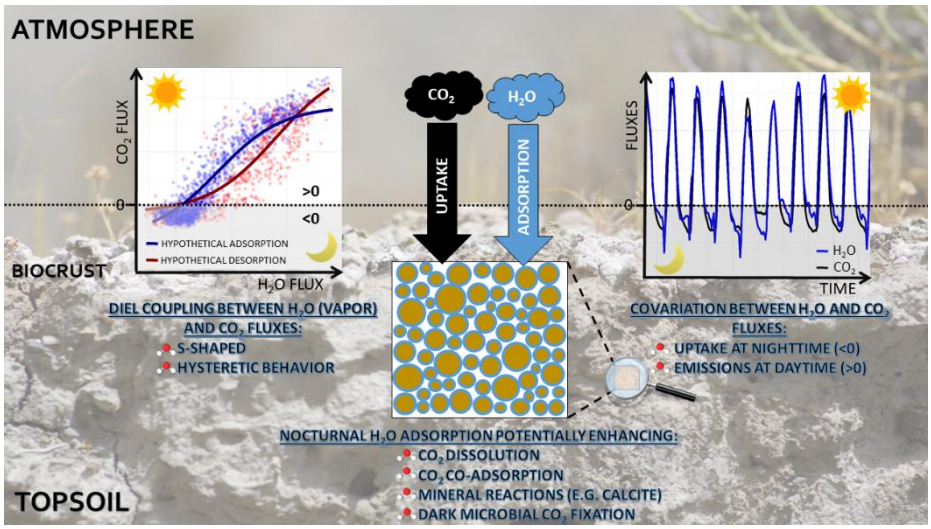

Abstract

Water vapor adsorption (WVA) by soil is a potential contributor to the water cycle in drylands. However, continuous *in-situ* estimates of WVA are still scarce and the understanding of its coupling with carbon cycle and ecosystem processes remains at an incipient stage.

Here we aimed to (1) identify periods of WVA and improve the understanding of the underlying processes involved in its temporal patterns by using the gradient method; (2) characterize a potential coupling between water vapor and CO_2 fluxes, and (3) explore the effect of soil properties and biocrusts ecological succession on fluxes. We assumed that the nocturnal soil CO_2 uptake increasingly reported in those environments could come from WVA enhancing geochemical reactions involving calcite.

We measured continuously during ca. 2 years the relative humidity and CO_2 molar fraction in soil and atmosphere, in association with below- and aboveground variables, over the biocrusts ecological succession. We estimated water vapor and CO_2 fluxes with the gradient method, and cumulative fluxes over the study. Then, we used statistical modelling to explore relationships between variables.

Our main findings are (1) WVA fluxes during hot and dry periods, and new insights on their underlying mechanisms; (2) a diel coupling between water vapor and CO_2 fluxes and between cumulative fluxes, well predicted by our models; and (3) cumulative CO_2 influxes increasing with specific surface area in early succession stages, thus mitigating CO_2 emissions.

During summer drought, as WVA was the main water source, it probably maintained ecosystem processes such as microbial activity and mineral reactions in this dryland. We suggest that WVA could drive the nocturnal CO_2 uptake in those moments and discuss biogeochemical mechanisms potentially involved. Additional research is needed to monitor soil water vapor and CO_2 uptake and separate their biotic and abiotic components as those sinks could grow with climate change.

3.3.1. Introduction

Non-rainfall water inputs (NRWIs) are critical components of the water cycle in drylands [*Agam & Berliner*, 2006; *Wang et al.*, 2017]; in the absence of precipitation, three processes contribute to soil water inputs to the topsoil: (1) fog deposition, (2) dew formation, and (3) water vapor adsorption (WVA). Fog deposition occurs when water vapor pressure reaches saturation, forming water droplets in the air that can deposit on surfaces. Dew formation occurs on a surface when its temperature is lower than or equal to the dew-point temperature of air, at which time the atmospheric water vapor in contact with the surface cools down, reaches saturation and condenses on the surface. WVA occurs when the water vapor pressure of the atmosphere is greater than the water vapor pressure of the soil air, triggering its diffusion from atmosphere towards soil and its retention on the surface of soil particles in a liquid form (water films), through complex physico-chemical mechanisms still not fully constrained [*Akin & Likos*, 2017]. Hence, which NRWI is preponderant in an ecosystem depends on micrometeorological conditions.

In most drylands, atmospheric conditions required for fog formation are rarely met [*McHugh et al.*, 2015]. Dew formation was considered until recently as the main NRWI, sometimes exceeding precipitation in amount or frequency, or being the sole source of water for plants and biological soil crusts [*Agam & Berliner*, 2006]. Therefore, dew formation has been extensively studied; however, it has been regularly confounded with WVA and its contribution to the water cycle has probably been overestimated, as favorable thermal conditions for dew deposition are rather uncommon in drylands, particularly on bare soil in hot environments or seasons [*Agam & Berliner*, 2006]. In comparison, WVA by soil has received little attention despite the fact that it can occur on a more regular basis, even when soil surface temperature is greater than dew point temperature. It is now considered as a likely substantial contributor to the water cycle in drylands [*McHugh et al.*, 2015], which cover about 41% of the Earth´s terrestrial surface. Moreover, since warmer air has the capacity to hold more water vapor, and soil drying is predicted with high confidence in some regions of the globe [*Collins et al.*, 2013], WVA by soil might be enhanced by climate change.

In spite of the potential global importance of WVA, *in situ* estimates of the process are still very scarce. Only few studies aimed to monitor WVA fluxes and they were almost always restricted to short time periods [*Agam & Berliner*, 2006; *Kosmas et al.*, 2001; *Uclés et al.*, 2015; *Verhoef et al.*, 2006], with few exeptions [*Kohfahl et al.*, 2021; *Saaltink et al.*, 2020]. That is partly due to a methodological gap as traditional approaches to estimate WVA fluxes include either complex numerical modelling using numerous parameters that require substantial effort to collect, or expensive lysimeters that can disturb the natural soil profile and pedoclimatic conditions. By contrast, the gradient method that has been increasingly used recently to determine soil-atmosphere greenhouse gases fluxes [*Maier & Schack-Kirchner*, 2014; *Sánchez-Cañete et al.*, 2017] could represent a suitable approach to obtain estimates of WVA as it is easy to deploy, generates only limited soil perturbation, and can provide long-term continuous measurements and further understanding of the belowground mechanisms involved in WVA.

The gradient method is based on the main assumption that molecular diffusion is the dominant gas transport process between soil and atmosphere, a condition that is generally considered to be fulfilled both for CO_2 [*Šimůnek and Suarez*, 1993] and water vapor [*Liu et al.*, 2020]. The only drawback of this method is that the estimated flux is highly dependent on the chosen coefficient of diffusion and therefore, it is recommended to apply a site-specific calibration to improve the accuracy the flux estimation. For CO_2, this calibration can be performed with soil chamber measurements [*Sánchez-Cañete et al.*, 2017]. However, for water vapor, no standardized procedure exist yet as soil-atmosphere diffusive fluxes of water vapor have seldom been estimated and most studies were limited to laboratory experiments [e.g. *Jabro & Jabro*, 2008; *Rao & Rekapalli*, 2020; *Reyzabal & Bazán*, 1992]. Only one study estimating those fluxes in-situ was found in the literature [*Bittelli et al.*, 2008]. If a substantial contribution of WVA to the water cycle in drylands were confirmed by more observational studies including accurate continuous monitoring, the process could potentially impact other element cycles and ecosystem processes, as they are strongly constrained by water availability in those environments.

In particular, the understanding of the coupling between WVA, carbon cycle and ecosystem processes remains at an incipient stage; nevertheless,

WVA could enhance water-limited microbial activity and mineral reactions in drylands. For example, some lichens have the capacity to use water vapor [*Lange et al.*, 1992, 1994; *Zheng et al.*, 2018]. A previous study found that WVA increased soil CO_2 production revealing that dryland microorganisms were able to use this water input to sustain their metabolic activity [*McHugh et al.*, 2015]. Other studies reported that dew contributed to rock weathering and karst development in drylands [*Agam & Berliner*, 2006]. Therefore, WVA is also expected to be a weathering agent of soil minerals. In particular, WVA on calcite is energetically favorable [*Rahaman et al.*, 2008] and can lead to the formation of carbonate species and reorganization of the mineral surface [*Rubasinghege & Grassian*, 2013]. Since microbial and mineral (e.g. calcite) processes can produce/consume CO_2 via respiration/assimilation and precipitation/dissolution respectively, the enhancement of those processes by WVA is likely to affect the soil-atmosphere CO_2 exchange in drylands.

Nocturnal CO_2 uptake by soil has been increasingly reported in water-limited ecosystems [*Fa et al.*, 2016; *Hamerlynck et al.*, 2013; *Ma et al.*, 2013], including at our study site [*Lopez Canfin et al.*, n.d.], and its origin remains debated [*Sagi et al.*, 2021]; different abiotic forces have been suggested to drive the phenomenon but the potential effect of WVA on both biotic and abiotic components of the ecosystem has not been explored yet. On the one hand, drylands shelter a rich biodiversity of biological soil crusts (hereafter, biocrusts), key ecosystem engineers that sustain many important ecological functions including an ability to fix CO_2 by photosynthesis. In addition, there is growing evidence that among those communities, chemotrophs able to perform CO_2 fixation in the dark coexist with phototrophs [*Bay et al.*, 2021; *Liu et al.*, 2021]. On the other hand, the abiotic assumption of calcite dissolution consuming CO_2 to explain the nocturnal CO_2 uptake by soil has been challenged by the supposition that, since the geochemical reaction consumes water, such uptake should not occur in dry soils [*Schlesinger et al.*, 2009]. This is without considering WVA as a potential link between the water and carbon cycle in drylands. Biotic and abiotic processes could also be tightly coupled, as for example microorganisms such as *Cyanobacteria* or fungi can promote the dissolution of $CaCO_3$ [*Garcia-Pichel et al.*, 2010; *Tian et al.*, 2021].

Assessing the role of WVA in drylands requires improved characterization of its drivers *in-situ*. The amount of adsorbed water in the soil depends on the magnitude of the soil-atmosphere vapor gradient, and the total surface area of soil particles [*Kool et al.*, 2021]. Since clay particles have the largest surface area, the amount of adsorbed water generally increases with the soil clay content; the clay type also affects the amount of adsorbed water as surface area varies between clay types [*Agam & Berliner*, 2006]. Soil organic carbon content and salinity have been reported as well as factors controlling WVA [*Amer*, 2019; *Arthur et al.*, 2020]. However, to our knowledge, the soil content in gypsum, a common salt at Earth surface, has never been investigated as a potential driver of soil-atmosphere water vapor fluxes; gypsum is more soluble than calcite and has strong hydration/dehydration properties, with dehydration starting at ca. 40°C [*Azimi et al.*, 2007], a temperature range that can be easily reached in drylands topsoil.

In this research we aimed to (i) identify periods of WVA and improve the understanding of the underlying processes involved in its temporal patterns by using the gradient method; (ii) characterize a potential coupling between water vapor and CO_2 fluxes; and (iii) explore the effect of soil properties and biocrusts ecological succession on fluxes. We assumed that (i) the gradient method could be used to measure the diffusion of water vapor from atmosphere to soil, considering those influxes as proxies of WVA; WVA should be substantial during the dry period due to enhanced soil drying during daytime, magnifying the soil-atmosphere water vapor pressure gradient; (ii) fluxes of water vapor and CO_2 could be tightly coupled. In particular, WVA was expected to be the underlying process controlling nocturnal CO_2 uptake; and (iii) soil surface area, gypsum content and biocrusts ecological succession could significantly affect WVA.

3.3.2. Material and methods

3.3.2.1. Experimental Site

This study was conducted in the experimental site of El Cautivo, an area of badlands located in the Tabernas Desert (Almería, Spain) (more information about the study site is provided in Section 2.1).

3.3.2.2. Environmental measurements and soil analyses

Continuous measurements of soil and above-surface variables were conducted during ca. two years (see Section 2.3.3). The soil-atmosphere CO_2 flux was also measured regularly with portable soil chambers (see Section 2.3.1).

In the topsoil (0-5cm), the porosity (ϕ), the soil total specific surface area (SSA_s), gypsum content, calcium carbonate equivalent content (CCE), calcite reactive surface area (RSA), calcite specific surface area (SSA_c, calcite RSA per weight of calcite) and soil organic content (SOC) were measured within each microsite described above. The SSA_s was estimated from the particle size distribution measured by a laser particle size analyzer (Mastersizer 3000 Hydro EV, Malvern Panalytical, Malvern, United Kingdom), assuming that the particles were spherical and non-porous. The SOC content was measured by a modified wet oxidation method [*Mingorance et al.*, 2007] and determined with a spectrophotometer (Spectronic Helios Alpha 9423 UVA 1002E, Thermo Fisher Scientific, Waltham, MA, USA). The gypsum content was determined by exploiting the gypsum-bassanite phase change [*Lebron et al.*, 2009]. The CCE and RSA were quantified by measuring the CO_2 released during an acidic reaction [*Lopez-Canfin et al.*, 2021].

3.3.2.3. Data processing, water vapor and CO_2 fluxes calculation

Hourly averages were calculated on the data. To fill data gaps and enable the modelling of time series as well as the determination of cumulative fluxes, a gap-filling procedure was applied (see Section 2.4.1).

The water vapor pressure in soil and atmosphere was calculated as:

$$P_{\mathrm{h}} = \frac{RH}{100} P_{\mathrm{s}} \qquad (1)$$

where P_h is the water vapor pressure (kPa), RH is the relative humidity (%) measured with the iButton® DS1923 loggers and P_s is the saturation water vapor pressure calculated according to Buck [1981] using the air temperature measured with the S-THB-M00x Smart Sensor (since it was protected against direct radiation and radiative cooling) and the soil temperature measured with the iButton® DS1923 logger.

The water vapor molar fraction in soil and atmosphere was calculated as:

$$\chi_{\mathrm{h}} = \frac{P_{\mathrm{h}}}{P_{\mathrm{a}}} \qquad (2)$$

where χ_{h} is the water vapor molar fraction (mol mol^{-1}, or KPa based on to Dalton`s law) and P_{a} is the atmospheric pressure (kPa).

The measured χ_{c} in soil and atmosphere were corrected for real-time changes in temperature atmospheric pressure (see Section 2.2.1) The soil-atmosphere fluxes of water vapor (F_{h}) and CO_2 (F_{c}) were calculated according to the gradient method (see Section 2.3.2)

The uncertainty in the estimation of F_{h} fluxes was calculated from the accuracy of the *RH* sensors used to calculate those fluxes. The following cumulative F_{h} and F_{c} were calculated from the data: effluxes, influxes and total fluxes. They refer to, respectively: positive fluxes (emissions, from soil to atmosphere), negative fluxes (uptake, from atmosphere to soil) and the sum of both fluxes (positive and negative).

3.3.2.4. Statistical modelling

All analyses were performed with R software v.3.6.3 and the significance level was set to 5%. The statistical protocol of Zuur and Ieno [2016] was used to analyze the data. Our model construction aimed to answer the following two questions: 1) is there a coupling between F_{h} and F_{c}, and in particular, is F_{h} a good predictor of F_{c}? and 2) Do soil variables (especially specific surface area and gypsum content) and biocrusts ecological succession significantly affect those fluxes?

We fitted models from both diel and cumulative fluxes over the study. For the former, the dataset was first split into a training set (first year) for calibration and a testing set (second year) for cross-validation. We selected only data from the summer season to exclude the effect of precipitation. Preliminary data exploration revealed a hysteretic relationship between F_{h} and F_{c} on a diel scale, presumably modellable with two sigmoid functions: one for the diel decrease in F_{c} and F_{h} from their maximum during daytime to their minimum at night, and *vice-versa* for the diel increase in those variables (Fig. S1B). Therefore, we additionally split the data into diel "decrease" and "increase" subsets, based on the average hour of minimum and maximum F_{h}, in order to model each part of the hysteresis independently. Since the "S-

shapes" exhibited substantial variation between crust types and replicates, non-linear mixed models were fitted [*Pinheiro & Bates*, 2000]. This approach allowed the parameters of the model to vary both with the fixed effect "crust type" and the random effect "replicate". The following four-parameter logistic model was chosen to model F_c as a function of F_h:

$$F_c = \phi_1 + \frac{\phi_2 - \phi_1}{1+\exp\left[(\phi_3 - F_h)/\phi_4\right]} \qquad (3)$$

where ϕ_1 is the horizontal asymptote as $F_h \to \infty$, ϕ_2 the horizontal asymptote as $F_h \to -\infty$, ϕ_3 the F_h value at the inflection point of the sigmoid (the value of F_h for which the response variable $F_c = \phi_1/2$), and ϕ_4 a scale parameter on the *x*-axis. Further information about this type of model, including a graphical visualization of the parameters, is available in Pinheiro and Bates [2000]. The serial correlation inherent to time series was modeled with a first-order autoregressive (AR1) process within each day.

Using a simple visual inspection of the time series, it was not clear whether the variation in F_h tended to lead or lag the variation in F_c. In general, negative F_h and F_c fluxes seemed to occur almost simultaneously but depending on the period and location, the variation in F_h could sometimes apparently lead or lag the variation in F_c. Therefore, a cross-correlation analysis was performed to determine whether F_c or F_h tended to lead or lag. In addition, relationships between pairs of variables were explored, and modelled either by linear or non-linear regression. All linear models' assumptions on residuals were checked with statistical tests: the Durbin-Watson's, Breusch-Pagan's, and Shapiro-Wilk's tests were used to assess independence, homoscedasticity, and normality, respectively. Non-linear models assumptions on residuals were checked visually.

3.3.3. Results

3.3.3.1. Temporal dynamics

3.3.3.1.1. General trends

In all stages of the biocrusts ecological succession, the soil relative humidity (RH_s) decreased sharply during summer drought (see for example in the mature *Cyanobacteria* microsite, Fig. 1A). During this period characterized

by the absence of precipitation, soil water content minima (Fig. 1E) and temperature maxima (Fig. 1F), RH_s became regularly lower than atmosphere relative humidity (RH_a). However, during this summer period, soil temperature (T_s) and atmosphere temperature (T_a) diverged substantially, with T_s exceeding T_a (Fig. 1F). Warmer air increases the saturation water vapor pressure, i.e. the capacity of air to store water vapor. Therefore, the molar fractions of water vapor (χ_h) were more relevant to understand the underlying processes involved in temporal patterns of water vapor fluxes (F_h), also because they were directly used to calculate F_h based on the gradient method. During summer drought, atmosphere χ_h regularly exceeded soil χ_h (Fig. 1B). Such conditions were often favorable to the inversion of the water vapor pressure gradient, thus generating negative F_h (Fig. 1C). Note that during another dry period but this time marked by winter temperatures (Fig. 1E and 2F), negative F_h fluxes were almost inexistent (Fig. 1C). Negative F_h always occurred at values of $RH_a > 40\%$ (see for example in the mature *Cyanobacteria* microsite, Fig. S2) but not exclusively, as positive F_h were also found in that interval. The conditions necessary for dew formation (i.e. $T_{surf} <$ dew point) and fog formation (i.e. $RH_a = 100\%$) were uncommon in summer (see example in Fig. 2E, and Fig. 1A, respectively).

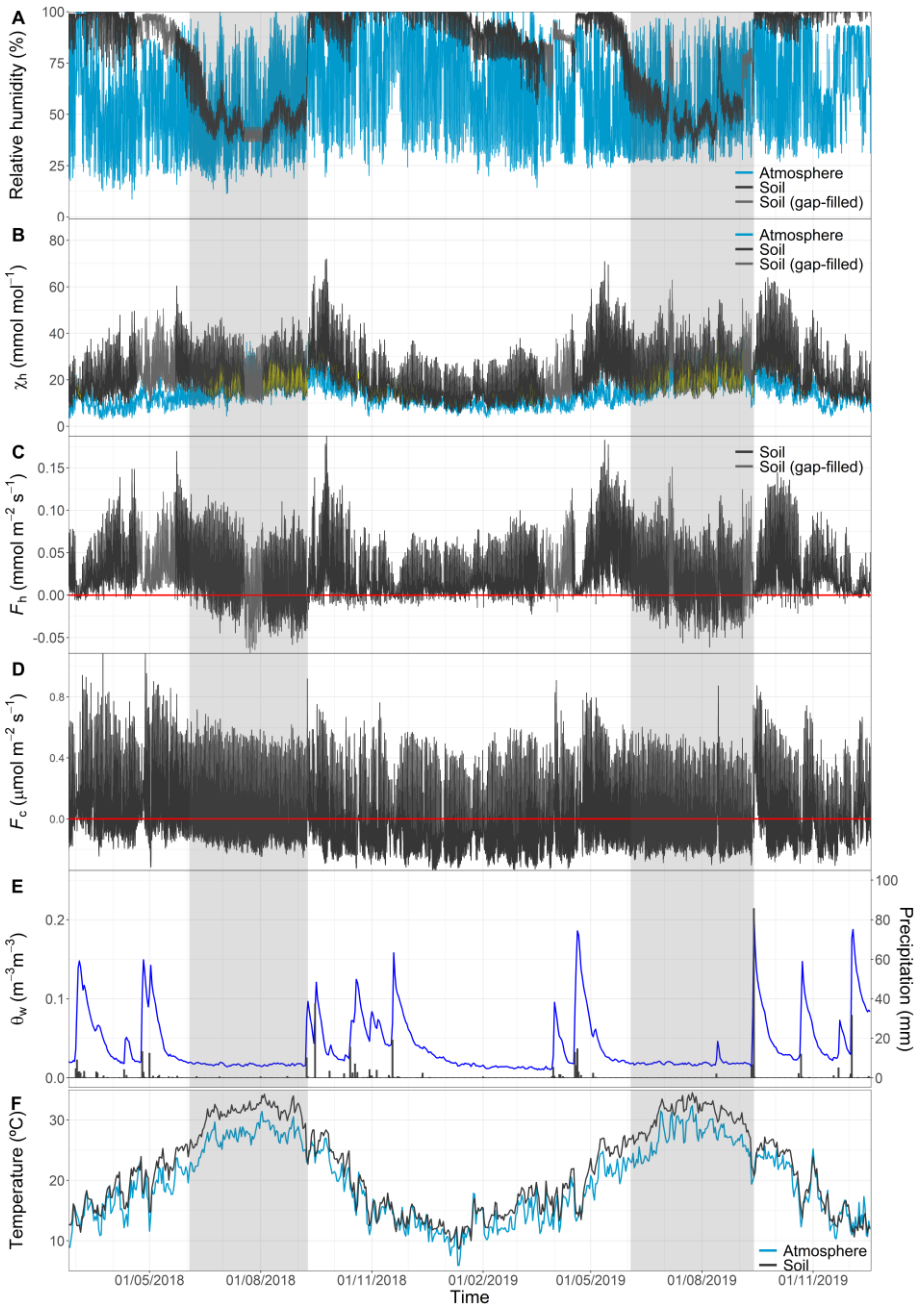

Figure 1 Time series of (A) hourly relative humidity in soil and atmosphere (B) hourly water vapor molar fraction (χ_h) in soil and atmosphere. The yellow areas delimit moments during which atmosphere χ_h exceeds soil χ_h; (C) hourly soil-atmosphere water vapor flux (F_h); (D) hourly soil-atmosphere CO_2 flux (F_c); (E) daily soil water content (θ_w, blue line) and precipitation (black bars); (F) daily temperature of soil and atmosphere. All time series come from the mature *Cyanobacteria* microsite. The shaded area highlights periods of consistent negative F_h during summer drought.

During a complete hydrological year from 01/09/2018 to 31/08/2019, the amount of water accumulated by precipitation was 174 mm while the amount of water accumulated through negative F_h ranged from 0.37 ± 0.02 mm to 1.58 ± 0.08 mm (i.e. from 0.21 ± 0.01% to 0.91 ± 0.05% of precipitation, respectively), depending on the microsite, using the model of Bittelli et al. [2015] to calculate the diffusion coefficient of water vapor between soil and atmosphere. By contrast, using the diffusion model of Xu et al. [1992], negative F_h accounted for between 1.42 ± 0.07 and 4.91 ± 0.25 mm, i.e. 0.82 ± 0.04% to 2.82 ± 0.14% of the annual precipitation over the same period. The amount of water accumulated through negative F_h only during summer of the same hydrological year ranged from 0.17 ± 0.01 mm to 1 ± 0.05 mm with the first model and from 0.67 ± 0.03 mm to 3.62 ± 0.18 mm with the second model. The amount of water accumulated through negative F_h only during summer represented between 47 and 75% of the annual negative F_h regardless of the diffusion model. By contrast with negative F_h that occurred predominantly during summer, negative CO_2 fluxes (F_c) occurred throughout the study period, with a slightly lower magnitude in summer (see for example in the mature *Cyanobacteria* microsite, Fig. 1D). The cumulative evaporation (positive F_h) ranged from 7.40 ± 0.37 mm to 15.21 ± 0.76 mm (i.e. from 4.25 ± 0.21% to 8.74 ± 0.44% of precipitation) based on the diffusion model of Bittelli et al. [2015]. It ranged from 23.02 ± 1.15 mm to 53.72 ± 2.69 mm (i.e. from 13.23 ± 0.66% to 30.87 ± 1.55% of precipitation) based on the diffusion model of Xu et al. [1992].

The ratio of cumulative negative F_h to cumulative positive F_h over the whole study period tended to increase over biocrusts succession (3%, 3%, 9%, 7%, 11% and 15% for the PD, IC, MC, MC2, SD and LI microsites, respectively). The average soil-atmosphere gradient of water vapor molar fraction decreased over succession (14.5, 12.5, 11.7, 10.6, 9.4, and 7.3 mmol mol^{-1} for the PD, IC, MC, MC2, SD and LI microsites, respectively).

3.3.3.1.2. Diel patterns in water vapor and CO_2 fluxes

A more detailed representation of the previously mentioned periods of summer and winter drought, during which negative F_h were respectively common and virtually absent, is provided in Fig. 2. During summer, negative F_h occurred due to a decrease in soil χ_h during the afternoon (reaching minima at nighttime) and a concomitant increase in atmosphere χ_h at nighttime inverting the soil-atmosphere water vapor pressure gradient (Fig. 2C). During winter, soil χ_h was lower in average but followed the same diel pattern whereas atmosphere χ_h was also lower in average but usually did not increase enough at nighttime to invert substantially the gradient (Fig. 2D). It is also worth noting that RH_s presented the opposite diel pattern to soil χ_h (Fig. 2A and 2B) and that the soil χ_h decrease during the afternoon and over night (Fig. 2C and 2D), occurred in synchrony with a decrease in temperature (Fig. 2E and 2F) and PAR (Fig. 2G and 2H). In addition, brief positive excursions in χ_h were frequently observed at sunrise, particularly in summer (Fig. 2C).

During summer, F_c and F_h covaried and used to be both negative at night (Fig. 3). The cross-correlation analysis revealed that overall, the variation in F_h slightly led the variation in F_c, i.e. by one hour (one hour being the maximum time resolution of the data). The moment when fluxes became negative used to coincide exactly with PAR reaching the zero value (Fig. 2G and Fig. 3), due to the inversion of the gradient of water vapor molar fractions at this moment (Fig. 2C).

There was a diel hysteresis between F_c and T_s as well as between F_c and F_h (Fig. S1A and S1B, Fig. 4A). The former was difficult to model whereas the latter could be modelled with two sigmoidal functions, one for the diel decrease from F_h maximum to F_h minimum and *vice-versa* for the diel increase (Fig. 4A, supporting information Table S1A). Note that in all succession stages, the diel "decrease" path of the observed hysteresis was on average longer than the diel "increase" path. The ratio of diel decrease time over diel increase time ranges from 1.6 in the PD and IC microsites to 3 in the LI site. After calibration of the model on the first summer of data, the model was cross-

validated with predictions on the second summer of data, which showed overall good performance (Fig. 4B and 4C).

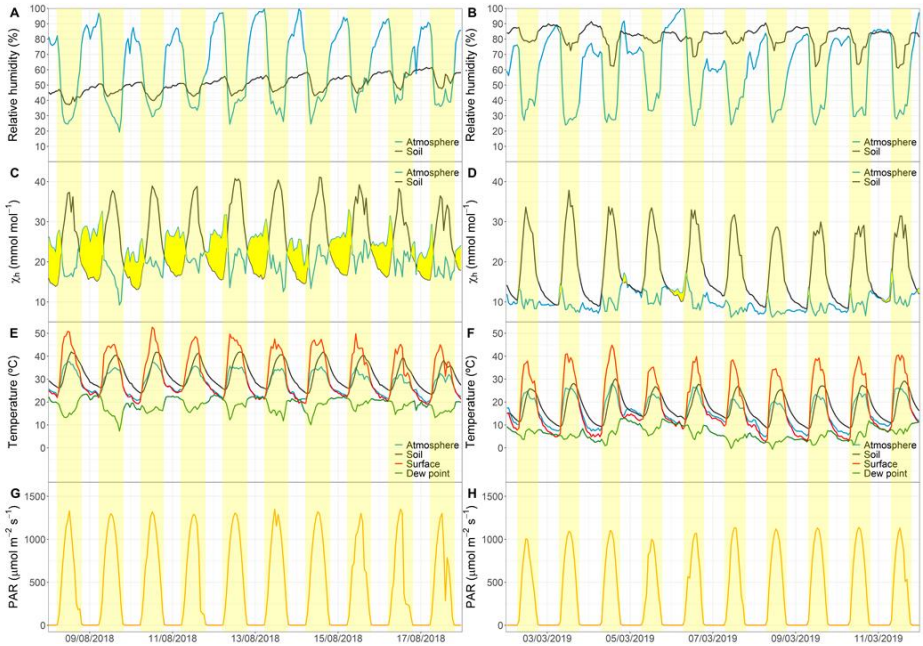

Figure 2 Variation of environmental variables over time during a drought period in summer (left column) and winter (right column); (A and B) relative humidity in soil and atmosphere; (C and D) molar fraction of water vapor (χ_h) in soil and atmosphere. The yellow area delimits moments during which atmosphere χ_h exceeds soil χ_h, leading to negative soil-atmosphere water fluxes, i.e. from atmosphere to soil; (E and F) temperature of soil (5 cm depth), atmosphere and soil surface, and dew point temperature; (G and H) photosynthetically active radiation (PAR). The yellowish shaded areas highlight daytime (i.e. positive PAR).

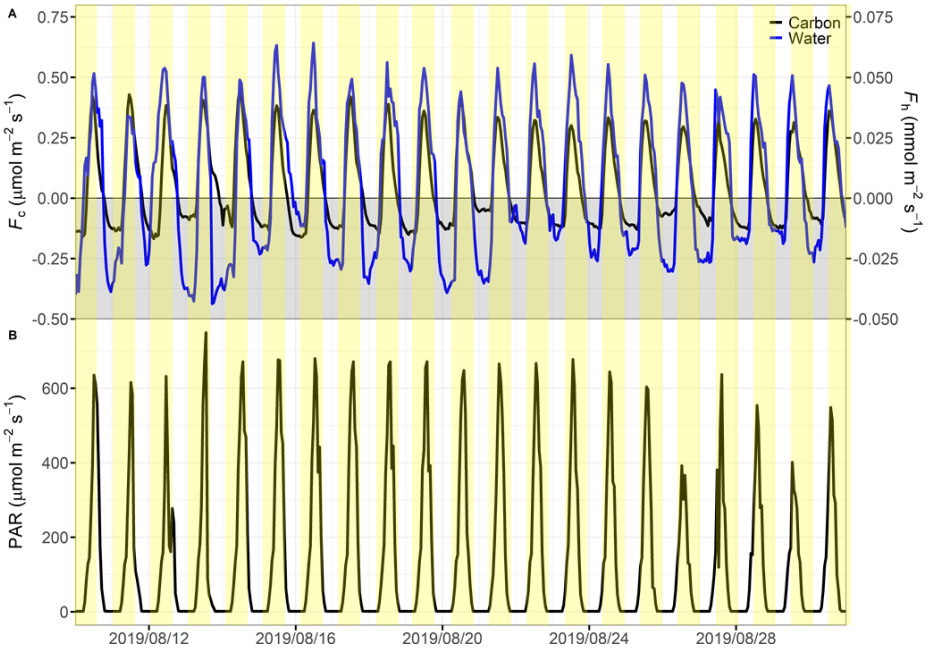

Figure 3 (A) Covariation between the soil-atmosphere CO_2 flux (F_c) and the soil-atmosphere water vapor flux (F_h) during a selected period in summer; (B) variation in photosynthetically active radiation (PAR) during the same period The dark shaded area highlights negative fluxes. The yellowish areas highlight daytime (i.e. positive PAR). Data were from the *Lepraria isidiata* (LI) microsite.

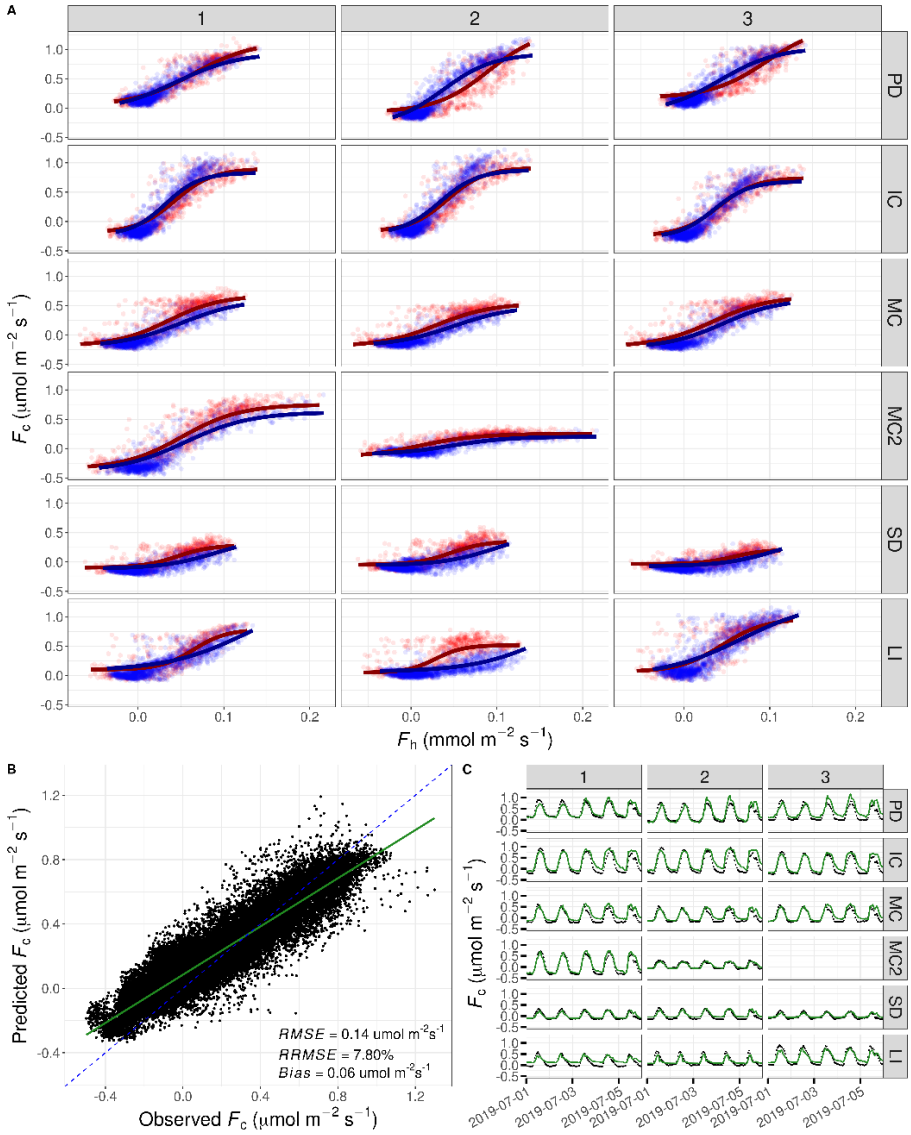

Figure 4 Non-linear modelling of the hysteretic relationship between the soil-atmosphere CO_2 flux (F_c) and the soil-atmosphere water vapor flux (F_h): (A) calibration of the model on the first summer of data. The blue lines and blue points correspond to the decrease from F_h maximum to minimum and *vice-versa* for the red line and red points. A summary of the model fixed effects is given in Table S2A; (B) Predicted F_c against observed F_c on the second summer of data for all microsites. The continuous green line is the model. The dashed blue line is the 1:1 line. (C) Example of predicted F_c against time during the second summer of data. The continuous green line is the model prediction. Black points correspond to the observed F_c. Stages of the biocrusts succession are labeled as: physical depositional crust (PD), incipient *Cyanobateria* (IC), mature *Cyanobacteria* (MC), lichen community dominated by *Squamarina lentigera* and *Diploschistes diacapsis* (SD), lichen community characterized by *Lepraria isidiata* (LI), and *Cyanobacteria* patches within the SD microsite (MC2).

3.3.3.2. Relations between cumulative water vapor and CO_2 fluxes, soil properties and biocrusts succession

There was a significant negative linear relationship ($p < 0.001$, adjusted $R^2 = 0.68$) between cumulative F_c and F_h estimated on the whole study period (Fig. 5). Mature *Cyanobacteria* microsites exhibited the least CO_2 emissions (very close to neutrality) and greatest water vapor emissions. By contrast, the *Lepraria isidiata* microsite exhibited the greatest CO_2 emissions and the least water vapor emissions. The other microsites exhibited intermediate values for these two variables. More details about the temporal patterns of cumulative total fluxes and cumulative negative fluxes for each stage of the succession can be found in Fig. S3. A particular covariation between cumulative negative F_c and F_h was found in the SD microsite with enhanced CO_2 influxes coinciding with water vapor influxes in summer (Fig. S3A).

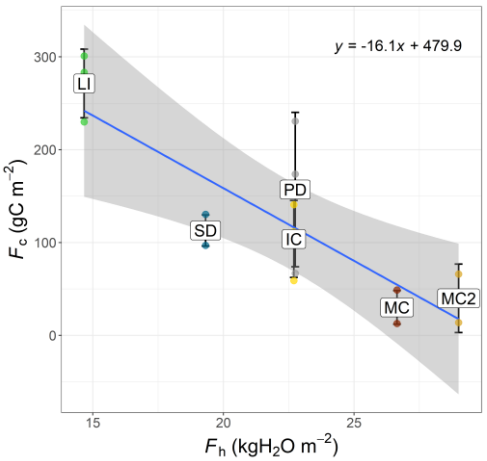

Figure 5 Fit of the linear model of the cumulative soil-atmosphere CO_2 flux (F_c) as a function of the cumulative soil-atmosphere water vapor flux (F_h), over the whole study period. Stages of the biocrusts succession are labeled as: physical depositional crust (PD), incipient *Cyanobateria* (IC), mature *Cyanobacteria* (MC), lichen community dominated by *Squamarina lentigera* and *Diploschistes diacapsis* (SD), lichen community characterized by *Lepraria isidiata* (LI), and *Cyanobacteria* patches within the SD microsite (MC2). Grey, yellow, red, orange, blue and green points correspond to the PD, IC, MC, MC2, SD and LI sites, respectively. Error bars represent the intra-microsite standard deviation for F_c. The shaded band represent the 95% confidence interval.

There was a significant positive linear relationship ($p < 0.001$, adjusted $R^2 = 0.85$) between cumulative CO_2 influxes and total soil specific surface area (SSA_s) among early successional stages (Fig. 6). In other words, the magnitude of the CO_2 influxes increased with SSA_s. This proportional increase was observed gradually during the early stages of the succession (from the physical depositional crust to incipient *Cyanobacteria* to mature *Cyanobacteria*). The SSA_s was strongly correlated with the soil clay fraction (Pearson´s $r = 0.92$).

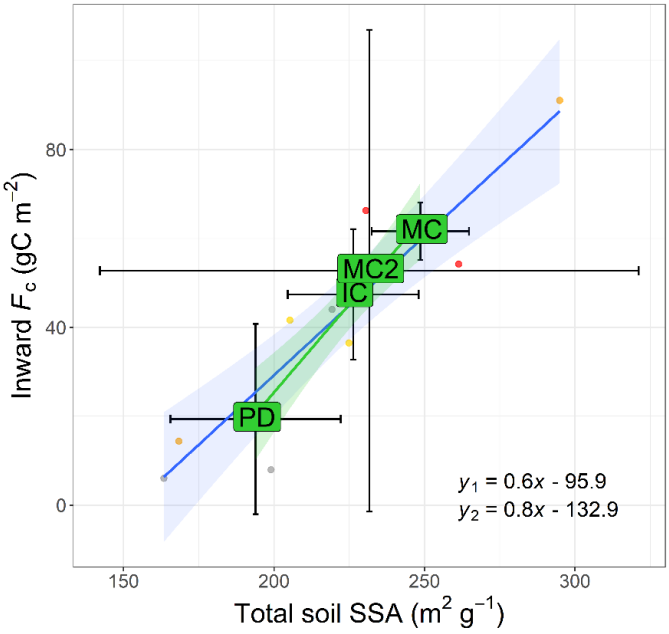

Figure 6 Fits of linear models of the absolute cumulative inward soil-atmosphere CO_2 flux (F_c) as a function of the total soil specific surface area. The blue and green lines are the model fits from the whole dataset and from averages by crust, respectively (corresponding to the y_1 and y_2 equations, respectively). Stages of the biocrusts succession are labeled as: physical depositional crust (PD), incipient *Cyanobateria* (IC), mature *Cyanobacteria* (MC), and *Cyanobacteria* patches within a lichen site (MC2). Grey, yellow, red and orange points correspond to data from the PD, IC, MC and MC2 microsites, respectively. Error bars correspond to the intra-microsite standard deviation. Shaded bands represent the 95% confidence intervals. The high spatial variation in the MC2 microsite is attributable to soil heterogeneity and less replicates ($n = 2$ for MC2 and $n = 3$ for other microsites).

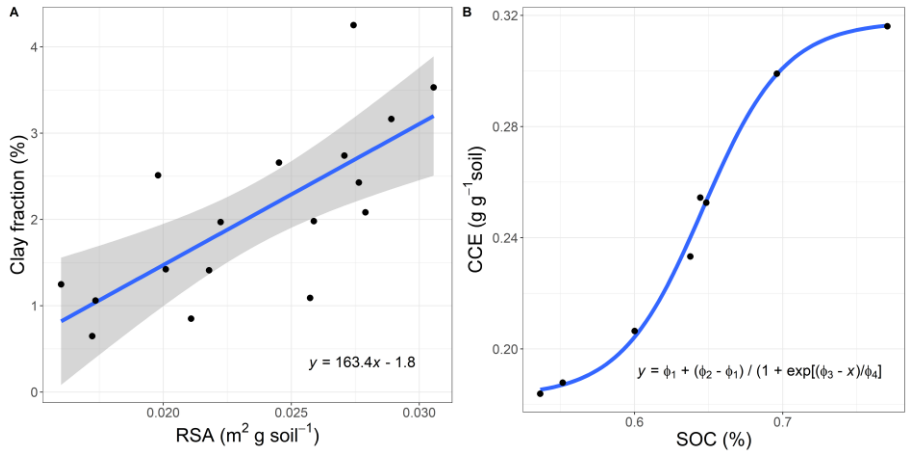

Figure 7 Fits of (A) linear model of the soil clay fraction as a function of the reactive surface area of calcite (RSA). The shaded band represent the 95% confidence interval, (B) non-linear model of the calcium carbonate equivalent content (CCE) as a function of soil organic carbon content (SOC). Values of the parameters of the model are given in Table S1B.

There was a significant positive linear relationship ($p < 0.001$, adjusted $R^2 = 0.53$) between the clay fraction and the reactive surface area of calcite (RSA) (Fig. 7A). The RSA was strongly correlated to the calcium carbonate equivalent content (CCE) (Pearson´s $r = 0.91$). There was a sigmoidal relationship (relative root mean square error (*RRMSE*) = 1.4%) between the CCE and the soil organic carbon content (SOC) within early stages of the succession (Fig. 7B, supporting information Table S1B), that did not follow the order of the succession.

3.3.4. Discussion

In this research, we report for the first time using the gradient method (1) negative water vapor fluxes at night during hot and dry periods, attributable to water vapor adsorption (WVA) by soil; (2) a tight coupling between soil-atmosphere CO_2 and water vapor fluxes (F_c and F_h, respectively), and (3) significant relationships between F_c, soil properties and biocrust ecological succession.

3.3.4.1. The gradient method as a novel approach to estimate water vapor adsorption by soil

Using the gradient method, negative F_h were consistently and predominantly detected at night during hot and dry periods (i.e. summer) (Fig. 1C). In congruence with this result, *in-situ* studies have reported that WVA occurs predominantly in those conditions [*Agam & Berliner*, 2006; *Kool et al.*, 2021; *Kosmas et al.*, 1998]. In addition, negative F_h always occurred at RH_a > ca. 40% (Fig. S2). In agreement with this result, according to theoretical equations, a water film starts to form on a solid surface at *RH* > 30-40% [*Kharitonova et al.*, 2010]. Therefore, our observations match those of both *in-situ* and theoretical studies, thus confirming that our measured negative F_h are attributable to WVA. However, the use of *RH* alone can be misleading to disentangle the temporal patterns involved in WVA *in-situ* as it is based on the saturation water vapor pressure of air which varies with temperature. By contrast, our results, using the water vapor molar fraction (χ_h) in soil and atmosphere to estimate F_h, provided a more accurate understanding of the underlying processes involved in WVA, as χ_h is independent of temperature, which can vary substantially between soil and atmosphere (Fig. 1F, Fig. 2E and 2F). As a result, soil χ_h and *RH* exhibited opposite diel patterns, and thus the observation of *RH* alone could lead to misleading conclusions. It has been previously stated that WVA occurs when RH_s is lower than RH_a [*Agam and Berliner*, 2006] and can be attributed to soil drying during daytime and an increase in RH_a at nighttime [*Kosmas et al.*, 1998]. However, although WVA occurred during a phase of decreasing χ_h during afternoon and overnight (Fig. 2C), it could not be due to soil drying since both temperature and PAR were decreasing during those moments. On the light of our results, the observed diel decrease in soil χ_h can be attributed to lower temperature reducing the capacity of air to store water vapor.

Furthermore, during an unusually dry period in winter, the soil water content (θ_w) decreased to values similar to those observed during summer (Fig. 1E) but soil χ_h decreased to values even lower in average than during summer due to the same physical process, i.e. low temperature decreasing the saturation water vapor pressure of air (Fig. 1B and 1F). In spite of that, WVA were scarce and of small magnitude in winter because atmosphere χ_h

was also lower in average than in summer and did not increase enough at night to exceed soil χ_h (Fig. 2D). Therefore, the decrease in soil χ_h alone does not seem sufficient to trigger WVA. Two additional conditions seem to be critical for the process to occur: (1) a substantial average atmosphere χ_h and (2) a sharp and substantial increase in atmosphere χ_h at night. The first condition can be fulfilled in summer due to greater temperature triggering more oceanic evaporation and as previously explained, the increased capacity of warmer air to store water vapor. Most studies reporting WVA fluxes were conducted in coastal drylands [e.g. *Kohfahl et al.*, 2021; *Kool et al.*, 2021; *Kosmas et al.*, 2001], where atmosphere is usually wetter. Our study site was also close to the sea (ca. 20 km). Therefore, further research is needed to clarify if WVA can also occur in non-coastal drylands. The second condition is most likely met due to stable stratification of the atmosphere boundary layer at night accumulating water molecules in the vapor form close to the ground. Previous studies have stated that such nocturnal conditions might be fulfilled due to incoming sea breeze at night [*Kosmas et al.*, 2001; *Uclés et al.*, 2015]. However, since sea breeze is a daytime process, it seems rather unlikely at our site. By contrast, here, the movement of wetter air from the surrounding mountains could also have played a role in explaining the sharp increase in atmosphere χ_h at night. We also suggest that the early morning peak in atmosphere χ_h, coinciding with the rise in PAR (Fig. 2C and Fig. 2G), is due to rapid soil surface evaporation at sunrise. This movement of water vapor from soil surface to the overlying low part of the atmosphere only occurs briefly probably because sun radiation rapidly heats the soil surface (Fig. 2E), thus triggering atmospheric turbulences that moves water vapor to higher atmosphere layers.

To our knowledge, it is the first time that the gradient method has been used to estimate WVA. Other approaches traditionally used either complex numerical modelling with numerous parameters that require substantial effort to collect, or expensive lysimeters that can disturb the natural soil profile and pedoclimatic conditions [*Agam & Berliner*, 2006; *Kohfahl et al.*, 2021; *Kosmas et al.*, 2001; *Saaltink et al.*, 2020; *Uclés et al.*, 2015; *Verhoef et al.*, 2006]. By contrast, the gradient method traditionally used to determine soil-atmosphere greenhouse gas fluxes [*Maier & Schack-*

Kirchner, 2014; *Sánchez-Cañete et al.*, 2017] is easy to deploy, generates only limited perturbation of the soil profile, and can provide long-term continuous low-cost measurements and further understanding of belowground mechanisms involved in WVA. It is therefore suitable to obtain estimates of WVA, based on the assumption that all the water vapor that diffuses from atmosphere to soil is adsorbed onto soil particles. The values estimated in this study ranging from 0.21 ± 0.01% to 0.91 ± 0.05% of annual precipitation should be considered as a proxy rather than absolute estimates of WVA because they are highly dependent on the selected model of water vapor diffusion. For example, using a different diffusion model [*Xu et al.*, 1992], our WVA estimates ranged this time from 0.82 ± 0.04% to 2.82 ± 0.14% of the annual precipitation. This difference in the estimated WVA is thus the result of potential errors in the quantification of F_h attributable to the choice of the diffusion model. That is because in the gradient method, the estimated flux is highly dependent on the chosen coefficient of diffusion. Whereas the diffusion coefficient used to estimate F_c was calibrated empirically with a portable soil chamber according to Sánchez-Cañete et al. [2017], no standardized procedure exists yet to calibrate this coefficient *in-situ* for F_h as, so far, most studies were limited to laboratory experiments [e.g. *Jabro and Jabro*, 2008; *Rao and Rekapalli*, 2020*; Reyzabal and Bazán*, 1992]. In order to obtain reliable absolute estimates of WVA, we suggest to calibrate the diffusion model with another validated method, e.g. using lysimeter measurements. However, since the main objectives of this research were to identify moments of WVA as well as their drivers and potential interactions with F_c, the use of a general model to estimate the coefficient of diffusion of water vapor was reasonable; it was still useful to compare the magnitude of WVA between microsites, analyze temporal patterns and explore correlations with other variables. Although our estimated contribution of WVA to annual precipitation is apparently small, WVA was barely the only source of water in summer when microclimatic conditions necessary for other non-rainfall water inputs, i.e. fog or dew formation, were uncommon. Hence, this water input is likely important for maintaining ecosystem processes during those periods. Our estimated values of evaporation (positive F_h) accounted for up to 30.9% of annual precipitation, indicating that the water balanced was not closed regardless of the diffusion model that was used. The remaining water could have (1) been

lost by runoff; (2) infiltrated deeper horizons and (3) been consumed by biocrusts and geochemical reactions.

3.3.4.2. Coupling between water vapor and CO_2 fluxes

3.3.4.2.1. Coupling between fluxes on a diel scale

During summer, F_c and F_h used to be both negative at night (Fig. 3) and our cross-correlation analysis revealed that the variation in F_h tended to slightly lead the variation in F_c (by one hour). This is in agreement with our hypothesis that WVA could be the underlying process controlling nocturnal CO_2 uptake in dry soils at this site, but due to the small lag corresponding to the maximum time resolution of the data, this result should be taken with caution and requires further confirmation with higher sampling frequency.

A diel hysteresis between F_c and T_s as well as between F_c and F_h was found (Fig. S1A and S1B, and Fig. 4A). The former has been extensively described in plants and generally attributed to a lag in the delivery of recent photosynthates to the soil [*Dusza et al.*, 2020; *Zhang et al.*, 2018], stimulating microbial activity, a process known as "priming effect" [*Guenet et al.*, 2018]; priming effect mediated by biocrusts has been less studied but does occur [*Beymer & Klopatek*, 1991]. However, this relationship between F_c and T_s was difficult to model in our study. By contrast, the hysteresis between F_c and F_h could be modelled with two sigmoidal functions, one for the diel decrease from maximum to minimum F_h and *vice-versa* for the diel increase (Fig. 4A, Table S1A), and the models performed well at predicting F_c from a new dataset (Fig. 4B and 4C). A lag due to a priming effect induced by biocrusts is possible to a certain extent as a fraction of their photosynthates is assimilated by the underlying microbial community, benefiting heterotrophic microbes which are often carbon-limited in drylands [*Belnap et al.*, 2003]. However, the duration of this lag is expected to be limited due to the absence of large phloem structures to transport those photosynthates such as in plants [*Mencuccini & Hölttä*, 2010]. In addition, biocrusts gross photosynthesis is almost inexistent during the dry season at our site [*Miralles et al.*, 2018] and the hysteresis was observed even in the absence of biocrusts, in the physical depositional crust. We therefore suggest that an abiotic mechanism

depending on F_h could be involved in the hysteresis between F_c and F_h. Adsorption-desorption of water vapor on solid particles is a good candidate process as it exhibits a well-known hysteresis which is considered to be crucial for accurate modelling of water vapor flow in drylands soils [*Arthur et al.*, 2020]. It has been reported from *ex-situ* experiments on soils that the adsorption time was always greater than the desorption time, with ratios of adsorption time to desorption time ranging from 1.3 to 2.9 [*Akin & Likos*, 2020]. Here we found that the diel "decrease" path of the observed hysteresis was always longer than the diel "increase" path, with ratios of the decrease time to increase time ranging from 1.6 to 3, thus matching closely the previous values; we therefore further assume that the observed paths of "decrease" and "increase" were likely due to underlying adsorption and desorption processes, respectively. Noteworthy, the hysteresis reported in Arthur et al. [2020] characterizes the relation between θ_w and relative humidity, whereas our assumption that water vapor adsorption and desorption processes are involved is based on the relation between F_c and F_h. Our θ_w measurements did not provide enough diel resolution to confirm the former relationship. However, we assume that a greater water content during the desorption phase that during the adsorption phase [*Arthur et al.*, 2020] should enhance F_c in this water-limited ecosystem, and therefore that it could generate the observed hysteresis exhibiting greater F_c during the hypothetical desorption phase at most microsites (Fig. 4A). In addition, during the hypothetical adsorption phase, fluxes became negative only at the end of the curve. We suggest that this might be due to (1) a threshold effect [*Kharitonova et al.*, 2010] and/or (2) different thermal conditions between laboratory and *in-situ* studies. Although similitudes can be found comparing observations of laboratory and *in-situ* measurements, they are only comparable to a certain extent as laboratory results are usually based on isotherms whereas temperature is not constant in the field but seems to be the motor of WVA (Fig. 2E). Therefore, we suggest that incubations of dry soils placed on lysimeters at constant temperature and varying *RH*, or *in-situ* temperature and *RH* manipulation could help to validate our assumption.

The abiotic process of WVA could have affected F_c, contributing to a nocturnal CO_2 uptake in different ways, enhancing other abiotic processes and/or biotic processes. Abiotic processes likely to be enhanced by WVA

include (1) dissolution of CO_2 in water; (2) mineral reactions such as dissolution of the surface of $CaCO_3$ particles, consuming CO_2 through the following reversible geochemical reaction:

$$CaCO_{3\,(s)} + H_2O_{\,(l)} + CO_{2\,(g)} \leftrightarrow Ca^{2+} + 2HCO_3^- \qquad (4)$$

It has been shown that WVA on the surface of calcite is energetically favorable and that adsorbed water can affect particle reactivity by enhancing surface ion mobility, by providing a medium for reactions or by serving as a reactant in surface-catalyzed hydrolysis reactions [*Rahaman et al.*, 2008]. Moreover, much evidence has already supported such a geochemical origin for the nighttime CO_2 uptake at this site [*Lopez Canfin et al.*, n.d.]. Alternatively, due the co-occurrence of gypsum with calcite and the greater solubility of the former (exceeding calcite by two orders of magnitude), its potential interaction through a common ion effect deserves to be investigated as calcite precipitation from Ca^{2+} released by gypsum could act as a carbon sink [*Yu et al.*, 2019]; that is because although calcite precipitation releases one mole of CO_2, it still consumes two moles of CO_2 as bicarbonate (eq. 4); (3) co-adsorption of CO_2. In the presence of equilibrium pressures of water vapor above 1% RH, co-adsorbed water enhances CO_2 adsorption and influences the chemical nature of the predominant adsorbed product from bicarbonate, which is no longer formed, to carbonate [*Rubasinghege & Grassian*, 2013]. Note that if co-adsorption occurs on calcite, this process could potentially push eq. 4 to the right. In a desert soil with low inorganic carbon content (ca. 4%), it has been reported through an isotope labeling experiment that most of the labeled atmospheric CO_2 was retained in the soil solid phase [*Liu et al.*, 2015]. The authors found that the CO_2 may be conserved in certain minerals but did not discuss adsorption as an explanatory process, though WVA can lead to the reorganization of mineral surfaces and the formation of “ice-like” structures (i.e. similar to solid water) [*Rubasinghege & Grassian*, 2013]. It has been estimated that CO_2 adsorption on mineral and soil surfaces can account for 1-3% of the average annual North American terrestrial carbon sink and that the greatest increases are predicted in regions with lower soil CO_2 concentrations (like at our study site), because soils and rock in these regions have a larger proportion of unused adsorption sites [*Davidson et al.*, 2013].

Biotic processes likely to be enhanced by WVA include (1) WVA could stimulate microbial activity of chemotrophs on the surface of soil particles. Other authors have found that WVA increased soil CO_2 production revealing that dryland microorganisms were able to use this water input to sustain their metabolic activity [*McHugh et al.*, 2015]. Since there is growing evidence that chemotrophs that are able to perform CO_2 fixation in the dark are present among biocrust communities in drylands [*Bay et al.*, 2021; *Liu et al.*, 2021], WVA could enhance the activity of these organisms that consume CO_2 at night. Moreover, as negative fluxes of water vapor and CO_2 used to start exactly when PAR reached zero values (Fig. 2 and Fig. 3), the hypothesis of dark fixation by chemotrophs deserves further investigation. Note that we measured maximal CO_2 uptake below *Cyanobacteria* (Fig. S3A). Those microorganisms could also promote the dissolution of calcite as they are able to decrease the local extracellular ion activity product of $CaCO_3$ by taking up Ca^{2+}, the weathering capacity of *Cyanobacteria* being optimal in the presence of a short daily dark phase [*Garcia-Pichel et al.*, 2010]; (2) WVA could favor the biomineralization of $CaCO_3$ from atmospheric CO_2, either by stimulating the activity of biomineralizing microorganisms or indirectly through the formation of dissolved inorganic carbon species involved in the process. Biomineralization has been frequently identified in *Actinobacteria,* and *Proteobacteria* phyla [*Cuezva et al.*, 2012; *Hervé et al.*, 2016; *Meier et al.*, 2017] including in desert soils [*Liu et al.*, 2018] as well as in *Cyanobacteria* [*Benzerara et al.*, 2014]. Those phyla were abundant at our study site [*Miralles et al.*, 2020] and thus deserve further attention in future research.

3.3.4.2.2. Coupling between cumulative fluxes

A significant negative linear relationship between total cumulative F_c and F_h over the study was identified (Fig. 5), with minimum CO_2 emissions occurring in mature *Cyanobacteria* microsites, where water vapor emissions were maximum. Those microsites were also the driest, as they exhibited minimum average values of soil water content (not shown). They also sustained the greatest magnitude of soil CO_2 uptake (Fig. S3A). Therefore, on the one hand, the low liquid water availability in *Cyanobacteria* microsites was related to greater water vapor losses from soil to atmosphere, thus probably

limiting microbial activity and CO_2 production. On the other hand, the greater CO_2 uptake in mature *Cyanobacteria* microsites contributed to mitigate CO_2 emissions there.

We did not find any significant relationship between annual cumulative negative F_c and F_h, most likely because negative F_c occurred over the whole study period, whereas WVA occurred mainly in summer (Fig. 1C and 1D) and/or because of high intra-microsite variation in F_h that was not captured by our measurements. However, the significant relationship between total cumulative F_c and F_h deserves additional research integrating more years of data and more spatial coverage for F_h in order to cross-validate a model. A predictive model of annual F_c from annual F_h would present the enormous advantage of providing annual estimates of a variable that is relatively costly to measure (i.e. F_c) from a variable that is very affordable to measure (i.e. F_h).

3.3.4.3. Effect of soil properties on water vapor adsorption

We found a strong positive linear relationship between cumulative CO_2 influxes and total soil specific surface area (SSA_s) among early successional stages (Fig. 6). The controlled adsorption of gases on surfaces through the Brunauer-Emmett-Teller (BET) technique is widely used to measure the surface area of solid materials, as adsorption increases with surface area. Therefore, many porous materials of high surface area - clays, carbonates and volcanic residues - have been investigated in laboratory conditions for their adsorbent properties to capture CO_2 [*Davidson et al.*, 2013; *Ouadjenia et al.*, 2017]. However, to our knowledge, this relationship between soil CO_2 uptake and surface area has never been evidenced *in-situ*. It could result from (1) direct adsorption of CO_2 onto soil particles; (2) an indirect effect of WVA enhancing CO_2 adsorption or triggering the dissolution of CO_2 in the adsorbed water; (3) enhanced chemotrophs/biomineralizers growth due to more available surface area and/or water.

We found no convincing relationship between cumulative negative F_h and SSA_s to confirm an indirect role of WVA. However, that was likely due to the lack of intra-microsite replicates of relative humidity measurements to

capture the spatial variability of F_h, and thus this assumption should not be discarded. The absence of consistent relationship between cumulative CO_2 influxes and SSA_s in late succession stages is most likely due to higher CO_2 production masking CO_2 consumption in those microsites. Other factors such as soil organic carbon (SOC) and salinity could also have affected adsorption [*Amer*, 2019; *Arthur et al.*, 2020; *Ravikovitch et al.*, 2005], but we did not find evidence of such relationships between adsorption and those parameters (including the content of a common salt, gypsum) at our site.

Furthermore, the strong relationship between SSA_s and clay fraction indicates that this soil CO_2 uptake was related to clay particles. Even if clays were not abundant at this site (ranging from 0.6 to 4.3% in the measured samples), they contained highly adsorbent smectite [*Hatch et al.*, 2012; *Michels et al.*, 2015]. Although smectite could have contributed to a certain extent to adsorption, its contribution was probably limited since it was only present in minor amounts (< 5 % of the clay fraction) [*Solé-Benet et al.*, 1997]. However, we found a significant relationship between the clay fraction and the reactive surface area of carbonates (RSA) (Fig. 7A), suggesting that there was a substantial amount of clay-size carbonate at this site. Clay-size carbonates are highly reactive [*Loeppert & Suarez*, 1996] and thus might have reacted with adsorbed CO_2 and/or water according to eq. 4.

3.3.4.4. Effect of biocrusts ecological succession on water vapor adsorption

The ratio of cumulative negative to positive F_h and the average soil-atmosphere gradient of water vapor molar fraction respectively increased and decreased over biocrust ecological succession, suggesting that those variables might be used as indices of succession status. However, further research is needed to explore the potential biophysical mechanisms controlling those patterns.

In early successional stages, the SSA_s increased following the order of ecological succession (physical depositional crust – incipient *Cyanobacteria* – mature *Cyanobacteria*) and was associated with an increase in the magnitude of soil CO_2 uptake (Fig. 6). In agreement with those results, on sandy soils, biocrusts are known to accumulate windblown silt and clay particles at the

surface, and clay particles in particular may be tightly bound to the sticky sheaths of some *Cyanobacteria* [*Warren*, 2003]; therefore, *Cyanobacteria* could indirectly favor WVA by accumulating fine particles. Moreover, at our experimental site, the dominance of *Cyanobacteria* in the driest microsites though those organisms require liquid water to develop is somewhat paradoxical. Since the greatest magnitude of summer WVA was observed in the mature cyanobacterial microsite (Fig. S3A), it is possible that *Cyanobacteria* take advantage of enhanced WVA in the driest microsites and use adsorbed water films to develop. Furthermore, as those organisms have the size of fine-silt particles, it is also possible that they favor WVA by providing additional adsorbent surface, surface that would be free for more adsorption once the water has been consumed by the microorganisms, thus generating a positive feedback loop between WVA and their development. Other authors have found that WVA capacity was increased by up to 157% in moss-dominated soils compared to bare soils [*Li et al.*, 2021], hence this assumption regarding *Cyanobacteria* deserves further research. The enhanced CO_2 uptake by soil coinciding with WVA in the SD lichen community during summer also requires further investigation to clarify the involved processes (Fig. S3A).

The logistic relationship found within early successional stages between the calcium carbonate equivalent content and SOC (Fig. 7B, supporting information Table S1B) is assumed to be due to the cementing effect of carbonates on aggregates [*Rowley et al.*, 2018]. Therefore, $CaCO_3$ might be crucial to stabilize organic matter in early successional stages. In late stages, other factors might contribute to organic carbon accumulation such as lichen and plant turnover and secretion of organic compounds. In agreement with those results, a previous study at this experimental site has found a trend of increase in small-size carbonates over succession [*Lopez-Canfin et al.*, 2021]. Those particles could potentially affect F_h and F_c due to their highly adsorbent and reactive properties. Additional research is needed to determine if this accumulation of small-size carbonates has an abiotic origin (through mineral dissolution and precipitation processes) or is mediated by biocrusts (e.g. through interception of fine particles or biomineralization).

3.3.5. Conclusions

In conclusion, this study identified for the first time WVA periods with the gradient method and provided further understanding on the underlying processes involved in the temporal patterns (diel and seasonal) of WVA. We also found that WVA was the main source of water in summer when microclimatic conditions necessary to other non-rainfall water inputs were uncommon. Our main finding is the existence of a tight coupling between F_c and F_h. So far, F_c has commonly been modelled as a function of T_s, θ_w and proxies of photosynthesis. Here, for the first time, F_c was modelled as a function of F_h during summer, providing robust predictions and thus this relation deserves to be tested in other ecosystems. We attribute the detected diel hysteresis between F_c and F_h to a potential water vapor adsorption/desorption process. The occurrence of both CO_2 and water vapor uptake by soil at night suggests that both processes might be connected. We propose different biogeochemical mechanisms through which WVA could contribute or interact with this CO_2 uptake, including the potential co-adsorption of those gases on highly reactive clay-size calcite and the potential enhancement of the activity of specialized microorganisms.

More efforts are now needed to confirm the role of WVA on soil CO_2 uptake and disentangle the suggested involved processes, as well as to confirm its occurrence in other non-coastal drylands. In particular, the assumption according to which the soil CO_2 uptake could not arise from calcite dissolution due to the lack of water in drylands, should be revisited, as it did not consider WVA as a potential link between the water and carbon cycle in those environments. Additional research is needed to monitor soil water vapor and CO_2 uptake as those sinks could grow with climate change in different ways: (1) warmer air has the capacity to hold more water vapor, and a soil drying is predicted in some regions of the globe, thus potentially enhancing WVA; (2) the atmospheric CO_2 increase is expected to enhance CO_2 adsorption by soils, especially in areas of low biological activity (typically, drylands) and where highly adsorbent phases are present; (3) little is known about the effect of future elevated CO_2 on the rate of CO_2 fixation by microorganisms.

In addition, the significance of the water input through WVA in hot and dry conditions leaves the door open for novel or growing research areas, for example to explore the role of WVA on ecosystem processes such as microbial and mineral reactions, on the growth of plants of agricultural interest in drylands, and as a potential source of liquid water in extra-terrestrial environments. Finding ways of optimizing WVA for agriculture in water-limited ecosystems is particularly relevant as they cover about 41% of Earth´s terrestrial surface and support more than two billion people (about one third of the world´s total population), 90% of whom are in developing countries.

Acknowledgements

This work was funded by the research project CGL2016-78075-P, Biocrust Dinamics (DINCOS), of the Spanish National Program of Scientific and Technical Research, and by the ICAERSA research project (P18-RT-3629) of the Andalusian Regional Government including European Union ERDF funds. We are grateful to Andrew S. Kowalski for the proofreading and insightful suggestions that considerably improved the manuscript, to Consuelo Rubio who performed the particle size analysis; and we are grateful to the Viciana brothers, landowners of the El Cautivo experimental site, without whose kind consent to set up semi-permanent installations on their land, this research would not have been possible.

Supporting information

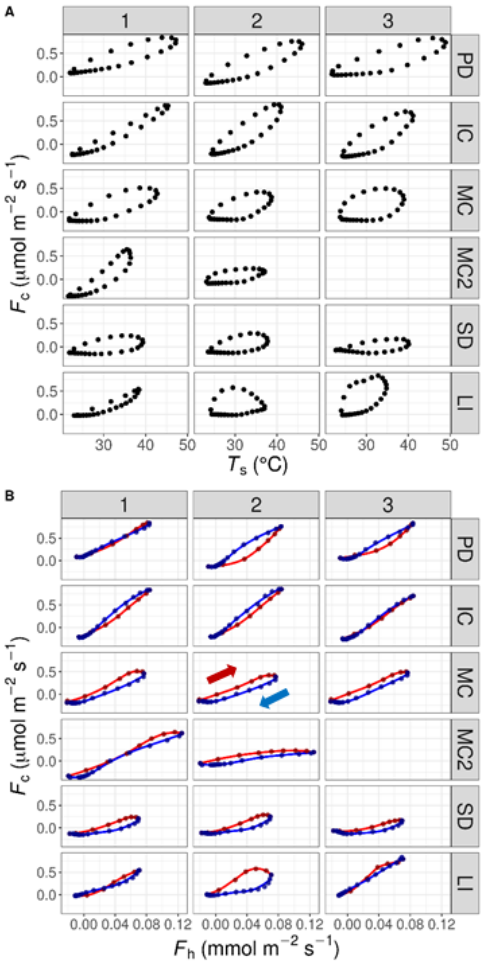

Figure S1 Diel hysteresis between the soil-atmosphere CO_2 flux (F_c) and (A) soil temperature (T_s), and (B) the soil-atmosphere water vapor flux (F_h). The blue line represents the decrease from F_h maximum (during daytime) to minimum (during nighttime) and *vice-versa* for the red line. Stages of the biocrusts succession are labeled as: physical depositional crust (PD), incipient *Cyanobateria* (IC), mature *Cyanobacteria* (MC), lichen community dominated by *Squamarina lentigera* and *Diploschistes diacapsis* (SD), lichen community characterized by *Lepraria isidiata* (LI), and *Cyanobacteria* patches within the SD microsite (MC2).

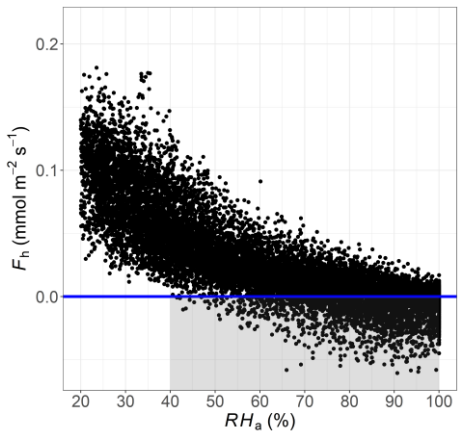

Figure S2 Relationship between the soil-atmosphere water vapor flux and the relative humidity in atmosphere (RH_a) within the mature *Cyanobacteria* site (MC2).

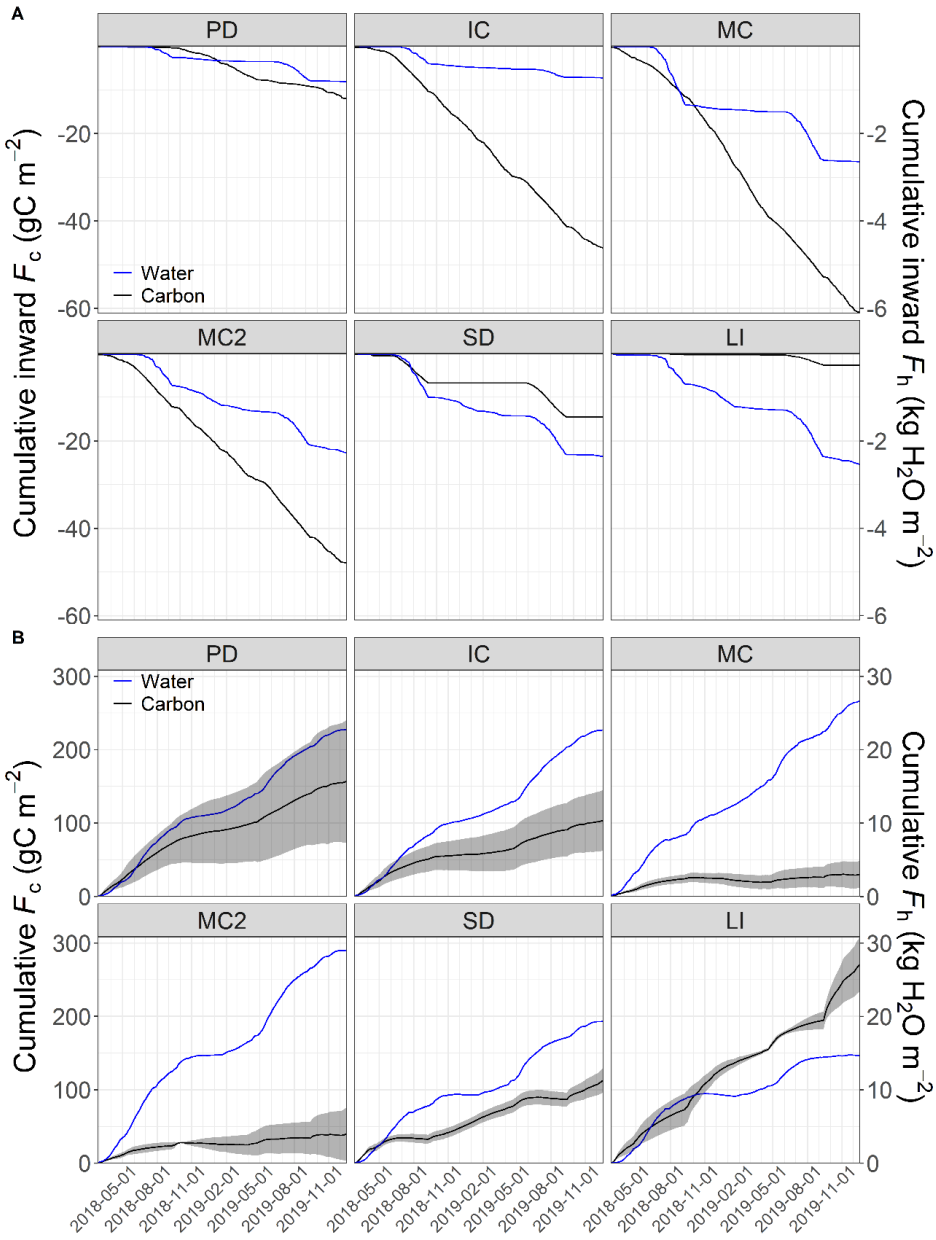

Figure S3 Cumulative (A) inward and (B) total fluxes of water vapor (F_h) and carbon (F_c). The shaded areas delimit the spatial standard variation. Represented water vapor fluxes were estimated with the diffusion model of Bittelli et al. (2015) while carbon fluxes were calibrated empirically. Stages of the biocrusts succession are labeled as: physical depositional crust (PD), incipient *Cyanobateria* (IC), mature *Cyanobacteria* (MC), lichen community dominated by *Squamarina lentigera* and *Diploschistes diacapsis* (SD), lichen community characterized by *Lepraria isidiata* (LI), and *Cyanobacteria* patches within the SD microsite (MC2).

Table S1A Summary of fixed effects of non-linear models of the diel hysteresis between CO_2 and water vapor fluxes

		Diel decrease model			Diel increase model		
Parameter	Crust	Value	SE	p-value	Value	SE	p-value
φ_1	PD	0.892	0.056	<0.001	1.284	0.099	<0.001
	IC	0.749	0.078	0.07	0.817	0.125	<0.001
	MC	0.546	0.080	<0.001	0.611	0.126	<0.001
	MC2	0.395	0.087	<0.001	0.488	0.136	<0.001
	SD	0.451	0.131	<0.001	0.283	0.126	<0.001
	LI	1.182	0.125	<0.05	0.736	0.126	<0.001
φ_2	PD	-0.077	0.045	0.09	0.068	0.039	0.08
	IC	-0.216	0.063	<0.05	-0.189	0.054	<0.001
	MC	-0.195	0.063	0.06	-0.191	0.055	<0.001
	MC2	-0.240	0.070	<0.05	-0.248	0.062	<0.001
	SD	-0.079	0.062	0.98	-0.059	0.054	<0.05
	LI	0.054	0.063	<0.05	0.073	0.054	0.94
φ_3	PD	0.041	0.009	<0.001	0.084	0.007	<0.001
	IC	0.032	0.013	0.53	0.040	0.010	<0.001
	MC	0.047	0.014	0.68	0.032	0.010	<0.001
	MC2	0.051	0.015	0.51	0.030	0.011	<0.001
	SD	0.095	0.017	<0.01	0.049	0.010	<0.001
	LI	0.113	0.015	<0.001	0.045	0.010	<0.001
φ_4	PD	0.028	0.002	<0.001	0.032	0.002	<0.001
	IC	0.019	0.002	<0.001	0.021	0.003	<0.001
	MC	0.033	0.003	0.06	0.031	0.003	0.88
	MC2	0.034	0.003	<0.05	0.033	0.003	0.79
	SD	0.030	0.004	0.61	0.020	0.003	<0.001
	LI	0.043	0.004	<0.001	0.020	0.003	<0.001

Table S1B Summary of the non-linear relationship between CCE and SOC contents

Parameter	Value	SE	p-value
φ_1	0.318	0.005	<0.001
φ_2	0.183	0.005	<0.001
φ_3	0.646	0.004	<0.001
φ_4	0.028	0.005	<0.01

SE, standard error, φ_n are the fitted parameters of the four-parameter logistic model $(y = \varphi_1 + (\varphi_2 - \varphi_1)/ (1 + exp[(\varphi_3 - x)/\varphi_4)]$, with ϕ_1 the horizontal asymptote as $x \rightarrow \infty$, ϕ_2 the horizontal asymptote as $x \rightarrow -\infty$, ϕ_3 the x value at the inflection point of the sigmoid (the value of x for which the response variable $y = \phi_1/2$), and ϕ_4 a scale parameter on the x-axis. SE is the standard error.

References

Agam, N., Berliner, P.R., 2006. Dew formation and water vapor adsorption in semi-arid environments—a review. J. Arid Environ. 65, 572–590.

Akin, I.D., Likos, W.J., 2020. Relationship between water vapor sorption kinetics and clay surface properties. J. Geotech. Geoenvironmental Eng. 146, 6020015.

Akin, I.D., Likos, W.J., 2017. Implications of surface hydration and capillary condensation for strength and stiffness of compacted clay. J. Eng. Mech. 143, 4017054.

Amer, A.M., 2019. Soil moisture adsorption capacity and specific surface area in relation to water vapor pressure in arid and tropical soils. Eurasian J. Soil Sci. 8, 289–297. https://doi.org/10.18393/EJSS.580889

Arthur, E., Tuller, M., Moldrup, P., de Jonge, L.W., 2020. Clay content and mineralogy, organic carbon and cation exchange capacity affect water vapour sorption hysteresis of soil. Eur. J. Soil Sci. 71, 204–214.

Azimi, G., Papangelakis, V.G., Dutrizac, J.E., 2007. Modelling of calcium sulphate solubility in concentrated multi-component sulphate solutions. Fluid Phase Equilib. 260, 300–315.

Bay, S.K., Waite, D.W., Dong, X., Gillor, O., Chown, S.L., Hugenholtz, P., Greening, C., 2021. Chemosynthetic and photosynthetic bacteria contribute differentially to primary production across a steep desert aridity gradient. ISME J. 1–18.

Belnap, J., Prasse, R., Harper, K.T., 2003. Influence of biological soil crusts on soil environments and vascular plants, in: Biological Soil Crusts: Structure, Function, and Management. Springer, Berlin, Heidelberg, pp. 281–300. https://doi.org/10.1007/978-3-642-56475-8_21

Benzerara, K., Skouri-Panet, F., Li, J., Férard, C., Gugger, M., Laurent, T., Couradeau, E., Ragon, M., Cosmidis, J., Menguy, N., 2014. Intracellular Ca-carbonate biomineralization is widespread in cyanobacteria. Proc. Natl. Acad. Sci. 111, 10933–10938.

Beymer, R.J., Klopatek, J.M., 1991. Potential contribution of carbon by microphytic crusts in pinyon-juniper woodlands. Arid L. Res. Manag. 5, 187–198. https://doi.org/http://doi.org/10.1080/15324989109381279

Bittelli, M., Ventura, F., Campbell, G. S., Snyder, R. L., Gallegati, F., & Pisa, P. R.

(2008). Coupling of heat, water vapor, and liquid water fluxes to compute evaporation in bare soils. Journal of Hydrology, 362(3–4), 191–205. https://doi.org/10.1016/J.JHYDROL.2008.08.014

Bittelli, M., Campbell, G.S., Tomei, F., 2015. Soil physics with Python: transport in the soil-plant-atmosphere system. OUP Oxford.

Buck, A.L., 1981. New equations for computing vapor pressure and enhancement factor. J. Appl. Meteorol. 20, 1527–1532.

Collins, M., Knutti, R., Arblaster, J., Dufresne, J.-L., Fichefet, T., Friedlingstein, P., Gao, X., Gutowski, W.J., Johns, T., Krinner, G., 2013. Long-term climate change: projections, commitments and irreversibility, in: Climate Change 2013-The Physical Science Basis: Contribution of Working Group I to the Fifth Assessment Report of the Intergovernmental Panel on Climate Change. Cambridge University Press, pp. 1029–1136.

Cuezva, S., Fernandez-Cortes, A., Porca, E., Pašić, L., Jurado, V., Hernandez-Marine, M., Serrano-Ortiz, P., Hermosin, B., Cañaveras, J.C., Sanchez-Moral, S., 2012. The biogeochemical role of Actinobacteria in Altamira cave, Spain. FEMS Microbiol. Ecol. 81, 281–290.

Davidson, G.R., Phillips-Housley, A., Stevens, M.T., 2013. Soil-zone adsorption of atmospheric CO2 as a terrestrial carbon sink. Geochim. Cosmochim. Acta 106, 44–50.

Dusza, Y., Sanchez-Cañete, E.P., Le Galliard, J.-F., Ferriere, R., Chollet, S., Massol, F., Hansart, A., Juarez, S., Dontsova, K., Van Haren, J., 2020. Biotic soil-plant interaction processes explain most of hysteretic soil CO 2 efflux response to temperature in cross-factorial mesocosm experiment. Sci. Rep. 10, 1–11.

Fa, K.-Y., Zhang, Y.-Q., Wu, B., Qin, S.-G., Liu, Z., She, W.-W., 2016. Patterns and possible mechanisms of soil CO2 uptake in sandy soil. Sci. Total Environ. 544, 587–594. https://doi.org/10.1016/j.scitotenv.2015.11.163

Garcia-Pichel, F., Ramírez-Reinat, E., Gao, Q., 2010. Microbial excavation of solid carbonates powered by P-type ATPase-mediated transcellular Ca2+ transport. Proc. Natl. Acad. Sci. 107, 21749–21754. https://doi.org/10.1073/pnas.1011884108

Guenet, B., Camino-Serrano, M., Ciais, P., Tifafi, M., Maignan, F., Soong, J.L., Janssens, I.A., 2018. Impact of priming on global soil carbon stocks. Glob. Chang. Biol. 24, 1873–1883. https://doi.org/10.1111/gcb.14069

Hamerlynck, E.P., Scott, R.L., Sánchez-Cañete, E.P., Barron-Gafford, G.A., 2013. Nocturnal soil CO2 uptake and its relationship to subsurface soil and ecosystem carbon fluxes in a Chihuahuan Desert shrubland. J. Geophys. Res. Biogeosciences 118, 1593–1603. https://doi.org/10.1002/2013JG002495

Hatch, C.D., Wiese, J.S., Crane, C.C., Harris, K.J., Kloss, H.G., Baltrusaitis, J., 2012. Water adsorption on clay minerals as a function of relative humidity: application of BET and Freundlich adsorption models. Langmuir 28, 1790–1803.

Hervé, V., Junier, T., Bindschedler, S., Verrecchia, E., Junier, P., 2016. Diversity and ecology of oxalotrophic bacteria. World J. Microbiol. Biotechnol. 32, 28.

Jabro, J. D., & Jabro, J. D. (2008). Water Vapor Diffusion Through Soil as Affected by Temperature and Aggregate Size. Transport in Porous Media 2008 77:3, 77(3), 417–428. https://doi.org/10.1007/S11242-008-9267-Z

Kargas, G., Londra, P., Sgoubopoulou, A., 2020. Comparison of Soil EC Values from Methods Based on 1:1 and 1:5 Soil to Water Ratios and ECe from Saturated Paste Extract Based Method. Water 2020, Vol. 12, Page 1010 12, 1010. https://doi.org/10.3390/W12041010

Kharitonova, G. V, Vityazev, V.G., Lapekina, S.I., 2010. A mathematical model for the adsorption of water vapor by soils. Eurasian Soil Sci. 43, 177–186.

Kohfahl, C., Saaltink, M.W., Ruiz Bermudo, F., 2021. Vapor flow control in dune sediments under dry bare soil conditions. Sci. Total Environ. 786, 147404. https://doi.org/10.1016/J.SCITOTENV.2021.147404

Kool, D., Agra, E., Drabkin, A., Duncan, A., Fendinat, P.P., Leduc, S., Lupovitch, G., Nambwandja, A.N., Ndilenga, N.S., Thị, T.N., 2021. The overlooked non-rainfall water input sibling of fog and dew: Daily water vapor adsorption on a! Nara hummock in the Namib Sand Sea. J. Hydrol. 598, 126420.

Kosmas, C., Danalatos, N.G., Poesen, J., Van Wesemael, B., 1998. The effect of water vapour adsorption on soil moisture content under Mediterranean climatic conditions. Agric. water Manag. 36, 157–168.

Kosmas, C., Marathianou, M., Gerontidis, S., Detsis, V., Tsara, M., Poesen, J., 2001. Parameters affecting water vapor adsorption by the soil under

semi-arid climatic conditions. Agric. water Manag. 48, 61–78.

Lange, O.L., Kidron, G.J., Budel, B., Meyer, A., Kilian, E., Abeliovich, A., 1992. Taxonomic composition and photosynthetic characteristics of thebiological soil crusts' covering sand dunes in the western Negev Desert. Funct. Ecol. 519–527.

Lange, O.L., Meyer, A., Zellner, H., Heber, U., 1994. Photosynthesis and Water Relations of Lichen Soil Crusts: Field Measurements in the Coastal Fog Zone of the Namib Desert. Funct. Ecol. 8, 253. https://doi.org/10.2307/2389909

Lebron, I., Herrero, J., Robinson, D.A., 2009. Determination of gypsum content in dryland soils exploiting the gypsum–bassanite phase change. Soil Sci. Soc. Am. J. 73, 403–411.

Li, S., Xiao, B., Sun, F., Kidron, G.J., 2021. Moss-dominated biocrusts enhance water vapor sorption capacity of surface soil and increase non-rainfall water deposition in drylands. Geoderma 388, 114930.

Liu, F. fei, Mao, X. song, Zhang, J. xun, Wu, Q., Li, Y. ying, & Xu, C. (2020). Isothermal diffusion of water vapor in unsaturated soils based on Fick's second law. *Journal of Central South University 2020 27:7*, *27*(7), 2017–2031. https://doi.org/10.1007/S11771-020-4427-6

Liu, J., Fa, K., Zhang, Y., Wu, B., Qin, S., Jia, X., 2015. Abiotic CO2 uptake from the atmosphere by semiarid desert soil and its partitioning into soil phases. Geophys. Res. Lett. 42, 5779–5785.

Liu, Z., Sun, Y., Zhang, Y., Feng, W., Lai, Z., Qin, S., 2021. Soil Microbes Transform Inorganic Carbon into Organic Carbon by Dark Fixation Pathways in Desert Soil. J. Geophys. Res. Biogeosciences e2020JG006047.

Liu, Z., Zhang, Y., Fa, K., Zhao, H., Qin, S., Yan, R., Wu, B., 2018. Desert soil bacteria deposit atmospheric carbon dioxide in carbonate precipitates. Catena 170, 64–72.

Loeppert, R.H., Suarez, D.L., 1996. Carbonate and gypsum. Methods Soil Anal. Part 3 Chem. Methods 5, 437–474. https://doi.org/10.2136/sssabookser5.3.c15

Lopez-Canfin, C., Sánchez-Cañete, E.P., Lazaro, R., 2021. Development of a new low-cost device to measure calcium carbonate content, reactive surface area in solid samples and dissolved inorganic carbon content in

water samples. Methods Ecol. Evol. https://doi.org/10.1111/2041-210X.13579

Lopez Canfin, C., Lázaro, R., Sánchez-Cañete P, E., in review. Disparate responses of soil-atmosphere CO2 exchange to biophysical and geochemical factors over a biocrust ecological succession in the Tabernas Desert. Biogeochemistry.

Ma, J., Wang, Z.-Y., Stevenson, B.A., Zheng, X.-J., Li, Y., 2013. An inorganic CO2 diffusion and dissolution process explains negative CO2 fluxes in saline/alkaline soils. Sci. Rep. 3, 2025. https://doi.org/10.1038/srep02025

Maier, M., Schack-Kirchner, H., 2014. Using the gradient method to determine soil gas flux: A review. Agric. For. Meteorol. 192, 78–95.

McHugh, T.A., Morrissey, E.M., Reed, S.C., Hungate, B.A., Schwartz, E., 2015. Water from air: an overlooked source of moisture in arid and semiarid regions. Sci. Rep. 5, 1–6.

Meier, A., Kastner, A., Harries, D., Wierzbicka-Wieczorek, M., Majzlan, J., Büchel, G., Kothe, E., 2017. Calcium carbonates: induced biomineralization with controlled macromorphology. Biogeosciences 14, 4867–4878.

Mencuccini, M., Hölttä, T., 2010. The significance of phloem transport for the speed with which canopy photosynthesis and belowground respiration are linked. New Phytol. 185, 189–203.

Michels, L., Fossum, J.O., Rozynek, Z., Hemmen, H., Rustenberg, K., Sobas, P.A., Kalantzopoulos, G.N., Knudsen, K.D., Janek, M., Plivelic, T.S., 2015. Intercalation and retention of carbon dioxide in a smectite clay promoted by interlayer cations. Sci. Rep. 5, 1–9.

Mingorance, M.D., Barahona, E., Fernández-Gálvez, J., 2007. Guidelines for improving organic carbon recovery by the wet oxidation method. Chemosphere 68, 409–413. https://doi.org/10.1016/j.chemosphere.2007.01.021

Miralles, I., Ladrón de Guevara, M., Chamizo, S., Rodríguez-Caballero, E., Ortega, R., van Wesemael, B., Cantón, Y., 2018. Soil CO2 exchange controlled by the interaction of biocrust successional stage and environmental variables in two semiarid ecosystems. Soil Biol. Biochem.

124, 11–23. https://doi.org/10.1016/J.SOILBIO.2018.05.020

Miralles, I., Lázaro, R., Sánchez-Marañón, M., Soriano, M., Ortega, R., 2020. Biocrust cover and successional stages influence soil bacterial composition and diversity in semiarid ecosystems. Sci. Total Environ. 709, 134654. https://doi.org/10.1016/J.SCITOTENV.2019.134654

Ouadjenia, F., Marouf, R., Schott, J., 2017. Mechanism sorption of carbon dioxide onto dam silt. Cogent Chem. 3, 1300974.

Pinheiro, J.C., Bates, D.M., 2000. Mixed-Effects Models in S and S-Plus. Springer-Verlag New York, New York, NY.

Rahaman, A., Grassian, V.H., Margulis, C.J., 2008. Dynamics of water adsorption onto a calcite surface as a function of relative humidity. J. Phys. Chem. C 112, 2109–2115.

Rao, S. M., & Rekapalli, M. (2020). Identifying the dominant mode of moisture transport during drying of unsaturated soils. Scientific Reports 2020 10:1, 10(1), 1–9. https://doi.org/10.1038/s41598-020-61302-w

Ravikovitch, P.I., Bogan, B.W., Neimark, A. V, 2005. Nitrogen and carbon dioxide adsorption by soils. Environ. Sci. Technol. 39, 4990–4995.

Reyzabal, M. L., & Bazán, J. C. (1992). A method for measurement of water vapor diffusion in dry soils. Geoderma, 53(1–2), 105–110. https://doi.org/10.1016/0016-7061(92)90024-2

Rowley, M.C., Grand, S., Verrecchia, É.P., 2018. Calcium-mediated stabilisation of soil organic carbon. Biogeochemistry 137, 27–49.

Rubasinghege, G., Grassian, V.H., 2013. Role (s) of adsorbed water in the surface chemistry of environmental interfaces. Chem. Commun. 49, 3071–3094.

Saaltink, M.W., Kohfahl, C., Molano Leno, L., 2020. Analysis of water vapor adsorption in soils by means of a lysimeter and numerical modeling. Vadose Zo. J. 19, e20012: 1-e20012: 18.

Sagi, N., Zaguri, M., Hawlena, D., 2021. Soil CO2 influx in drylands: A conceptual framework and empirical examination. Soil Biol. Biochem. 156, 108209. https://doi.org/10.1016/J.SOILBIO.2021.108209

Sánchez-Cañete, E.P., Scott, R.L., van Haren, J., Barron-Gafford, G.A., 2017. Improving the accuracy of the gradient method for determining soil carbon dioxide efflux. J. Geophys. Res. Biogeosciences 122, 50–64.

Schlesinger, W.H., Belnap, J., Marion, G., 2009. On carbon sequestration in

desert ecosystems. Glob. Chang. Biol. 15, 1488–1490.

Šimůnek, J., & Suarez, D. L. (1993). Modeling of carbon dioxide transport and production in soil: 1. Model development. *Water Resources Research*, *29*(2), 487–497.

Solé-Benet, A., Calvo, A., Cerda, A., Laīzaro, R., Pini, R., Barbero, J., 1997. Influences of micro-relief patterns and plant cover on runoff related processes in badlands from Tabernas (SE Spain). Catena 31, 23–38.

Tian, D., Su, M., Zou, X., Zhang, L., Tang, L., Geng, Y., Qiu, J., Wang, S., Gao, H., Li, Z., 2021. Influences of phosphate addition on fungal weathering of carbonate in the red soil from karst region. Sci. Total Environ. 755, 142570. https://doi.org/10.1016/J.SCITOTENV.2020.142570

Uclés, O., Villagarcía, L., Cantón, Y., Lázaro, R., Domingo, F., 2015. Non-rainfall water inputs are controlled by aspect in a semiarid ecosystem. J. Arid Environ. 113, 43–50.

Verhoef, A., Diaz-Espejo, A., Knight, J.R., Villagarcía, L., Fernandez, J.E., 2006. Adsorption of water vapor by bare soil in an olive grove in southern Spain. J. Hydrometeorol. 7, 1011–1027.

Wang, L., Kaseke, K.F., Seely, M.K., 2017. Effects of non-rainfall water inputs on ecosystem functions. Wiley Interdiscip. Rev. Water 4, e1179. https://doi.org/10.1002/WAT2.1179

Warren, S.D., 2003. Synopsis: influence of biological soil crusts on arid land hydrology and soil stability, in: Biological Soil Crusts: Structure, Function, and Management. Springer, pp. 349–360.

Xu, X., Nieber, J.L., Gupta, S.C., 1992. Compaction effect on the gas diffusion coefficient in soils. Soil Sci. Soc. Am. J. 56, 1743–1750.

Yu, L., Daniels, L.M., Mulders, J.J.P.A., Saldi, G.D., Harrison, A.L., Liu, L., Oelkers, E.H., 2019. An experimental study of gypsum dissolution coupled to CaCO3 precipitation and its application to carbon storage. Chem. Geol. 525, 447–461. https://doi.org/10.1016/J.CHEMGEO.2019.08.005

Zhang, Q., Phillips, R.P., Manzoni, S., Scott, R.L., Oishi, A.C., Finzi, A., Daly, E., Vargas, R., Novick, K.A., 2018. Changes in photosynthesis and soil moisture drive the seasonal soil respiration-temperature hysteresis relationship. Agric. For. Meteorol. 259, 184–195.

Zheng, J., Peng, C., Li, H., Li, S., Huang, S., Hu, Y., Zhang, J., Li, D., 2018. The role

of non-rainfall water on physiological activation in desert biological soil crusts. J. Hydrol. 556, 790–799. https://doi.org/10.1016/J.JHYDROL.2017.12.003

Zuur, A.F., Ieno, E.N., 2016. A protocol for conducting and presenting results of regression-type analyses. Methods Ecol. Evol. 7, 636–645. https://doi.org/10.1111/2041-210X.12577

3.4. CHAPTER 4

Nocturnal soil CO_2 uptake driven by coupled gypsum dissolution and calcite precipitation in the Tabernas Desert: an active and potential long-term carbon sink

Clément Lopez-Canfin, Roberto Lázaro, Enrique P. Sánchez-Cañete

In preparation to submit for publication to *Science of the Total Environment*

Lopez-Canfin, C.; Lázaro R.; Sánchez-Cañete, E.P (in prep.). Nocturnal soil CO_2 uptake by coupled gypsum dissolution and calcite precipitation in the Tabernas Desert: an active and potential long-term carbon sink.

Graphical abstract

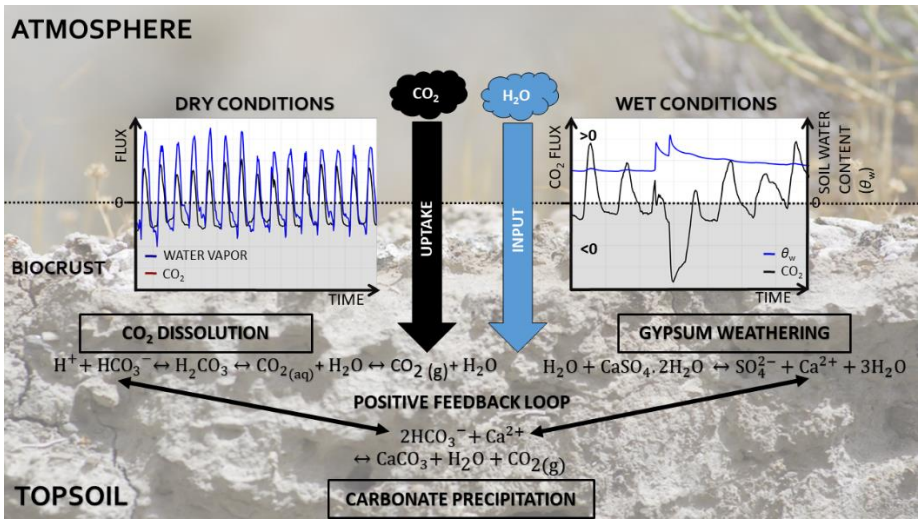

Abstract

Drylands soils have been increasingly reported to absorb CO_2 at nighttime. However, there is no consensus so far about which biogeochemical processes cause this uptake. Recent evidences in a semiarid ecosystem in Southern Spain suggested that geochemical reactions with calcite could be involved and favored by the adsorption of water vapor by dry soils.

In order to test this assumption in this ecosystem, we ran continuous measurements of the soil-atmosphere CO_2 and water vapor fluxes in association with soil temperature and soil water content. Those measurements were combined with analyses of the composition of the soil solution after simulated rain events and subsequent geochemical and statistical modelling.

We found strong evidence for the occurrence of a geochemical mechanism of coupled gypsum dissolution-carbonate precipitation, due to a common-ion effect. The soil CO_2 uptake can be explained by decreasing temperature favoring the dissolution of CO_2 in the soil water, forming HCO_3^- that can combine with the Ca inherited from gypsum dissolution to precipitate $CaCO_3$. The continuous removal of HCO_3^- by $CaCO_3$ precipitation might generate a positive feedback between the mineral precipitation and CO_2 dissolution in soil water.

The main factor limiting the process in this dryland was water availability, but our observations support that nocturnal water vapor adsorption by soil might lift this limitation under drought conditions. In addition, dissolved organic carbon seemed to inhibit the CO_2 uptake by calcite precipitation, and a possible connection with the nitrogen cycle and biomineralizing microorganisms deserves to be further investigated. We suggest that this natural geochemical process has the potential to constitute an active long-term carbon sink since the Ca involved in $CaCO_3$ precipitation came from an exogenic source.

3.4.1. Introduction

The soil-atmosphere CO_2 flux (F_c) is a critical component of the terrestrial carbon (C) cycle because of (1) its magnitude. The carbon of soils is estimated to be exchanged with the atmosphere at a rate of ca. 98 Gt C yr^{-1} [*Bond-Lamberty & Thomson*, 2010a]. This is *ca*. 15 times higher than the annual rate of C emission through fossil fuel combustion [*Denman et al.*, 2007] and makes F_c the second largest contributor to terrestrial CO_2 exchanges, similar in scale to uptake by terrestrial photosynthesis [*Raich & Schlesinger*, 1992; *Schimel et al.*, 2001]; (2) its feedback with climate. Since soil temperature and moisture are the main biophysical factors controlling F_c [*Lopez-Canfin et al.*, 2018], the current global warming and changes in precipitation patterns are likely to modify the amount of CO_2 released by soils, potentially affecting in return the greenhouse effect. However, F_c remains the least constrained component of the terrestrial carbon cycle [*Bond-Lamberty & Thomson*, 2010b] and is often interpreted as being under the influence of biological processes, thus neglecting the role of important abiotic drivers on its dynamics [*Rey*, 2015; *Serrano-Ortiz et al.*, 2010].

This is because in most instances, F_c can be considered as the result of dominant processes of CO_2 production and transport: respiration and diffusion, respectively [*Šimůnek & Suarez*, 1993]. The biological production of CO_2 by respiration maintains a gradient of decreasing CO_2 concentrations from soil to atmosphere. As CO_2 mainly flows following the Fick´s first law of molecular diffusion, F_c is usually positive (efflux or CO_2 emission towards atmosphere). Nevertheless, it has been recently reported that a considerable fraction of soil CO_2 is not emitted directly towards atmosphere, but rather reacts into the soil where it is consumed by various biogeochemical processes [*Sánchez-Cañete et al.*, 2018]. In ecosystems where biological activity is limited, the prevalence of CO_2 consumption rates over CO_2 production rates can sometimes result in negative values of F_c (influx or CO_2 uptake by the soil). Therefore, such “anomalies” in F_c have generally been reported in drylands [e.g. *Fa et al.*, 2016; *Hamerlynck et al.*, 2013; *Liu et al.*, 2015], revealing the non-negligible role of soil CO_2 consumption processes on the carbon balance of these ecosystems.

However, there is no consensus so far about which biogeochemical

processes are involved in these anomalies of F_c, and they are not necessarily unique nor identical from one site to another. Both biotic and abiotic mechanisms can explain such observations. Several biotic processes are able to consume CO_2 in the soil gaseous phase at night: (1) root uptake by plants [*Stemmet et al.*, 1962]; (2) chemoautotrophy: Chemoautotrophic microorganisms can fix CO_2 into organic matter via the oxidation of reduced organic or inorganic compounds [*Bay et al.*, 2021; *Liu et al.*, 2021]; (3) bioweathering and/or biomineralization [*Cuezva et al.*, 2011; *Liu et al.*, 2018]. The abiotic mechanisms that can consume gaseous CO_2 in soil are (1) CO_2 adsorption on soil particles [*Davidson et al.*, 2013]; (2) CO_2 dissolution in the aqueous phase [*Ma et al.*, 2013, 2014] producing dissolved inorganic carbon (DIC) species according to the reaction:

$$CO_{2\,(g)} + H_2O_{\,(l)} \leftrightarrow CO_{2\,(aq)} + H_2O_{\,(l)} \leftrightarrow H_2CO_3 \leftrightarrow H^+_{(aq)} + HCO_3^-{}_{(aq)} \leftrightarrow 2H^+_{(aq)} + CO_3^-{}_{(aq)} \quad (1)$$

Soils can store an order of magnitude greater CO_2 as DIC in the aqueous phase than in the gas phase [*Angert et al.*, 2015]. The amount of DIC depends mainly on the partial pressure of CO_2 and temperature according to Henry´s law, as well as pH; (3) solubilization of some minerals, such as carbonates [*Liu et al.*, 2011; *Roland et al.*, 2013], the solubility of carbonates being inversely related to temperature; (4) precipitation of secondary carbonates [*Hasinger et al.*, 2015]. Carbonate dissolution and precipitation processes occur according to the following reversible reaction:

$$CaCO_{3\,(s)} + H_2O_{\,(l)} + CO_{2\,(g)} \leftrightarrow Ca^{2+}{}_{(aq)} + 2HCO_3^-{}_{(aq)} \quad (2)$$

Among abiotic processes, whether $CaCO_3$ dissolution or precipitation can be considered as a net carbon sink depends on both the considered time-scale and the origin of calcium [*Monger et al.*, 2015]. The $CaCO_3$ dissolution immediately consumes gaseous CO_2 (eq. 2). This CO_2 removal from the gaseous phase could therefore be detected by instruments measuring CO_2 fluxes on short-time scales (e.g. at nighttime). However the DIC formed can return subsequently to the atmosphere as CO_2, e.g. when the soil dries out during daytime. The DIC should be exported to aquifers in order to capture carbon transiently, from hundreds up to thousands of years [*Kessler & Harvey*, 2001]. Over longer term, DIC is exported to the ocean and reprecipitate as $CaCO_3$, thus compensating the initial CO_2 uptake. Therefore, only the

weathering of non-carbonated rocks such as silicates can be considered as a long-term CO_2 sink since it initially consumes two moles of CO_2 and thus still removes one mole of CO_2 from the atmosphere even after reprecipitation as $CaCO_3$ according to the reactions:

$$CaSiO_{3\,(s)} + H_2O_{\,(l)} + 2CO_{2\,(g)} \leftrightarrow Ca^{2+}{}_{(aq)} + 2HCO_3{}^{-}{}_{(aq)} + SiO_{2\,(aq)} \leftrightarrow$$
$$CaCO_{3\,(s)} + H_2O_{\,(l)} + CO_{2\,(g)} + SiO_{2\,(aq)} \quad (3)$$

Similarly, although the $CaCO_3$ precipitation apparently produces gaseous CO_2 (eq. 2) potentially detectable on a short-time scale, the net balance of the equation is a carbon uptake since two moles of carbon are consumed for each mole of carbon that is produced. Instruments measuring gaseous CO_2 would detect a net CO_2 consumption only if bicarbonate ions involved in carbonate precipitation are actively renewed by rapid CO_2 dissolution in water (eq. 1). The precipitation of pedogenic carbonates represents an interesting long-term carbon sink since the residence time of mineral carbon is much greater than organic matter: 10^2-10^6 years and 0.1-10^3 years, respectively [*Bernoux & Chevallier*, 2014; *Cailleau et al.*, 2004]. Over the long term, in dryland soils inherited from carbonate bedrock, the alternance of $CaCO_3$ precipitation/dissolution due to drying/wetting cycles is expected to be carbon neutral, except (1) temporarily during large precipitation events able to export DIC by leaching to a transient aquifer reservoir; (2) in the presence of another source of calcium to increase the pool of precipitated $CaCO_3$ over time. Main sources of calcium exogenous to carbonates include the deposition of marine aerosols and atmospheric dust as well as the alteration of minerals [*Derry & Chadwick*, 2007] such as gypsum ($CaSO_4.H_2O$), a common salt at Earth´s surface [*Verheye & Boyadgiev*, 1997]. Hence, in order to understand the mechanisms driving nocturnal soil CO_2 uptake, it is crucial to consider the specific soil properties of the concerned sites.

In the experimental site of *El Cautivo* located in the Tabernas Desert (Almería, Spain), recent continuous measurements of pedoclimatic variables revealed a net uptake of CO_2 by soil at nighttime [*Lopez Canfin et al.*, n.d.]. The exact biogeochemical mechanisms explaining this uptake are not completely understood but recent evidences suggest that the water vapor adsorption by dry soil at nighttime could provide an input of liquid water on the surface of highly reactive clay-size carbonates [*Lopez Canfin et al.*, 2022]. The soil at this

experimental site inherits from a bedrock consisting of gypsum-calcareous mudstones and calcaric sandstones. In particular, the calcium carbonate equivalent content is high (*ca.* 15 to 30%) and soil pH ranges from ca. 7.5 to 9. From the one hand, soils with pH > 6.5, can retain substantial amounts of CO_2 in the solution phase [*Sparling & West*, 1990] and a soil solution charged with CO_2 has an enhanced capacity to dissolve minerals such as carbonates. In addition, the well-known increase in CO_2 and carbonates solubility with decreasing temperature (a condition typically occurring at night) together with local observations [*Lopez Canfin et al.*, n.d.] supports the hypothesis of a potential $CaCO_3$ dissolution process driving the nocturnal CO_2 uptake by soil at this site. From the other hand, due the co-occurrence of gypsum with calcite and the greater solubility of the former (exceeding calcite by two orders of magnitude), its potential interaction through a common ion effect deserves to be investigated.

Therefore, in this study we aimed to explore (1) whether carbonate reactions of precipitation/dissolution could drive the nocturnal CO_2 uptake by soil and (2) evaluate the potential of this CO_2 uptake as a long-term net carbon sink. In particular, we assumed that (1) the soil CO_2 uptake would be enhanced at nighttime and in winter due to lower temperature favoring both CO_2 dissolution in water according to Henry´s law and carbonate dissolution; (2) the magnitude of the CO_2 uptake would increase in soils with greater $CaCO_3$ contents due to more mineral reactions; (3) the presence of gypsum could interfere with $CaCO_3$ reactions due to a common-ion effect.

3.4.2. Material and Methods

3.4.2.1. Experimental site

This study was conducted in the experimental site of El Cautivo, an area of badlands located in the Tabernas Desert (Almería, Spain) (more information about the study site is provided in Section 2.1)

Since the magnitude of the nocturnal soil CO_2 uptake was greater in the mature cyanobacterial succession stage [*Lopez Canfin et al.*, n.d.], it was selected to conduct this study. In order to test the assumption according to which the magnitude of the soil CO_2 uptake would increase in soils with greater

$CaCO_3$ contents due to more mineral reactions, we chose two microsites (plots) belonging to the MC succession stage with different calcium carbonate equivalent contents (CCE). The first microsite (MC) had a CCE of 0.25 ± 0.01 g g^{-1} and the second microsite (MC2) had a CCE of 0.31 ± 0.03 g g^{-1} [*Lopez-Canfin et al.*, 2021]. In the MC2 microsite, *Cyanobacteria* were present as patches within the lichen SD site which had overall a greater biomass of biocrusts.

3.4.2.2. Environmental measurements

Continuous measurements of soil and above-surface variables were conducted since December 2017 (see Section 2.3.3). The soil-atmosphere CO_2 flux was also measured regularly with portable soil chambers (see Section 2.3.1).

3.4.2.3. Data processing, water vapor and CO_2 fluxes calculation

In order to determine cumulative fluxes over the study, a gap-filling procedure was applied to the data (see Section 2.4.1)

The soil and atmosphere χ_c were corrected for real-time changes in temperature and atmospheric pressure (see Section 2.2.1).

The water vapor pressure in soil and atmosphere was calculated as:

$$P_{\mathrm{h}} = \frac{RH}{100} P_{\mathrm{s}} \qquad (4)$$

where P_h is the water vapor pressure (kPa), *RH* is the relative humidity (%), and P_s is the saturation vapor pressure calculated according to Buck [1981].

The water vapor molar fraction in soil and atmosphere was calculated as:

$$\chi_{\mathrm{h}} = \frac{P_{\mathrm{h}}}{P_{\mathrm{a}}} \qquad (5)$$

where χ_h is the water vapor molar fraction (mol mol^{-1}) and P_a is the atmospheric pressure (kPa).

The soil-atmosphere fluxes of water vapor (F_h) and CO_2 (F_c) were calculated according to the gradient method (see Section 2.3.2).

The following cumulative F_h and F_c were calculated from the data: emissions, uptake and total resultant fluxes. They refer to, respectively: positive fluxes (from soil to atmosphere), negative fluxes (from atmosphere to soil) and the sum of both fluxes (positive and negative).

3.4.2.4. Rain simulations and soil solution sampling

The soil solution was sampled after simulating rainfall during the fall and winter season, both at nighttime and daytime. To this end, two 30 cm-diameter PVC tubes were inserted in the topsoil layer ensuring to include sensors measuring χ_c, θ_w and T_s within the delimited perimeters. Three soil solution samplers (1910PL06, Soilmoisture Equipment Corp., CA, USA) were installed at 5-cm depth within each microsite, randomly inside the area of the PVC tubes. The "zero dead volume" of those samplers and the sampling procedure described hereafter ensured to minimize potential pH measurement errors due to CO_2 degassing [*Suarez*, 1986, 1987]. Before each extraction, soil solution samplers were irrigated with rainwater previously collected in the area. An amount of 40 mm of rainwater was applied within each of the PVC tubes, two times. The first 40 mm were applied half a day before the extraction and the next 40 mm were applied just before the extraction. This amount of rainwater was selected based on preliminary tests, as it ensured to collect enough water for the subsequent analyses. The extraction was started once all the rainwater infiltrated. To this end, a vacuum of 50 kPa was applied to two buried 10 mL sampling vials and a 100 mL reservoir container connected in line with each extractor. The experimental design of the soil solution sampling experiment is summarized in Figure 1.

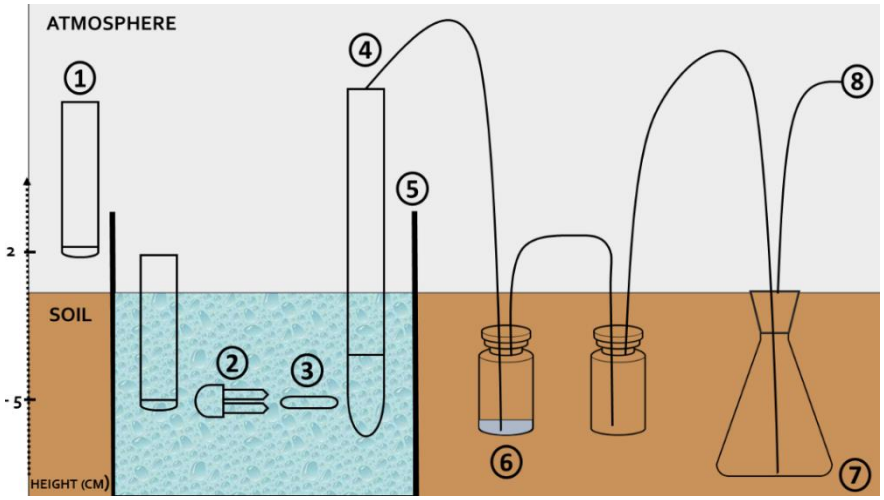

Figure 1 Experimental design of the soil water sampling experiment: (1) CO_2 molar fraction sensor; (2) soil water content sensor; (3) soil temperature sensor; (4) soil solution sampler; (5) PVC tube delimiting the watering area; (6) 5 mL sampling vial; (7) 100 mL sampling container; (8) vacuum (-50 kPa).

Once 3 times the total volume of the sampling vials was flushed through each extraction line, water samples were ready for collection. The pH electrode (HI1330B, Hannah instruments, Woonsocket, RI, USA) coupled to a pH-meter (PCE-228, PCE Iberica S.L., Tobarra, Spain) was calibrated by manually compensating the pH measurements for T_s. To this end, the pH buffers (4.01 and 7.00) were cooled or heated to reach the instantaneous readings of T_s. Once the vacuum was released, the pH electrode was equilibrated into the large sampling container. This ensured a faster response of the pH electrode for the subsequent pH determination from the sampling vial. A fast response is necessary to obtain a pH measurement representative of belowground conditions because once exposed to the atmosphere, the sample pH could drift due to CO_2 release or uptake. After measuring the pH in a sampling vial, two subsamples of 5 mL were withdrawn from the vial with a 10 mL syringe, filtered (0.22 µm, 25 mm Nylon filters) and saved in 5mL cryotubes for alkalinity analysis. Then the second sampling vial was disconnected and sealed quickly with an aluminum cap and a pressure gun. Two subsamples of 5 mL were withdrawn from this vial, filtered as well and saved in 5mL cryotubes for DIC determination. Particular care was taken to ensure that no air chamber were left inside the cryotubes. From the reservoir container, a 20 mL sample was filtered and saved for dissolved organic carbon (DOC) analysis. Two 10 mL samples were also filtered and saved for major anions and cations determination. The sample for cations was acidified with some drops of concentrated nitric acid (65%). If water was remaining in the reservoir, it was filtered and saved to measure conductance. Samples were transported to the laboratory in a cooler.

3.4.2.5. Geochemical analyses

The DIC and alkalinity were measured in the laboratory immediately after sampling, and the other samples were stored at 4°C until analysis. The DIC content was quantified by measuring the CO_2 released during an acidic reaction [*Lopez-Canfin et al.*, 2021]. Alkalinity was determined by titration with 0.1M HCl, using the inflection point method and calculator of the United States Geological Survey (https://or.water.usgs.gov/alk/). The acidified samples were analyzed for Ca, Mg, Na, K and S by a 720 series ICP Optical

Emission Spectrometer (Agilent, Santa Clara, CA, USA) according to APHA [2005]. Unacidified samples were used to determine Cl^- and NO_3^- with a Bran+Luebbe AA3 autoanalyzer (SPXFlow, Charlotte, NC, USA), according to ISO [2000] and ISO [1996], respectively. The DOC was estimated by difference between total carbon and DIC, both measured with a carbon analyzer TOC-Vcsh coupled to an automatic sampler ASI-V (Shimadzu, Kyoto, Japan), according to [*ASTM*, 1994]. The electrical conductivity (EC) of the soil solution was measured with a conductimeter Basic 30 (Crison Instruments, Barcelona, Spain). The gypsum content was determined by exploiting the gypsum-bassanite phase change [*Lebron et al.*, 2009]. The pH, alkalinity and major ionic species of the rainwater used for irrigation was analyzed using the same procedures as described previously.

3.4.2.6. Geochemical modelling

Saturation indices of calcite ($SI_{calcite}$) and gypsum (SI_{gypsum}) were calculated with the PHREEQC software (see Section 2.4.3).

3.4.2.7. Statistical analysis

All analyses were performed with R software v.4.1.0. A simple correlation analysis was performed to explore relationships between pairs of variables in the whole dataset and in subsets from each microsite. To this end, a correlation matrix with p-values was computed based on the non-parametric Kendall´s correlation and a strict significance level was used ($\alpha = 0.01$). Then, relevant relationships were plotted using the Siegel regression, an improved version of the Kendall–Theil Sen robust regression [*Siegel*, 1982].

3.4.3. Results

3.4.3.1. Soil CO_2 uptake in natural conditions

In natural conditions, over two years, the cumulative negative F_c (i.e. CO_2 uptake by soil (averaged among spatial replicates) were -65 gC m^{-2} and -55 gC m^{-2}, respectively in the MC and MC2 microsites (Figure 2A). They represented 64% and 54% of the cumulative positive F_c (101 gC m^{-2} in both microsites), i.e. CO_2 emission by soil, generating a resultant cumulative F_c close

to neutrality (36 and 46 gC m^{-2} for the MC and MC2 microsites, respectively). Those cumulative CO_2 fluxes are represented over time, together with the cumulative negative F_h (i.e. water vapor adsorption by soil) in Fig. 2A. During dry conditions in summer, the soil CO_2 uptake mainly occur at night during periods of water vapor adsorption by soil (see example in Fig. 2B). The soil CO_2 uptake was also often enhanced after rainfalls but not always, as the observed temporal patterns usually depended on antecedent θ_w. To illustrate that, the effect of two consecutive rainfalls in spring on F_c is represented in Fig. 2C. The rewetting of dry soil mainly produced CO_2 emissions immediately after rain (during two days in this example), after what the nocturnal CO_2 uptake started. As illustrated in this example, the consecutive rainfall on a previously wet soil immediately enhanced the soil CO_2 uptake.

3.4.3.2. Soil CO_2 uptake after rain simulation

All irrigations triggered or magnified the soil CO_2 uptake (Table 1). In general, the soil CO_2 uptake was particularly enhanced after the second rainwater pulse. An example of the effect of irrigation on F_c is shown in Fig. 3. Overall, the decrease in χ_c (from its basal value before the first irrigation to its minimum) was enhanced in winter compared to fall (Fig. 4A). The cumulative F_c during soil water extractions differed between sites and between day and night (Fig. 4B). More soil CO_2 uptake was observed when the soil water extraction was performed at nighttime and in the MC site. Note than in the MC2 site, the cumulative F_c during daytime was positive because of some CO_2 emissions in the last moments of the soil solution sampling.

3.4.3.3. Water composition and saturation indices

The composition of the soil water extracts is provided in Table 2. The composition of the rainwater used for irrigation is also provided in Supplementary Information (Table S1). Almost all the SI_{gypsum} were negative, indicating overall undersaturation of the soil water with respect to gypsum. The only few positive values were very close to zero, i.e. close to the equilibrium. By contrast, almost all $SI_{calcite}$ were positive, indicating overall supersaturation of the soil water with respect to calcite. The pH of the soil solution tended to be higher in the MC2 site, especially at nighttime (Fig. 4C).

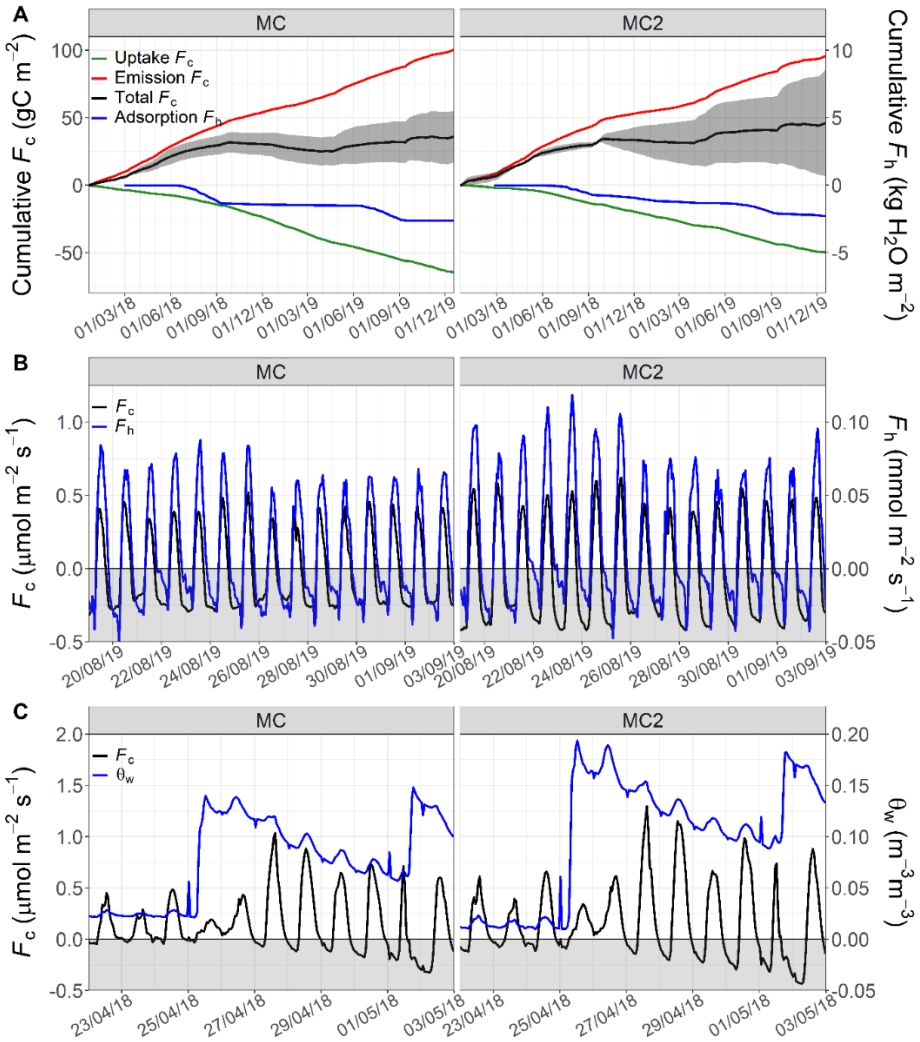

Figure 2 Time series of (A) cumulative soil-atmosphere CO_2 fluxes (F_c) and water vapor fluxes (F_h) of adsorption by soil; (B) hourly F_c and F_h during a dry period in summer. Negative values of F_h are attributed to water vapor adsorption by soil; (3) hourly F_c and soil water content (θ_w) after two consecutive rain pulses in spring. Measurements were conducted in two microsites dominated by mature *Cyanobacteria* (MC and MC2).

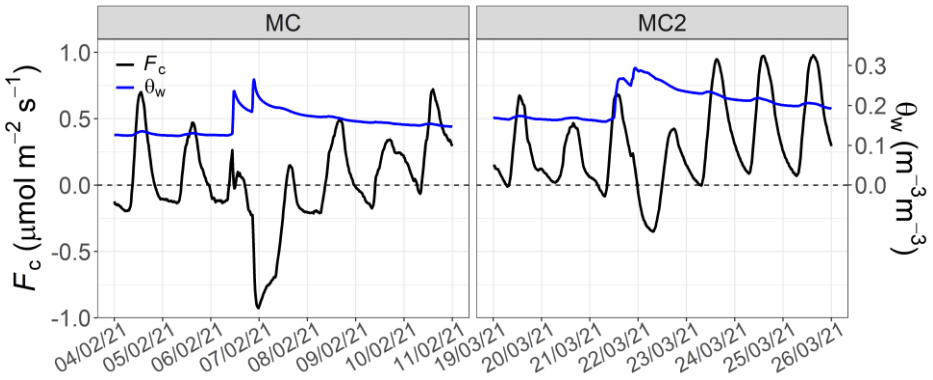

Figure 3 Time series of the soil-atmosphere CO_2 fluxes (F_c) and soil water content (θ_w) during simulated rain pulses at nightime in winter. Measurements were conducted in two microsites dominated by mature *Cyanobacteria* (MC and MC2).

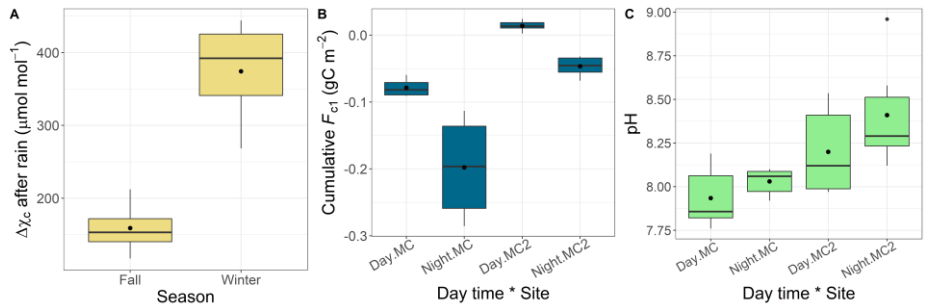

Figure 4 Boxplots of (A) the decrease in soil CO_2 molar fraction ($\Delta\chi_c$) after simulated rain pulses (from basal value before the first irrigation to minimum) against season; (B) the cumulative CO_2 fluxes (F_c) during soil water extractions (F_{c1}) against the interaction between site and day time; (C) the pH of soil solution against the interaction between site and day time. The black points are the means. Measurements were conducted in two microsites dominated by mature *Cyanobacteria* (MC and MC2).

Table 1 Effect of simulated rain pulses on pedoclimate

Date	Day time	Site	Basal χ_c	Final χ_c	Cumulative CO_2 uptake	T_s during extraction	θ_w during extraction
-	-	-	µmol mol^{-1}	µmol mol^{-1}	gC m^2	ºC	m^3 m^{-3}
09-10-20	day	MC	395	236	-0.26	22.3	0.23
14-10-20		MC2	423	275	-0.11	16.4	0.26
19-10-20	night	MC	472	260	-0.46	14.9	0.22
23-10-20		MC2	346	228	-0.45	13.6	0.27
26-01-21	day	MC	663	244	-0.11	17.1	0.22
29-01-21		MC2	608	340	-0.06	13.0	0.28
06-02-21	night	MC	521	155	-0.49	10.3	0.22
21-03-21		MC2	688	244	-0.13	8.2	0.29

χ_c, CO_2 molar fraction; T_s, soil temperature; θ_w, soil water content. Basal χ_c refers to χ_c before the rain simulation. Final χ_c refers to χ_c minimum after the rain simulation. The cumulative CO_2 uptake refers to the uptake since the occurrence of the first negative CO_2 flux until it became positive again.

3.4.3.4. Relationships between variables

The plots of Kendall correlations from the whole dataset as well as from the MC and MC2 sites subsets are presented in Figure 5. Over the whole dataset, the most relevant correlations came from the positive relationships between alkalinity and DIC (Fig. 6A) as well as between Ca and S (Fig. 6B). There was also a significant positive relationship between $SI_{calcite}$ and pH but due to five outliers that had their own non-significant relationship, this correlation was not highlighted by the correlation plot (Fig. 6C). All those outliers came from the MC2 site, and corresponded to negative values of $SI_{calcite}$, or very close to the equilibrium.

Over the MC subset, the most relevant correlations came from the positive relationship between cumulative F_c during extraction and T_s during extraction (Fig. 6D), the positive relationship between cumulative F_c after rain and DOC concentration (Fig. 6E), the negative relationship between the χ_c decrease after rain and pH (Fig. 6F), the negative relationship between the χ_c decrease after rain and the NO_3^- concentration (Fig. 6G), and the positive relationship between pH and NO_3^- concentration (Fig. 6H).

Over the MC2 subset, the most relevant correlations came from the negative relationship between DOC concentration and pH (Fig. 6I) and the negative relationships between the χ_c decrease and T_s after rain (however, since the information of this relationship was redundant with Fig. 6D, it is not plotted).

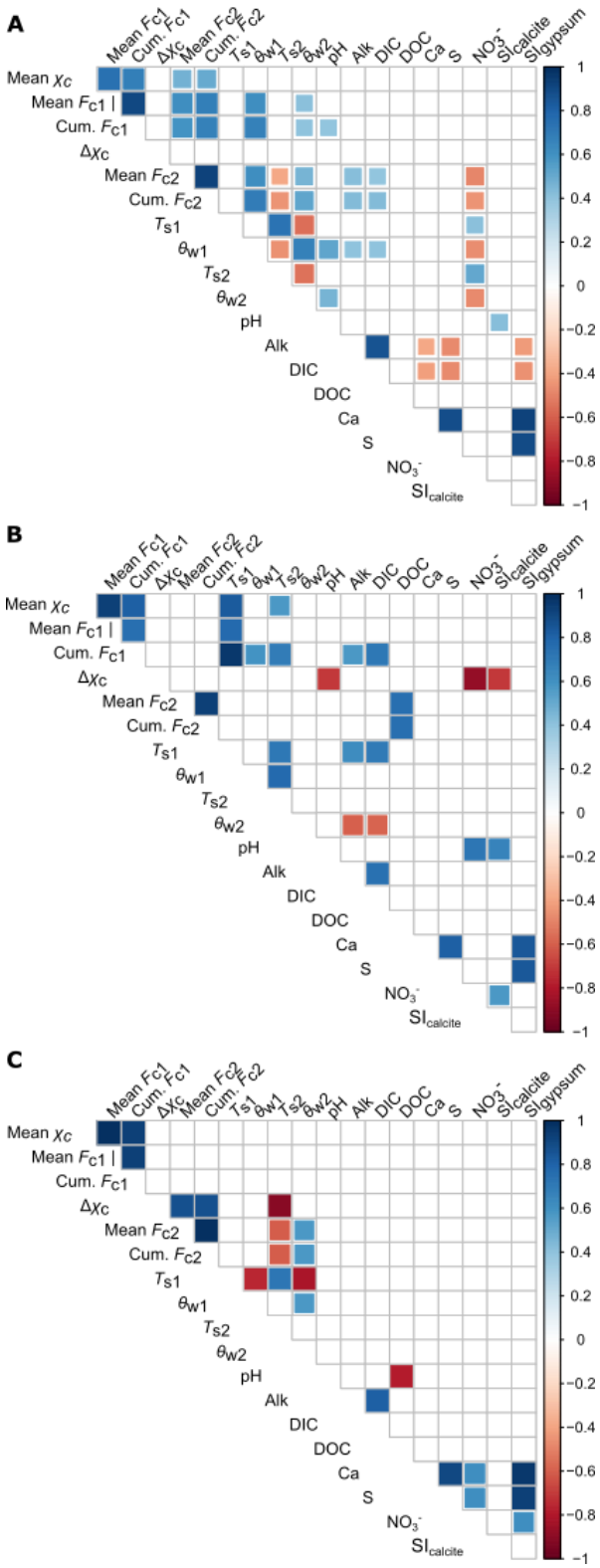

Figure 5 Plots of significant Kendall´s correlations over (A) the whole dataset; (B) the MC (mature cyanobacterial) microsite subset; (C) the MC2 microsite subset.

Mean χ_c, mean soil CO_2 molar fraction (χ_c) during soil water extraction; Mean F_{c1} ,mean soil-atmosphere CO_2 flux (F_c) during extraction; Cum. F_{c1}, cumulative F_c during extraction; $\Delta\chi_c$, decrease in χ_c after irrigation (from basal value before the first irrigation to minimum); Mean F_{c2} , mean F_c after irrigation (from basal χ_c value before the first irrigation to minimum); Cum. F_{c2}, cumulative F_c after irrigation (from basal χ_c value before the first irrigation to minimum); T_{s1} , mean soil temperature during extraction; θ_{w1} , mean soil water content during extraction; T_{s2} , mean T_s after irrigation (from basal χ_c value before the first irrigation to minimum); θ_{w2} , mean θ_w after irrigation (from basal χ_c value before the first irrigation to minimum)Alk, alkalinity; DIC, dissolved inorganic carbon content; DOC, dissolved organic carbon content; Ca, calcium concentration; S, sulfur concentration; NO_3^-, nitrate concentration; $SI_{calcite}$, calcite saturation index; SI_{gypsum}, gypsum saturation index.

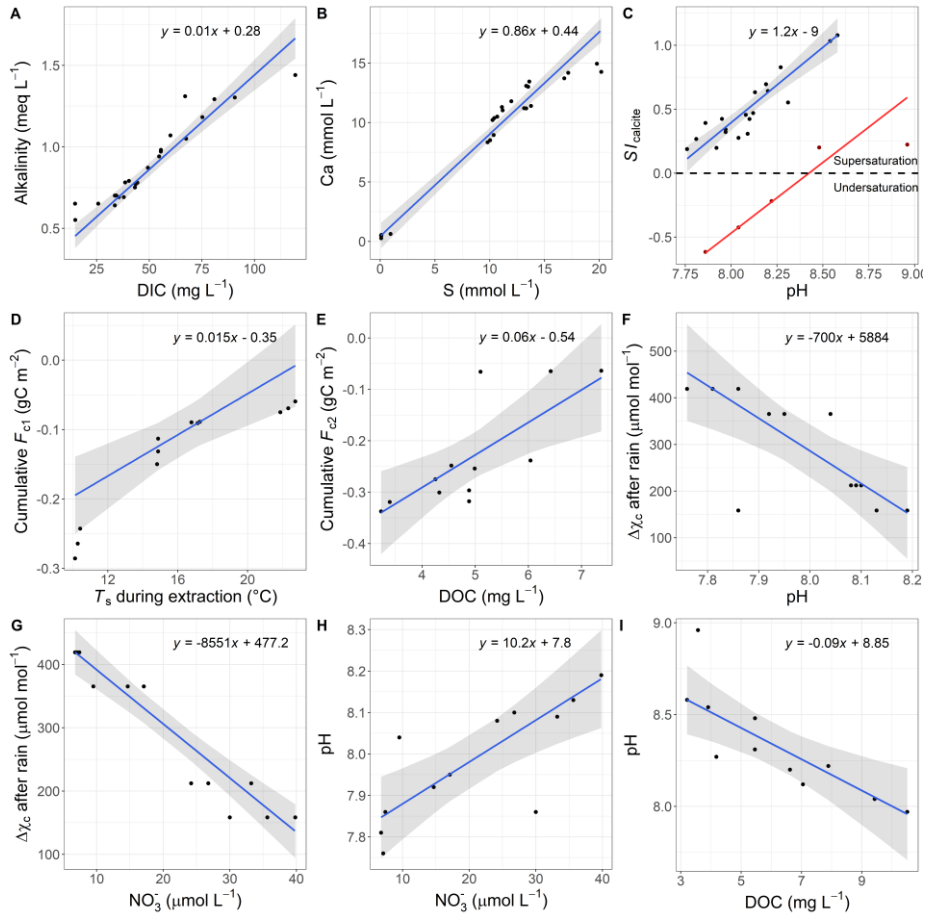

Figure 6 Relevant significant relationships between variables (A-C) over the whole dataset; (D-H) over the MC (mature cyanobacterial) microsite subset; (I) over the MC2 microsite subset.

DIC, dissolved inorganic carbon content; Ca, calcium content; S, sulfur content; $SI_{calcite}$, saturation index of calcite; χ_c, soil CO_2 molar fraction; $\Delta\chi_c$ after rain, decrease in χ_c after irrigation (from basal χ_c value before the first irrigation to minimum); F_{c1}, soil-atmosphere CO_2 flux (F_c) during extraction; F_{c2}, F_c after irrigation (from basal χ_c value before the first irrigation to minimum); NO_3^-, nitrate concentration; DOC, dissolved organic carbon content. The blue lines are the models fits and the shaded bands are the confidence intervals. The redline in (C) is a linear regression fit on outliers form the MC2 microsite.

3.4.4. Discussion

3.4.4.1. Evidences of coupled gypsum dissolution and carbonate precipitation

This study found several evidences of calcite precipitation from the calcium inherited from gypsum dissolution:

(1) The soil solution was most of the time undersaturated with respect to gypsum (Table 2) and there was a strong correlation between Ca and S concentration (Fig. 6B), indicating that the dissolution of this mineral was favored, according to the following reaction:

$$CaSO_4.2H_2O_{(s)} + H_2O_{(l)} \leftrightarrow Ca^{2+}{}_{(aq)} + SO_4^{2-}{}_{(aq)} + 3H_2O_{(l)} \quad (6)$$

(2) By contrast, the soil solution was most of the time supersaturated with respect to calcite (Table 2) and $SI_{calcite}$ increased with pH (Fig. 6C), indicating that the precipitation of this mineral was favored according to eq. 2, and enhanced by pH in the observed pH range (ca. 7.8 to 9). Non-equilibrium conditions with soil solution supersaturated with respect to calcite is a common condition in drylands soils that can be due to other sources of Ca, such as silicates [*Suarez et al.*, 1992; *Suarez & Rhoades*, 1982]. The presence of gypsum has also been reported to favor $CaCO_3$ precipitation due to the common-ion effect [*Bischoff et al.*, 1994; *Suarez*, 2017].

Therefore, we suggest that at our site, gypsum dissolution releases Ca that increases the IAP of calcite, thus favoring the precipitation of the latter mineral. In agreement with our results, pH >7.5 are known to favor gypsum dissolution and precipitation of calcite at atmospheric CO_2 concentrations [*Yu et al.*, 2019]. The coupled reaction can be summarized as:

$$CaSO_4.2H_2O_{(s)} + HCO_3^-{}_{(aq)} \leftrightarrow CaCO_{3(s)} + H^+{}_{(aq)} + SO_4^{2-}{}_{(aq)} + 3H_2O_{(l)} \quad (7)$$

3.4.4.2. Potential of coupled gypsum dissolution-carbonate precipitation as a long-term carbon sink

This study was motivated by *in-situ* observations of CO_2 uptake by soil, mitigating soil CO_2 emissions (Fig. 2). To explain this uptake, we formulated a conjecture according to which although the $CaCO_3$ precipitation apparently

produces gaseous CO_2 (eq. 2), the net balance of the equation is a carbon uptake since two moles of carbon are consumed for each mole of carbon that is produced. As a result, instruments measuring gaseous CO_2 would only detect a net CO_2 consumption if bicarbonate ions involved in carbonate precipitation are actively renewed by rapid CO_2 dissolution in water (eq. 1). Based on the CO_2 uptake by soil after irrigation (Fig. 3, Table 1) in association with the previously explained evidences of coupled gypsum dissolution and calcite precipitation, this assertion is likely. Carbonate precipitation, by removing HCO_3^- from the soil solution, would shift the equilibrium of eq. 1 towards more CO_2 dissolution, generating a positive feedback loop between those processes. Note that since saturation indexes are theoretical, they mean that $CaCO_3$ precipitation was favored but the observed CO_2 uptake could also have been due to the formation of ionic species ($CaCO_3^0$ y $CaHCO_3^+$), without immediate $CaCO_3$ precipitation. However, $CaCO_3$ would precipitate anyway during subsequent soil drying due to the removal of water and increasing Ca^{2+} and HCO_3^- concentrations shifting eq. 2 to the left.

One of the objectives of this study was to evaluate the potential of the observed CO_2 uptake as a long-term net carbon sink. The precipitation of secondary $CaCO_3$ can be considered as an effective carbon sink only when the Ca originates from an exogenic source (i.e. independently of the carbonate parent material), due to precipitation/dissolution cycles of $CaCO_3$ that would result in a neutral carbon balance [*Hasinger et al.*, 2015; *Monger et al.*, 2015]. For this reason, the weathering of silicate rocks represents a well-known carbon sink (eq. 3). However, this reaction is generally considered to be slow, except for kinetically labile silicates such as plagioclase [*Sánchez-Cañete et al.*, 2018; *Suarez & Rhoades*, 1982], and has usually been considered to be a carbon sink regulating Earth climate over geological times. By contrast, the carbonation from gypsum dissolution is rapid (on timescales of hours) and has therefore been considered as a promising way to store CO_2 in subsurface caprocks [*Yu et al.*, 2019]. However, the later authors concluded that since the reaction releases protons (eq. 7), the acidification of the medium could potentially tend to destabilize calcite over time. At the pH range observed at our sites, calcite dissolution is rather unlikely to occur, except during ephemeral soil respiration pulses after extended drought, typically once a year

at the end of the summer under this climate [*Vargas et al.*, 2018]. During those moments, the respired CO_2 has the potential to acidify the soil solution. Therefore, in order to confirm that the coupled gypsum dissolution and calcite precipitation constitutes a long-term carbon sink in those soils, further research should monitor the composition of the soil solution during those events as well as the gypsum and soil $CaCO_3$ content over time. The use of isotope techniques would also contribute to better characterize the pathways of Ca and carbon.

3.4.4.3. Factors related to the CO_2 uptake

3.4.4.3.1. Water availability

In this dryland, the main factor controlling the soil CO_2 uptake appeared to be water availability, as it is required for the initial gypsum dissolution. Our observations reveal that CO_2 uptake could be triggered or enhanced by rainfall (Fig.3C, Fig. 4). Remarkably, this uptake used to only occur at nighttime in natural dry conditions (Fig. 3B) but also occurred during daytime after irrigation (Table 1). Those results support the recent assumption according to which water vapor adsorption in natural dry conditions enhances mineral reactions at this site [*Lopez Canfin et al.*, 2022]. During daytime, liquid water was not available for mineral reactions in natural conditions but our irrigation lifted this limitation. Note that since gypsum is a hydrated salt with strong hydration/dehydration properties, it could potentially favor the process of water vapor adsorption and its dissolution could provide a non-negligible additional input of water at nighttime during drought.

3.4.4.3.2. Soil temperature

When water was available, the second most critical factor driving the CO_2 uptake in natural conditions was certainly the decrease in temperature at night due to Henry´s law according to which CO_2 dissolution in water increases at lower temperature [*Wilhelm et al.*, 2002]. To test this assumption, we performed our soil water extractions from fall to winter in order to capture the natural seasonal decrease in T_s, as well as at daytime and nighttime to capture the diel pattern of T_s (Table 1). We found that the decrease in χ_c from basal

pre-irrigation conditions was magnified in winter (Fig. 4A), and that the soil CO_2 uptake was enhanced at nighttime (Fig. 4B) following the expected relationship with temperature (Fig. 6E), thus confirming our hypothesis. Such inverse relationship between soil CO_2 uptake and temperature has already been reported *in-situ* in other drylands [*Ma et al.*, 2013; *Parsons et al.*, 2004]. At our experimental site, this uptake was also site-dependent (Fig. 4B).

3.4.4.3.3. Dissolved organic carbon

The third factor that seemed to drive the soil CO_2 uptake was the presence of organic matter. At the beginning of this study, we assumed that soil CO_2 uptake would be greater in the site with higher $CaCO_3$ content, i.e. in the MC2 site. However, we found the opposite trend (Table1, Fig.3, Fig. 4B) with the MC2 site even transiently emitting CO_2 at daytime (Fig. 4B). We suggest that this result is attributable to the greater soil organic carbon (SOC) content at the MC2 site (11.2 mg g^{-1}) compared to the MC site (6.4 mg g^{-1}) [*Lopez Canfin et al.*, n.d.] that could have acted in different ways: (1) by providing more available substrate for biological CO_2 production, thus partly masking the CO_2 uptake. However, over two years, soil CO_2 emissions were similar between the two sites (101 gC m^{-2}) and hence, this process could only have played a minor role; (2) by inhibiting calcite precipitation [*Lebron & Suarez*, 1996] through surface coating of the growing crystals by DOC [*Lebron & Suárez*, 1998]. We found several evidences supporting this mechanism: the soil solution pH used to be lower in the MC site (Fig. 4C) potentially as a result of more coupled gypsum dissolution-calcite precipitation releasing protons in this site (eq. 7) and conversely, more inhibition of the calcite growth in the MC2 "SOC-richer" site. The acidification triggered by the coupled gypsum dissolution-calcite precipitation seems to be confirmed by the greater magnitude of the CO_2 decrease after irrigation at lower pH in the MC site (Fig. 6F). Otherwise, if the process of carbonation from gypsum were not involved, the CO_2 uptake would have been expected to be enhanced by pH [*Ma et al.*, 2013; *Sparling & West*, 1990] due to aqueous CO_2 rapidly converting to HCO_3^- or CO_3^{2-}; that would provoke a depletion of aqueous CO_2 shifting the equilibrium of eq. 1 towards more CO_2 dissolution. As another evidence for the inhibition of calcite nucleation at the MC2 site, greater values of DOC were

associated to a lower pH (6I) thus limiting $SI_{calcite}$ which is pH-dependent (Fig 6C); in addition outliers in the relationship between $SI_{calcite}$ and pH all came from the MC2 "SOC-richer" site. Greater DOC values associated to lower pH might be due to an acidifying effect of organic matter on soil solution. In particular, organic acids are commonly produced by microorganisms and have the ability to enhance mineral weathering [*Drever & Stillings*, 1997; *Finlay et al.*, 2020], potentially explaining the relationship between DOC and pH (Fig. 6I) and why all the previously mentioned outliers were the only samples undersaturated with respect to $CaCO_3$ (Fig. 6C).

3.4.4.3.4. Nitrogen

In the MC site, we found a strong relationship between the χ_c decrease after irrigation and the NO_3^- concentration, with the latter variable related to pH of the soil solution (Fig. 6G and 6H). However, the potential mechanisms involved in those relationships remain unclear, as several processes could contribute. Both pH and NO_3^- have been shown to affect the activity of carbonic anhydrase, an enzyme produced by microorganisms that catalyzes the hydration of CO_2 [*Jones et al.*, 2021]. Soil pH can influence nitrification, denitrification and dissimilatory reduction NO_3^- reduction to NH_4^+ in a variety of ways [*Šimek & Cooper*, 2002; *Stevens et al.*, 1998]. In soils covered by biocrusts such as at our site, nitrifying microbes producing nitric acid are widespread and numerous [*Garcia-Pichel et al.*, 2016; *Marusenko et al.*, 2013]. In addition, biocrusts can release very rapidly NO_3^- or NH_4^+ after rewetting that can be readily taken up by the surroundings microorganisms and the release of NH_4^+ from nitrogen-fixing organisms supports very intense rates of nitrification in biocrusts [*Barger et al.*, 2016]. More recently, [*Liu et al.*, 2018] reported that under laboratory conditions, desert bacteria were able to trap atmospheric CO_2 in carbonate presumably *via* a biomineralization process mediated by ammonification through its positive effect on pH. The authors concluded that more empirical results were needed to confirm that such atmospheric CO_2 biomineralization processes actually occur in desert soils. Further *in-situ* research should combine soil-atmosphere CO_2 and N_2O fluxes measurements to explore the potential participation of nitrogen-related ecosystem processes on the nocturnal soil CO_2 uptake, as well as well as

scanning electron microscopy to investigate a potential biotic origin of the precipitated $CaCO_3$.

3.4.5. Conclusions

This study emphasizes the role of soil mineral reactions in the nocturnal CO_2 uptake by soil that has been increasingly reported in drylands and which origin is debated. At the studied site, analyses point out that coupled gypsum dissolution-carbonate precipitation can explain this uptake. In this dryland, the availability of water appears to be the main factor limiting the process. Empirical evidences show that this geochemical process was enhanced by rainfalls and probably by nocturnal water vapor adsorption by soil in dry conditions. In the presence of water, the second main factor driving the process appears to be temperature. Decreasing temperature, either at nighttime or in winter favored the dissolution of CO_2 in the soil water, forming HCO_3^- that could combine with the Ca inherited from gypsum dissolution to precipitate $CaCO_3$, generating a net CO_2 uptake by soil. The continuous removal of HCO_3^- by $CaCO_3$ precipitation might generate a positive feedback between the mineral precipitation and CO_2 dissolution in soil water. By contrast, the presence of DOC seemed to inhibit the process, most likely due to surface coating during crystal growth. Our results also show that the CO_2 uptake could be connected to nitrogen cycling but the possibly involved mechanisms remain to be clarified. We suggest that this natural pathway of CO_2 trapping in soil $CaCO_3$ potentially constitutes an active long-term carbon sink.

Acknowledgements

This work was funded by the research project CGL2016-78075-P, Biocrust Dinamics (DINCOS), of the Spanish National Program of Scientific and Technical Research, and by the ICAERSA research project (P18-RT-3629) of the Andalusian Regional Government including European Union ERDF funds. We are grateful to Andrew S. Kowalski for the proofreading and insightful suggestions that considerably improved the manuscript, and we are grateful to the Viciana brothers, landowners of the El Cautivo experimental site, without whose kind consent to set up semi-permanent installations on their land, this research would not have been possible.

Supporting Information

Table S1 Composition of the rainwater used for irrigation

Sample	pH	Alkalinity	Ca	K	Mg	Na	S	Cl^-	NO_3^-
-	-	meq L-1				mmol L-1			
1	6.74	0.022	0.034	0.003	0.005	0.033	< 0.0016	0.042	0.004
2	6.51	0.03	0.017	0.003	0.007	0.040	< 0.0016	0.048	0.003

References

American Public Health Association. (2005). Standard methods for the examination of water and wastewater (21st ed.). Port City Press.

Angert, A., Yakir, D., Rodeghiero, M., Preisler, Y., Davidson, E., & Weiner, T. (2015). Using O2 to study the relationships between soil CO2 efflux and soil respiration. *Biogeosciences*, *12*, 2089–2099. https://doi.org/10.5194/bg-12-2089-2015

ASTM. (1994). Standard Test Method for Total Organic Carbon in water. In *Annual Book of ASTM Standards.* American Soc. Testing & Materials.

Barger, N. N., Weber, B., Garcia-Pichel, F., Zaady, E., & Belnap, J. (2016). *Patterns and Controls on Nitrogen Cycling of Biological Soil Crusts*. 257–285. https://doi.org/10.1007/978-3-319-30214-0_14

Bay, S. K., Waite, D. W., Dong, X., Gillor, O., Chown, S. L., Hugenholtz, P., & Greening, C. (2021). Chemosynthetic and photosynthetic bacteria contribute differentially to primary production across a steep desert aridity gradient. *The ISME Journal*, 1–18.

Bernoux, M., & Chevallier, T. (2014). Carbon in dryland soils. Multiple essential functions. *Les Dossiers Thématiques Du CSFD*, *10*.

Bischoff, J. L., Juliá, R., Shanks III, W. C., & Rosenbauer, R. J. (1994). Karstification without carbonic acid: Bedrock dissolution by gypsum-driven dedolomitization. *Geology*, *22*(11), 995–998.

Bond-Lamberty, B., & Thomson, A. (2010a). Temperature-associated increases in the global soil respiration record. *Nature*, *464*(7288), 579–582.

Bond-Lamberty, B., & Thomson, A. (2010b). A global database of soil respiration data. *Biogeosciences*, *7*(6), 1915–1926.

Buck, A. L. (1981). New equations for computing vapor pressure and enhancement factor. *Journal of Applied Meteorology*, *20*(12), 1527–1532.

Cailleau, G., Braissant, O., & Verrecchia, E. P. (2004). Biomineralization in plants as a long-term carbon sink. *Naturwissenschaften 2004 91:4*, *91*(4), 191–194. https://doi.org/10.1007/S00114-004-0512-1

Cuezva, S., Fernandez-Cortes, A., Benavente, D., Serrano-Ortiz, P., Kowalski, A. S., & Sanchez-Moral, S. (2011). Short-term CO 2 (g) exchange between a

shallow karstic cavity and the external atmosphere during summer: role of the surface soil layer. *Atmospheric Environment*, *45*(7), 1418–1427.

Davidson, G. R., Phillips-Housley, A., & Stevens, M. T. (2013). Soil-zone adsorption of atmospheric CO2 as a terrestrial carbon sink. *Geochimica et Cosmochimica Acta*, *106*, 44–50.

Denman, K. L., Brasseur, G., Chidthaisong, A., Ciais, P., Cox, P. M., Dickinson, R. E., Hauglustaine, D., Heinze, C., Holland, E., Jacob, D., Lohmann, U., Ramachandran, S., da Silva Dias, P. L., Wofsy, S. C., & Zhang, X. (2007). *Couplings Between Changes in the Climate System and Biogeochemistry, in Climate Change 2007: The Physical Science Basis, Contribution of Working Group I to the Fourth Assessment Report of the Intergovernmental Panel on Climate Change, Cambridge Univ. Press, Cambridge, 499–587.*

Derry, L. A., & Chadwick, O. A. (2007). Contributions from Earth's Atmosphere to Soil. *Elements*, *3*(5), 333–338. https://doi.org/10.2113/GSELEMENTS.3.5.333

Drever, J. I., & Stillings, L. L. (1997). The role of organic acids in mineral weathering. *Colloids and Surfaces A: Physicochemical and Engineering Aspects*, *120*(1–3), 167–181. https://doi.org/10.1016/S0927-7757(96)03720-X

Fa, K.-Y., Zhang, Y.-Q., Wu, B., Qin, S.-G., Liu, Z., & She, W.-W. (2016). Patterns and possible mechanisms of soil CO2 uptake in sandy soil. *Science of the Total Environment*, *544*, 587–594. https://doi.org/10.1016/j.scitotenv.2015.11.163

Finlay, R. D., Mahmood, S., Rosenstock, N., Bolou-Bi, E. B., Köhler, S. J., Fahad, Z., Rosling, A., Wallander, H., Belyazid, S., Bishop, K., & Lian, B. (2020). Reviews and syntheses: Biological weathering and its consequences at different spatial levels - From nanoscale to global scale. *Biogeosciences*, *17*(6), 1507–1533. https://doi.org/10.5194/BG-17-1507-2020

Garcia-Pichel, F., John, V., Noah, M., Felde, L., Drahorad, S. L., & Weber, B. (2016). *Microstructure and Weathering Processes Within Biological Soil Crusts*. 237–255. https://doi.org/10.1007/978-3-319-30214-0_13

Hamerlynck, E. P., Scott, R. L., Sánchez-Cañete, E. P., & Barron-Gafford, G. A. (2013). Nocturnal soil CO2 uptake and its relationship to subsurface soil and ecosystem carbon fluxes in a Chihuahuan Desert shrubland. *Journal*

of Geophysical Research: Biogeosciences, *118*(4), 1593–1603. https://doi.org/10.1002/2013JG002495

Hasinger, O., Spangenberg, J. E., Millière, L., Bindschedler, S., Cailleau, G., & Verrecchia, E. P. (2015). Carbon dioxide in scree slope deposits: A pathway from atmosphere to pedogenic carbonate. *Geoderma*, *247–248*, 129–139. https://doi.org/10.1016/J.GEODERMA.2015.02.012

International Organization of Standardization. (1996). *ISO 13395:1996. Water quality - Determination of nitrite nitrogen and nitrate nitrogen and the sum of both by flow analysis (CFA and FIA) and spectrometric detection*. https://www.iso.org/standard/21870.html

International Organization of Standardization. (2000). *ISO 15682:2000. Water quality - Determination of chloride by flow analysis (CFA and FIA) and photometric or potentiometric detection*. https://www.iso.org/standard/27984.html

Jones, S. P., Kaisermann, A., Ogée, J., Wohl, S., Cheesman, A. W., Cernusak, L. A., & Wingate, L. (2021). Oxygen isotope exchange between water and carbon dioxide in soils is controlled by pH, nitrate and microbial biomass through links to carbonic anhydrase activity. *SOIL*, *7*(1), 145–159. https://doi.org/10.5194/SOIL-7-145-2021

Kessler, T. J., & Harvey, C. F. (2001). The global flux of carbon dioxide into groundwater. *Geophysical Research Letters*, *28*(2), 279–282. https://doi.org/10.1029/2000GL011505

Lebron, I., Herrero, J., & Robinson, D. A. (2009). Determination of gypsum content in dryland soils exploiting the gypsum–bassanite phase change. *Soil Science Society of America Journal*, *73*(2), 403–411.

Lebron, I., & Suarez, D. L. (1996). Calcite nucleation and precipitation kinetics as affected by dissolved organic matter at 25°C and pH > 7.5. *Geochimica et Cosmochimica Acta*, *60*(15), 2765–2776. https://doi.org/10.1016/0016-7037(96)00137-8

Lebron, I., & Suárez, D. L. (1998). Kinetics and Mechanisms of Precipitation of Calcite as Affected by PCO2 and Organic Ligands at 25°C. *Geochimica et Cosmochimica Acta*, *62*(3), 405–416. https://doi.org/10.1016/S0016-7037(97)00364-5

Liu, J., Fa, K., Zhang, Y., Wu, B., Qin, S., & Jia, X. (2015). Abiotic CO2 uptake from the atmosphere by semiarid desert soil and its partitioning into soil phases. *Geophysical Research Letters*, *42*(14), 5779–5785.

Liu, Z., Dreybrodt, W., & Liu, H. (2011). Atmospheric CO2 sink: Silicate weathering or carbonate weathering? *Applied Geochemistry*, *26*(SUPPL.), S292–S294. https://doi.org/10.1016/J.APGEOCHEM.2011.03.085

Liu, Z., Sun, Y., Zhang, Y., Feng, W., Lai, Z., & Qin, S. (2021). Soil Microbes Transform Inorganic Carbon into Organic Carbon by Dark Fixation Pathways in Desert Soil. *Journal of Geophysical Research: Biogeosciences*, e2020JG006047.

Liu, Z., Zhang, Y., Fa, K., Zhao, H., Qin, S., Yan, R., & Wu, B. (2018). Desert soil bacteria deposit atmospheric carbon dioxide in carbonate precipitates. *Catena*, *170*, 64–72.

Lopez Canfin, C., Lázaro, R., & Sánchez-Cañete P, E. (n.d.). Disparate responses of soil-atmosphere CO2 exchange to biophysical and geochemical factors over a biocrust ecological succession in the Tabernas Desert. *Geoderma*.

Lopez Canfin, C., Lázaro, R., & Sánchez-Cañete P, E. (2022). Water vapor adsorption by dry soils: a potential link between the water and carbon cycles. *Science of the Total Environment*.

Lopez-Canfin, C., Sánchez-Cañete, E. P., & Lazaro, R. (2021). Development of a new low-cost device to measure calcium carbonate content, reactive surface area in solid samples and dissolved inorganic carbon content in water samples. *Methods in Ecology and Evolution*. https://doi.org/10.1111/2041-210X.13579

Lopez-Canfin, C., Sánchez-Cañete, E. P., Serrano-Ortiz, P., López-Ballesteros, A., Domingo, F., Kowalski, A. S., & Oyonarte, C. (2018). From microhabitat to ecosystem: identifying the biophysical factors controlling soil CO2 dynamics in a karst shrubland. *European Journal of Soil Science*, *69*(6), 1018–1029. https://doi.org/10.1111/ejss.12710

Ma, J., Liu, R., Tang, L.-S., Lan, Z.-D., & Li, Y. (2014). A downward CO2 flux seems to have nowhere to go. *Biogeosciences Discussions*, *11*(7), 10419–10450.

Ma, J., Wang, Z.-Y., Stevenson, B. A., Zheng, X.-J., & Li, Y. (2013). An inorganic CO2 diffusion and dissolution process explains negative CO2 fluxes in

saline/alkaline soils. *Scientific Reports*, *3*, 2025. https://doi.org/10.1038/srep02025

Marusenko, Y., Bates, S. T., Anderson, I., Johnson, S. L., Soule, T., & Garcia-Pichel, F. (2013). Ammonia-oxidizing archaea and bacteria are structured by geography in biological soil crusts across North American arid lands. *Ecological Processes*, *2*(1), 1–10. https://doi.org/10.1186/2192-1709-2-9/TABLES/3

Monger, H. C., Kraimer, R. A., Khresat, S., Cole, D. R., Wang, X., & Wang, J. (2015). Sequestration of inorganic carbon in soil and groundwater. *Geology*, *43*(5), 375–378. https://doi.org/10.1130/G36449.1

Parsons, A. N., Barrett, J. E., Wall, D. H., & Virginia, R. A. (2004). Soil carbon dioxide flux in Antarctic dry valley ecosystems. *Ecosystems*, *7*(3), 286–295. https://doi.org/10.1007/s10021-003-0132-1

Raich, J. W., & Schlesinger, W. H. (1992). The global carbon dioxide flux in soil respiration and its relationship to vegetation and climate. *Tellus B*, *44*(2), 81–99.

Rey, A. (2015). Mind the gap: non-biological processes contributing to soil CO2 efflux. *Global Change Biology*, *21*(5), 1752–1761.

Roland, M., Serrano-Ortiz, P., Kowalski, A. S., Goddéris, Y., Sánchez-Cañete, E. P., Ciais, P., Domingo, F., Cuezva, S., Sanchez-Moral, S., & Longdoz, B. (2013). Atmospheric turbulence triggers pronounced diel pattern in karst carbonate geochemistry. *Biogeosciences*, *10*(7), 5009–5017. https://doi.org/10.5194/bg-10-5009-2013

Sánchez-Cañete, E. P., Barron-Gafford, G. A., & Chorover, J. (2018). A considerable fraction of soil-respired CO2 is not emitted directly to the atmosphere. *Scientific Reports*, *8*(1), 13518. https://doi.org/10.1038/s41598-018-29803-x

Schimel, D. S., House, J. I., Hibbard, K. A., Bousquet, P., Ciais, P., Peylin, P., Braswell, B. H., Apps, M. J., Baker, D., & Bondeau, A. (2001). Recent patterns and mechanisms of carbon exchange by terrestrial ecosystems. *Nature*, *414*(6860), 169.

Serrano-Ortiz, P., Roland, M., Sanchez-Moral, S., Janssens, I. A., Domingo, F., Goddéris, Y., & Kowalski, A. S. (2010). Hidden, abiotic CO 2 flows and

gaseous reservoirs in the terrestrial carbon cycle: review and perspectives. *Agricultural and Forest Meteorology*, *150*(3), 321–329.

Siegel, A. F. (1982). Robust regression using repeated medians. *Biometrika*, *69*(1), 242–244. https://doi.org/10.1093/BIOMET/69.1.242

Šimek, M., & Cooper, J. E. (2002). The influence of soil pH on denitrification: progress towards the understanding of this interaction over the last 50 years. *European Journal of Soil Science*, *53*(3), 345–354. https://doi.org/10.1046/J.1365-2389.2002.00461.X

Šimůnek, J., & Suarez, D. L. (1993). Modeling of carbon dioxide transport and production in soil: 1. Model development. *Water Resources Research*, *29*(2), 487–497.

Sparling, G. P., & West, A. W. (1990). A comparison of gas chromatography and differential respirometer methods to measure soil respiration and to estimate the soil microbial biomass. *Pedobiologia*, *34*(2), 103–112.

Stemmet, M. C., De Bruyn, J. A., & Zeeman, P. B. (1962). The uptake of carbon dioxide by plant roots. *Plant and Soil*, *17*(3), 357–364.

Stevens, R. J., Laughlin, R. J., & Malone, J. P. (1998). Soil pH affects the processes reducing nitrate to nitrous oxide and di-nitrogen. *Soil Biology and Biochemistry*, *30*(8–9), 1119–1126. https://doi.org/10.1016/S0038-0717(97)00227-7

Suarez, D. (2017). Inorganic Carbon: Land Use Impacts. *Encyclopedia of Soil Science, Third Edition*, 1210–1212. https://doi.org/10.1081/E-ESS3-120001765

Suarez, D. L. (1986). A soil water extractor that minimizes CO2 degassing and pH errors. *Water Resources Research*, *22*(6), 876–880.

Suarez, D. L. (1987). Prediction of pH Errors in Soil-water Extractors Due to Degassing 1. *Soil Science Society of America Journal*, *51*(1), 64–67.

Suarez, D. L., & Rhoades, J. D. (1982). The Apparent Solubility of Calcium Carbonate in Soils. *Soil Science Society of America Journal*, *46*(4), 716–722.

Suarez, D. L., Wood, J. D., & Ibrahim, I. (1992). Reevaluation of calcite supersaturation in soils. *Soil Science Society of America Journal*, *56*(6), 1776–1784.

Vargas, R., Sánchez-Cañete P, E., Serrano-Ortiz, P., Curiel Yuste, J., Domingo, F., López-Ballesteros, A., & Oyonarte, C. (2018). Hot-moments of soil CO2

efflux in a water-limited grassland. *Soil Systems*, *2*(3), 47. https://doi.org/10.3390/soilsystems2030047

Verheye, W. H., & Boyadgiev, T. G. (1997). Evaluating the land use potential of gypsiferous soils from field pedogenic characteristics. *Soil Use and Management*, *13*(2), 97–103. https://doi.org/10.1111/J.1475-2743.1997.TB00565.X

Wilhelm, E., Battino, R., & Wilcock, R. J. (2002). Low-pressure solubility of gases in liquid water. *Chemical Reviews*, *77*(2), 219–262. https://doi.org/10.1021/CR60306A003

Yu, L., Daniels, L. M., Mulders, J. J. P. A., Saldi, G. D., Harrison, A. L., Liu, L., & Oelkers, E. H. (2019). An experimental study of gypsum dissolution coupled to CaCO3 precipitation and its application to carbon storage. *Chemical Geology*, *525*, 447–461. https://doi.org/10.1016/J.CHEMGEO.2019.08.005

4. GENERAL DISCUSSION

4.1. Variation of CO_2 fluxes and other environmental variables over ecological succession

In the Chapter 2 of the thesis, a predictive spatio-temporal model was developed in order to predict the evolution of the CO_2 molar fraction (χ_c) of soil over time, as accurate predictions of χ_c could be used to predict the soil CO_2 flux (F_c) by using the gradient method. This model was developed in a parsimonious way, as it included as less terms as possible: (1) a qualitative variable: the stage of biocrusts ecological succession; (2) two quantitative variables: the soil water content (θ_w) and soil temperature (T_s); (3) up to three-way interactions between those variables. In spite of its simplicity, the model performed very well at predicting from a new dataset. During the model development, it was observed that removing the stage of the biocrusts ecological succession considerably deteriorated the quality of the fit and predictions. Those results seem to support the statement that a successional community framework has a strong potential to provide predictive and scaling power regarding biocrust relationships with function [*Ferrenberg et al.*, 2017].

However, it is important to not attribute all the improvement of the explained variability in the developed model to biocrusts succession, since this variable was included as a factor (i.e. categorical variable). As a result, this variable could have accounted for other environmental variables not measured or not included in the model. For example, in this thesis, it was found that many variables tended to vary over biocrusts succession. Overall, most of the variables tended to increase over succession: the soil porosity, the soil organic carbon (SOC) content, the soil nitrogen content, the specific surface area of $CaCO_3$ (SSA_c), the ratio between cumulative negative water vapor fluxes (F_h) and cumulative positive F_h; more specifically in later succession stages, the CO_2 production tended to increase over succession; more specifically in early succession stages: the total specific surface area of soil (SSA_s) and the magnitude of CO_2 influxes tended to increase over succession. Few variables tended to decrease over biocrusts succession: the gradient of water vapor molar fraction (χ_h) between soil and atmosphere; and specifically in late succession stages: the ratio between cumulative CO_2

influxes and cumulative CO_2 influxes. All those variables (and potentially others that were not measured) could have affected the χ_c dynamics through feedback processes with biocrusts. Many of these variables were highly collinear, thus challenging our ability to disentangle the controlling effects without *a priori* knowledge on the processes affecting χ_c. To improve modelling, further research should explore the relevance of a synthetic index of the succession status taking into account those variables, in order to minimize collinearity, which represents an issue in model development.

In spite of that, pedoclimatic variables such as θ_w and T_s that were included in our model were probably the main underlying variables driving χ_c dynamics, as they control decomposition rates of organic matter and the availability of nutrients that affect biological CO_2 production [*Luo & Zhou*, 2006]; θ_w and T_s are also modulated by biocrusts [*Chamizo et al.*, 2012; *Xiao et al.*, 2013], and have positive feedbacks on their development [*Grote et al.*, 2010; *Maestre et al.*, 2013]. Those variables also present the enormous advantage to be easy to measure at high frequency and with good spatial coverage. This is especially important in water-limited ecosystems where χ_c and F_c are known to exhibit "hot-moments" and "hot-spots" which depend on θ_w and T_s [*Leon et al.*, 2014; *Lopez-Canfin et al.*, 2018; *Vargas et al.*, 2018], including soils covered by biocrusts [*Bowling et al.*, 2011; *Castillo-Monroy et al.*, 2011]. In comparison, in this thesis, most of the soil physicochemical properties were only sampled once and thus deserve to be sampled at higher frequency in the future. In particular, monitoring organic and inorganic pools (SOC and $CaCO_3$) could provide further explanatory and predictive power to models, as well as critical information on the fate of the carbon that is emitted or captured by the soil (i.e. the carbon storage capacity of soil) in each stage of the biocrusts succession.

At the beginning of this thesis, it has been assumed that since biocrusts ecological succession can last decades to centuries [*Belnap & Lange*, 2001], measuring and sampling different succession stages could be approached by space-for-time substitution, i.e. to infer long-term temporal dynamics from spatial data [*Pickett*, 1989]. In the light of our results, we suggest that biocrusts development could drive the succession towards a climax state that maximizes organic carbon storage. That is because in spite of greater soil CO_2 emissions in late stages, the soil tended to accumulate SOC over succession. Therefore,

photosynthetic rates should also increase over succession in order to exceed those enhanced CO_2 emissions (i.e. net CO_2 fluxes should increase over succession) and allow carbon accumulation in soil. Recent evidences at our site suggest that biocrusts respiration is at least compensated by photosynthesis thus resulting in similar net CO_2 fluxes regardless of the biocrust type [*Miralles et al.*, 2018]. However, those measurements were performed with manual chambers that probably did not capture completely the sporadic activation of biocrusts photosynthesis after rain pulses. Therefore, continuous measurements of aboveground CO_2 fluxes with transparent and opaque chambers should be performed to confirm our assumption.

At the beginning of this thesis, it has also been assumed that the ecological succession of biocrusts could represent a convenient *in-situ* model to study the interaction between biotic and abiotic factors on F_c as the biotic influence on soil was expected to increase gradually from physical crusts to lichens-dominated late succession stages. In the light of our results, some evidences seem to support this assumption: in Chapter 3, it was found that the magnitude of the nocturnal CO_2 uptake by soil increased only over early successional stages and this increase was highly correlated to a concomitant increase in SSA_s. The latter variable depended mainly on the soil clay fraction which was correlated to the reactive surface area of calcite. That suggested the potential contribution of an abiotic mechanism of CO_2 adsorption [*Davidson et al.*, 2013] on highly reactive clay-size calcite [*Loeppert & Suarez*, 1996]. The accumulation of fine $CaCO_3$ particles can be mediated by biocrusts through the interception of particles from wind [*Warren*, 2003] and/or through biomineralization [*Liu et al.*, 2018]. This enhancement of CO_2 uptake with SSA_s was not observed in late successional stages. However, in Chapter 1, the SSA_c tended to increase over the whole succession (including in late successional stages), suggesting that as expected, processes consuming CO_2 and presumably involving $CaCO_3$ were masked in late successional stages due to enhanced CO_2 production. Further determinations of SSA_c with greater spatial coverage in combination with analyses of the morphology of those small-size carbonates with electronic microscopy are required to respectively

confirm with more confidence their accumulation over succession and assess their potential biotic origin.

4.2. Water vapor adsorption by dry soils

In the Chapter 3 of this thesis, water vapor adsorption (WVA) fluxes were identified for the first time in the scientific literature by using the gradient method. Compared to the traditionally used lysimeters, the gradient method has several advantages: (1) it is easy to deploy in the field; (2) it generates only limited perturbation of the soil profile (only a thin PVC tube is inserted in the topsoil); (3) it can provide long-term continuous measurements of water vapor fluxes at high frequency; (4) it can provide further understanding of the above- and belowground mechanisms involved in WVA; (5) it has a very low-cost, as relative humidity sensors used to calculate the water vapor molar fraction involved in the fluxes estimation, are very affordable; (6) its low-cost facilitates the acquisition of measurements replicated in space, allowing to combine both spatial and temporal resolution; (7) it does not require complex numerical modelling, providing a direct estimation of the water vapor uptake by soil without the need to filter data based on environmental conditions to discard other non-rainfall water inputs. The only drawback of the gradient method is that the estimated flux is highly dependent on the chosen gas transfer coefficient. For water vapor, no standardized procedure exists yet to calibrate this coefficient. Therefore, future research could combine measurements from the gradient method and measurements with lysimeters to calibrate this coefficient in order to obtain more accurate estimates of WVA. Moreover, the WVA estimates obtained by the gradient method are based on the assumption that all the water vapor that diffuses from atmosphere to soil is adsorbed onto soil particles, and thus this assumption requires validation or correction to improve the accuracy of WVA estimates.

The gradient method provided new insights on the underlying processes involved in WVA. In the past, WVA has been attributed to a soil drying during daytime and an increase in atmosphere relative humidity (RH_a) at nighttime, magnifying the soil-atmosphere water vapor pressure gradient [*Kosmas et al.*, 1998]. Based on our measurements, those statements were partially true. First, future research should prefer to analyze the variations in the water

vapor molar fraction (χ_h) instead of *RH* as the latter is influenced by temperature and hence can be misleading. Second, although we indeed observed an increase in atmosphere χ_h at nighttime and a decrease in soil χ_h during daytime, the latter could not be attributed to soil drying (the soil was already dry) but rather to a decrease in temperature reducing the capacity of air to store water vapor. In addition, a third condition seemed necessary for the process to occur: a substantial average atmosphere χ_h. This condition could only be fulfilled in summer due to greater temperature triggering more oceanic evaporation and the increased capacity of warmer air to store water vapor. Most studies reporting WVA fluxes were conducted in coastal drylands [e.g. *Kohfahl et al.*, 2021; *Kool et al.*, 2021; *Kosmas et al.*, 2001], where atmosphere is usually wetter. Since our study site was also close to the sea, further research is needed to clarify if WVA can also occur in non-coastal drylands or if the proximity of the sea only affects the magnitude of WVA fluxes. In addition, the vicinity of mountains could also be involved in the increase in atmosphere χ_h at night due to katabatic winds enriched with water vapor.

After combining continuous measurements of f_h and f_c, the main finding of Chapter 3 was that WVA could represent a potential link between the water and carbon cycle. At the beginning of this thesis, it has been assumed that WVA could enhance microbial activity and mineral reactions, thus impacting f_c. In particular, we assumed that WVA could be the driver of the nocturnal CO_2 uptake increasingly reported in drylands by providing water to sustain either biotic or abiotic CO_2 consumption processes. This thesis provided several evidences that this is likely to occur: (1) f_h and f_c covaried, both becoming negative at night; (2) a cross-correlation analysis revealed that the variation in f_h slightly led the variation in f_c. However, the lag was small and thus requires further confirmation with measurements at higher frequency; (3) a diel hysteretic relationship was found between f_h and f_c. In agreement with this result, adsorption/desorption processes are known to exhibit this kind of hysteretic behavior [*Arthur et al.*, 2020]. In spite of those evidences, it is still unclear whether a biotic and/or abiotic process links water vapor and CO_2 uptake by soil. Besides, since no convincing relationship was found between cumulative absorption f_h and cumulative absorption f_c, and because

absorption f_c was strongly correlated to SSA_s (which is an important factor controlling the adsorption of gases), a process of CO_2 adsorption independent of WVA cannot be completely discarded. However, if both gases were adsorbed at the same time (co-adsorption), they would still be expected to interact as WVA can enhance CO_2 adsorption [*Rubasinghege & Grassian*, 2013]. It is also very likely that more spatial replicates of f_h are needed to find a significant relationship between cumulative absorption f_h and cumulative absorption f_c, as well as between WVA and SSA_s, due to soil heterogeneity.

Many questions remain about the impact of WVA on the carbon cycle in drylands, especially: what is the fate of the adsorbed water? Is water vapor reemitted to the atmosphere during daytime due to desorption? Do microorganisms such as *Cyanobacteria* or chemotrophs use the adsorbed water films in their carbon-fixing metabolism? Is the adsorbed water consumed by geochemical reactions involving minerals such as calcite? If those processes occur, in which proportions? The use of appropriate isotopic techniques can probably help to answer those questions. The assumption of a potential enhancement of WVA by *Cyano*bacteria generating a positive feedback loop on their development also deserves further investigation. In addition, the significance of the water input through WVA leaves the door open for novel or growing multidisciplinary research, for example (1) on the use of WVA to grow plants of agricultural interest in drylands. For example, highly adsorbent material such as volcanic ashes could be used to optimize both water vapor and CO_2 adsorption by soils; (2) to assess the potential of WVA as a source of liquid water in extra-terrestrial environments. For example, strong water vapor adsorption and desorption processes have recently been found on Mars [*Savijärvi & Harri*, 2021].

4.3. The role of carbonates in nocturnal CO_2 uptake by soil

In the chapter 4 of this thesis, empirical evidences were found supporting that coupled gypsum dissolution-calcite precipitation could explain the nocturnal CO_2 uptake by soil observed at the experimental site. The main evidences came from saturation indexes (SI) with overall SI_{gypsum} and $SI_{calcite}$ indicating clear dissolution and precipitation of the respective minerals during the consumption of CO_2 by soil. However, the use of SI´s alone to assess calcite

dynamics is not entirely satisfactory. The SI´s can only be considered as semi-quantitative indicators of carbonate dynamics as they do not take into account key parameters that can either inhibit or enhance calcite precipitation. The analyses performed in this thesis suggested that the CO_2 uptake apparently due to calcite precipitation was inhibited by DOC. That is because the rates of precipitation and dissolution of calcite and more generally of minerals increase with the mineral surface area. When DOC is present in the soil solution, it can adsorb on the surface of growing calcite crystals, thus limiting precipitation rates [*Lebron & Suarez*, 1996; *Lebron & Suarez*, 1998]. Due to contamination of crystal surfaces by DOC, solutions can remain almost indefinitely calcite-supersaturated [*Suarez & Rhoades*, 1982]. Evaporation has also the potential to provoke supersaturation by concentrating ionic species [*Suarez*, 2017]. However, in our experiment, evaporation is unlikely to explain the supersaturation of the soil solution since water extractions were performed immediately after irrigation and evaporation was strongly limited at nighttime, especially at lower temperature in winter. Therefore, in our case, the rate of gypsum dissolution surely exceeds the rate of $CaCO_3$ precipitation due to contamination of calcite crystal surfaces. This unbalanced input of Ca increases the ion activity product (IAP) of calcite, provoking supersaturation of the soil solution. Due to the key role of DOC and mineral surface area in calcite precipitation, an accurate quantification of the rates of formation of pedogenic carbonates should take into account those parameters.

Quantifying with accuracy the rate of $CaCO_3$ precipitation would allow to better assess and validate the efficiency of this apparently active carbon sink. Such quantification requires the use of special kinetic models, such as the UNSATCHEM model developed by Suarez and Šimůnek, [1997]. Apart of using DOC and reactive surface area (RSA) as inputs for calculations of precipitation rates, this mechanistic model has also the advantage of incorporating a submodel to predict the dynamics of soil CO_2 from fundamental variables, and thus its outputs would also disserve to be compared with continuous measurements of the soil CO_2 dynamics at our experimental site. Incorporating a submodel of soil CO_2 dynamics is an advantage over most available models that generally consider the CO_2 as a fixed infinite reservoir (open-system) in equilibrium with the soil solution. Although those models are

more realistic than closed-system models, they are not entirely satisfactory to represent field conditions due to the highly variable χ_c and common deviations from the equilibrium state [*Suarez*, 1995]. In spite of the availability of powerful tools such as UNSATCHEM to model the precipitation-dissolution dynamics of soil carbonates, we found limited use of this software for this purpose in the scientific literature. That is partly attributable to the fact that carbon storage in the form of organic matter has received much more scientific attention, probably because carbonates have a slower dynamic. However, the limited experimental observations indicate that carbonate dynamics are not slow and insignificant; for example, it has been estimated that pedogenic $CaCO_3$ forms at a rate of 0.07-0.266 Gt C $year^{-1}$ in arid and semiarid regions [*Bernoux & Chevallier*, 2014]. Those estimates are still largely uncertain and thus require to be better constrained. Therefore, future research in drylands where fluxes of soil CO_2 uptake have been reported should consider to apply such kinetic models to compare rates of $CaCO_3$ formation to rates of soil CO_2 uptake, in particular in arid and hyperarid climates where the inhibition effect of DOC on $CaCO_3$ growth should be limited due to $CaCO_3$ stocks largely exceeding SOC stocks [*Lal*, 2019; *Plaza et al.*, 2018].

Several other challenges remain to explore the effect of biology and microclimate on $CaCO_3$ precipitation, in particular to which extent water vapor adsorption can contribute to the process and activate microorganisms involved in $CaCO_3$ precipitation. In the Chapter 3 of this thesis, we found that the nocturnal soil CO_2 uptake increase with total soil specific surface area (SSA_s) in early stages of the biocrust ecological succession. Since the SSA_s is mainly due to the clay fraction and a correlation was found between the clay fraction and calcite RSA, it was inferred that highly reactive clay-size carbonates might have reacted with the adsorbed CO_2 and/or water. In the light of results from Chapter 4, it can be postulated that those relationships are likely due to the growth of small-size calcite crystals during the early stages of biocrust succession. Those results raise the question of whether the development of microbial communities over succession could favor the precipitation of $CaCO_3$. Under purely abiotic control, the precipitation rate of $CaCO_3$ is often considered to occur slowly; however, microbes have the ability to create conditions that can enhance $CaCO_3$ precipitation, a process named

biomineralization. The mechanism appears to be widespread in ecosystems. For example, Meier et al. [2017] isolated bacteria from limestone-associated groundwater, rock and soil; they found that 92% of isolates were able to form carbonates. The diversity of the microorganisms involved in this process is large; it has generally been associated to bacteria [*Dhami et al.*, 2013; *Görgen et al.*, 2020], although fungi can also contribute, sometimes through bacterial-fungal interactions [*Bindschedler et al.*, 2016; *Hervé et al.*, 2016]. Since biocrusts are regarded as hotspots of bacterial and fungal diversity [*Maier et al.*, 2016], they are very likely to shelter biomineralizing organisms. Four groups of microorganisms are seen to be mainly involved in the process [*Dhami et al.*, 2013]: (1) photosynthetic organisms, such as *Cyanobacteria* and algae; (2) sulphate reducing bacteria; (3) organisms utilizing organic acids, and (4) organisms involved in the nitrogen cycle. The first group is particularly congruent with our measurements over biocrusts succession revealing that the soil CO_2 uptake had the greatest magnitude in the mature *Cyanobacteria* stage. The fourth group is also congruent with our observations of the soil CO_2 uptake being related to the NO_3^- concentration of the soil solution. In particular, the greater CO_2 uptake at lower NO_3^- could have been favored by biomineralizing nitrate reducers [*Eltarahony et al.*, 2019; *Hou et al.*, 2011; *Singh et al.*, 2015]. The two other groups of biomineralizers could also have participated to the process in some way. Although sulfate reducers are anaerobic, their presence has been reported in oxic desert soils [*Peters & Conrad*, 1995] and favorable anoxic conditions can be locally created in soil aggregates or transiently after rain pulses [*Lafuente et al.*, 2020]. Biomineralizers utilizing organic acids could have played a role in late succession stages dominated by lichens. Those organisms can produce large amounts of oxalic acid and calcium oxalate that can serve as a substrate to sustain the metabolism of bacteria that oxidize oxalate into $CaCO_3$ [*Braissant et al.*, 2004]. In this thesis, the soil solution of late succession stages was not sampled to assess their calcite precipitation-dissolution status but they also exhibited a non-negligible soil CO_2 uptake, although probably limited by greater DOC contents and partly masked by greater CO_2 production. For those reasons, we recommend for future research (1) to sample the soil solution over the whole succession (as well as during more seasons in order to capture

the annual variability of temperature); (2) to isolate potential microorganisms able to precipitate $CaCO_3$.

4.4. Climate-carbon cycle feedbacks

One of the most important results of this thesis from Chapter 2 is that θ_w was the main driver of the χ_c dynamics and that overall, its effect tended to be enhanced by T_s, regardless of the successional stage (Fig. 6, Chapter 2). Due to the good prediction accuracy of the model, this result can be interpreted with good confidence and has considerable implications in the context of climate change. It provides relevant information to the ongoing debate on whether the main regulator of the net terrestrial carbon flux is temperature or moisture variability, supporting recent studies stating that it is becoming increasingly evident that their interaction is fundamental but still largely neglected in most studies [*Piao et al.*, 2020; *Quan et al.*, 2019]. This is particularly true in drylands where the effect of T_s is strongly constrained by θ_w and antecedent moisture conditions play a key role in triggering ephemeral soil CO_2 pulses [*Lopez-Canfin et al.*, 2018; *Vargas et al.*, 2018]. This result also confirms that even if a positive feedback between the F_c and temperature is likely [*Hashimoto et al*. 2015], global models still underrepresent drylands and are often simplified in those areas with respect to their hydric status; therefore, future predictions require confirmation of their modelled processes in water-limited ecosystems.

The main difficulty in establishing predictions of the future feedback between F_c and climate change in drylands comes from the fact that climate change can have disparate effects: (1) from the one hand, the soil drying predicted with high confidence in some regions of the globe [*Collins et al.*, 2013] has the potential to reduce basal respiration over long periods of drought; (2) from the other hand, the rewetting of soils that have previously experienced long droughts can trigger short-lived but very large CO_2 emissions, which according to the results at our site, should be enhanced by the future rise in temperature. Therefore, one question arises: which of these disparate effects will dominate the carbon balance of water-limited ecosystems? It could be argued that the future precipitation patterns will play an important role, as some drylands are expected to undergo a rise in the total precipitation amount and others are expected to undergo a decrease in total

precipitation amount; however, even in areas where precipitation will increase, the global warming will concomitantly increase evapotranspiration rates, which may cancel out the expected positive effects of enhanced precipitation on θ_w; as a consequence, θ_w is projected to decrease by 25% in a substantial portion of drylands worldwide [*Maestre et al.*, 2012]. In the ecosystem studied in this thesis, it was observed that basal F_c was close to zero most of the year, except after rain pulses (Fig. 1, Chapter 2). As a result, a reduction of basal F_c in response to increasing drought should be limited in comparison with the enhanced pulse response to precipitation in response to the combined effect of rising temperature and increasing drought that stimulates the Birch effect [*Unger et al.*, 2010]. Consequently, a future enhancement of soil CO_2 emissions is a more likely outcome of global warming at this site. However, the future response of F_c might differ in other drylands such as in those from subhumid climates as they are expected to sustain a greater basal respiration. In Chapter 2, we suggested that since climate change is predicted to have a harmful effect on biocrusts cover and their carbon assimilation capacity [*Ferrenberg et al.*, 2015; *Maestre et al.*, 2013, 2015], biocrusted drylands like the one studied here which often have a carbon balance close to neutrality, could dangerously switch from carbon sinks to carbon sources. That could potentially generate a vicious cycle of positive feedback with climate change. In agreement with our speculations, Darrouzet-Nardi *et al*. [2015] found that biocrusted soils that were warmed by 2°C emitted more CO_2 (biocrusted soils took up less carbon and/or lost more carbon in warmed plots), thus highlighting a substantial risk of increased carbon loss from biocrust soils with higher future temperatures.

In order to predict with higher confidence the future trajectory of ecosystem carbon-climate feedbacks in drylands, it is urgent to invest more research efforts in studying natural ecosystem processes that mitigate CO_2 emissions. Many of those processes still suffer from a gap in both their understanding and quantification, including:

- The potential adaptation of soil microbial communities. Due to adaptation processes, responses of microbial communities might differ on the long-term compared to results obtained from short-term experiments. Several studies pointed out that soil microbial respiration can adapt to warming

[*Bradford*, 2013; *Bradford et al.*, 2008, 2019], including in drylands [*Dacal et al.*, 2019]. Regarding biological soil crusts, although some evidences exist regarding a potential adaptation of their respiration to warming [*Tucker et al.*, 2020], most studies suggest a negative effect of climate change on biocrusts cover and their carbon assimilation capacity [*Ferrenberg et al.*, 2015; *Maestre et al.*, 2013, 2015].

- Dark CO_2 fixation by soil chemotrophs. This process has been increasingly reported in soils recently [*Akinyede et al.*, 2020; *Bay et al.*, 2021; *Yang et al.*, 2017], including in drylands [*Liu et al.*, 2021]. The fixation rates of CO_2 by those microorganisms has been shown to increase with CO_2 concentration [*Spohn et al.*, 2020], and thus their activity could be enhanced by climate change. However, the sensitivity of respiration and carbon assimilation by soil chemotrophs to environmental factors such as χ_c, θ_w and T_s remains largely unexplored.

- Adsorption of water vapor and CO_2 by soils. Additional research is needed to monitor soil water vapor and CO_2 uptake as those sinks could grow with climate change in different ways: (1) warmer air has the capacity to hold more water vapor, and a soil drying is predicted in some regions of the globe, thus potentially enhancing WVA; (2) the atmospheric CO_2 increase is expected to enhance CO_2 adsorption by soils, especially in areas of low biological activity (typically, drylands) and where highly adsorbent phases are present [*Davidson et al.*, 2013].

- Mineral carbonation in soils. The fixation of CO_2 into stable carbonates through industrial processes has been recommended to mitigate climate change [*Mazzotti et al.*, 2005]. However, its natural occurrence in ecosystems has been overlooked as most research has focused on carbon storage into soil organic matter so far. Carbonates represents a much more interesting carbon sink since the residence time of mineral carbon is much greater than organic matter: 10^2-10^6 years and 0.1-10^3 years, respectively [*Bernoux & Chevallier*, 2014; *Cailleau et al.*, 2004]. Therefore, future research should dedicate further effort to assess the importance in the global carbon cycle of natural mineral carbonation, occurring either

through abiotic processes such as those investigated in Chapter 4 of this thesis or through biomineralization processes such as the oxalate-carbonate pathway [*Verrecchia et al.*, 2006].

- Leaching of soil dissolved inorganic carbon towards aquifers. The exportation of dissolved inorganic carbon (either inherited from carbonate weathering or soil respiration) to aquifers has the potential to capture carbon transiently, from hundreds up to thousands years [*Kessler and Harvey*, 2001]. Such downward fluxes have been reported in drylands [*Li et al.*, 2015; *Ma et al.*, 2014] and have been suggested to contribute to the unbalance in the global carbon budget, i.e. "the residual terrestrial carbon sink" [*Houghton et al.*, 2018]. At the scale of Europe, the leaching of carbon has also been proposed to explain this "missing sink" [*Siemens*, 2003].

Many of those processes of mitigation of CO_2 emissions depend on critical environmental conditions such as θ_w, T_s, RH and χ_c. Therefore, besides monitoring those processes, more manipulation experiments of those variables are required to anticipate their future response to climate change. Most of those processes are not included yet into current Earth System Models, i.e. climate models that take into account biogeochemical processes such as those involved in the carbon cycle [*Kawamiya et al.*, 2020]. In particular, more Free Air CO_2 Enrichment (FACE) facilities are needed worldwide, as they provide a strong foundation for next-generation experiments in unexplored ecosystems, and inform coupled climate-biogeochemical models of the ecological mechanisms controlling ecosystem response to the rising atmospheric CO_2 concentration [*Norby & Zak*, 2011]. At this time, FACE facilities are still inexistent in Africa and Latin America; and several areas still deserve further attention in order to attain a better knowledge of drylands worldwide and further increase our ability to predict global change impacts [*Maestre et al.*, 2012].

References

Akinyede, R., Taubert, M., Schrumpf, M., Trumbore, S., & Küsel, K. (2020). Rates of dark CO2 fixation are driven by microbial biomass in a temperate forest soil. *Soil Biology and Biochemistry*, *150*, 107950. https://doi.org/10.1016/j.soilbio.2020.107950

Arthur, E., Tuller, M., Moldrup, P., & de Jonge, L. W. (2020). Clay content and mineralogy, organic carbon and cation exchange capacity affect water vapour sorption hysteresis of soil. *European Journal of Soil Science*, *71*(2), 204–214.

Bay, S. K., Waite, D. W., Dong, X., Gillor, O., Chown, S. L., Hugenholtz, P., & Greening, C. (2021). Chemosynthetic and photosynthetic bacteria contribute differentially to primary production across a steep desert aridity gradient. *The ISME Journal*, 1–18.

Belnap, J., & Lange, O. L. (2003). Structure and Functioning of Biological Soil Crusts: a Synthesis. Springer. https://doi.org/10.1007/978-3-642-56475-8_33

Bernoux, M., & Chevallier, T. (2014). Carbon in dryland soils. Multiple essential functions. *Les Dossiers Thématiques Du CSFD*, *10*.

Bindschedler, S., Cailleau, G., Verrecchia, E., Benzerara, K., Miot, J., & Coradin, T. (2016). Role of Fungi in the Biomineralization of Calcite. *Minerals 2016, Vol. 6, Page 41*, *6*(2), 41. https://doi.org/10.3390/MIN6020041

Bowling, D. R., Grote, E. E., & Belnap, J. (2011). Rain pulse response of soil CO2 exchange by biological soil crusts and grasslands of the semiarid Colorado Plateau, United States. *Journal of Geophysical Research: Biogeosciences*, *116*(G3). https://doi.org/10.1029/2011JG001643

Bradford, M. A. (2013). Thermal adaptation of decomposer communities in warming soils. *Frontiers in Microbiology*, *4*(NOV). https://doi.org/10.3389/FMICB.2013.00333

Bradford, M. A., Davies, C. A., Frey, S. D., Maddox, T. R., Melillo, J. M., Mohan, J. E., Reynolds, J. F., Treseder, K. K., & Wallenstein, M. D. (2008). Thermal adaptation of soil microbial respiration to elevated temperature. *Ecology Letters*, *11*(12), 1316–1327. https://doi.org/10.1111/J.1461-0248.2008.01251.X

Bradford, M. A., McCulley, R. L., Crowther, T. W., Oldfield, E. E., Wood, S. A., &

Fierer, N. (2019). Cross-biome patterns in soil microbial respiration predictable from evolutionary theory on thermal adaptation. *Nature Ecology & Evolution 2019 3:2*, *3*(2), 223–231. https://doi.org/10.1038/s41559-018-0771-4

Braissant, O., Cailleau, G., Aragno, M., & Verrecchia, E. P. (2004). Biologically induced mineralization in the tree Milicia excelsa (Moraceae): its causes and consequences to the environment. *Geobiology*, *2*(1), 59–66. https://doi.org/10.1111/J.1472-4677.2004.00019.X

Cailleau, G., Braissant, O., & Verrecchia, E. P. (2004). Biomineralization in plants as a long-term carbon sink. *Naturwissenschaften 2004 91:4*, *91*(4), 191–194. https://doi.org/10.1007/S00114-004-0512-1

Castillo-Monroy, A. P., Maestre, F. T., Rey, A., Soliveres, S., & García-Palacios, P. (2011). Biological soil crust microsites are the main contributor to soil respiration in a semiarid ecosystem. *Ecosystems*, *14*(5), 835–847.

Chamizo, S., Cantón, Y., Miralles, I., & Domingo, F. (2012). Biological soil crust development affects physicochemical characteristics of soil surface in semiarid ecosystems. *Soil Biology and Biochemistry*, *49*, 96–105. https://doi.org/10.1016/J.SOILBIO.2012.02.017

Collins, M., Knutti, R., Arblaster, J., Dufresne, J.-L., Fichefet, T., Friedlingstein, P., Gao, X., Gutowski, W. J., Johns, T., & Krinner, G. (2013). Long-term climate change: projections, commitments and irreversibility. In *Climate Change 2013-The Physical Science Basis: Contribution of Working Group I to the Fifth Assessment Report of the Intergovernmental Panel on Climate Change* (pp. 1029–1136). Cambridge University Press.

Dacal, M., Bradford, M. A., Plaza, C., Maestre, F. T., & García-Palacios, P. (2019). Soil microbial respiration adapts to ambient temperature in global drylands. *Nature Ecology & Evolution 2019 3:2*, *3*(2), 232–238. https://doi.org/10.1038/s41559-018-0770-5

Darrouzet-Nardi, A., Reed, S. C., Grote, E. E., & Belnap, J. (2015). Observations of net soil exchange of CO2 in a dryland show experimental warming increases carbon losses in biocrust soils. *Biogeochemistry, 126*(3), 363–378. https://doi.org/10.1007/S10533-015-0163-7

Davidson, G. R., Phillips-Housley, A., & Stevens, M. T. (2013). Soil-zone adsorption of atmospheric CO2 as a terrestrial carbon sink. *Geochimica*

et Cosmochimica Acta, *106*, 44–50.

Dhami, N. K., Reddy, M. S., & Mukherjee, M. S. (2013). Biomineralization of calcium carbonates and their engineered applications: A review. *Frontiers in Microbiology*, *4*(OCT), 314. https://doi.org/10.3389/FMICB.2013.00314/BIBTEX

Eltarahony, M., Zaki, S., Kamal, A., Abd-El-Haleem, D., & Zaki, S. A. (2019). Calcite and vaterite biosynthesis by nitrate dissimilating bacteria in carbonatogenesis process under aerobic and anaerobic conditions. *Biogeosciences Discussions*, 1–33. https://doi.org/10.5194/BG-2019-444

Ferrenberg, S., Reed, S. C., Belnap, J., & Schlesinger, W. H. (2015). Climate change and physical disturbance cause similar community shifts in biological soil crusts. *Proceedings of the National Academy of Sciences of the United States of America*, *112*(39), 12116–12121. https://doi.org/10.1073/PNAS.1509150112/-/DCSUPPLEMENTAL

Ferrenberg, S., Tucker, C. L., & Reed, S. C. (2017). Biological soil crusts: diminutive communities of potential global importance. *Frontiers in Ecology and the Environment*, *15*(3), 160–167. https://doi.org/10.1002/fee.1469

Görgen, S., Benzerara, K., Skouri-Panet, F., Gugger, · Muriel, Chauvat, · Franck, & Cassier-Chauvat, C. (2020). The diversity of molecular mechanisms of carbonate biomineralization by bacteria. *Discover Materials 2020 1:1*, *1*(1), 1–20. https://doi.org/10.1007/S43939-020-00001-9

Grote, E. E., Belnap, J., Housman, D. C., & Sparks, J. P. (2010). Carbon exchange in biological soil crust communities under differential temperatures and soil water contents: implications for global change. *Global Change Biology*, *16*(10), 2763–2774. https://doi.org/10.1111/j.1365-2486.2010.02201.x

Hashimoto, S., Carvalhais, N., Ito, A., Migliavacca, M., Nishina, K., & Reichstein, M. (2015). Global spatiotemporal distribution of soil respiration modeled using a global database. *Biogeosciences*, *12*, 4121–4132. https://doi.org/10.5194/bg-12-4121-2015

Hervé, V., Junier, T., Bindschedler, S., Verrecchia, E., & Junier, P. (2016). Diversity and ecology of oxalotrophic bacteria. *World Journal of Microbiology and Biotechnology*, *32*(2), 28.

Hou, W., Lian, B., & Zhang, X. (2011). CO2 mineralization induced by fungal

nitrate assimilation. *Bioresource Technology*, *102*(2), 1562–1566. https://doi.org/10.1016/J.BIORTECH.2010.08.080

Houghton, R. A., Baccini, A., & Walker, W. S. (2018). Where is the residual terrestrial carbon sink? *Global Change Biology*, *24*(8), 3277–3279. https://doi.org/10.1111/gcb.14313

Kawamiya, M., Hajima, T., Tachiiri, K., Watanabe, S., & Yokohata, T. (2020). Two decades of Earth system modeling with an emphasis on Model for Interdisciplinary Research on Climate (MIROC). *Progress in Earth and Planetary Science*, *7*(1), 1–13. https://doi.org/10.1186/S40645-020-00369-5

Kessler, T. J., & Harvey, C. F. (2001). The global flux of carbon dioxide into groundwater. Geophysical Research Letters, 28(2), 279–282. https://doi.org/10.1029/2000GL011505

Kohfahl, C., Saaltink, M. W., & Ruiz Bermudo, F. (2021). Vapor flow control in dune sediments under dry bare soil conditions. *Science of The Total Environment*, *786*, 147404. https://doi.org/10.1016/J.SCITOTENV.2021.147404

Kool, D., Agra, E., Drabkin, A., Duncan, A., Fendinat, P. P., Leduc, S., Lupovitch, G., Nambwandja, A. N., Ndilenga, N. S., & Thị, T. N. (2021). The overlooked non-rainfall water input sibling of fog and dew: Daily water vapor adsorption on a! Nara hummock in the Namib Sand Sea. *Journal of Hydrology*, *598*, 126420.

Kosmas, C., Danalatos, N. G., Poesen, J., & Van Wesemael, B. (1998). The effect of water vapour adsorption on soil moisture content under Mediterranean climatic conditions. *Agricultural Water Management*, *36*(2), 157–168.

Kosmas, C., Marathianou, M., Gerontidis, S., Detsis, V., Tsara, M., & Poesen, J. (2001). Parameters affecting water vapor adsorption by the soil under semi-arid climatic conditions. *Agricultural Water Management*, *48*(1), 61–78.

Lafuente, A., Durán, J., Delgado-Baquerizo, M., Recio, J., Gallardo, A., Singh, B. K., & Maestre, F. T. (2020). Biocrusts Modulate Responses of Nitrous Oxide and Methane Soil Fluxes to Simulated Climate Change in a Mediterranean Dryland. *Ecosystems*, *23*(8), 1690–1701.

https://doi.org/10.1007/S10021-020-00497-5

Lal, R. (2019). Carbon Cycling in Global Drylands. *Current Climate Change Reports 2019 5:3*, *5*(3), 221–232. https://doi.org/10.1007/S40641-019-00132-Z

Lebron, I., & Suarez, D. L. (1996). Calcite nucleation and precipitation kinetics as affected by dissolved organic matter at 25°C and pH > 7.5. *Geochimica et Cosmochimica Acta*, *60*(15), 2765–2776. https://doi.org/10.1016/0016-7037(96)00137-8

Lebron, I., & Suarez, D. L. (1998). Kinetics and mechanisms of precipitation of calcite as affected by PCO2 and organic ligands at 25 C. *Geochimica et Cosmochimica Acta*, *62*(3), 405–416.

Leon, E., Vargas, R., Bullock, S., Lopez, E., Panosso, A. R., & La Scala, N. (2014). Hot spots, hot moments, and spatio-temporal controls on soil CO2 efflux in a water-limited ecosystem. *Soil Biology and Biochemistry*, *77*, 12–21. https://doi.org/10.1016/j.soilbio.2014.05.029

Li, Y., Wang, Y., Houghton, R. A., & Tang, L. (2015). Hidden carbon sink beneath desert. *Geophysical Research Letters*, *42*(14), 5880–5887.

Liu, Z., Sun, Y., Zhang, Y., Feng, W., Lai, Z., & Qin, S. (2021). Soil Microbes Transform Inorganic Carbon into Organic Carbon by Dark Fixation Pathways in Desert Soil. *Journal of Geophysical Research: Biogeosciences*, e2020JG006047.

Liu, Z., Zhang, Y., Fa, K., Zhao, H., Qin, S., Yan, R., & Wu, B. (2018). Desert soil bacteria deposit atmospheric carbon dioxide in carbonate precipitates. *Catena*, *170*, 64–72.

Loeppert, R. H., & Suarez, D. L. (1996). Carbonate and gypsum. *Methods of Soil Analysis: Part 3 Chemical Methods*, *5*, 437–474. https://doi.org/10.2136/sssabookser5.3.c15

Lopez-Canfin, C., Sánchez-Cañete, E. P., Serrano-Ortiz, P., López-Ballesteros, A., Domingo, F., Kowalski, A. S., & Oyonarte, C. (2018). From microhabitat to ecosystem: identifying the biophysical factors controlling soil CO2 dynamics in a karst shrubland. *European Journal of Soil Science*, *69*(6), 1018–1029. https://doi.org/10.1111/ejss.12710

Luo, Y., & Zhou, X. (2006). *Soil respiration and the environment*. Academic Press.

Ma, J., Liu, R., Tang, L.-S., Lan, Z.-D., & Li, Y. (2014). A downward CO2 flux

seems to have nowhere to go. *Biogeosciences Discussions*, *11*(7), 10419–10450.

Maestre, F. T., Escolar, C., Bardgett, R. D., Dungait, J. A. J., Gozalo, B., & Ochoa, V. (2015). Warming reduces the cover and diversity of biocrust-forming mosses and lichens, and increases the physiological stress of soil microbial communities in a semi-arid Pinus halepensis plantation. *Frontiers in Microbiology*, *6*(AUG). https://doi.org/10.3389/FMICB.2015.00865/ABSTRACT

Maestre, F. T., Escolar, C., de Guevara, M. L., Quero, J. L., Lázaro, R., Delgado-Baquerizo, M., Ochoa, V., Berdugo, M., Gozalo, B., & Gallardo, A. (2013). Changes in biocrust cover drive carbon cycle responses to climate change in drylands. *Global Change Biology*, *19*(12), 3835–3847. https://doi.org/10.1111/GCB.12306

Maestre, F. T., Salguero-Gó Mez, R., Quero, J. L., Rey, U., Carlos, J., & Tulipán, C. /. (2012). It is getting hotter in here: determining and projecting the impacts of global environmental change on drylands. *Philosophical Transactions of the Royal Society B: Biological Sciences*, *367*(1606), 3062–3075. https://doi.org/10.1098/RSTB.2011.0323

Maier, S., Muggia, L., Kuske, C. R., & Grube, M. (2016). *Bacteria and Non-lichenized Fungi Within Biological Soil Crusts*. 81–100. https://doi.org/10.1007/978-3-319-30214-0_5

Mazzotti, M., Abanades, J. C., Allam, R., Lackner, K. S., Meunier, F., Rubin, E., Sanchez, J. C., Yogo, K., & Zevenhoven, R. (2005). Mineral carbonation and industrial uses of carbon dioxide. In *IPCC special report on carbon dioxide capture and storage*. Cambridge University Press.

Meier, A., Kastner, A., Harries, D., Wierzbicka-Wieczorek, M., Majzlan, J., Büchel, G., & Kothe, E. (2017). Calcium carbonates: induced biomineralization with controlled macromorphology. *Biogeosciences*, *14*(21), 4867–4878.

Miralles, I., Ladrón de Guevara, M., Chamizo, S., Rodríguez-Caballero, E., Ortega, R., van Wesemael, B., & Cantón, Y. (2018). Soil CO2 exchange controlled by the interaction of biocrust successional stage and environmental variables in two semiarid ecosystems. *Soil Biology and Biochemistry*, *124*, 11–23.

https://doi.org/10.1016/J.SOILBIO.2018.05.020

Norby, R. J., & Zak, D. R. (2011). Ecological Lessons from Free-Air CO2 Enrichment (FACE) Experiments. *Http://Dx.Doi.Org/10.1146/Annurev-Ecolsys-102209-144647*, *42*, 181–203. https://doi.org/10.1146/ANNUREV-ECOLSYS-102209-144647

Peters, V., & Conrad, R. (1995). Methanogenic and other strictly anaerobic bacteria in desert soil and other oxic soils. *Applied and Environmental Microbiology*, *61*(4), 1673–1676. https://doi.org/10.1128/AEM.61.4.1673-1676.1995

Piao, S., Wang, X., Wang, K., Li, X., Bastos, A., Canadell, J. G., Ciais, P., Friedlingstein, P., & Sitch, S. (2020). Interannual variation of terrestrial carbon cycle: Issues and perspectives. *Global Change Biology*, *26*(1), 300–318. https://doi.org/10.1111/gcb.14884

Pickett, S. T. A. (1989). Space-for-Time Substitution as an Alternative to Long-Term Studies. *Long-Term Studies in Ecology*, 110–135. https://doi.org/10.1007/978-1-4615-7358-6_5

Plaza, C., Zaccone, C., Sawicka, K., Méndez, A. M., Tarquis, A., Gascó, G., Heuvelink, G. B. M., Schuur, E. A. G., & Maestre, F. T. (2018). Soil resources and element stocks in drylands to face global issues. *Scientific Reports 2018 8:1*, *8*(1), 1–8. https://doi.org/10.1038/s41598-018-32229-0

Quan, Q., Tian, D., Luo, Y., Zhang, F., Crowther, T. W., Zhu, K., Chen, H. Y. H., Zhou, Q., & Niu, S. (2019). Water scaling of ecosystem carbon cycle feedback to climate warming. *Science Advances*, *5*(8), eaav1131. https://doi.org/http://dx.doi.org/10.1126/sciadv.aav1131

Rubasinghege, G., & Grassian, V. H. (2013). Role (s) of adsorbed water in the surface chemistry of environmental interfaces. *Chemical Communications*, *49*(30), 3071–3094.

Savijärvi, H. I., & Harri, A. M. (2021). Water vapor adsorption on Mars. *Icarus*, *357*, 114270. https://doi.org/10.1016/J.ICARUS.2020.114270

Siemens, J. (2003). The European Carbon Budget: A Gap. *Science*, *302*(5651), 1681–1681. https://doi.org/10.1126/SCIENCE.302.5651.1681A

Singh, R., Yoon, H., Sanford, R. A., Katz, L., Fouke, B. W., & Werth, C. J. (2015). Metabolism-Induced CaCO3 Biomineralization during Reactive Transport in a Micromodel: Implications for Porosity Alteration. *Environmental*

Science and Technology, *49*(20), 12094–12104. https://doi.org/10.1021/ACS.EST.5B00152/SUPPL_FILE/ES5B00152_SI_001.PDF

Spohn, M., Müller, K., Höschen, C., Mueller, C. W., & Marhan, S. (2020). Dark microbial CO2 fixation in temperate forest soils increases with CO2 concentration. *Global Change Biology*, *26*(3), 1926–1935. https://doi.org/10.1111/gcb.14937

Suarez, D. (2017). Inorganic Carbon: Land Use Impacts. *Encyclopedia of Soil Science, Third Edition*, 1210–1212. https://doi.org/10.1081/E-ESS3-120001765

Suarez, D. L. (1995). Carbonate chemistry in computer programs and application to soil chemistry. *SSSA SPECIAL PUBLICATION*, *42*, 53.

Suarez, D. L., & Rhoades, J. D. (1982). The Apparent Solubility of Calcium Carbonate in Soils. *Soil Science Society of America Journal*, *46*(4), 716–722.

Suarez, D. L., & Šimůnek, J. (1997). UNSATCHEM: Unsaturated water and solute transport model with equilibrium and kinetic chemistry. *Soil Science Society of America Journal*, *61*(6), 1633–1646.

Tucker, C., Ferrenberg, S., & Reed, S. C. (2020). Modest Residual Effects of Short-Term Warming, Altered Hydration, and Biocrust Successional State on Dryland Soil Heterotrophic Carbon and Nitrogen Cycling. *Frontiers in Ecology and Evolution*, *8*, 364. https://doi.org/10.3389/FEVO.2020.467157/BIBTEX

Unger, S., Máguas, C., Pereira, J. S., David, T. S., & Werner, C. (2010). The influence of precipitation pulses on soil respiration–Assessing the "Birch effect" by stable carbon isotopes. *Soil Biology and Biochemistry*, *42*(10), 1800–1810.

Vargas, R., Sánchez-Cañete P, E., Serrano-Ortiz, P., Curiel Yuste, J., Domingo, F., López-Ballesteros, A., & Oyonarte, C. (2018). Hot-moments of soil CO2 efflux in a water-limited grassland. *Soil Systems*, *2*(3), 47. https://doi.org/10.3390/soilsystems2030047

Verrecchia, E. P., Braissant, O., & Cailleau, G. (2006). The oxalate-carbonate pathway in soil carbon storage: the role of fungi and oxalotrophic bacteria. *Fungi in Biogeochemical Cycles*, 289–310.

Warren, S. D. (2003). Synopsis: influence of biological soil crusts on arid land hydrology and soil stability. In *Biological soil crusts: Structure, function, and management* (pp. 349–360). Springer.

Xiao, B., Wang, H., Fan, J., Fischer, T., & Veste, M. (2013). Biological soil crusts decrease soil temperature in summer and increase soil temperature in winter in semiarid environment. *Ecological Engineering*, *58*, 52–56. https://doi.org/10.1016/J.ECOLENG.2013.06.009

Yang, J., Kang, Y., Sakurai, K., & Ohnishi, K. (2017). Fixation of carbon dioxide by chemoautotrophic bacteria in grassland soil under dark conditions. *Acta Agriculturae Scandinavica, Section B—Soil & Plant Science*, *67*(4), 362–371. https://doi.org/10.1080/09064710.2017.1281433

5. GENERAL CONCLUSIONS

This thesis contributed to improve the understanding and modelling of the soil-atmosphere CO_2 and water vapor exchange in semiarid biocrusted soils, by identifying the environmental variables and potential biogeochemical processes controlling those fluxes. The main conclusions of the thesis are the following:

- The interactive effect of soil water content and temperature on CO_2 fluxes is still largely neglected in most studies but is fundamental in water-limited ecosystems to assess their future response to climate change. In addition, taking into account biocrusts ecological succession has the potential to enhance the predictive power of models of the soil-atmosphere CO_2 exchange. Overall, the combination of observations and predictions suggest that soil CO_2 emissions are likely to be enhanced by climate change at the studied site. That is because, in the future, the interactive effect of increasing drought and temperature magnifying the pulse response of soil CO_2 to rewetting seems likely to override the expected decrease in basal soil respiration with drought. Since climate change is predicted to have a harmful effect on biocrusts cover and their carbon assimilation capacity, biocrusted drylands like the one studied here which often have a carbon balance close to neutrality, could dangerously switch from carbon sinks to carbon sources. That could potentially generate a vicious cycle of positive feedback with climate change. Upcoming research in this site should evaluate the future response of natural CO_2 mitigation processes that differ from photosynthesis.

- Processes of CO_2 consumption in soil were detected at night in all stages of the biocrusts succession. However, the magnitude of this CO_2 uptake was greater in early successional stages and particularly in sites dominated by *Cyanobacteria.* Our results indicate that the increased CO_2 production in late successional stages partially masked those CO_2 consumption processes throughout the year, except during periods of droughts that

substantially reduced biological activity. That is also probably why, in the scientific literature, CO_2 consumption processes have been essentially reported in drylands, as they sustain a low biological CO_2 production. The role of natural soil CO_2 consumption processes in mitigating soil CO_2 emissions and their sensitivity to climate change has been overlooked so far as most research has focused on soil respiration and water-limited ecosystems are still largely underrepresented in research on the soil-atmosphere CO_2 exchange. As a result, the potential of drylands to act as substantial carbon sinks has been neglected so far in comparison to other ecosystems such as forests. However, highlighting the capacity of those extensive ecosystems to mitigate CO_2 emissions could help to improve their conservation in the future.

- This thesis has provided several evidences regarding the potential biogeochemical processes involved in the nocturnal CO_2 uptake by soil. During most of the year, when liquid water inputs are available, though limited in this ecosystem, our geochemical analyses suggest that the dissolution of gypsum coupled to $CaCO_3$ precipitation might act as a net CO_2 sink at nighttime. During summer drought, our results point out that water vapor adsorption by soil was the main input of liquid water in this ecosystem, and has the potential to link the water and carbon cycles by maintaining those geochemical reactions. However, we cannot discard the potential activation of specialized microorganisms (chemotrophs/biomineralizers) by the adsorbed water and/or CO_2 co-adsorption to explain the nocturnal CO_2 uptake by soil; hence, further investigation is required to evaluate the potential contribution of those processes.

- By the way, this thesis participated in improving the methodology required (1) to quantify *in situ* the water vapor adsorption by soils, by using for the first time the gradient method for this purpose, and (2) to measure the $CaCO_3$ equivalent content and its reactive surface area in soils samples as well as the dissolved inorganic carbon in aqueous samples, by developing a device that measures the CO_2 release after samples acidification. The latter contribution gave rise to the registration of a

Utility Model (nº U202032735) in the Oficina Española de Patentes y Marcas (Spanish office of Patents and Registered trademarks). The parameters measured by the device can now be used as inputs in a kinetic model of coupled carbonate precipitation-gypsum dissolution, to accurately quantify the rates of $CaCO_3$ accumulation in soils through this active and potential long-term carbon sink. Such quantitative results would constitute a solid argument to improve the protection status of the Tabernas Desert.

LIST OF ABREVIATIONS

AEV	Air entry value
AIC	Akaike information criteria
AR1	Autoregressive of order 1
CCE	Calcium carbonate equivalent content
CV	Coefficient of variation
DIC	Dissolved Inorganic Carbon or Deviance Information Criteria
DOC	Dissolved organic carbon
EC	Electrical conductivity
IAP	Ion Activity Product
IC	Incipient *Cyanobacteria*
IGME	Instituto Geológico y Minero de España
FPI	Fabry-Pérot interferometer
LI	*Lepraria isidiata*
MC	Mature *Cyanobacteria*
MC2	Mature *Cyanobacteria* (second microsite)
NRWI	Non-rainfall water input
PAR	Photosynthetically active radiation
PD	Physical depositional crust
RMSE	Root mean square error
RRMSE	Relative root mean square error
RSA	Reactive surface area
SD	*Squamarina lentigera* and *Diploschistes diacapsis*
SI	Saturation index
SOC	Soil organic carbon
SOM	Soil organic matter
SSA_c	Calcite specific surface area
SSA_s	Total soil specific surface area
VIF	Variance inflation factor
WVA	Water vapor adsorption

LIST OF SYMBOLS

a_i	Activity of aqueous species *i*
C_i	Molar concentration of aqueous spcies *i*
χ_c	Soil CO_2 molar fraction
χ_s	Soil CO_2 molar fraction (in Chapter 2)
χ_a	Atmosphere CO_2 molar fraction
χ_{CO2}	CO_2 molar fraction (in Chapter 1)
χ_h	Water vapor molar fraction
D_a	Diffusion coefficient in free air
e	Partial pressure of water vapor
F_c	Soil-atmosphere CO_2 flux
F_h	Soil-atmosphere water vapor flux
F_s	Soil-atmosphere CO_2 flux (in Chapter 2)
γ_i	Activity coefficient of the aqueous species *i*
I	Ionic strength
k_s	Diffusion coefficient, or empirical soil transfer coefficient.
K_{sp}	Solubility product
P	Pressure
P_h	Water vapor pressure
P_s	Saturation vapor pressure
ϕ	Porosity
R	Universal gas constant
RH	Relative humidity
RH_s	Soil relative humidity
RH_a	Atmosphere relative humidity
R_s	Radius of maximum pore size
T	Temperature
T_a	Atmosphere temperature
T_s	Soil temperature or surface tension
T_{surf}	Surface temperature
θ_a	Air filled pore space
θ_w	Soil water content
V	Volume
z_i	Ionic charge of aqueous species *i*